NANOSTRUCTURED LIPID CARRIERS (NLC) IN DERMAL AND PERSONAL CARE FORMULATIONS

Inaugural-Dissertation

to obtain the academic degree

Doctor rerum naturalium (Dr. rer. nat.)

submitted to the Department of Biology, Chemistry and Pharmacy
of the Freie Universität Berlin

by

Aiman Hommoss

from Damascus, Syria

Berlin 2008

1st Reviewer: Prof. Dr. Rainer H. Müller
2nd Reviewer: Prof. Dr. Hans-Hubert Borchert

Date of defence: 20th January 2009

To my mom and dad

With all love and gratitude

Das Fehlen einer besonderen Kennzeichnung oder eines entsprechenden Hinweises auf ein Warenzeichen, ein Gebrauchmuster oder einen Patentschutz lässt nicht den Schluss zu, dass über die in dieser Arbeit angegebenen Dinge frei verfügt werden kann.

INDEX OF CONTENTS

ABBREVIATIONS

BCO	black currant seed oil
BMBM	butyl methoxydibenzoylmethane
DSC	differential scanning calorimetry
e.g.	*exempli gratia*
EDX	energy dispersive X-ray spectroscopy
FDA	US food and drug administration
GRAS	generally recognized as safe
HLB	hydrophilic lipophilic balance
HPLC	high performance liquid chromatography
hr	Hour
LD	laser diffractometry
NLC	nanostructured lipid carriers
o/w	oil in water
PCS	photon correlation spectroscopy
PI	polydispersity index
ppm	part per million
Q10	coenzyme Q 10
RI	recrystallization index
rpm	rotation per minute
SEM	Scanning electron microscopy
SLN	solid lipid nanoparticles
SPF	sun protection factor
SPME	solid phase microextraction
TEWL	transepidermal water loss
TiO_2	titanium dioxide
UV	ultraviolet
ZP	zeta potential

AIMS AND ORGANIZATION OF THE THESIS

Since the beginning of the 1990s the lipid nanoparticles were getting a growing interest from the pharmaceutical technology research groups world wide. Nowadays solid lipid nanoparticles (SLN) and nanostructured lipid carriers (NLC) have been already investigated as carrier systems for many applications.

In this thesis different NLC formulations were developed to be incorporated in dermal and personal care formulations. The advantages of using NLC in these preparations and the factors affecting these advantages were studied in details.

The thesis consists of six main chapters. The first chapter contains a literature review with respect to the uses of SLN and NLC as topical drug delivery systems. The features that SLN and NLC have, as topical delivery systems, were mentioned and the market products based on these systems were listed. The second chapter contains the materials and methods used in this work. The other four chapters contain different studies. The aims of these studies were:

- In chapter 3: To determine the optimal production conditions of NLC.

- In chapter 4: To develop NLC formulations which provide chemical protection to the chemically labile actives. The first NLC formulation contains coenzyme Q 10 and black currant seed oil. A formulation that contains a high load of black currant seed oil while maintaining the physical stability of the particles and the chemical stability of the oil was to be developed. The chemical stability of coenzyme Q 10 and black currant seed oil was to be determined in the developed NLC formulation and in a reference emulsion. The second NLC formulation contains retinol. The developed formulations were to have high load of retinol while maintaining the physical stability of the particles and the chemical stability of the incorporated retinol.

- In chapter 5: To develop NLC formulations to be used in sunscreen products as a UV blocker enhancer and to study the factors affecting this enhancement. Three NLC formulations were to be developed. A placebo NLC formulation that does not contain any UV blocker, an organic UV blocker-loaded NLC formulation (BMBM) and a TiO_2-

loaded NLC formulation. The different NLC formulations were to be incorporated in conventional creams and the enhancement of the UV blocking activity was to be measured.

- In chapter 6: To develop stable perfume-loaded NLC formulations that have a controlled perfume release profile and to study the factors affecting this release. Perfume-loaded NLC that have a positive charge were to be developed and incorporated in a conventional textile softener. The sustainability of the perfume was to be determined from this NLC containing softener and a conventional perfumed one.

1. LITERATURE REVIEW

1.1 Colloidal drug carriers

The new technologies employed in drug discovery lead to find many new powerful substances. The development of new drugs alone is not sufficient to ensure progress in drug therapy. Poor water solubility and insufficient bioavailability of the new drug molecules are main and common problems. Therefore, there is an increasing need to develop a drug carrier system that overcomes these drawbacks.

This carrier system should have no toxicity (acute and chronic), have a sufficient drug loading capacity and the possibility of drug targeting and controlled release characteristics. It should also provide chemical and physical stability for the incorporated drug. The feasibility of production scaling up with reasonable overall costs should be available [1-3].

Size reduction is one of the methods to increase the solubility and hence the bioavailability of poorly water soluble actives, which belong to the classes II and IV in the biopharmaceutical classification system (BCS). Colloidal systems, particularly those in the nanosize range, have been increasingly investigated in the last years because they can fulfill the requirements mentioned above [4-6].

1.1.1 Liposomes

Liposomes consist of one or more lipid bilayers of amphiphilic lipids, i.e. phospholipids, cholesterol and glycolipids [7]. Liposomes were described in 1965 by Bangham et al. as a cell membrane model [8, 9]. Later on they were used as a carrier system and were introduced to the cosmetic market by Dior in 1986. The first pharmaceutical marketed topical liposomal product was Pevaryl®-Lipogel, produced by Cilag A.G. Comprehensive biodisposition studies indicated the superiority of the liposomal form over the commercial Pevaryl cream, gel, and lotion forms. The liposomal products resulted in an increase in drug concentration in the epidermis (7-9 folds), where the site of action is. On the other hand, the drug concentration in internal organs was less, or similar to that of the treatment with the commercial preparations [10]. This product was followed by few others (AmBisome®, DaunoXome®). These products expressed less toxicity in comparison to the conventional dosage forms of the same drugs [11, 12]. Parenteral and topical administrations are the main application routes for liposomes. The size of liposomes varies from 20 nm to few micrometers, with lipid membranes of approximately 5 nm [13]. They can be prepared by many different methods, e.g. mechanical dispersion, solvent dispersion and detergent dialysis [14, 15].

Liposomes can encapsulate hydrophilic and lipophilic drugs and they are accepted for intravenous dosage forms due to their composition [16]. On the other hand, liposomes often

suffer rapid degradation by the pH of the stomach or by the intestinal enzymes and the bile salts if taken orally. They also have limited physical and chemical stability during storage. This is due to the hydrolysis of the ester bindings of the phospholipids and the oxidation of the unsaturated fatty acids. Moreover, there is a lack of large-scale production methods and organic solvents are used in some production procedures. All of these points make liposomes not optimal as a pharmaceutical carrier system. To overcome some of the liposomes drawbacks, niosomes were invented. Saturated hydrocarbon chains and intramolecular ether bindings increase the chemical stability of the niosomes [7, 17].

1.1.2 Microemulsions and nanoemulsions

Microemulsions are optically isotropic, transparent or translucent, low-viscous, single-phase liquid solutions. They are thermodynamically stable bicontinuous systems, which are essentially composed of water, oil, surfactant and co-surfactant [18-20]. Microemulsions show greater solubilizing capacities for both hydrophilic and lipophilic drugs than micellar solutions, e.g. Sandimmun Optoral® and Neoral® preconcentrate [21]. Due to the high surfactant concentration in microemulsions they are usually limited to dermal and peroral applications [22].

In the 1950's, nanoemulsions were introduced for the purposes of parenteral nutrition [23]. Nanoemulsions are heterogeneous systems composed of two immiscible liquids in which one liquid is dispersed as droplets in the other one [24-26]. In order to produce nanoemulsions an energy input is necessary and the obtained liquid-in-liquid dispersion is thermodynamically unstable [27].

Nanoemulsions have been used since some decades as drug carriers for lipophilic actives. Several pharmaceutical products based on nanoemulsion system have been introduced to the market e.g. Etomidat Lipuro®, Diazepam Lipuro®, Disoprivan®, Stesolid® and Lipotalon® [23, 28, 29].

The benefits of nanoemulsions over solubilization-based formulations (microemulsions) in terms of drug delivery are the reduction of the local and systemic side effects, e.g. reducing pain during injection and hemolytic activity caused by the high emulsifying agent concentration in the solubilization-based formulation [30]. However, the lipophilic loaded drug can partition between the oil droplets and the aqueous medium and hence, stability problems arise [31]. Moreover, the possibility of controlled drug release from nanoemulsions is limited due to the high mobility of the loaded drug which is dissolved in the oily phase. In

several studies a rapid release of the drug from its carrier system (nanoemulsion) was reported [32].

1.1.3 Nanocapsules and polymeric nanoparticles

Nanocapsules consist of a barrier made from polymers between the core (usually oil) and the aqueous surrounding environment. Solvent displacement [33] and interfacial polymerization [34] methods are often used for nanocapsules preparation. Polymers used in the preparation of nanoparticles include cellulose derivatives, poly (alkylcyanoacrylates), poly (methylidene malonate), polyorthoesters, polyanhydrides and polyesters such as poly (lactid acid), poly (glycolic acid) and poly (ε-caprolactone) and their copolymers [1]. Various procedures are applied for polymeric nanoparticles production e.g. coacervation technique, solvent evaporation [35], solvent diffusion methods, interfacial polymerization [36], denaturation or desolvation of natural proteins or carbohydrates [36] and the degradation by high-shear forces, e.g. by high pressure homogenization [37] or by micro fluidization [38].

In contrast to emulsions and liposomes, nanocapsules and polymeric nanoparticles can provide more protection to the incorporated sensitive drug molecules. This is due to the polymeric barrier and the solid polymeric matrix respectively. It is also possible to achieve controlled drug release from these carrier systems [39-42]. However, polymer-based nanoparticles have several drawbacks, e.g. the residues of the organic solvents used in the production process, the toxicity from the polymer itself and the difficulty of the large-scale production [43, 44]. Also polymer erosion, drug diffusion through the matrix or desorption from the surface may occur. Moreover, the concentration of prepared polymeric nanoparticle suspensions is low and mostly less than 2%. Nowadays there are many market products for therapy based on polymeric nanoparticles e.g. Decapeptyl ®, Gonapeptyl Depot ®, and Enantone Depot®.

1.2 Lipid nanoparticles

1.2.1 Definitions

Solid lipid nanoparticles (SLN) are produced by replacing the oil of an o/w emulsion by a solid lipid or a blend of solid lipids, i.e. the lipid particle matrix being solid at both room and body temperatures [45]. SLN are composed of 0.1% (w/w) to 30% (w/w) solid lipid dispersed in an aqueous medium and if necessary stabilized with preferably 0.5% (w/w) to 5% (w/w) surfactant. The incorporation of cosmetic and pharmaceutical actives is feasible. The mean particle size of SLN is in the submicron rage, ranging from about 40 nm to 1000 nm [45].

Nanostructured lipid carriers (NLC) are produced using blends of solid lipids and liquid lipids (oils). To obtain the blends for the particles matrix, solid lipids are mixed with liquid lipids, preferably in a ratio of 70:30 up to a ratio of 99.9:0.1. Because of the oil presence in these mixtures, a melting point depression compared to the pure solid lipid is observed, but the blends obtained are also solid at room and body temperatures [46]. The overall solid content of NLC could be increased up to 95% [47].

SLN are formulated from solid lipids only. Therefore, after preparation at least a part of the particles crystallizes in a higher energy modification (α or β`). During storage, these modifications can transform to the low energy, more ordered β modification. Due to this modification high degree of order, the number of imperfections in the crystal lattice is small, this leads to drug expulsion. NLC have been developed to overcome the drawbacks associated with SLN. They are considered to be the second generation of lipid nanoparticles. Compared to SLN, NLC show a higher loading capacity for active compounds by creating a less ordered solid lipid matrix, i.e. by blending a liquid lipid with the solid lipid, a higher particle drug loading can be achieved. Therefore, the NLC have an increased drug loading capacity in comparison to SLN and the possibility of drug expulsion during storage is less [2, 30, 48, 49]. NLC have also a lower water content of the particle suspension and a less tendency of unpredictable gelation [49-51].

1.2.2 SLN and NLC as drug delivery systems

At the beginning of the 1990s, SLN have been introduced as an alternative carrier system to emulsions, liposomes and polymeric nanoparticles. Primarily they were developed by three research groups namely the groups of Müller, Gasco, and Westesen. Afterwards, a growing

interest from many other research groups worldwide has been given to these carrier systems [52]. Many drugs have been successfully incorporated into SLN and NLC for different routes of administration. Table 1-1 shows some drugs that have been incorporated into lipid nanoparticles. SLN and NLC revealed several advantages compared to the other colloidal carrier systems. They provide a controlled drug release and an increase in chemical stability of the incorporated drugs. Moreover, they are safe carriers which can be produced easily on large scale [2, 16, 49, 53, 54].

Table 1-1: Examples of drug incorporated in lipid nanoparticles.

Incorporated drug	Reference
Aciclovir	[55]
Albumin	[56]
Amphotericin B	[57, 58]
Ascorbyl palmitate	[59, 60]
Azidothymidine palmitate	[61]
Betamethasone valerate	[62]
Bupivacaine	[63]
Calcitonin	[64]
Calixarenes	[65]
Camptothecin	[66-68]
Cholesteryl butyrate	[69]
Clobetasol proprionate	[70]
Clotrimazole	[71]
Clozapine	[72, 73]
Cortisone	[74]
Cyclosporin A	[75, 76]
Dexamethasone	[77]
Diazepam	[78]
Doxorubicin	[79]
Etomidate	[80]
Etoposide	[81]
Ferrulic acid	[82]
5-Fluorouracil	[83]
Gadolinium (III) complexes	[84]
Gonadorelin	[85]
Hydrocortisone	[86]
Idarubicin	[79, 87]
Indometacin	[88]
Insect repellents	[89, 90]
Insulin	[91]
Ketoconazole	[92]
Magnetite	[93]
Mifepristone	[94]
Nitrendipine	[95]
Oxazepam	[74]
Oxytetracycline	[96]
Paclitaxel	[69, 97]
Podophyllotoxin	[98]
Prednicarbate	[99]
Prednisolone	[80]
Retinoids	[100]
Thymopentin	[101]
Tobramycin	[102]
Tocopherol	[31]
Triptolide	[103, 104]
Ubidecarenone	[105-107]
Vitamin K	[108]

1.2.3 SLN and NLC as topical drug delivery systems

Topical drug application has been introduced since long time to achieve several purposes on different levels (skin surface, epidermis, dermis and hypodermis). However, several problems have been reported with the conventional topical preparations e.g. low uptake due to the barrier function of the stratum corneum and absorption to the systemic circulation. A lot of research groups paid attention to the topical application of the SLN and NLC. Many features, which these carrier systems exhibit for dermal application of cosmetics and pharmaceutics, have been pointed out. SLN and NLC are composed of physiological and biodegradable lipids that show low toxicity. The small size ensures a close contact to the stratum corneum and can increase the amount of drug penetrated into the skin. Due to the occlusive properties of lipid nanoparticles, an increased skin hydration effect is observed. Furthermore, lipid nanoparticles are able to enhance the chemical stability of compounds sensitive to light, oxidation and hydrolysis [30].

1.2.3.1 Increase of skin occlusion

The lipid film formation on the top of the skin and the subsequent occlusion effect was reported for lipid nanoparticles [109-111]. By using very small lipid particles, which are produced from highly crystalline and low melting point lipids, the highest occlusion will be reached. Particles smaller than 400 nm containing at least 35% lipid of high cystallinity have been most effective [112]. Souto et al. found a higher occlusive factor for SLN in comparison to NLC of the same lipid content [71]. Comparing NLC with different oil content showed that an increase in oil content leads to a decrease of the occlusive factor [113].

1.2.3.2 Increase of skin hydration and elasticity

The reduction of transepidermal water loss (TEWL) caused by occlusion leads to an increase in skin hydration after dermal application of SLN, NLC or formulations containing them. An *in vivo* study showed that the SLN-containing o/w cream increased the skin hydration significantly more than the conventional o/w cream. In this study the skin hydration effect after repetitive application of an o/w cream containing SLN and a conventional o/w cream was investigated for 28 days [112]. A significant higher increase in skin hydration was found by Müller et al. for an NLC-containing cream compared to conventional cream [114].

1.2.3.3 Enhancement of skin permeation and drug targeting

The stratum corneum in healthy skin has typically a water content of 20% and provides relatively an effective barrier against percutaneous absorption of exogenous substances. Skin hydration after applying SLN or NLC leads to a reduction of corneocytes packing and an increase in the size of the corneocytes gaps. This will facilitate the percutanious absorption and drug penetration to the deeper skin layers [115, 116].

An increase of skin penetration was reported for coenzyme Q 10 (Q10)-loaded SLN compared to Q10 in liquid paraffin and isopropanol. The cumulative amounts of Q10 were determined performing a tape stripping test. After five strips the cumulative amount of Q10 was 1%, 28% and 53% of the applied amount from the liquid paraffin, the isopropanol and the SLN formulation, respectively [117]. Similar results were achieved by another study for Q10-loaded NLC [118]. Another tap stripping test study showed that the tocopherol-loaded SLN formulation enhances the tocopherol penetration into the skin [117]. Jenning et al. showed that enhanced penetration of retinol with epidermal targeting of this active could be achieved by applying retinol-loaded NLC [119]. Application of antiandrogen drug cyproterone acetate-loaded SLN increased the skin penetration at least four folds over the uptake from the conventional cream and emulsion [120]. SLN were found to increase the triptolide penetration into the skin as well as the anti-inflammatory activity. This strategy improved the bioavailability at the site of action, reduces the required dose and the dose-dependent side effects like irritation and stinging [104].

Chen et al. compared podophyllotoxin-loaded SLN with podophyllotoxin tincture with regards to skin permeation, skin penetration and epidermal targeting effect. The podophyllotoxin permeated porcine skin from the tincture while no permeation was found for drug-loaded SLN. For one SLN formulation an increased penetration into porcine skin up to about four times over the tincture was reported. Furthermore, it was found that podophyllotoxin was located in the epidermis and hair follicles when applied as SLN formulation. No drug was found in the dermis after SLN application while podophyllotoxin after tincture application was distributed in each layer of the skin. Therefore, a localization effect in the epidermis was suggested and a reduction in systemic side effects is expected after application of podophyllotoxin using a formulation containing SLN [98]. Liu et al. found that epidermal targeting of isotretinoin could also be achieved using SLN [121].

Ricci et al. investigated the *in vitro* penetration of indomethacin from NLC-containing gel and gel without NLC through the stratum corneum and epidermis. He also investigated the *in vivo* indomethacin release by tape-stripping test and the *in vivo* anti-inflammatory activity using

the UV-B induced erythrema model. In this work it was found that the anti-inflammatory effect following the topical application of indomethacin was more prolonged with indomethacin-loaded NLC gel. In the tape stripping test higher amounts of indomethacin were found in the stratum corneum after application of the indomethacin-loaded NLC gel. The *in vitro* permeation through the stratum corneum and epidermis from indomethacin-loaded NLC gel was less than from gel without NLC [88].

Joshi et al. compared an NLC based gel of the nonsteroidal anti-inflammatory drug celecoxib with a micellar gel of the same composition regarding the *in vitro* skin penetration using rat skin and the pharmacodynamic efficiency by Aerosil induced rat paw edema. The *in vitro* permeation of celecoxib from NLC gel was less than the permeation from the micellar based gel. This confirms former findings about nanoparticles leading to a drug deposit in the skin resulting in sustained release. The *in vivo* comparison of the percentage edema inhibition produced by NLC and micellar gels showed a significant higher inhibition after application of the NLC based gel up to 24 hrs [122].

1.2.3.4 Improve benefit/risk ratio

Skin atrophy and systemic side effect occurred after applying conventional prednicarbate cream could be avoided when this drug was formulated as SLN. Predinicarbate uptake was enhanced and it was accumulated in the epidermis with a low concentration in the dermis [99, 116].

In another study Joshi et al. compared a valdecoxib-loaded NLC carbopol gel with a valdecoxib market product. The NLC containing gel showed no skin irritation while the market gel showed slight irritation after 48 hrs. Moreover, the NLC based gel showed prolonged activity up to 24 hrs while the activity of the market gel was shorter. This indicates a better skin tolerability and a longer activity of the NLC formulation compared to the marketed formulation [123].

Tretinoin loaded-SLN formulation was studied by Shah et al. concerning skin irritation. One of the major disadvantages associated with the topical application of tretinoin is the local skin irritation such as erythrema, peeling and burning as well as increased sensitivity to sunlight. In the *in vitro* permeation studies through rat skin they found that SLN based tretinoin gel has a permeation profile comparable to that of the market tretinoin cream. But on the other hand, Draize patch test showed that SLN based tretinoin gel resulted in remarkably less erythremic episodes compared to the currently marketed tretinoin cream and hence, a better benefit/risk ratio is expected for the formulations containing tretinoin-loaded SLN [124].

Conclusively, applying SLN or NLC can enhance skin penetration of incorporated actives, promote the epidermal targeting and minimize the systemic side effects and therefore, the benefit/risk ratio is improved.

1.2.3.5 Enhancement of UV blocking activity

Some side effects of organic UV blockers were reported due to the penetration of these compounds into the skin causing skin irritation and allergic reaction. This penetration can be reduced by incorporating these compounds in lipid nanoparticles. It was found that incorporating benzophenone in SLN not only improves the UV blocking activity evaluated using *in vitro* photoprotection assay but also reduces the absorption of the benzophenone into the skin in comparison to a conventional nanoemulsion. Improving the UV blocking activity allows the reduction of the concentration of the UV blocker while maintaining the protective level of the conventional formulation [30, 110, 125, 126]. These findings were confirmed by Song and Lui comparing UV absorption properties of 3,4,5-trimethoxybenzochitin-loaded SLN and SLN free system [127].

Furthermore, a significant increase in SPF up to about 50 was reported after the encapsulation of titanium dioxide into NLC. Encapsulation of inorganic sunscreens into NLC is therefore a promising approach to obtain well tolerable sunscreens with high SPF [128].

1.2.3.6 Enhancement of chemical stability of chemically labile compounds

Enhancement of chemical stability after incorporation into lipid nanocarriers was proven for many cosmetic actives, e.g. coenzyme Q 10 [117], ascorbyl palmitate [129], tocopherol (vitamin E) [117] and retinol (vitamin A) [100, 130].

1.2.4 Preparation methods of SLN and NLC

Many methods are used for the preparation of lipid nanoparticles (SLN, NLC). These methods are high pressure homogenization [2, 131, 132], microemulsion technique [133-135], emulsification-solvent diffusion [70, 136], emulsification-solvent evaporation [137], solvent injection (or solvent displacement) [138], multiple emulsion technique [139], phase inversion [140], ultrasonication [141], and membrane contractor technique [142, 143].

However, high pressure homogenization is the most used method due to the many advantages it has compared to the other methods, e.g. the avoidance of organic solvents, the short production time and the possibility of production on large scale. High pressure homogenizers are widely used in many industries including food industry (e.g. milk) and pharmaceutical

industry e.g. emulsions for parenteral nutrition. Therefore, no regulatory problems exist for the production of pharmaceutical and cosmetic preparations using this production technique.
Lipid nanoparticles can be produced by either the hot or cold high pressure homogenization technique [2]. More details about hot high pressure homogenization are mentioned in chapter 2.

1.2.5 Lipid nanoparticles based market products

The positive features of lipid nanoparticles leaded to the market introduction of many cosmetic products. Table 1-2 provides an overview of the cosmetic products containing lipid nanoparticles and the date of their market introduction.

Table 1-2: Examples of cosmetic products currently on the market containing lipid nanoparticles.

Product name	Producer	Market introduction	main active ingredients
Cutanova Cream Nano Repair Q10	Dr. Rimpler	10/2005	Q 10, polypeptide, Hibiscus extract, ginger extract, ketosugar
Intensive Serum NanoRepair Q10		10/2005	Q 10, polypeptide, mafane extract
Cutanova Cream NanoVital Q10		06/2006	Q 10, TiO_2, polypeptide, ursolic acid, oleanolic acid, sunflower seed extract
SURMER Crème Legère Nano-Protection SURMER Crème Riche Nano-Restructurante SURMER Elixir du Beauté Nano- Vitalisant SURMER Masque Crème Nano-Hydratant	Isabelle Lancray	11/2006	kukuinut oil, Monoi Tiare Tahiti®, pseudopeptide, milk extract from coconut, wild indigo, noni extract
NanoLipid Restore CLR	Chemisches Laboratorium Dr. Kurt Richter, (CLR)	04/2006	black currant seed oil containing ω-3 and ω-6 unsaturated fatty acids
Nanolipid Q10 CLR		07/2006	coenzyme Q10 and black currant seed oil
Nanolipid Basic CLR		07/2006	caprylic/capric triglycerides
NanoLipid Repair CLR		02/2007	black currant seed oil and manuka oil
IOPE SuperVital - Cream - Serum - Eye cream - Extra moist softener - Extra moist emulsion	Amore Pacific	09/2006	coenzyme Q10, ω-3 und ω-6 unsaturated fatty acids
NLC Deep Effect Eye Serum	Beate Johnen	12/2006	coenzyme Q10, highly active oligo saccharides
NLC Deep Effect Repair Cream			Q10, TiO_2, highly active oligo saccharides
NLC Deep Effect Reconstruction Cream NLC Deep Effect Reconstruction Serum			Q10, Acetyl Hexapeptide-3, micronized plant collagen, high active oligosaccharides in polysaccharide matrix
Regenerationscreme Intensiv	Scholl	6/2007	Macadamia Ternifolia seed oil, Avocado oil, Urea, Black currant seed oil
Swiss Cellular White Illuminating Eye Essence Swiss Cellular White Intensive Ampoules	la prairie	1/2007	Glycoprotiens, Panax ginseng root extract, Equisetum Arvense extract, Camellia Sinensis leaf extract, Viola Tricolor Extract
SURMER Creme Contour Des Yeux Nano-Remodelante	Isabelle Lancray	03/2008	kukuinut oil, Monoi Tiare Tahiti®, pseudopeptide, hydrolized wheet protien
Olivenöl Anti Falten Pflegekonzentrat	Dr. Theiss	02/2008	Olea Europaea Oil, Panthenol, Acacia Senegal, Tocopheryl Acetate
Olivenöl Augenpflegebalsam			Olea Europaea Oil, Prunus Amygdalus Dulcis Oil, Hydrolized Milk Protein, Tocopheryl Acetate, Rhodiola Rosea Root Extract, Caffeine

2 MATERIALS AND METHODS

2.1 Materials

The materials used in this work are only partially composed of individual chemical substances and their composition may differ according to the manufacturer. Therefore, the physicochemical properties and the producer details for all the materials which were used are given in the present section. All the materials have been used as received and were of reagent grade.

2.1.1 Solid lipids

The solid lipids used in this work consist of a mixture of several chemical compounds which have a relatively high melting point (higher than 40ºC). These solid lipids are well tolerated, of GRAS status, accepted for human use and they are also *in vivo* biodegradable.

2.1.1.1 Apifil®

It is a market product from Gattefossé GmbH (Weil am Rhein, Germany). It is nonionic, hydrophilic PEG-8 white beeswax having self-emulsifying properties with an HLB value of 9.4. Apifil melting point is between 59ºC and 70ºC. Due to its good emulsifying abilities it is used as lipid phase in o/w emulsions with high lipid content (40-80%). The acid value of this lipid is less than 5 mg KOH/g, saponification value is between 70-90 mg KOH/g and the iodine value is less than 10 g I_2/100g. It is soluble in chloroform and ethanol and insoluble in water [144].

2.1.1.2 Beeswax

Also called Cera alba was purchased from Caelo (Hilden, Germany). Beeswax is a hard wax formed consists of a mixture of several compounds mainly palmitate, palmitoleate, hydroxypalmitate and oleate esters of long chain (C30-C32). Beeswax has a melting point between 62°C and 64°C. According to the origin of the wax the saponification value will be between 3 and 9 mg KOH/g (European types have a lower value than oriental ones) [145, 146].

2.1.1.3 Carnauba wax 2442

It is a market product from Kahl (Trittau, Germany). Carnauba wax is a plant wax that is separated from the leafs of the Brazilian palm tree Copernicia Cerifera. It contains mainly esters of fatty acids (80-85%), fatty alcohols (10-15%), acids (3-6%) and hydrocarbons (1-3%). Specific for carnauba wax is the content of esterified fatty diols (about 20%),

hydroxylated fatty acids (about 6%) and cinnamic acid (about 10%). Cinnamic acid, an antioxidant, may be hydroxylated or methoxylated. Carnauba wax is insoluble in water and soluble in organic solvents like ethyl acetate and chloroform. The acid value is 2-7 mg KOH/g and the saponification value is between 78-95 mg KOH/g. Its melting point is between 78°C and 88°C and the relative density is about 0.97. Because of its hardness carnauba wax is an important additive in the cosmetic products It is also accepted in the food industry and has many uses [147].

Carnauba wax 2442 L

It is carnauba wax 2442 that has been treated with a special washing process to make it more suitable for the use in food, pharmaceutical industry and cosmetic products. It has less smell and taste. The peroxide number is almost 0 mEq O_2/kg [148].

2.1.1.4 Compritol®888 ATO

It is a market product from Gattefossé GmbH (Weil am Rhein, Germany) based on glycerol esters of behenic acid (C22). It is composed of glycerol tribehenate (28-32%), glycerol dibehenate (52-54%) and glycerol monobehenate (12-18%). The main fatty acid is behenic acid (>85%) but other fatty acids (C16-C20) are also present. The melting point of Compritol®888 ATO is between 69ºC and 74ºC. Due to the presence of partial acylglycerols, this lipid has an amphiphilic character. It has an HLB of about 2 and a density of 0.94 g/cm^3 [144]. Compritol®888 ATO has a peroxide value lower than 6 mEq O_2/kg, indicating a high chemical stability. It is soluble in chloroform, methylene chloride and xylene when heated and it is insoluble in ethanol, ethyl ether, mineral oils and water. It is used as lubricating agent for tablets and capsules, as a binding agent for direct compression and as a lipophilic matrix in sustained release formulations. In dermal preparations, this lipid is used as viscosity enhancer (to increase the viscosity) of oil phases in w/o or o/w emulsions and improves heat stability of emulsions. It has to be stored below 35ºC because of the risk of caking, avoiding the contact with air, light, heat and moisture in its original packing.

2.1.1.5 Cutina CP®

It is a market product from Cognis Deutschland GmbH (Düsseldorf, Germany) and consists of cetyl palmitate which is a wax consists predominantly of hexadecyl hexadecanoate ($C_{32}H_{64}O_2$), an ester of cetyl alcohol and palmitic acid. It is supplied in the form of white coarse pellets. Because of its characteristics this wax is used in cosmetic and pharmaceutical emulsions. The acid value of this lipid is max. 1 mg KOH/g, saponification value is between

112-123 mg KOH/g and the iodine value is max 1 g I_2/100. Its melting point is between 46°C and 51°C. It is soluble in chloroform and ethanol and insoluble in water and paraffin [145].

2.1.1.6 Dynasan®116

Dynasan® bases are market products from Sasol Germany GmbH (Witten, Germany). These products consist of lipid materials with a high content of microcrystalline triacylglycerols (90%) and monocarboxilic acids (10%). The triacylglycerols are glycerol esters of selected, even-numbered and unbranched fatty acids of natural origin. These triacylglycerols do not contain any antioxidants or stabilizing agents. The melting point of Dynasan®116 (triacylglycerol of palmitic acid) is between 62ºC and 64ºC [149]. The acid value is max 3 mg KOH/g, saponification value is between 205-215 mg KOH/g and the iodine value is max 1 g I_2/100g. This lipid is hardly soluble in *n*-hexane, ether and ethanol, and practically insoluble in water. If Dynasan®116 is rapidly cooled down from the melt, glassy amorphous masses are initially formed. On storage these amorphous masses change into crystalline modifications with volume expansion. The stable β modification has a very sharp melting point and is of triclinic structure. The lipid needs to be stored in sealed containers and protected from light. Under these conditions the shelf life of this product more than three years.

2.1.1.7 Elfacos® C 26

It is a market product from Akzo Nobel (Amsterdam, Netherlands). It is a synthetic wax of long chains of hyrdroxylated fatty acids and fatty alcohols, the INCI name is Hydroxyoctacosanyl Hydoxystearate. It has a melting point of 80°C. The acid value is 5-10 mg KOH/g, and the saponification value is between 75-90 mg KOH/g. Elfacos C 26 is used as a consistency regulating agent for w/o emulsions with emulsion stabilizing properties and as a waxy substance for decorative cosmetics. It can be used as a replacement for beeswax [145].

2.1.1.8 Imwitor 900®

It is a market product from Sasol Germany GmbH (Witten, Germany) and consists of vegetable-based monodiglyceride based on hydrogenated fats with a monoester content of about 45%. Its melting point is between 54°C and 64°C. Above its melting point it is soluble in oils and fats but it is insoluble in water. It is supplied in powder and flake form, and considered to be an additive permitted for general use (food, cosmetics and pharmaceuticals). The acid value of this lipid is max. 3 mg KOH/g, saponification value is between 160-180 mg KOH/g and the iodine value is max 3 g I_2/100 [149].

2.1.1.9 Precifac® ATO

It is a market product from Gattefossé GmbH (Weil am Rhein, Germany). It is a spray dried cetyl palmitate. DSC analysis showed that precifac ATO has a melting point between 51.9°C and 55.9°C. It is practically insoluble in water and ethanol. It is usually used to increase the consistency of the ointments, creams and liquid emulsions [144].

2.1.1.10 Syncrowax ERLC

It is a synthesized wax marketed by Croda GmbH (Nettetal Kaldenkirchen, Germany). It is an ethylene glycol ester of a long chain (C18-C36) fatty acid wax particularly suitable for emulsions and liquid polishes. It also improves emulsion stability and structure. DSC analysis showed that syncrowax ERLC has a melting point between 60°C and 68°C [150].

2.1.2 Liquid lipids (oils)

The oils used in this work are well tolerated, of GRAS status and accepted for human use.

2.1.2.1 Cetiol V

It is a market product from Gognis Deutschland GmbH (Düsseldorf, Germany). A clear, slightly yellowish polar oil with characteristic odor. The chemical name is decyl oleate, which is the ester of decyl alcohol and oleic acid. Decyl oleate is used as an emollient in body lotions and skin preparations [145].

2.1.2.2 Miglyol® 812

It is a liquid triacylglycerol obtained from Caelo GmbH (Hilden, Germany). This oil consists of medium chain triacylglycerols (C8-C10) (caprilic/capric triglycerides), having a density between 0.945 and 0.955 g/cm^3. It is used as skin oil and as dissolution medium for many substances. It is virtually colorless and of neutral odor and taste. It is soluble in Hexane, toluene, diethyl ether, ethyl acetate, acetone, isopropanol, and ethanol 96%. It is miscible in all ratios with paraffin hydrocarbons and natural oils. The acid value is 0.1 mg KOH/g, and the saponification value is between 325-345 mg KOH/g [149].

2.1.3 Emulsifying agents

The International Union of Pure and Applied Chemistry (IUPAC) defines the properties of an emulsifying agent as a surfactant, which is positively adsorbed at interfaces and lowers the interfacial tension [151]. When a surfactant is present in small amounts, it facilitates the formation of an emulsion or enhances its colloidal stability by decreasing either or both of the

rates of coalescence or aggregation. Surfactants have amphiphilic structures and are able to form micelles. Some polymers can function in the same manner, if they have a sufficient surface activity.

2.1.3.1 Miranol ultra 32

Is a market product of Henkel (Düsseldorf, Germany). The INCI name is sodium cocoampho-acetate. A pure mild amphoteric surfactant with an isoelectric point at pH=7. In a pH between 2 and 13 the substance is stable [152]. It has a small hydrophilic head and a short fatty acid chain (C6-C16), that makes the surfactant molecules very fast in covering the interfaces between the aqueous and oily phases [153]. The HLB value is about 34 [130].

2.1.3.2 PlantaCare® 2000 UP

Is a market product of Cognis (Düsseldorf, Germany). The INCI name is decyl glucoside. It is a cloudy, viscous, aqueous solution of a C8-C16 fatty alcohol polyglycoside. The turbidity of the product is because of a combination of its magnesium oxide content (max. 500 ppm magnesium) and the pH value at which it is supplied. This turbidity has no negative effects on the products properties and disappears if the pH value is adjusted to below 7. PlantaCare 2000 UP is a nonionic surfactant with excellent foaming capacity and good dermatological compatibility. Therefore, it is used as a base surfactant or a co-surfactant in cosmetic products of cleansing preparations. This surfactant has a high pH value and for this reason the product contains no preservatives (suffix UP = unpreserved) [154].

2.1.3.3 Tego®Care 450

Is a market product of the company Goldschmidt AG (Essen, Germany). Chemically it is polyglyceryl-3 methyl-glucose distearate. Tego®Care 450 is a non-ionic and a polyethylene glycol (PEG) free emulsifier based on natural renewable raw materials. It is suitable for the formulation of o/w creams and lotions. The HLB of this emulsifier is approximately 12 and it exists as solid pellets with ivory color [155].

2.1.3.4 Tween™80

The Tween™ series of surfactants are polyoxyethylene (POE) derivatives of the Span™ series products produced by Uniqema (Everberg, Belgium). Tween surfactants are hydrophilic, generally soluble or dispersible in water, and soluble to varying degrees in organic liquids. They are used for o/w emulsification, dispersion or solubilization of oils and wetting. These products are widely used in pharmaceutical and cosmetic products as well as in detergents and

food industry. Tween 80 is a POE-(20)-sorbitan monooleate, the HLB is 15. It is a yellow liquid with a viscosity of 400 mPas at 25°C [156].

2.1.3.5 Maquat® SC 18

Is a market product of Mason Chemical Company (Illinois, USA). It is characterized as a stearyl dimethylbenzyl ammonium chloride available in either paste or flake form. Maquat SC18 is a high quality, low color cationic surfactant used in personal care formulations, textiles and paper [157].

2.1.3.6 Maquat® BTMC-85%

Is a market product of Mason Chemical Company (Illinois, USA). It is an 85% active behenyl trimethyl ammonium chloride in a convenient pastille form. The antistatic properties of the behenyl moiety, BTMC-85% is suitable for use in wide range of products including personal care, textiles and paper. Maquat BTMC-85% has wetting, cleaning, conditioning, softening, suspending and emulsifying properties [158].

2.1.4 Coenzyme Q 10 (Q10)

Coenzyme Q 10 is also known as ubiquinone or ubidecarenone. It is a benzoquinone where Q refers to the quinone and the 10 refers to the isoprenyl chemical subunits.

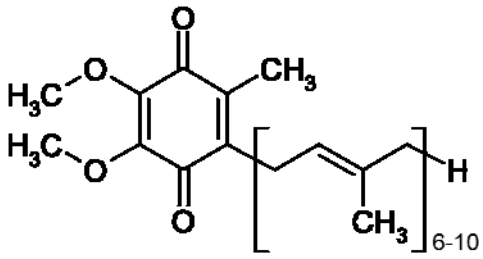

Figure 2-1: The chemical structure of coenzyme Q 10.

The vitamin-like substance is naturally present in all human cells and responsible for the production of the required cell energy. In each human cell food energy is converted into energy in the mitochondria with the aid of Q10. 95% of the energy requirements (ATP) in the body are converted with the aid of Q10. Therefore, the organs with the highest energy requirements such as heart, lungs, and liver have the highest Q10 concentrations [159]. Coenzyme Q10 is also used as a dietary supplement because of its ability to transfer electrons and hence being an antioxidant. Young people are able to make Q10 from the lower-numbered ubiquinones, while sick and elderly people may not be able to make enough.

Therefore, Q10 becomes a vitamin later in life and in illness. Q10 was prescribed for mitochondrial disorders, migraine headaches, cancers, cardiovascular disorders, brain health and neurodegenerative diseases. In cosmetics Q10 is used as antioxidant in skin care products [160]. Some studies suggest that the combination of carotenoids and Q10 in topical skin care products may provide enhanced protection from inflammation and premature aging caused by sun exposure [161].

Crystalline Q10 is a yellowish powder that has a melting point around 48 ºC, and transfers to the amorphous state after melting. Due to the isoprenyl side chain Q10 is very lipophilic. It is soluble in oils, lipids and organic solvents [162]. Q10 is sensitive to light and heat and will decompose when it is exposed to these conditions [163, 164]. Oxidation of Q10 might also occur in personal care products [117]. Q10 can be synthesised chemically or by biotechnological means. The product produced biotechnologically is more expensive.

The Q10 used in this work was purchased from BIK Internationaler Handel GmbH (Horgen, Switzerland).

2.1.5 Black currant seed oil (BCO)

The Black currant (*Ribes nigrum*) is a species of Ribes berry, native to central and northern Europe and Asia. Other names for Black currant are Schwarze Johannisbeer and Gichtbeer [165].

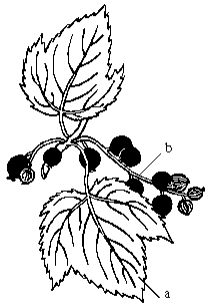

Figure 2-2: Black currant (*Ribes nigrum*) leaves and fruits.

Black currant seed oil is a rich source of omega 6 (ω−6) fatty acids (gamma linolenic acid (GLA)), along with other important polyunsaturated fatty acids (Table 2-1). Fatty acids are involved in many body functions, such as maintaining body temperature, insulating nerves, cushioning and protecting tissues and creating energy. It is also used in the treatment of arthritis and to stimulate the immune system. These essential fatty acids are precursors of prostaglandins, which must be present for functions involved with dilating blood vessels,

regulating arterial pressure, metabolizing cholesterol, activating T-lymphocytes, protecting against platelet aggregation, controlling abnormal cell proliferation, and other functions. BCO is an alternative acne treatment. It boosts the skin moisture retention ability, making the skin soft and increases the skin resistance to environmental factors [165, 166]. Due to the high content of the unsaturated fatty acids in the BCO it is susceptible to oxidation during storage [167]. BCO was purchased from Henry Lamotte GmbH (Bremen, Germany).

Table 2-1: Approximate fatty acids content in black currant seed oil [168].

Fatty acid	Carbon chain length	Degree of unsaturation	% (w/w)
Palmitic acid	C16	0	6.0
Stearic acid	C18	0	1.5
Oleic acid	C18	1, n=9	11.0
Linoleic acid	C18	2, n=6	46.0
alpha-Linolenic acid	C18	3, n=3	14.0
gamma-Linolenic acid	C18	3, n=6	14.0
Stearidonic acid	C18	4, n=3	3.0
others			4.5

2.1.6 Retinol

Retinol (Afaxin) is a fat soluble, unsaturated isoprenoid. It is the animal form of Vitamin A, which is important in vision, veins epithelial cells differentiation and bone growth. It belongs to the family of chemical compounds known as retinoids [169].

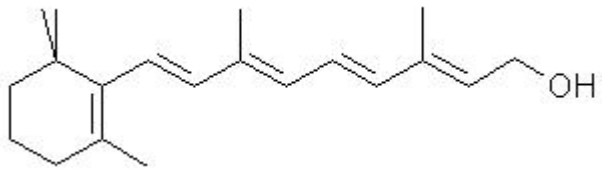

Figure 2-3: The chemical structure of retinol.

Retinol is ingested in a precursor form, the animal sources like eggs and liver containing retinyl esters, while plants like carrots and spinach contain pro-vitamin A carotenoids. Hydrolysis of retinyl esters gives retinol while pro-vitamin A carotenoids can be cleaved to produce retinal [170]. Retinal, also known as retinaldehyde, can be reversibly reduced to produce retinol or it can be irreversibly oxidized to produce retinoic acid. Retinol is an active ingredient in many cosmetic skin care products. It is active against ageing and skin damage

caused by UV radiation. Retinol accelerates mitosis, increases enzyme activity and normalizes keratinisation. Hence, it enhances the barriers function, increases the water uptake and skin elasticity [171, 172]. Because of the five conjugated double bonds, retinol is not stable and susceptible to oxidation and isomerization [173].

In this work two market products of retinol were used. Retinol 15 D, which is a 15% retinol solution in medium chain triglycerides (caprylic/capric triglycerides) produced by the company BASF AG (Ludwigshafen, Germany) and Retinol 50 C, which is a 50% retinol solution in polysorbate 20 produced by the same company.

2.1.7 UV blockers

Also know as sunscreens, sun blockers or UV blockers. These materials help to protect the skin from the ultraviolet radiation of the sun and reduce sunburn and other skin damages, with the goal of lowering the risk of skin cancer. Sunscreen products contain either an organic chemical compound that absorbs UV light (e.g. avobenzone) or an opaque material that reflects light, which is also called inorganic or physical UV blocker (e.g. titanium dioxide), or a combination of both [174].

2.1.7.1 Avobenzone (BMBM)

It is also known as Parsol 1789 or butyl methoxydibenzoylmethane (BMBM), molecular formula $C_{20}H_{22}O_3$. Parsol 1789 is a market product of Roche Vitamins (Basel, Switzerland).

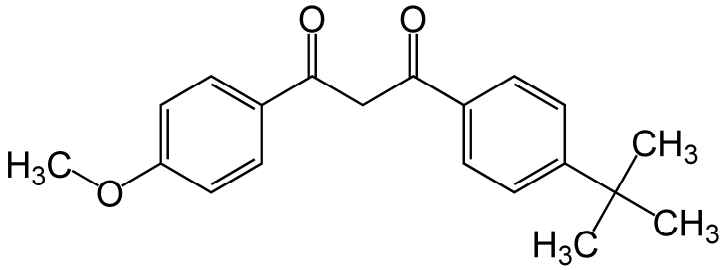

Figure 2-4: The chemical structure of Avobenzone (BMBM).

It is a compound used in sunscreens to absorb the full spectrum of the UV-A radiation (maximum absorption at 357 nm). Its ability to absorb ultraviolet light over a wider range of wavelengths better than many organic sunscreen agents has led to its use in many commercial preparations marketed as "broad spectrum" sunscreens. It is a lipophilic compound and has a melting point between 81-86ºC. It is a yellowish white powder with faint aromatic smell. It has been approved by FDA in 1988 to be used in sun protection products up to 3%.

Avobenzone has been shown to degrade significantly in light, resulting in less protection over time [175-178].

2.1.7.2 Titanium Dioxide (TiO_2)

Titanium dioxide is the naturally occurring oxide of Titanium, the chemical formula is TiO_2. It is used in many applications like paints, sunscreens and food coloring. Titanium dioxide is one of the most widely used pigments because of its brightness and very high refractive index (n=2.7). In personal care products it protects against the whole range of UV radiation through reflection, scattering and absorption [179]. TiO_2 is considered to be save but the penetration of the ultrafine TiO_2 particles are till now questionable [180, 181]. TiO_2 might decrease the activity of the organic UV blockers when they are present in one formulation by facilitating photodegradation [182].

In this work different nanonized TiO_2 (UV-TITAN) from the company Kemira (Finland) were used (Table 2-2).

Table 2-2: The nanosized TiO_2 pigments.

UV-TITAN	Surface coat	Specific surface area (m^2/g)	Size (nm)	Hydrophobicity
M160	alumina, stearic acid	70	17	hydrophobic
M170	alumina, silicone	80	14	very hydrophobic
M195	Silica, silicon	50	14	very hydrophobic

2.1.8 Perfumes

CA:

It is the natural green apple fragrance provided by the company PharmaSol (Berlin, Germany).

CT:

It is the natural lemon fragrance provided by the company Quest PharmaSol (Berlin, Germany).

Kenzo:

It is a mixture of volatile oils provided by the company Kimex (Seoul, South Korea).

2.1.9 β-carotene

The term carotene is used for several related substances having the formula $C_{40}H_{56}$. Carotene is an orange photosynthetic pigment important for photosynthesis in plants. It is responsible

for the orange color of the carrot and many other fruits and vegetables. It contributes to photosynthesis by transmitting the light energy it absorbs to chlorophyll. Chemically, carotene is a terpene, synthesized biochemically from eight isoprene units [183]. As hydrocarbons, carotenes are fat-soluble and insoluble in water. β-carotene is composed of two retinyl groups, and is broken down in the mucosa of the small intestine to retinal, a form of vitamin A. Carotene can be stored in the liver and converted to vitamin A as needed, thus making it a provitamin.

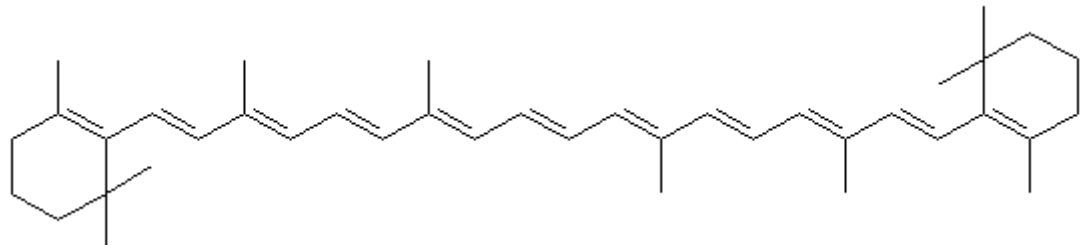

Figure 2-5: The chemical structure of β-carotene.

The β-carotene used in this work was a 10% (w/w) β-carotene solution dissolved in sunflower oil, Lucarotin 10 Sun, which is a product of BASF AG (Ludwigshafen, Germany). β-carotene loses its yellowish color upon exposure to UV radiation. β-carotene is easily degraded by photo-irradiation, this is because of the hydroxylation of carotenes and esterification of xanthophylls [184, 185]. Exposure to UV radiation causes decomposition of the β-carotene chromophore and hence, bleaching occurs i.e. loss of color due to breaking of the chromophore [183, 186, 187].

2.1.10 Water

The water used in all experiments was purified water by reverse osmosis and was obtained from a Milli Q Plus, Millipore system (Schwalbach, Germany). The water had an electrical conductivity of 0.5-1.5 μS/cm.

2.2 Methods

2.2.1 Lipid screening

Prior to the production of an NLC formulation a lipid screening should be performed to determine the most suitable lipid for the active ingredient to be incorporated in the NLC. This is performed by dissolving increasing amounts of the active ingredient in various melted solid lipids and determining the maximum amount of the active that could be dissolved in each lipid. After dissolution, the lipid/active mixtures are cooled down to room temperature for solidification. The solid mixtures are visually observed for the presence or absence of crystalline active (when this ingredient is a solid substance at room temperature). If the active ingredient is oil, the miscibility of the two materials (melted lipid and oil) is observed. After cooling down the mixture to room temperature the lipid will solidify again and the incorporation of the oil in the solid lipid matrix is investigated. This can be performed by smearing a piece of the solid mixture on a filter paper and observing if there are any oil spots on the filter paper. Calorimetric analysis can be performed on the solid solutions obtained using differential scanning calorimeter (DSC). These analyses will detect any presence of crystalline active (i.e. undissolved active) and also can show if there is an unincorporated part of active ingredient in the lipid matrix (i.e. oil).

2.2.2 Production of the nanoparticles

2.2.2.1 High pressure homogenisation

Homogenization is a fluid mechanical process that involves the subdivision of droplets or particles into micro- or nanosize to create a stable emulsion or dispersion. Homogenization is a very common processing step in the food and dairy industries. It improves product stability, shelf life, digestion and taste [188, 189]. Homogenization can also significantly reduce the amount of additives (e.g. stabilizer) needed in a product. In the cosmetic industry homogenization is essential for the quality and stability of the products and their texture (skin feeling). The bioavailability of the pharmaceutical products can be enhanced by homogenization, also the tolerance of some drugs can be improved [190-192]. Moreover, high pressure homogenization has some advantages over other size-reducing processes (e.g. ball milling). It is considered to be a superior process from an economical and product quality prospects. The contamination of the products caused by the personnel or coming from the

machine (machine parts wearing) is reduced [193]. Also the exposure to thermal stress and microbiological contamination is clearly less due to the shorter production times.

There are two types of high pressure homogenizers available on the market, the jet-stream homogenizers e.g. Mircofluidizer (Microfluidics, Newton, USA), and the piston-gap homogenizers e.g. Micron LAB 40 (APV Deutschland GmbH, Unna, Germany).

2.2.2.2 Operation principle of piston-gap high pressure homogenizer

The process occurs in a special homogenizing valve, the design of which is the heart of the homogenizing equipment. Figure 2-6 and Figure 2-7 help to understand its mode of operation and to explain the homogenization process in a piston-gap homogenizer.

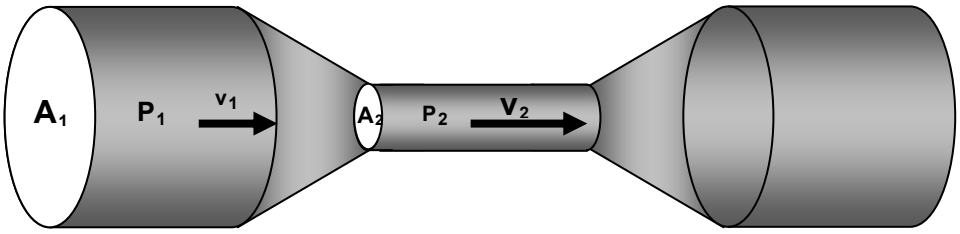

Figure 2-6: A 3-dimensional drawing showing the principle of the high pressure homogenization. The cross-section narrowing of the tubes ($A_2<A_1$) results in a decrease in the static pressure ($P_2<P_1$) and an increase in the streaming velocity ($v_2>v_1$).

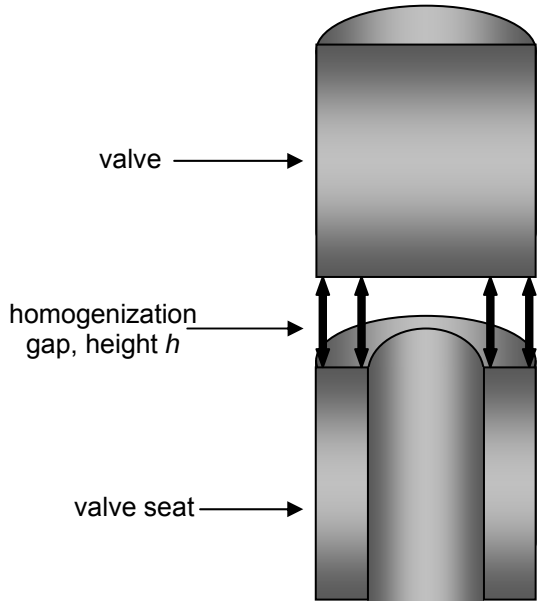

Figure 2-7: The geometry of the homogenization valve (valve and valve seat) and the resulted homogenization gap between them.

The fluid passes through a small gap in the homogenizing valve. This creates conditions of high turbulence, cavitation and shear, combined with compression, acceleration, pressure drop and impact. This causes particles disintegration or droplets fine-dispersion throughout the

dispersion medium. After homogenization, the particles (or droplets) are of a uniform size, typically from 0.1 to 5 micron, depending on the homogenized material properties, the operating pressure and the number of homogenization cycles. The actual properties of the product vary with pressure and product type in a complex relationship. In general, higher processing pressure produces smaller particles, down to a certain limit of micronization or nanonization [191, 194, 195].

Under the consideration that the fluid to be homogenized has a laminar streaming of an ideal liquid, and at continuous conditions, the operation principle can be mathematically described by the *Bernoulli equation* which shows that the sum of static pressure in the flow plus the dynamic pressure is equal to a constant throughout the flow (total pressure of the flow).
From the continuity equation:

$$A_1 v_1 = A_2 v_2$$

where A is the cross-section area of the tubes and v is the streaming velocity.
By applying the *Bernoulli equation*:

$$P_1 + \frac{\rho v_1^{\,2}}{2} = P_2 + \frac{\rho v_2^{\,2}}{2} = K$$

where: P_1 and P_2 are the static pressure, ρ is the density, v_1 and v_2 are the streaming velocity and K is the constant pressure of the flow.

Explaining the homogenization operation in more details, during the process the suspension (or the emulsion) is contained in a compartment and it will be pushed through the narrow homogenisation gap (around 3 μm). This will dramatically increase the streaming velocity and therefore the dynamic pressure. Simultaneously, the static pressure decreases and falls below the vapour pressure of the dispersion medium (normally water) at room temperature. This makes the water boil and gas bubbles will form, which implode when the liquid leaves the gap and the pressure suffers an abrupt decrease (cavitation). The implosion of the gas bubbles cause shock waves which originate the diminution of particles or droplets. It is understood that the formation of bubbles and the turbulences resulting of them (i.e. shear forces) are a decisive factor for the reduction in particle size [196].

Form what previously mentioned it can be concluded that many factors affect the homogenization process in a piston-gap homogenizer at a given homogenization pressure. The geometry of the homogenization valve plays a crucial role in the homogenization process as it determines the streaming velocity of the product to be homogenized during the homogenization process (Figure 2-7).

The homogenization gap size is adjusted automatically according to the required homogenization pressure. If the product to be homogenized is of a high viscosity, the required pressure is reached with a larger homogenization gap size. When the gape size is larger the streaming velocity in the gape becomes lower and hence the homogenization efficacy decreases. In other words, preparations with higher viscosity are harder to be homogenized.

The influence of the temperature on the homogenization efficacy can also be attributed to the viscosity change. Usually the viscosity of the dispersion medium decreases when the temperature increases. Also, at higher temperatures, the dispersion medium (water) will reach the boiling point at lower pressure and hence, the consequent cavitation occurs easier and therefore, the homogenization efficacy is higher.

2.2.2.3 Preparation of nanoemulsions

Nanoemulsions are o/w emulsions which consist of a lipid phase (oil), a surfactant and an aqueous phase (water). These nanoemulsions can be prepared at RT, but to maintain the same production conditions for all preparations (as for NLC) they were prepared at higher temperatures (80-90ºC). The lipid (oil) phase and the aqueous surfactant solution were heated up to about 80ºC, and the active substance (if any) was dissolved in the hot oil phase which is subsequently dispersed by a high speed stirrer at 8000 rpm for 20-30 sec in the hot aqueous surfactant solution. The obtained pre-emulsion is homogenized in a high pressure homogenizer applying a pressure of 800 bar and two homogenization cycles yielding a hot o/w nanoemulsion. The obtained product was filled in silanized glass vials, which were immediately sealed. A thermostated water bath adjusted to 15ºC has been used as cooling system to control the rate of cooling of the obtained product.

2.2.2.4 Preparation of aqueous NLC dispersions

Lipid nanoparticles with solid particle matrix are derived from o/w emulsions by replacing the liquid lipid (oil) by a solid lipid at room temperature. The first generation of solid lipid nanoparticles (SLN) was developed at the beginning of the nineties [45]. They were produced from a solid lipid only. In the second generation technology the nanostructured lipid carriers (NLC) are produced by using a blend of solid and liquid lipids, this blend is solid at room temperature [46]. The production process is identical for both particles SLN and NLC. The solid lipid or lipid blend is melted at 5-10ºC above the melting point of the solid lipid, the active substance is dissolved in the melted lipid phase, which is subsequently dispersed by a high speed stirrer at 8000 rpm for 20-30 sec in the aqueous surfactant solution previously heated up to the same temperature. The obtained pre-emulsion is homogenized in a high pressure homogenizer applying a pressure of 800 bar and two homogenization cycles (unless otherwise mentioned) yielding a hot o/w nanoemulsion. The obtained product was filled immediately in silanized glass vials and the vials were sealed properly. The obtained samples were cooled down to room temperature in a thermostated water bath adjusted to 15ºC. After cooling down the emulsion droplets crystallize forming lipid nanoparticles with solid particle matrix, depending on the lipids used either SLN or NLC are obtained [196].

2.2.2.5 Machines used in NLC production

I. Ultra-Turrax T25

The machine is produced by the company Janke & Kunkel GmbH (Staufen, Germany). It is a high-speed stirrer with different sizes of homogenization heads. Head size B was used to prepare the hot pre-emulsions.

II. Micron LAB 40

It is the laboratory scale homogenizer produced by the company APV Deutschland GmbH (Unna, Germany). In the standard design of the machine the homogenization operation is performed discontinuously with a maximum batch size of 40 ml. The pre-emulsion or the dispersion will be pushed out of the sample container by a plunger through the homogenization gap to the product container. This process is called "homogenization cycle". To make many homogenization cycles the sample must be transferred again into the sample container and the same process must be performed again. Although this procedure might be a disadvantage (tedious work) but the fact that the product can be very well controlled (number of cycles for each partition) makes the machine optimal for product development and study. The machine has also good homogenization efficacy and reproducibility.

2.2.3 Characterization of particles

Several techniques were employed in this work to determine the particle size of the preparations. These techniques were direct measurements (microscopy) and indirect measurements (laser diffractometry and photon correlation spectroscopy).

2.2.3.1 Imaging analysis

The major advantage that microscopic techniques have over most of the other methods used for size analysis is that the particle size itself is measured, rather than some property which is dependent on particle size. In other words, microscopic technique is a direct measurement and do not depend on any other factors that might influence the measurements (e.g. temperature, refractive index, etc.). In this work both light and electron microscopy have been used.

2.2.3.1.1 Light microscopy

The size of a particle which can be detected by microscopy is limited by the diffraction of the light used to form the image. The resolution of a microscope is calculated approximately as the wavelength of the light divided by the numerical aperture of the microscope objective. All substances, which are transparent when they are examined by microscope that has crossed

polarizing filters, are either isotropic or anisotropic [197]. Amorphous substances, such as supercooled melts and non-crystalline solid organic compounds, or substances with cubic crystal lattices, are isotropic materials, having one refractive index. On the other hand, anisotropic materials have more than one refractive index and appear bright with brilliant colors (birefringence) against a black polarized background. The interference colors depend upon the thickness of the crystal and the differences are either uniaxial, having two refractive indices or biaxial, having three principal refractive indices. Most materials are biaxial corresponding to either, an orthorhombic, a monoclinic or a triclinic crystal system.

The light microscope used in this work was an Orthoplan Leitz (Wetzlar, Germany) and the magnifications used were 160x, 400x, 630x and 1000x (1000x with immersion oil). The microscope was attached to a camera CMEX 3200, Euromex (Arnhem, Netherlands). The use of polarized light enables the imaging of crystals if any. General overview of the particles prepared was obtained in terms of particle size and presence of aggregations or agglomerations as well as crystals formation (both solid lipids and loaded drug if existed). Light microscopy is an important procedure to know if the relatively larger particles detected by laser diffractometry (LD) technique are really particles or agglomerates of nanosized particles.

2.2.3.1.2 Scanning electron microscopy (SEM)

This technique was used to investigate the shape of the particles prepared and to assess the particle size of these particles. Aqueous NLC dispersions were applied and spread on a sample holder (thin carbon film). The samples were placed inside of the vacuum column of the microscope and the air was pumped out of the chamber. An electron gun placed at the top of the column emits a beam of high energy primary electrons. The beam of the electrons passes through the lenses which concentrates the electrons to a fine spot and scan across the specimen row by row. As the focused electron beam hits a spot on the sample, secondary electrons are emitted by the specimen through ionization. A detector counts these secondary electrons. The electrons are collected by a laterally placed collector and these signals are sent to an amplifier. The particles (NLC) have been observed with a scanning electron microscope S-4000, Hitachi High Technologies Europe GmbH (Krefeld, Germany) using secondary electron imaging at 5-20 kV. SEM studies have been performed together with Mr. Gernert at the Zentraleinrichtung Elektronenmikroskopie (ZELMI) at the Technische Universität Berlin. The samples were spread on carbon slides and left to dry for 30 min before placing them in the microscope chamber for analysis.

2.2.3.2 Energy dispersive X-ray spectroscopy (EDX)

EDX is an analytical technique used predominantly for the elemental analysis or chemical characterization of a sample. Being a type of spectroscopy, it relies on the investigation of a sample through interactions between the electromagnetic radiation and the matter, analyzing X-rays emitted by the matter in this particular case. Its characterization capability is mainly due to the fundamental principle that each element of the periodic table has a unique atomic structure. This allows the x-rays, which are characteristic of the atomic structure of the element, to be uniquely distinguished from each other. EDX systems are most commonly found on scanning electron microscopes. In this work the EDX system or the X-ray analyzer sam X (Saint Laurent du Var, France), which was installed on the scanning electron microscope S-4000, was used.

2.2.3.3 Laser Diffractometry (LD)

Laser diffractometry (LD) is a technique used for the determination of particle size in the range of 10 nm to 2000 μm [198]. It is based on the phenomenon that particles scatter light in all directions. The laser light is diffracted by the particle surface in a pattern depending on the particle size. Simply, the diffraction angle is small for a large particle, as its surface is less curved, while for a small particle, with a more curved surface, the diffraction angle is larger. Figure 2-8 shows the simplified principle of the operation of a laser diffractometer.

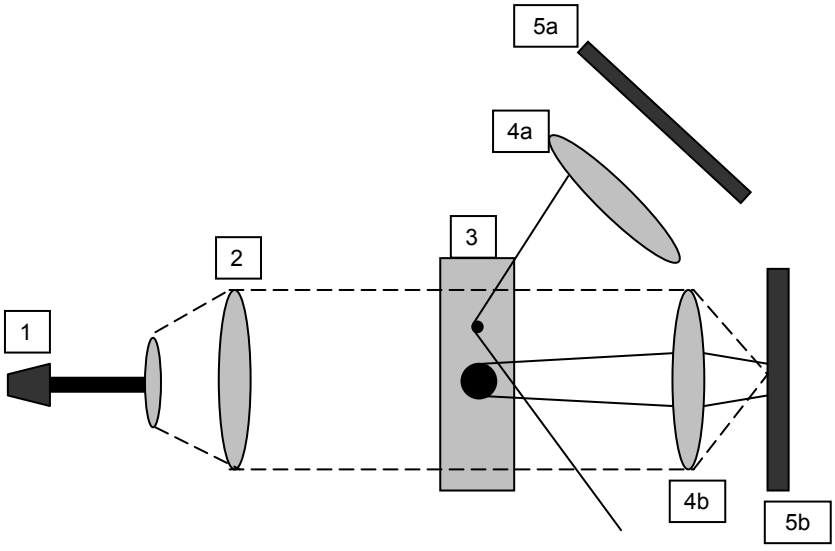

Figure 2-8: The laser diffractometer schematic assembly showing its operation principle. The diffraction angles caused by the particles are characteristic for each one. The diffraction angle is small for large particles and large for small particles (modified after [199]).
1- laser
2- lenses system
3- measuring cell with particles
4- Fourier lenses (a- high angle, b- low and middle angle)
5- detector (a- high angle, b- low and middle angle).

All LD instruments assume that the particles have spherical shapes. Moreover, the laser diffraction technique cannot distinguish between scattering by single particles and scattering by clusters of particles forming aggregates or agglomerates.

In this work the instrument Coulter® LS 230, Beckman-Coulter Electronics (Krefeld, Germany) was used. This instrument has a laser wavelength of 750 nm as a light source. An optical system conducts the laser beam towards the particles in the measuring cell (Figure 2-8), were it will reach the particles to be absorbed, refracted or diffracted. At a certain distance a Fourier lens will project the patterns of the moving particles in the measuring cell on the multi-element detector. The simultaneous presence of particles with different sizes leads to diffraction patterns, which are the superposition of the patterns specific for each size. This pattern can be mathematically resolved to yield a volume distribution of the particles.

Formerly, instruments used scattering angles smaller than 14°, which limited the application of these instruments to a lower minimal size of about 1 μm. The reason for this limitation is that smaller particles show most of their distinctive scattering at larger angles and the intensity of the scattered light is below the detection limits. Many new instruments (including the Coulter LS 230) measure at larger scattering angles, usually from 60 to 146 degrees. This will make it possible to measure small particles down to about 0.01 μm and bigger particles up to 2000 μm. This is based on the Polarization Intensity Differential Scattering technology (PIDS). This complements the detection system, which allows, with high resolution, the detection of particles below 1 μm. In PIDS technology, a light beam (of intensity I) with several wavelengths (from typically a tungsten-halogen lamp) is polarized in either vertical (V) or horizontal (H) directions passing the sample. The detected scattering intensities I_V and I_H at a given angle will be different. The difference between the I_V and the I_H is termed the PIDS signal. The scattered light is detected by detectors located at a wide angular range (60-146 degrees) [200, 201].

The volume distribution can be calculated applying the Fraunhofer theory or the Mie theory, depending on the characteristics of the sample. This means, for the data analysis of particles bigger than 4 μm, the Fraunhofer theory is applicable [202], while for particles smaller than 4 μm the Mie theory must be used for calculations. However, in contrast to the Fraunhofer theory, the Mie model takes into account the real and the imaginary refractive indices of the particles. The real refractive index corresponds to the refraction properties and the imaginary refractive index represents the absorption. A completely transparent material would have an imaginary refractive index of zero. Alternatively, a coloured material would have both a real refractive index (describing its refractive properties) and an imaginary refractive index

(describing its absorbing properties). Both of these indices influence the light scattering. Unfortunately, data on the complex refractive index of many substances is difficult to find in the literature, since it has only been investigated in detail for a small number of well characterized materials [199]. Concerning lipid nanoparticles, the real part was considered to be 1.456 and the imaginary part was 0.01 [203].

LD data were evaluated using the volume distribution diameters d50%, d90%, d95% and d99%. For example, a diameter 95% (d95%) value of 1 μm indicates that 95% of the particles possess a diameter below 1 μm. Each sample was measured three times consecutively.

2.2.3.4 Photon Correlation Spectroscopy (PCS)

Photon correlation spectroscopy (PCS) is a technique used to determine the mean particle size diameter (mean PCS diameter) and the width of the particle size distribution expressed as polydispersity index (PI) [199, 204-206]. The measurement using PCS is based on the light scattering phenomena in which the statistical intensity fluctuations of the scattered light from the particles in the measuring cell are measured. These fluctuations are due to the random movement of the particles in the dispersion medium because of the Brownian motion of the dispersion medium molecules (e.g. water). The measuring range of PCS is approximately from 3 nm to approximately 3 μm.

Usually a PCS device consists of a laser light which is focused to illuminate a small volume of the sample, which is a dilute suspension of particles. The light scattered from these particles is collected again by a lens and its intensity is measured by a photomultiplier. The diffusion rate of the particles depends on their size (at a known fluid viscosity and temperature). Hence, the size of these particles can be calculated from the rate of fluctuation of the scattered light intensity. The lower particle size limit for a measurement is determined by the scattering intensity and the experimental noise. When the suspended particles are small, they diffuse relatively fast, and the fluctuations in the scattered light are rapid. On the other hand, if the particles are large, they move slowly, and the fluctuations in the scattered light are slow. The detected intensity signals are used to calculate the auto-correlation function G(τ), from the decay of this correlation function the diffusion coefficient *D* of the particles is obtained. Once the diffusion coefficient is known, the equivalent diffusional spherical diameter can be calculated applying the *Stokes-Einstein equation*, which relates the diffusion coefficient *D* of a spherical particle to its diameter *r*:

$$r = \frac{kT}{3\pi\rho D}$$

where ρ is the viscosity of the surrounding medium, k is Boltzmann's constant, T is the absolute temperature.

The apparatus consists of a laser, a temperature controlled sample cell and a photomultiplier for the detection of the scattered light at a certain angle (e.g. 90º or 173º) [204]. The photomultiplier (or photodiode in the new apparatus) signal is transferred to a correlator for

calculation of the G(τ). This G(τ) is after that sent to a microprocessor for the calculation of *D* and the correlated mean particle size.

As it was previously mentioned, small particles diffuse faster than large ones causing a stronger fluctuation in the scattering signal and a more rapid decaying G(τ). For a monodisperse particle population G(τ) is a single exponential, but if more than one size of particles is present the function is polyexponential. Deviation from a single exponential is used to calculate the PI, which is a measure of the width of the size distribution. The PI is 0.0 when a monodisperse particles population is measured. PI values of around 0.10-0.20 indicate a relatively narrow distribution, values of 0.5 and higher are obtained in case of very broad distributions.

In this work, a Zetasizer Nano ZS, Malvern Instruments (Malvern, UK) was used to measure the particles produced. The instrument was equipped with a laser beam (λ=633 nm). The scattered light detector is positioned at an angle of 173° (Figure 2-9). This detection angle is known as the backscatter detection and it has the advantages of improved sensitivity and possibility of measuring a wide range of sample concentrations [207]. The measuring range of this device is between 0.6 nm to 6 μm. Samples were diluted with bidistilled water to an appropriate concentration. The average particle size diameter and PI are given from 30 runs.

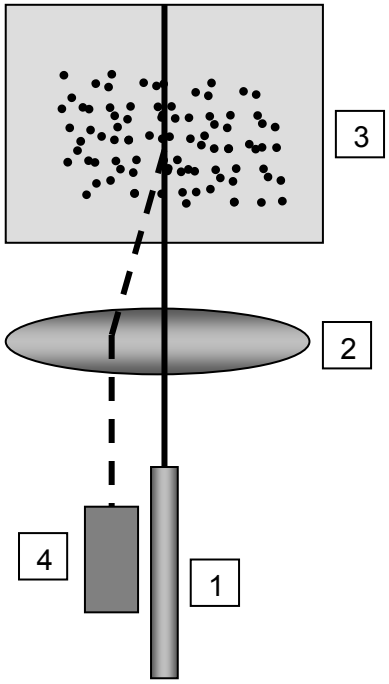

Figure 2-9: Schematic assembly of the Zetasizer Nano ZS device (modified after [207]).
1- laser
2- focusing lens
3- cuvette
4- detector

2.2.3.5 Zeta potential (ZP)

Zeta potential is the electric potential of a particle in a suspension. It is a parameter which is very useful for the assessment of the physical stability of colloidal dispersions [208-211]. In suspensions the surfaces of particles develop a charge due to ionization of surface groups or adsorption of ions. This charge depends on both the surface chemistry of the particles and the media around these particles. The surface charge generates a potential around the particle, which is at the highest near the surface and decays with distance into the medium (Figure 2-10). When the particle is placed in an electric field, it will move with a characteristic velocity *v*. The velocity of the particle per unit electric field strength is called the electrophoretic mobility, which is expressed in micrometers per second per volt per centimeter (μm/s)/(V/cm). The particle velocity *v* can be then expressed in relation to the electrical field strength *E* as electrophoretic mobility μ using the following equation:

$$\mu = \frac{v}{E}$$

As the particle moves in the medium due to the electric field it carries an ionic environment with it, which extends a small distance into the solvent. The spherical surface separating the moving particle, ions and solvent from the stationary surroundings is called the surface of hydrodynamic shear. The electrophoretic mobility is determined by the potential at this surface, which is the zeta potential (ζ). The zeta potential can be determined from the electrophoretic mobility using the *Helmholtz-Smoluchowski equation*, which is applied to large particles in a diluted electrolytes solution:

$$\xi = \frac{v}{\eta \varepsilon E}$$

where η is the viscosity of the dispersion medium and ε the permittivity of the environment (the dielectric constant).

In an aqueous medium of low electrolytes concentration the potential does not change rapidly with distance into the solvent. Therefore, the zeta potential is usually equated with the potential at the stern layer (the Stern Potential). The zeta potential is proportional to the

Nernst potential of the particle surface. For this reason, it is used to characterize the surface charge of the particles.

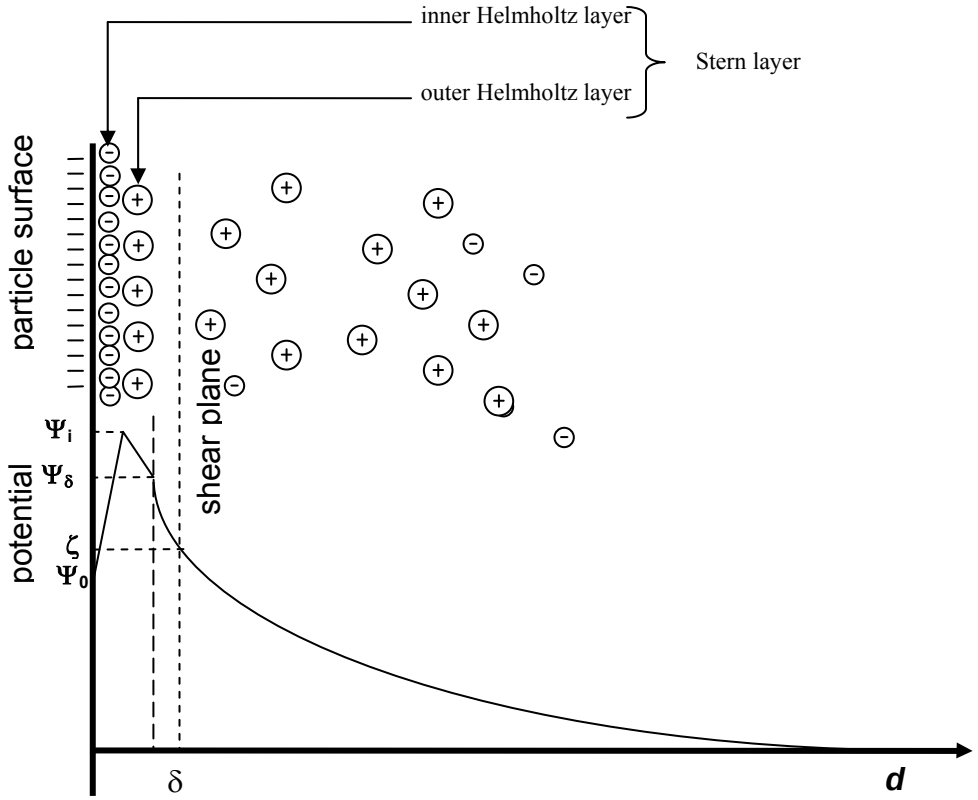

Figure 2-10: Schematic representation of the electric double layer model. Ψ0 is the Nernst potential, Ψi is the potential of inner Helmholtz layer, Ψδ is the Stern potential, δ is the thickness of the diffuse layer, ζ is the zeta potential at the surface of shear and *d* is the distance from the particle surface (modified after [204]).

The adsorbed monolayer of the ions at the surface of the particles consists of fixed, dehydrated and in most cases negatively charged ions (inner Helmholtz layer). These negative ions increase the surface potential (Nernst potential, Ψ_0) to the potential of the inner Helmholtz layer (Ψ_i). The second monolayer (outer Helmholtz layer) consists of fixed but hydrated positive ions reducing the potential to the potential of the Stern plane (Ψ_δ). Moving out to the dispersion medium through the diffuse layer the potential drops towards zero. During the movement of the particle a part of the diffuse layer will be sheared off to reveal a potential at the shear plane. This potential is called the zeta potential (ζ or ZP) and it is an indirect measurement of the surface charge because its magnitude depends on the Nernst potential.

The zeta potential can be measured by determining the velocity of the particles in an electrical field (electrophoresis measurement) [211].

The zeta potential measurements were performed using a Malvern Zetasizer Nano ZS, Malvern Instruments (Malvern, UK). Adjusting the conductivity of the distilled water used for diluting the samples avoids the fluctuations of the zeta potential due to variations in conductivity. The samples were either diluted with bidistilled water adjusted to a conductivity of 50 μS/cm using a 0.9% (w/v) NaCl solution or with a solution of the surfactant which was used in the formulation (having the same concentration as in the formulation). The pH was between 6.0 and 7.0. The average of the zeta potential is given from 30 runs.

2.2.4 Thermal analysis

As the International Confederation of Thermal Analysis and Calorimetry (ICTAC) defines the thermal analysis, it is "a group of techniques in which a physical property of a substance is measured as a function of temperature whilst the substance is subjected to a controlled temperature program". In this work differential scanning calorimetry (DSC) analysis was employed to characterize the particles which were produced.

2.2.4.1 Differential scanning calorimetry (DSC) analysis

DSC is usually used to get information about both the physical and the energetic properties of a compound or formulation. DSC measures the heat loss or gain as a result of physical or chemical changes within a sample as a function of the temperature. There are 2 types of DSC instruments, the power compensate DSC and the heat-flux DSC [212].

The power compensate DSC consists of 2 separate ovens while the heat-flux DSC consists of one oven that heat up both the reference and the sample pans (Figure 2-11). Heat is transferred through the disc (where the sample and the reference pans are placed) and through the sample pan to the contained sample and reference. The differential heat flow is monitored, as well as the sample temperature. Software linearization of the cell calibration is used to maintain calorimetric sensitivity. The cell has a volume of 2 ml and can be used with various inert atmospheres, as well as oxidizing and reducing atmospheres. Different sample pans (hermetic, open or sealed) allow sample volumes of 0.04 ml to 0.1 ml, which can be up to 100 mg depending on sample density.

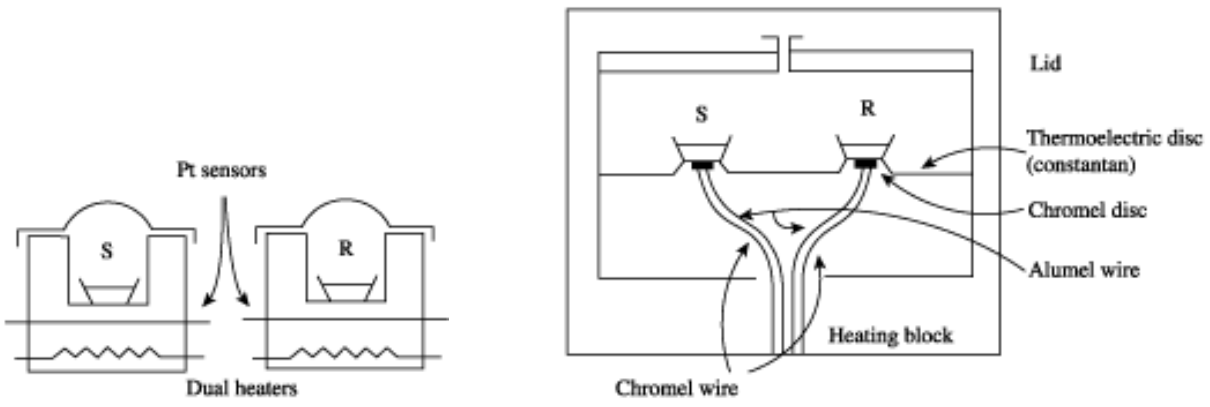

Figure 2-11: The 2 DSC types, the power compensate DSC (left) and the heat-flux DSC (right) [213].

Examples of endothermic (heat-absorbing) processes are fusion (melting), boiling, sublimation, vaporization, desolvation and solid-solid transitions. An important exothermic, (energy is liberated) process is crystallization. Qualitative measurements of these processes have many applications, such as materials identification, study of purity, polymorphism, solvation, degradation quantitative and qualitative analysis, aging, glass transition temperature and compatibility of substances.

DSC analysis has been used to determine the state and the degree of crystallinity of lipid dispersions, semi-solid systems, polymers and liposomes. It allows the study of the melting and crystallization behavior of crystalline material like lipid nanoparticles [214-217]. DSC analysis is useful to understand solid dispersions like solid solutions, simple eutectic mixtures or, as in the case of NLC, drug and lipid interactions and the mixtures of solid lipids and liquid lipids (oils). In general, a melting point depression is observed when transforming the bulk lipid to a particulate form in the nanometer range. This melting point depression is described by the *Gibbs-Thomson equation* which is derived from the *Kelvin equation*:

$$\ln\left(\frac{T}{T_0}\right) = -\frac{2\gamma V_s}{r\Delta H}$$

where T represents the melting point of the particle, and it is always smaller than the melting point of the bulk material T_0. The molar volume of the substance is characterized by V_s, r is the radius of the particle, ΔH is the molar melting enthalpy and γ is the interfacial energy at the solid lipid interface. For characterizing crystal forms, ΔH can be obtained from the area under the DSC curve of the melting thermogram.

Melting point depression might occur also when a second compound is dissolved in the lipid matrix, such as surfactant molecules, oils or active compounds (drugs). Therefore, drug-loaded NLC will show a melting point depression in case of a molecularly dispersed drug is present. In order to compare the crystallinity between the developed formulations a useful parameter is the recrystallization index (RI). RI is defined as the percentage of the lipid matrix that has recrystallized during storage time. The RI can be calculated according to the following equation [214].

$$RI(\%) = \frac{\Delta H_{NLC}}{\Delta H_{bulk} \times Concentration_{lipid}} \times 100$$

where ΔH_{NLC} is the melting enthalpy of 1 g NLC suspension, ΔH_{bulk} is the melting enthalpy of 1 g bulk lipid. ΔH is given in J/g and the concentration is given by the percentage of lipid phase.

The DSC measurements have been performed using a Mettler DSC 821e, Mettler Toledo (Gieβen, Germany). An accurately weighed amount of aqueous dispersion having approximately 1-2 mg of solid lipid has been placed in 40 µl aluminium pans and analyzed. DSC scans have been performed from 25ºC to 90ºC and back to 25ºC at a heating rate of 5 K/min (if not otherwise specified), using an empty pan as reference. Melting points (melting peak maximum) and melting enthalpies were determined if existed.

2.2.5 High performance liquid chromatography (HPLC) analysis

HPLC technique is a suitable and accurate way to determine the content of a substance and/or its chemical stability. In this work HPLC was used to determine the concentration and the chemical stability of coenzyme Q10 and retinol in their formulations.

The HPLC system used is from the company Kontron. It consists of an autosampler model 560, a pump system model 525 and a diode array detector model 540 Kontron Instruments (Groß-Zimmern, Germany). The system was linked to a KromaSystem 2000 v. 1.70 data acquisition and process system, which also controls the HPLC modules. Each formulation to be analyzed was weight twice and each weighed sample was measured in duplicate.

2.2.5.1 HPLC analysis method of Coenzyme Q10

In the literature there are many HPLC methods to determine the coenzyme Q10 [218, 219]. In this work a modified method by Dingler was used [117, 220]. The method specifications are listed below (Table 2-3).

Table 2-3: Coenzyme Q 10 HPLC analysis method specifications.

specification	details
column	Betasil C 8, 5µm, 125x4mm, with pre-column
mobile phase	acetonitrile:THF 90:10 v/v
flow	1.5 ml/min
injection	20µl
wave length	280nm
retention time	8 min at room temperature
measurement time	11 min at room temperature
calibration curve reggretion	$r^2 \geq 0.99$
calibration curve range	10 to 100 µg/mL
sample preparation	≅100 mg of the sample was dissolved in 10 ml acetone, placed for 5 min in ultrasound bath and centrifuged
samples number per formulation	n=2
sample repetetion	each sample was measured in duplicate

2.2.5.2 HPLC analysis method of Retinol

In this work the HPLC analysis method for the determination of the retinol concentration in NLC, nanoemulsions and creams was taken from the work performed by Jenning [130]. The method specifications are listed below (Table 2-4).

Table 2-4: Retinol HPLC analysis method specifications.

specification	details
column	Lichrospher 60 RP select B 5µm, 250x4mm, with pre-column
mobile phase	acetonitril/aqua bidest 80:20 v/v + 1 ml ortho-phosphoric acid/L
flow	1.0 ml/min
injection	20µl
wave length	325nm
retention time	4 min at room temperature
measurement time	10 min at room temperature
calibration curve reggretion	$r^2 \geq 0.99$
calibration curve range	10 to 100 µg/mL
Sample preparation	≅50 mg of the sample was dissolved in 10 ml acetone, placed for 5 min in ultrasound bath and centrifuged
samples number per formulation	n=2
sample repetetion	each sample was measured in duplicate

2.2.6 Oxidative stress test

This test was designed and performed to demonstrate the stabilizing effect of the NLC against peroxidation of black currant seed oil. 125g of both the NLC suspension and an o/w nanoemulsion as reference were kept in closed 1000ml dark glass flasks. The samples were exposed to permanent agitation at 20°C and 45°C over a period of 8 weeks. The flasks were filled with fresh oxygen every day after taking a sample for the analysis. The oxidation induced by the oxygen in the headspace of the flasks was determined daily by measuring the peroxide value of the black currant seed oil. The peroxide value was determined according to the Wheeler method. Each formulation was filled in 3 flasks, and each sample was assessed in triplicate (n=3).

2.2.7 Peroxide value according to Wheeler

According to DGF Standard Method C-VI 6a [221]:

Purpose and field of application

The peroxide value is a measurement for the amount of peroxide-bound oxygen, especially hydroperoxides, in a fat or oil. In addition to other analytical methods it helps to determine the degree of oxidation. This method can be applied to all oils, fats and fatty acids. It is worthy to mention that the results obtained from different methods are not comparable.

Definition

The peroxide value indicates the number of millimoles of oxygen contained in one kilogram of sample that oxidizes potassium iodide under the conditions provided by this method. The peroxide value is indicated as mmol O_2 per kilogram or milliequivalents (mEq) O_2 per kilogram.

Principle of the method

The sample is added to a mixture of glacial acetic acid and isooctane and then allowed to react with potassium iodide. The iodine released is determined by titration using sodium thiosulfate solution. End point is determined visually (iodometrically).

Reagents

Acetic acid (glacial), 96% w/w (R: 10-35; S: 2-23-36); isooctane, purest; glacial acetic acid/isooctane mixture, 60 ml / 40 ml v/v; potassium iodide; potassium iodide solution, saturated, freshly prepared; sodium thiosulfate standard solution, c = 0.01 mol/l (0.01 N); starch solution, approx. 1 g/100 ml, freshly prepared.

Equipment

250 ml Erlenmeyer, NS 29, with stopper; Metrohm titrator; 1 ml volumetric pipette (or dispenser); 50 ml graduated cylinder; analytical balance.

Preparation of Sample

Mix samples without warming and inclusion of air if possible. Avoid direct sunlight. Carefully heat solid samples to approx. 10°C above their melting point. Samples containing visible impurities must be filtered (filtration to be recorded in protocol).

Procedure

Conduct tests in diffuse daylight or artificial light. Avoid direct sunlight. Make sure all glassware is free of oxidizing or reducing substances. Introduce exactly 5 g of sample (accuracy: ± 0.1 mg) into the thoroughly cleaned Erlenmeyer. Dissolve sample in 50 ml of glacial acetic acid/ isooctane mixture with turning upside down. Using a pipette, add 0.5 ml of saturated potassium iodide solution, close the Erlenmeyer and shake vigorously for exactly 60 seconds (stopwatch!). Immediately add 30 ml of water and turn upside down. Titrate released iodine immediately with 0.1 N thiosulfate standard solution until yellow color appears, then add 0.5 ml of starch solution to titrate from violet/ purple to colorless. Titration is complete as soon as solution remains colorless for 30 seconds. Simultaneously, conduct blank test without using more than 0.1 ml of 0.01 N thiosulfate solution.

Result of determination

Use the following formula to calculate the peroxide value (POV) in mmol O_2/kg:

$$POV = (a-b) \times M \times 1000\ 2 \times \cdot Q$$

where: *a* is the consumption (ml) of sodium thiosulfate standard solution in main test, *b* is the consumption (ml) of sodium thiosulfate standard solution in blank test, *M* is the molarity of the sodium thiosulfate standard solution and *Q* is the quantity of the sample used.

2.2.8 Membrane-free release model

A release test model was developed to allow the relative (not absolute) comparison of perfume release from the different formulations e.g. o/w nanoemulsion and perfume-loaded NLC [222]. The test model consists of 2 phases, an aqueous phase (NLC dispersions or nanoemulsions) and an oil phase on the top of the aqueous phase as an acceptor medium. This release test model allows to determine the release profile of perfumes from their carrier systems independently of membranes, which is the case in the normal use of perfumes. Here the diffusion of the perfumes from the formulation to the acceptor medium (Miglyol 812) was observed. 10 ml of Miglyol 812 were placed on top of 5 ml aqueous phase (NLC dispersions or nanoemulsions) (Figure 2-12). Saturation of the perfume in the acceptor medium was not allowed to be reached. The two phases were put in a closed vial and kept in a temperature controlled shaking chamber at 70 shakes/ min and 32ºC, Innova 4230, New Brunswick Scientific (New Jersey, USA). The concentrations of the perfumes have been assessed at defined time intervals by withdrawing 1 ml from the acceptor medium and analysing it using a spectrophotometer, UV-1700 PharmaSpec, Shimadzu Deutschland GmbH (Duisburg, Germany), at a proper wave length (λ max of the perfume). 1 ml of Miglyol 812 was added to the acceptor medium to substitute the withdrawn volume.

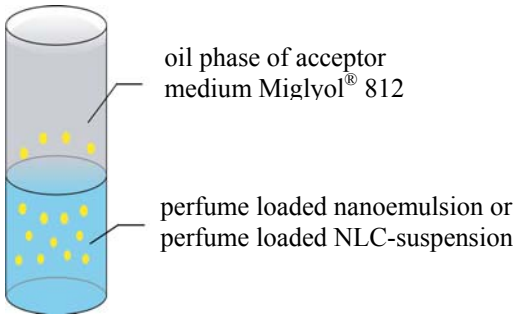

Figure 2-12: The membrane-free release model.

2.2.9 Panel's nose test

Materials

- Tap water
- Square towel (27cmX27cm)
- Conventional perfumed fabric softener
- NLC fabric softener
- Cyclodextrin-perfume complex fabric softener.

Preparation of Sample

Each fabric softener was dissolved in tap water (6 ml to 1 Litter).

4 pieces of non-perfumed towel were hand-agitated in one of the beakers containing one of the fabric softener formulations for 10 min.

The towels were then individually hanged and wrung, removing as much water as possible.

The towels were graded according to the odor impact using the below 1 to 5 scale (Table 2-5) after definite time intervals (3, 6, 12, 48, 72 hrs).

Table 2-5: Odor grading for strength was done by a panel of six people, using the following scale.

grade	Odor impact
1	No Perfume odor detected
2	Faint perfume odor detected
3	Definite perfume odor detected
4	Strong perfume odor detected
5	Very strong perfume odor detected

2.2.10 Solid phase microextraction (SPME)

SPME is a solvent free sample extraction technology that is fast, economical, and versatile. SPME is a fiber coated with a solid (sorbent), a liquid (polymer) or a combination of both. The fiber coating removes the compounds from the sample to be tested by absorption (liquid coatings) or adsorbtion (solid coatings). The SPME fiber is then inserted directly into the gas chromatograph for desorption and analysis. SPME is used in many applications including flavors and fragrances, toxicology, environmental and biological matrices, and product testing [223-225].

In this work samples were taken from the towels after treatment with the different fabric softeners (c.f. 2.2.9) and were analyzed for the presence of the different components of the perfume used. Samples were taken in triplicate from each towel.

2.2.11 UV blocking properties and UV protection determination

Three *in vitro* methods were used to determine the UV blocking properties of the formulations prepared for UV radiation protection.

2.2.11.1 UV spectral absorption

A UV spectral absorption of the aqueous dispersions (NLC, nanoemulsion) was performed using a spectrophotometer UV-1700 PharmaSpec, Shimadzu Deutschland GmbH (Duisburg, Germany). Before measuring, the formulations were diluted in the same rate and the wave length from 400-200 nm was scanned. To obtain valid results avoiding the size effect on UV scattering, samples of similar particle sizes were always measured.

2.2.11.2 UV blocking activity (β-carotene to asses UV protection)

This method has been developed in the working group of Prof. Müller. The principle of this method is that β-carotene loses its yellowish color upon exposure to UV radiation. β-carotene is easily degraded by photo-irradiation, this is because of the hydroxylation of carotenes and esterification of xanthophylls [184, 185]. Exposure to UV radiation causes decomposition of the β-carotene chromophore and hence bleaching occurs, i.e. loss of color due to breaking of the chromophore [183, 186, 187].

A 2.0 mg/ml Miglyol 812 solution of β-carotene was prepared using Lucarotin 10 Sun, BASF AG (Ludwigshafen, Germany), which is a 10% (w/w) β-carotene in sunflower oil. Quartz Petri dishes of 4.5 cm diameter were filled with 5.0 ml of this solution. Each Petri dish was covered with 0.3 g evenly spread layer of one of the formulations to be tested for their UV blocking activity. The most cited factor that influences the UV transmission during *in vitro* measurements is the nonhomogeneity of the residual film formed after the sunscreen application. The film thickness homogeneity is influenced by the amount of the sunscreen applied and by the way of spreading the film over the substrate of skin surface [226-228]. Therefore, special care was taken while applying the formulations on the dishes covers. The Petri dishes were placed inside the artificial sunlight chamber Suntest, Heraeus GmbH (Hanus, Germany) and were irradiated with a radiation intensity of about 830 W/m^2 (between 300 and 830 nm) for a period of time (60-120 min) till the concentration of β-carotene in the Petri dishes of one of the formulations (usually the placebo) is around zero. The exposure

time may differ from one set of formulations to another according to their UV blocking activity.

The concentration of the β-carotene solution in each Petri dish was assessed spectrophotometrically using a UV-1700 PharmaSpec, Shimadzu Deutschland GmbH (Duisburg, Germany) after definite times of exposure (e.g. 15, 30, 45 min). The higher the UV blocking activity of a formulation, the higher is the β-carotene concentration of the solution in the Petri dish covered with this formulation. Figure 2-13 shows the design of this method.

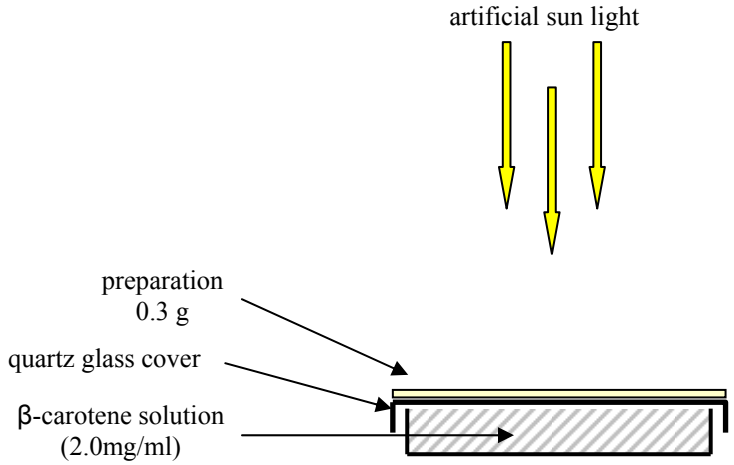

Figure 2-13: The design of the β-carotene method: The Petri dish is filled with β-carotene solution and covered with 0.3g of the formulation to be tested.

2.3 Data presentation and statistical treatment in figures and tables

The data points in figures correspond to the average (mean) value of *n* repetitions of the experiment. The error bars stand for the corresponding standard deviations (SD). Data given in tables and in the text are average (mean) values of *n* repetitions ± SD thereof.

3 PRODUCTION OPTIMIZATION OF NLC

The size and physical stability of an NLC formulation depends beside the composition (lipid phase concentration, surfactant type, surfactant concentration) on the production parameters, e.g. pre-emulsion quality, production temperature, homogenization pressure, number of homogenization cycles and cooling rate [2, 229-232]. The following experiments were performed to determine the optimal production parameters and conditions. A placebo NLC formulation containing 10% (w/w) lipid phase was used in these experiments. Table 3-1 shows the composition of this placebo NLC formulation.

Table 3-1: The composition of the NLC formulation.

Composition	% (w/w)
Apifil	8.0%
Mygliol 812	2.0%
TegoCare 450	2.0%
water	88.0%

The melting point of Apifil is between 59°C and 70°C. Therefore, the production temperature was adjusted to 85°C (5-15°C above the solid lipid melting point) for all the batches produced in this study. The lipid and aqueous phases were heated up to 85°C and they were pre-homogenized using a high speed stirrer (Ultra-Turrax) at 8000 rpm for 30 sec.

The homogenization tower was heated to 90°C using a water jacket. Controlling the production temperature is very crucial because it affects the viscosity of the emulsion during the homogenization process. Increasing the temperature usually decreases the viscosity of the lipid and aqueous phases and hence the efficiency of the homogenization is increased. In other words, increasing the homogenization temperature results in smaller droplet/particle size [233, 234].

3.1 Effect of cooling rate after homogenization

The NLC formulation (Table 3-1) was produced three times using the same homogenization conditions (90°C, 800 bar, 2 homogenization cycles). After homogenization the three batches were cooled down at different cooling rates. The first sample was placed in a 5°C water bath while the second was placed in a 15°C water bath and the third was left on the bench to cool down at room temperature. Figure 3-1 and Figure 3-2 show the particle size measured by LD and PCS of these samples at day 0 and after one month.

It can be concluded that the cooling rate does not influence the particle size of the NLC or their physical stability. To have a controlled cooling rate for all the NLC formulations after homogenization, the cooling down step was performed always using a 15°C water bath.

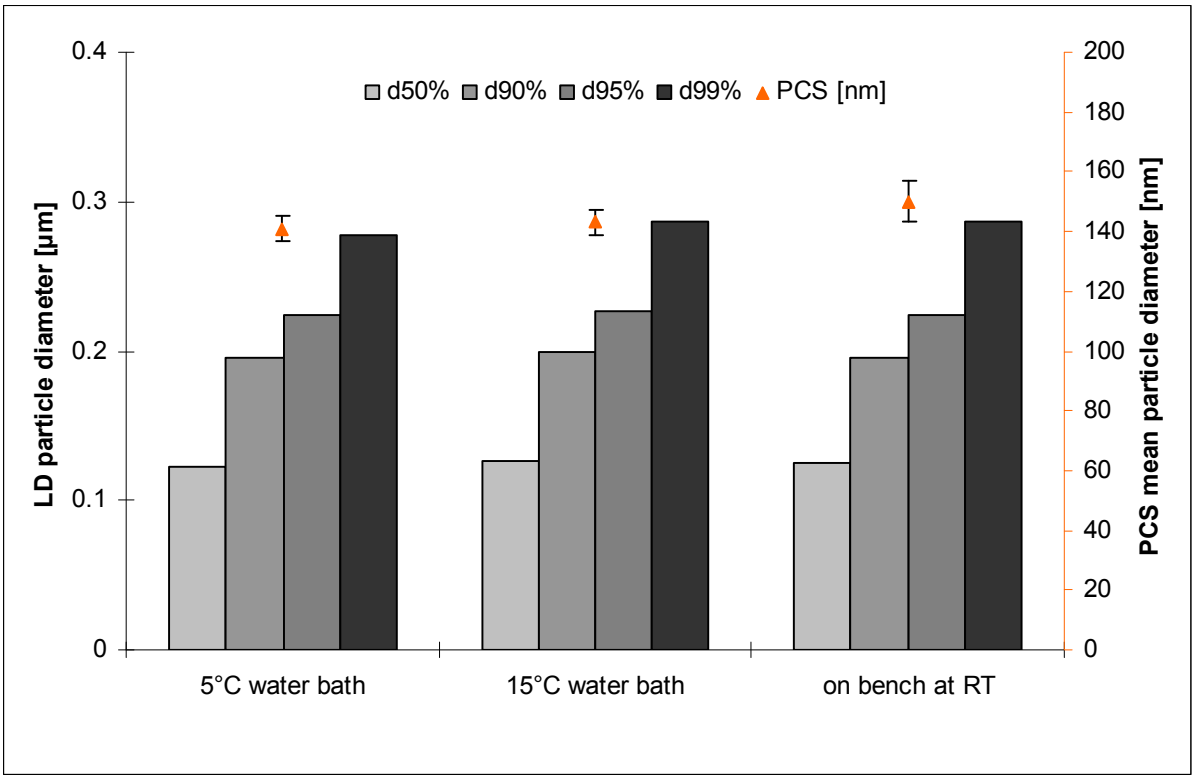

Figure 3-1: Day 0 PCS and LD particle size of the NLC samples cooled down at different temperatures (n=3).

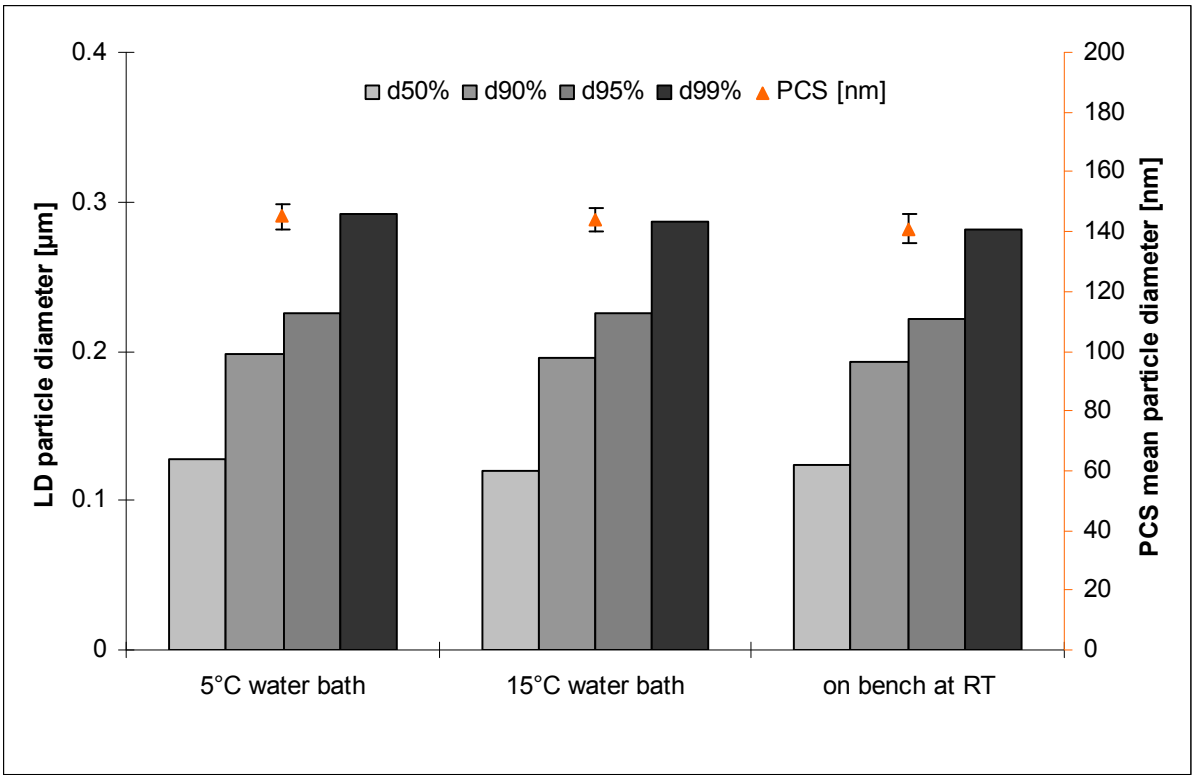

Figure 3-2: One month PCS and LD particle size of the NLC formulations cooled down at different temperatures (n=3).

3.2 Effect of increasing homogenization cycles and pressure

Maintaining all other variables constant, the NLC formulation (Table 3-1) has been homogenized at two different homogenization pressures (800 bar and 500 bar) and the number of homogenization cycles was 1, 2, 3 or 4 cycles.

At 800 bar the difference in particle size of the NLC after the 2nd homogenization cycle was neglectable. At 500 bar the 4th homogenization cycle resulted in a slight reduction of particle size when compared to the particle size after the 3rd homogenization cycle. Moreover, the particle size of the batch homogenized at 800 bar and with 2 homogenization cycles was similar to the particle size of the batch homogenized at 500 bar and 3 cycles (Figure 3-3). To reach a balance between the efficacy and economy of the homogenization process, 2 cycles at 800 bar were chosen to be the homogenization parameters.

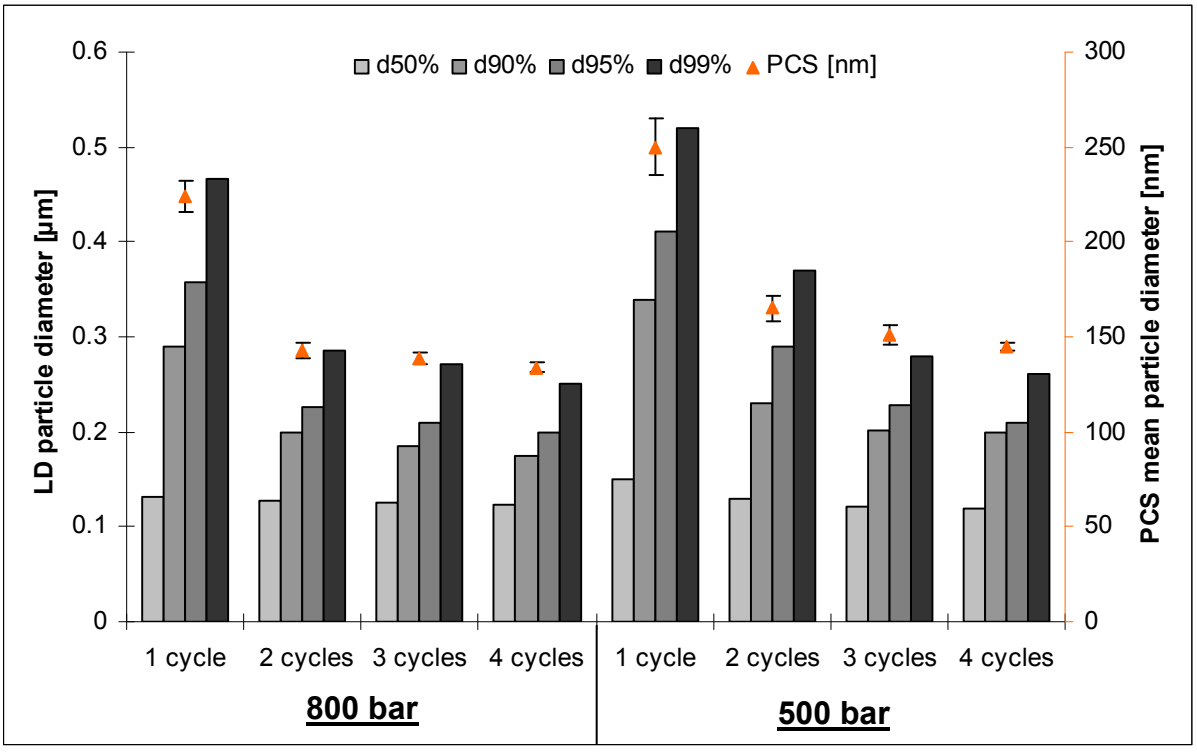

Figure 3-3: Day 0 PCS and LD particle size of the NLC formulations homogenized at different pressure and with increasing homogenization cycles (n=3).

3.3 Effect of adding the surfactant to the lipid or aqueous phase

During the production of NLC the surfactant can be dispersed in the aqueous phase or the melted lipid phase. To determine the best procedure two batches of the NLC formulation were produced under the same conditions. In the first batch the surfactant (TegoCare 450) was added to the aqueous phase and in the second batch it was added to the lipid phase. The particle size analysis showed that there is no difference between these two batches (Figure 3-4). Due to the TegoCare 450 nature (lipid) and the recommendation of the producer (Goldschmidt AG) it was added to the lipid phase while producing NLC formulations stabilized with it. The NLC formulations stabilized with Tween 80, PlantaCare 2000 or Miranol ultra 32 were produced by adding the surfactant to the aqueous phase.

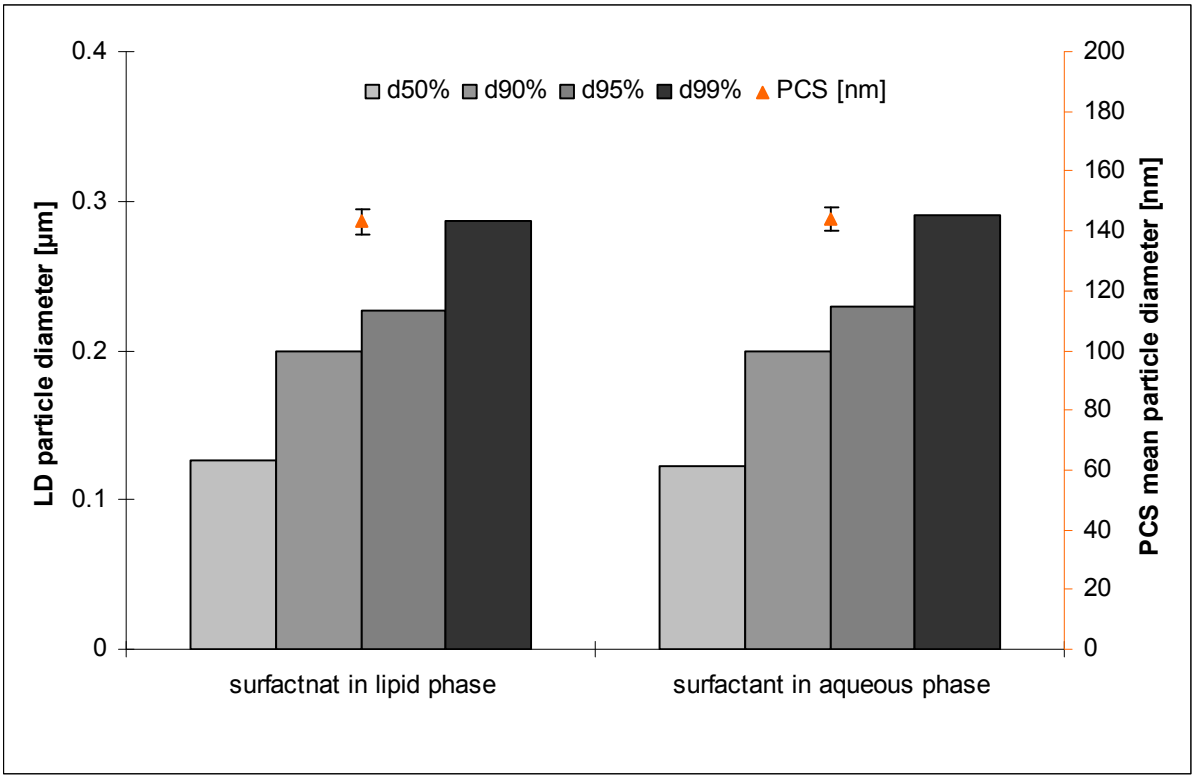

Figure 3-4: Day 0 PCS and LD particle size of the NLC formulations prepared by adding TegoCare 450 surfactant to the lipid phase or the aqueous phase (n=3).

3.4 Effect of increasing surfactant concentration

Maintaining all the production conditions the same, the NLC formulation was prepared using increasing concentration of TegoCare 450 and the particle size of the different batches was measured using PCS and LD on the production day and after one month (the following five figures). The zeta potential was also determined (Figure 3-10).

The formulation containing 1% (w/w) TegoCare 450 showed an increase in the d99% after one month indicating insufficient stabilization of the particles (Figure 3-8 and Figure 3-9). Increasing the TegoCare 450 concentration above 2% (w/w) did not cause a big reduction in particle size (Figure 3-5 and Figure 3-7). Moreover, the formulation containing 2% (w/w) was stable and particle growth did not occur after one month. On the other hand, the higher surfactant concentrations (above 2% (w/w)) led to foam formation during the homogenization process. This might cause loss of the sample, inaccuracy of the suspension contents and incomplete filling of the sample cylinder of the homogenizer because of the volume taken by the foam. Therefore, 2% (w/w) TegoCare 450 was found to be sufficient to produce a stable NLC suspension with 10% (w/w) lipid phase content.

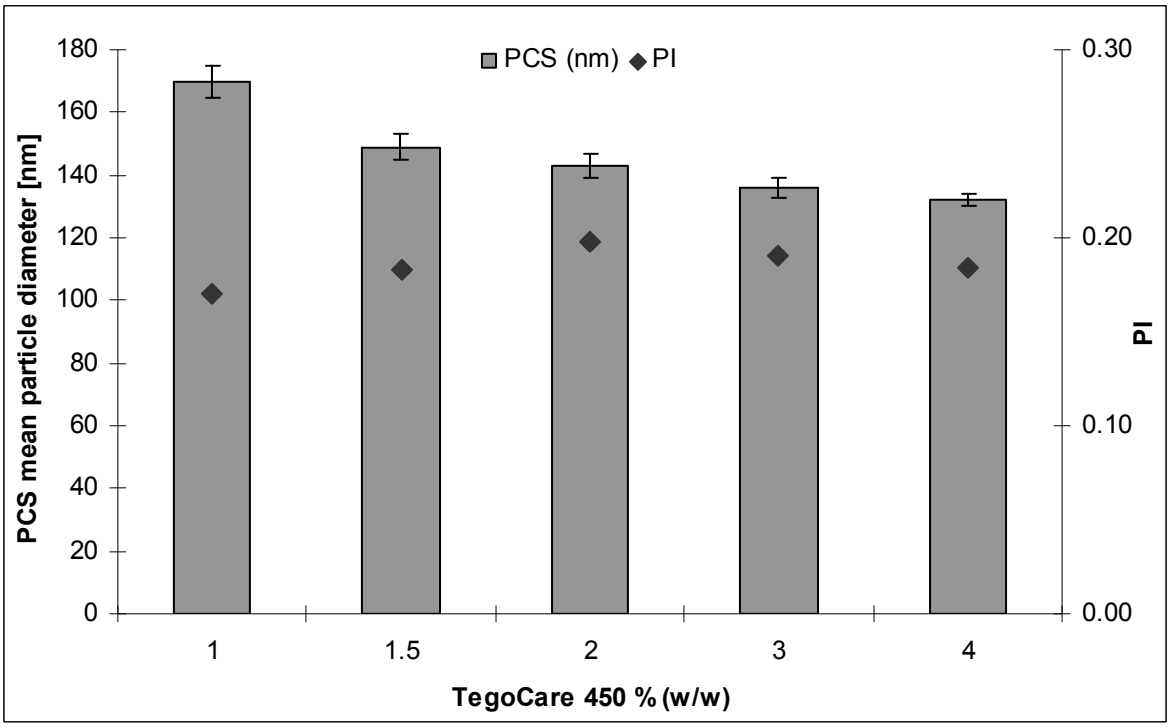

Figure 3-5: Day 0 PCS particle size of the NLC formulations with an increased surfactant concentration (n=3).

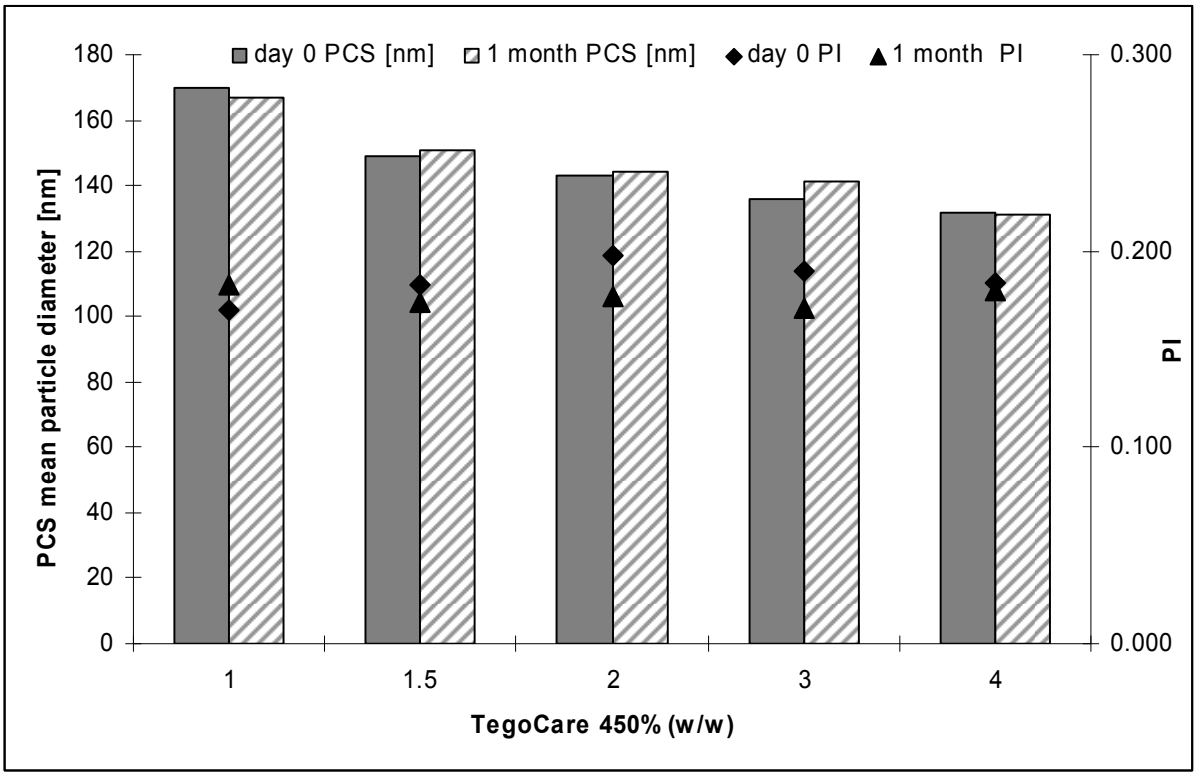

Figure 3-6: Day 0 and one month PCS particle size of the NLC formulations with an increased surfactant concentration (n=3).

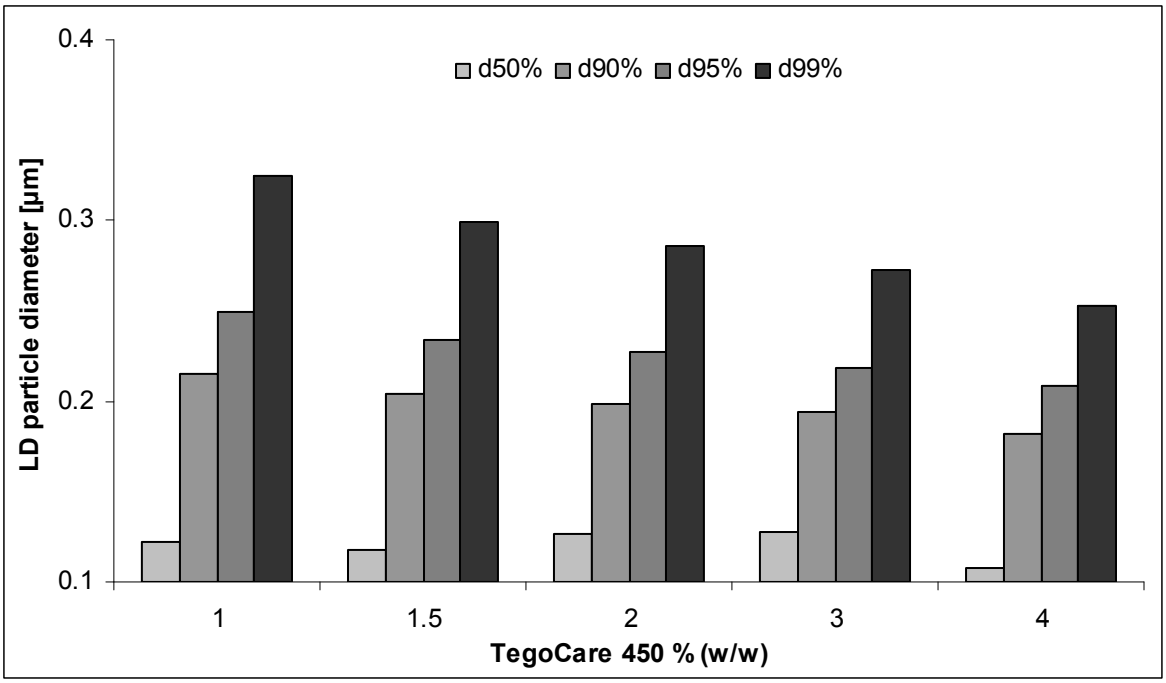

Figure 3-7: Day 0 LD particle size of the NLC formulations with an increased surfactant concentration (n=3).

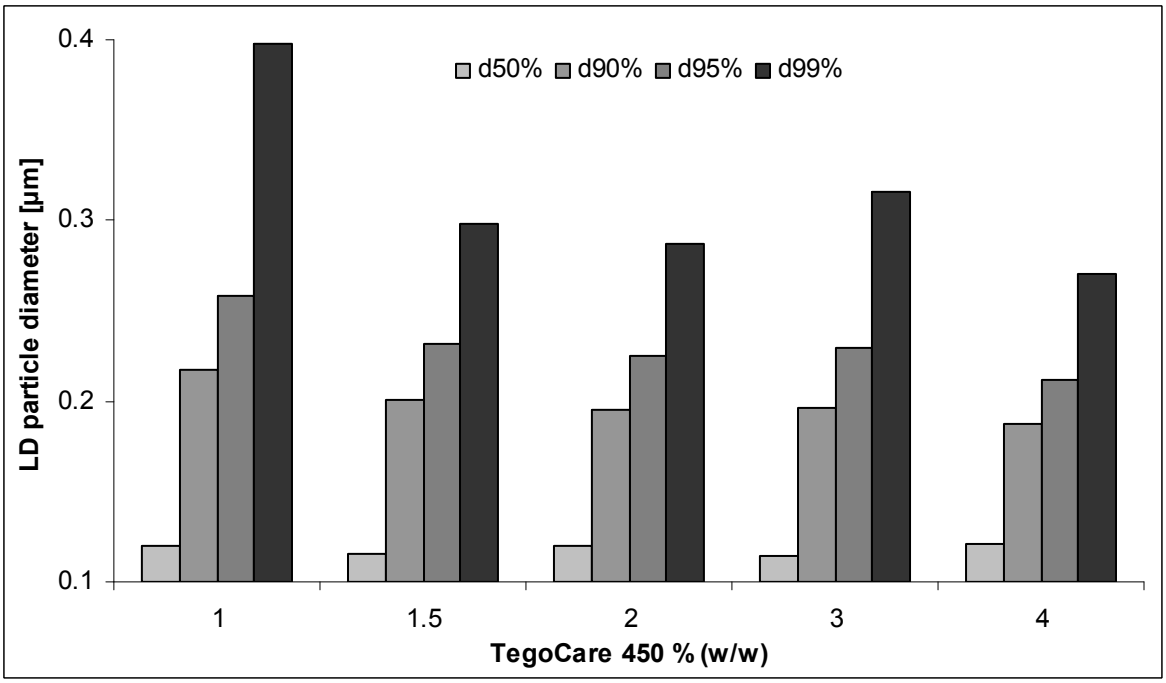

Figure 3-8: One month LD particle size of the NLC formulations with an increased surfactant concentration (n=3).

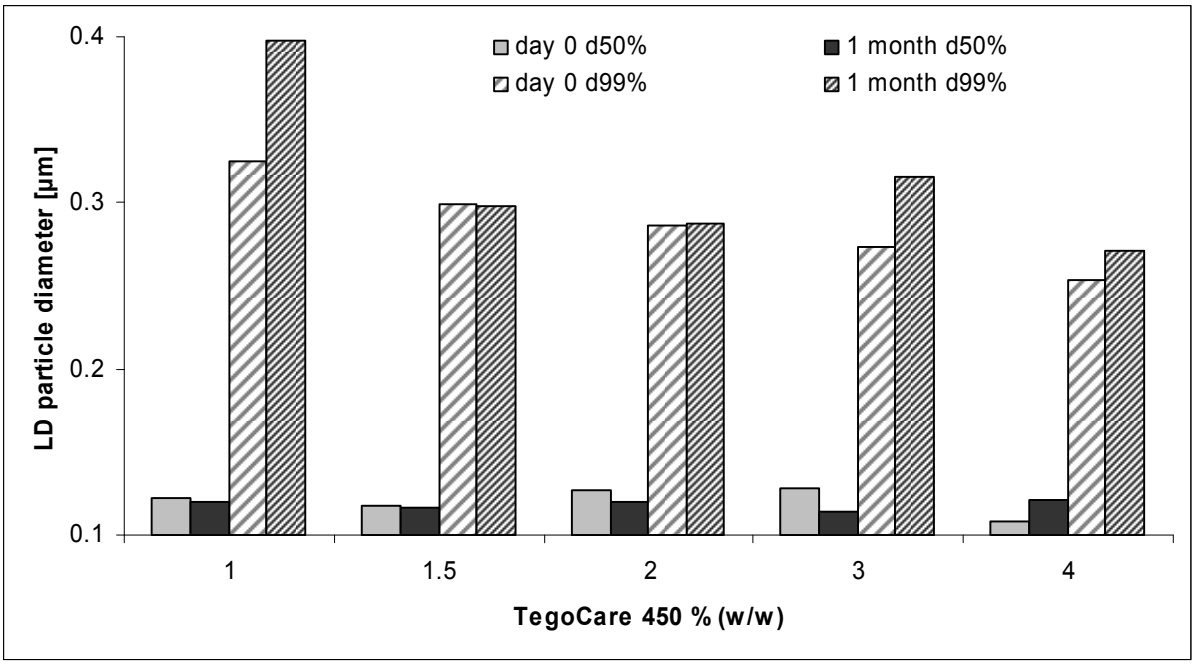

Figure 3-9: Day 0 and one month LD particle size of the NLC formulations with an increased surfactant concentration (n=3).

Regarding zeta potential, increasing the TegoCare 450 concentration led to an increase in the absolute value of the zeta potential (Figure 3-10). Chemically TegoCare 450 is a stearyl glucoside (polyglyceryl-3 methyl-glucose distearate). It is a nonionic surfactant but the OH groups of the sugar part in its molecule have a negative charge when it is in water. Therefore, the surface of the particles stabilized with this surfactant will have a negative zeta potential. This explains the increasing of the zeta potential value when the concentration of the surfactant is increased. Due to the steric stabilization of TegoCare 450 a value of -24.3 (2% (w/w) TegoCare 450 concentration) is considered to be sufficient to obtain a suspension with high physical stability [210].

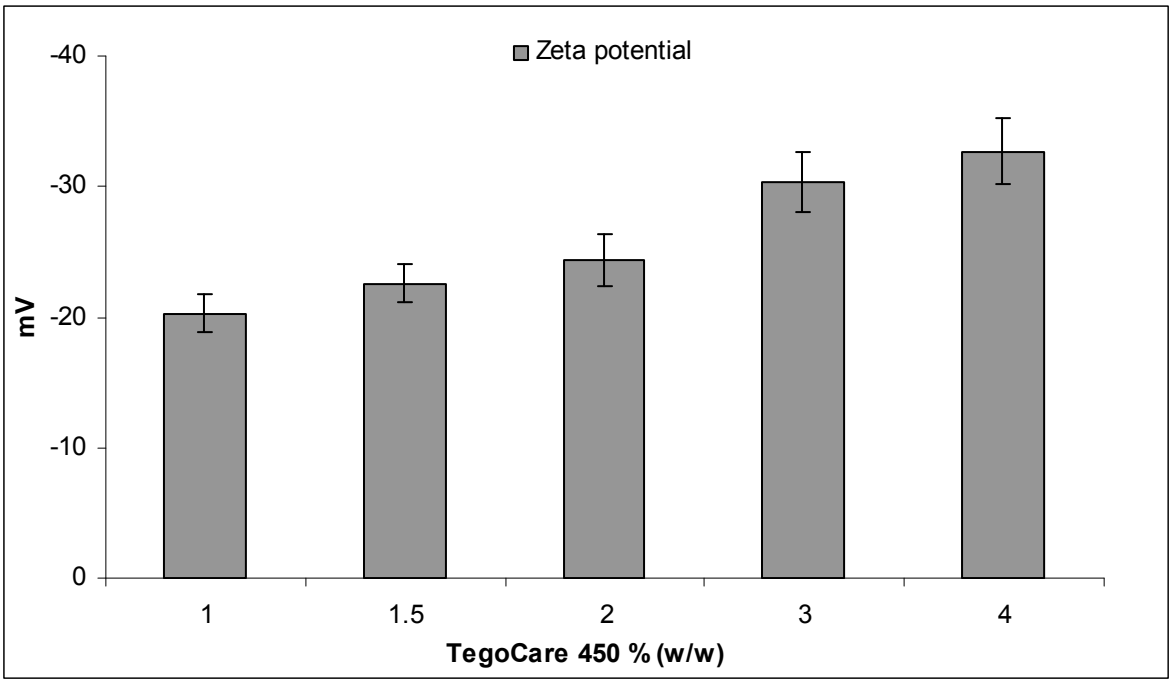

Figure 3-10: Day 0 zeta potential analysis of the NLC formulations with an increased surfactant concentration measured in water with adjusted conductivity (50 µS/cm) (n=3).

3.5 Conclusion

From this study the production conditions were decided to be 2 homogenization cycles and 800 bar homogenization pressure unless otherwise was required. The surfactant should be added to the aqueous phase unless otherwise was recommended. Increasing the surfactant concentration led to a decrease in the particle size but more than 2% did not cause a further decrease in the particle size. Moreover, excessive amount of surfactant led to foam formation during homogenization. Therefore, an optimal surfactant concentration should be determined. The cooling down step of the formulations after homogenization is to be performed using a 15°C water bath.

4 NLC AS A CARRIER SYSTEM FOR CHEMICALLY LABILE ACTIVES

4.1 Introduction

Many actives used in the pharmaceutical and cosmetic industries are chemically labile and difficult to stabilize in the final product. It is known that the incorporation of chemically labile substances in colloidal carriers, such as liposomes and polymeric nanoparticles, can improve drug stability [59, 235]. Liposomes and o/w emulsions are frequently employed as carriers for cosmetic actives. However, they are limitedly able to protect chemically labile actives against degradation. Due to the liquid state of oil droplets in o/w emulsions, relatively fast partitioning of lipophilic actives between oil phase and water takes place [236]. The active is degraded in the water phase, re-partitions into the oil phase and being replaced in the water phase by non-degraded active diffusing from the oil into the water phase (Figure 4-1, left). With liposomes, the lipophilic actives are localised in the phospholipids bilayer. These actives can also partition to the water phase. Hydrophilic actives dissolved in the water core of the liposomes are in exchange with the external water phase. This exchange can be slowed down (but not completely stopped) by increasing the viscosity of the phospholipid bilayers using some materials like cholesterol (Figure 4-1, middle). Mathematically the diffusion coefficient D is reversely proportional to the viscosity η of the medium (law by Einstein-Stokes):

$$D = \frac{kT}{6\pi\eta r}$$

where k is Blotzmann constant, T is the absolute temperature and r is the size/radius of the molecule or particle.

Moreover, liposomes are susceptible to hydrolysis and oxidation due to the contents of unsaturated fatty acids and ester bonds in their phospholipid bilayers [237]. This limits the long-term stability of liposomes. In contrast to this, a carrier in the solid state leads to a slow exchange between the solid particle phase and the external water phase, e. g. as in the case of polymeric nanoparticles or microparticles [59]. The same is valid for the NLC (Figure 4-1, right). Therefore, an optimized NLC formula can be a successful carrier system which provides the desired stability, as already previously documented in the literature [119].

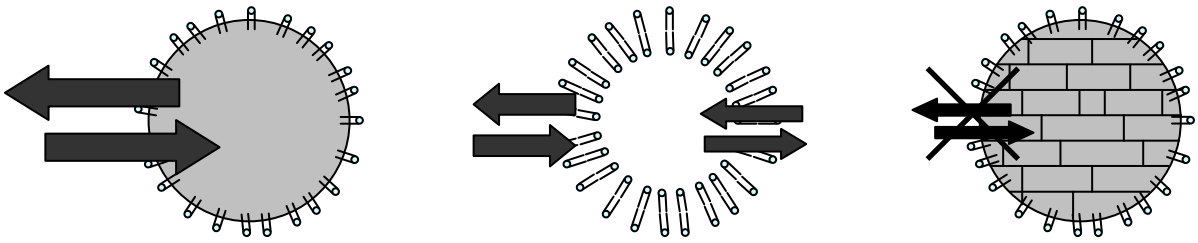

Figure 4-1: Exchange phenomena between the lipophilic oil phase of emulsions (left), and the lipophilic bilayers and aqueous core of liposomes (middle) with the surrounding water phase, and subsequent degradation taking place in the water phase. In case of a solid particle matrix (e. g. polymeric particles, lipid nanoparticles with solid matrix) these exchange phenomena and degradation are practically eliminated or at least distinctly slowed down/minimised (right) (modified after [238]).

4.2 Coenzyme Q 10 (Q10) and Black Currant seed Oil (BCO) loaded NLC

Coenzyme Q 10 (Q10) is sensitive to light and heat and will decompose when it is exposed to these conditions [162, 164, 239]. Oxidation of Q10 might also occur in personal care products [117].

Many trials to stabilize Q10 by incorporating it into liposomes [240], nanoliposomes [241], poly (lactic-co-glycolic acid) PLGA nanopartilces [242] and polyelectrolyte-fatty acid complex nanoparticles [243] were performed. Also Q10-loaded lipid nanoparticles were prepared and then lyophilizing to achieve higher stability [244]. Westesen et al. prepared Q10 nanoparticles by emulsifying the molten Q10 in an aqueous phase. The colloidal dispersion of the Q10 remains in the state of a supercooled melt and hence it is considered to be an o/w emulsion not a suspension [245]. Bunjes et al. incorporated Q10 into solid lipid nanoparticles and studied the structure and the physical stability of these particles [105].

In cosmetics Q10 is used as antioxidant in the skin care products [160]. Some studies suggest that Q10 in dermal products may provide enhanced protection against inflammation and premature aging caused by sun exposure [161]. But the penetration of Q10 into the skin is dubious. Principles of novel drug delivery systems need to be applied to significantly improve the performance of Q10. Recently, coupling agents, inclusion complexes (Lycopene and β-cyclodextrin), liposomes, microparticle and nanoparticle systems have been explored for the delivery of Q10 either for oral or dermal administration [246]. Teeranachaideekul et al. incorporated Q10 in NLC and studied the physicochemical properties of the system and performed an *in vitro* release study for the Q10 incorporated in the nanoparticles. Pardeike and Müller investigated the skin penetration of Q10 from an NLC and from a reference emulsion and paraffin. They found that there is an increase in Q10 penetration when the NLC

is applied [247]. NLC seems to be the optimal delivery system for Q10 having the advantages of stabilization and of skin penetration enhancement.
Black currant seed oil (BCO) contains polyunsaturated fatty acids, which makes it susceptible to oxidation [167, 248]. In this chapter Q10 and BCO were incorporated together in NLC to protect them from oxidation.

4.2.1 Production of Q10 and BCO loaded NLC

The NLC formulation to be produced is intended to be used in cosmetic products for dermal application. The nanoparticles should stay solid after applying to the skin, i.e. the melting temperature of the nanoparticles must be above 32ºC (skin temperature). Oil incorporation lowers the crystallisation and the melting temperature of the lipid particles matrix [48]. The high oil content (BCO) in the lipid phase makes the production of the lipid nanoparticles, which are solid at 32ºC, a challenge. Therefore, it was necessary to find a lipid that can still form a solid matrix at 32ºC with the high BCO load and in which the Q10 can be incorporated.

4.2.1.1 Investigation of lipid/BCO mixtures

15 high melting point lipids were selected and each lipid was mixed with BCO in three different ratios, namely: 60:40, 40:60 and 20:80 lipid to BCO. The miscibility of the melted lipid with BCO and the physical appearance of the mixture after cooling down were observed. Table 4-1 shows the results of this screening.

Table 4-1: The physical appearance of the lipid/BCO mixtures of different ratios at 32ºC. All melted lipids were miscible with the BCO at 90ºC. (- means no mixture was prepared and tested).

Lipid	Physical appearance at 32ºC Lipid:BCO ratio		
	60:40	40:60	20:80
Apifil	solid	solid	soft
Atowax	solid	solid	soft
Biogapress vegeta	solid	solid	soft
Compritol ATO888	solid	soft	-
Compritol HD 5 ATO	solid	soft	-
Dynasan116	solid	solid	soft
Dynasan118	solid	solid	solid
Imwitor 900	soft	-	-
Lanette 18	solid	soft	-
Lanette O	soft	-	-
Precifac ATO	soft	-	-
Precifac ATO 5	soft	-	-
Hydrine	soft	-	-
Softisan 154	solid	solid	soft
carnauba wax	solid	solid	solid

The lipids which formed soft mixtures at 32ºC with the first two ratios (60:40 or 40:60) were not mixed with the BCO at the other ratios (40:60 or 20:80). Carnauba wax and Dynasan 118 were chosen based on this primary screening, i.e. these lipids mixtures were solid at 32ºC with the highest BCO content (20:80 lipid:BCO). These mixtures were further investigated by running DSC analysis to determine the exact melting point (melting peak maximum) of the mixture and the melting enthalpy and recrystallization index (RI) of the lipid. The RI was calculated applying the following equation.

$$RI(\%) = \frac{\Delta H_{mixture}}{\Delta H_{bulk} \times Concentration_{lipid}} \times 100$$

where $\Delta H_{mixutre}$ is the melting enthalpy of 1 g lipid/BCO mixture, ΔH_{bulk} is the melting enthalpy of 1 g bulk solid lipid. ΔH is given in J/g and the concentration is given by the percentage of solid lipid.

Figure 4-2 shows the DSC diagrams of the bulk carnauba wax and the mixtures of carnauba wax/BCO with lipid:BCO ratios 40:60 and 20:80. As the BCO ratio increased the melting point of the mixture decreased from 80.5ºC to 77.7ºC. The RI decrease was 12% indicating a homogenous lipid/BCO matrix with a high BCO incorporation capacity.

Figure 4-3 shows the DSC diagrams of the bulk Dynasan 118 and the mixtures of Dynasan 118/BCO with lipid:BCO ratios 40:60 and 20:80. As the BCO ratio increased, the melting

point of the mixture decreased from 68.1ºC to 63.3ºC. The RI decrease was 13% indicating a homogenous lipid/BCO matrix with a high BCO incorporation capacity.

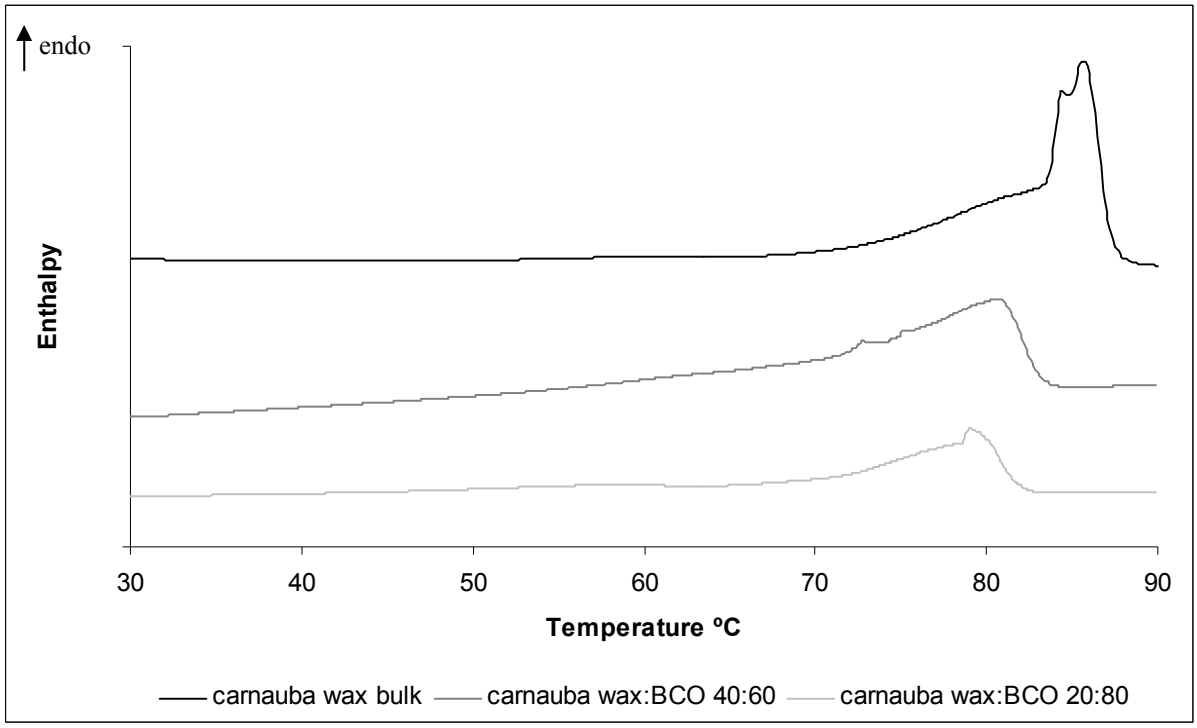

Figure 4-2: The thermogram of the bulk carnauba wax (upper curve) and the mixtures of carnauba wax/ BCO with the lipid:BCO ratios 40:60 and 20:80 (middle and lower curves, respectively). By increasing the BCO ratio a depression in melting point and melting enthalpy occurred.

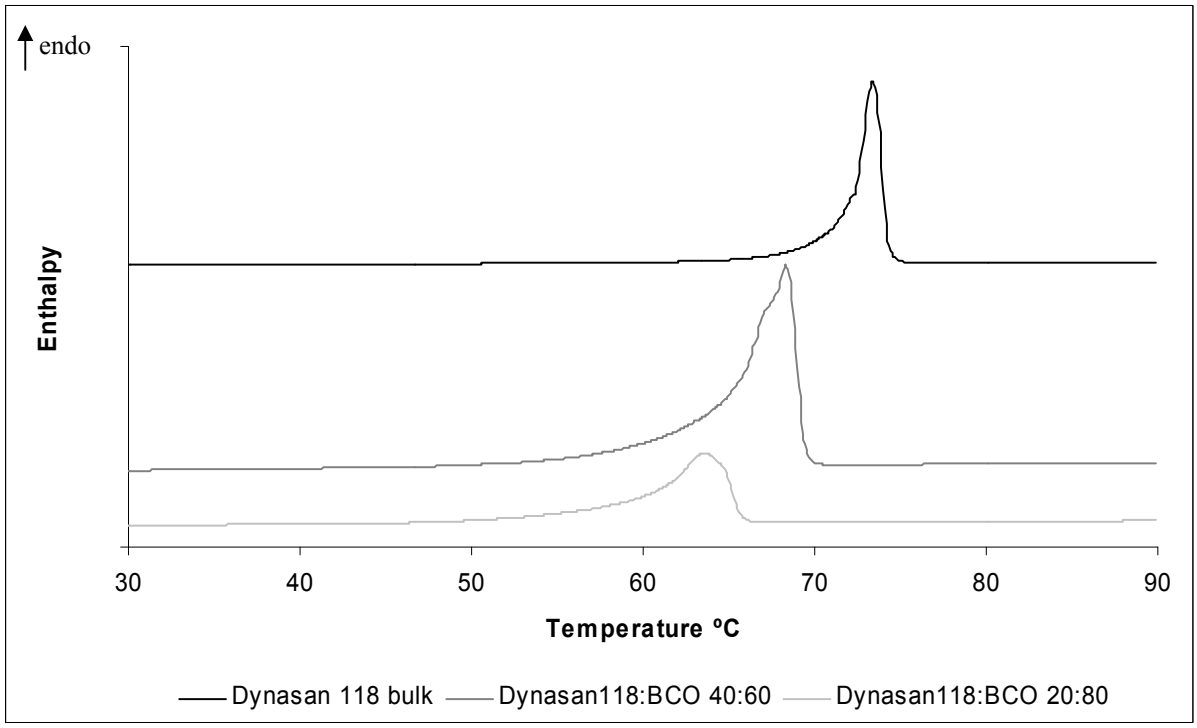

Figure 4-3: The thermogram of the bulk Dynasan 118 (upper curve) and the mixtures of Dynasan 118/ BCO with the lipid:BCO ratios 40:60 and 20:80 (middle and lower curves, respectively). By increasing the BCO ratio a depression in melting point and melting enthalpy occurred.

The melting enthalpy, melting point and RI of carnauba wax, Dynasan 118 and their mixtures are shown in Table 4-2. A decrease in the melting enthalpy and RI of the lipid in the lipid/BCO solid mixture by increasing the BCO part indicates good incorporation of the BCO in the solid lipid matrix.

Table 4-2: The DSC analysis of lipid/BCO mixtures with two different lipid:BCO ratios. The measurements were performed after 1 day of preparing the mixtures.

Lipid	Lipid:BCO ratio	Onset ºC	Melting point ºC	Enthalpy J/g	RI%
carnauba wax	100:0	82.8	85.0	175	**100**
	40:60	76.9	80.5	76.5	**77**
	20:80	71.8	77.7	38.4	**65**
Dynasan 118	100:0	71.7	72.7	201.0	**100**
	40:60	64.6	68.1	94.2	**79**
	20:80	59.6	63.3	39.8	**66**

The two lipid:BCO ratios 40:60 and 20:80 were chosen for the produced of the NLC. Although the matrix with the ratio 20:80 lipid:BCO was solid at 32ºC, it has been thought that a lower amount of the BCO in the matrix might provide an increased chemical stability to the BCO because it will be more enclosed inside the lipid particles. Therefore, the ratio 40:60 lipid:BCO was produced in parallel to the 20:80 one.

4.2.1.2 Optimization of the BCO-loaded NLC formulation

After selecting the lipids to be used for the production of the NLC, trials have been performed to optimize the formula. Different homogenization pressures were applied and the effect of an increasing number of homogenization cycles was investigated. The two solid lipids carnauba wax and Dynasan 118 were used as well as the two surfactants PlantaCare 2000 and Inutec SP1. The concentration of the lipid matrix was also optimized. According to the achieved results the necessary modifications on the formulation have been made and a new trial was performed.

4.2.1.2.1 Homogenization pressure and number of homogenization cycles

After fixing all other parameters (lipid phase concentration, lipid:BCO ratio and surfactant concentration), the homogenization pressure has been increased from 500 bar to 1000 bar and the number of homogenization cycles was either 1, 2 or 3 cycles. To perform this experiment the lipid phase concentration was decided to be 45% (w/w). The carnauba wax:BCO ratio was 40:60. PlantaCare 2000 was selected as surfactant and its concentration was 5% (w/w). The particle size measurements achieved after the different homogenization pressures and cycles are listed in Table 4-3.

Comparing the particle sizes after one cycle, a homogenization pressure higher than 800 bar (1000 bar) did not give much smaller particles. Moreover, two cycles at 800 bar did not give much smaller particles than one cycle at the same homogenization pressure either. Three cycles at 500 bar were a time consuming and costly procedure. To reach a balance between the efficacy and economy of the homogenization process, one cycle and 800 bar homogenization pressure were chosen to be the homogenization parameters.

Table 4-3: PCS mean particle size of carnauba wax NLC suspensions at different homogenization pressures and cycles (Lipid phase 45% (w/w), carnauba wax:BCO ratio 40:60, PlantaCare 2000 5% (w/w)).

Homogenization conditions		PCS mean particle size (nm)	PI
Pressure	*Number of cycles*		
500 bar	1	540 ±25	0.45
	2	294 ±10	0.25
	3	260 ±9	0.19
800 bar	1	279 ±8	0.14
	2	253 ±4	0.09
1000 bar	1	265 ±15	0.29

4.2.1.2.2 Lipid and lipid phase concentration

For economical and practical reasons the NLC suspension should contain as much lipid particles as possible. That means a high lipid phase concentration (mixture of solid lipid and BCO). On the other hand the NLC suspension should be physically stable. It means no significant growth in the particle size occurs and the suspension does not gel or solidify during the shelf life.

Samples with lipid phase concentration of 60% (w/w) and higher (using both PlantaCare 2000 and Inutec SP1) became highly viscous after production. These samples became solid after one week storage at room temperature. Samples containing 50% (w/w) lipid phase and produced using Dynasan 118 and PlantaCare 2000 or Inutec SP1 showed aggregations after adding the preservative system (2-phenylethanol and dehydroacetic acid sodium salt). Samples containing 50% (w/w) lipid phase and produced using carnauba wax and PlantaCare 2000 or Inutec SP1 maintained the same particle size after adding the preservatives mixture for 6 months. Therefore, carnauba wax was the solid lipid of choice and Dynasan 118 was excluded from further studies. The final lipid phase concentration was decided to be 45% to definitely avoid any instability on long-time storage.

4.2.1.2.3 Carnauba wax:BCO ratio

The aim was to have a high content of BCO in the lipid phase while maintaining the melting point of the particles above 32ºC and the chemical stability of the BCO. The BCO in the sample with the higher oil content (carnauba wax:BCO 20:80) was more susceptible to oxidation in the "oxidative stress test" (see chapter 2) than in the sample with the lower oil content (carnauba wax:BCO 40:60) (Table 4-4). Therefore, the ratio 40:60 was selected for further developments.

Table 4-4: The oxidative stress test results after 11 days for the two BCO-loaded NLC formulations with carnauba wax:BCO ratios 40:60 and 20:80 (PlantaCare 2000 as surfactant). The sample with the lower BCO content (carnauba wax:BCO 40:60) had a lower peroxide number value (n=3).

Carnauba wax:BCO ratio	Peroxide number (mmol O_2/kg)
40:60	73±1.1
20:80	115±0.8

4.2.1.2.4 Surfactant and its concentration

The two surfactants PlantaCare 2000 and Inutec SP1 were investigated. These surfactants are accepted in personal care products. The optimal concentration of these two surfactants has been determined for a 45% (w/w) lipid phase NLC (carnauba wax:BCO ratio 40:60). The NLC formulations were prepared using different concentrations of the two surfactants and the PCS particle size was measured (Figure 4-4, Figure 4-5). Increasing the PlantaCare 2000 concentration above 5% (w/w) did not cause any further reduction in particle size. Also increasing the Inutec SP1 concentration above 4% (w/w) did not cause any reduction in particle size. An undesired thin lipid film on the surface of the NLC suspension could be seen after production when the NLC are stabilized with Inutec SP1. This film did not appear when PlantaCare 2000 was used. Therefore, PlantaCare 2000 was chosen to be the surfactant of choice, using the concentration of 5% (w/w) for the 45% (w/w) lipid phase.

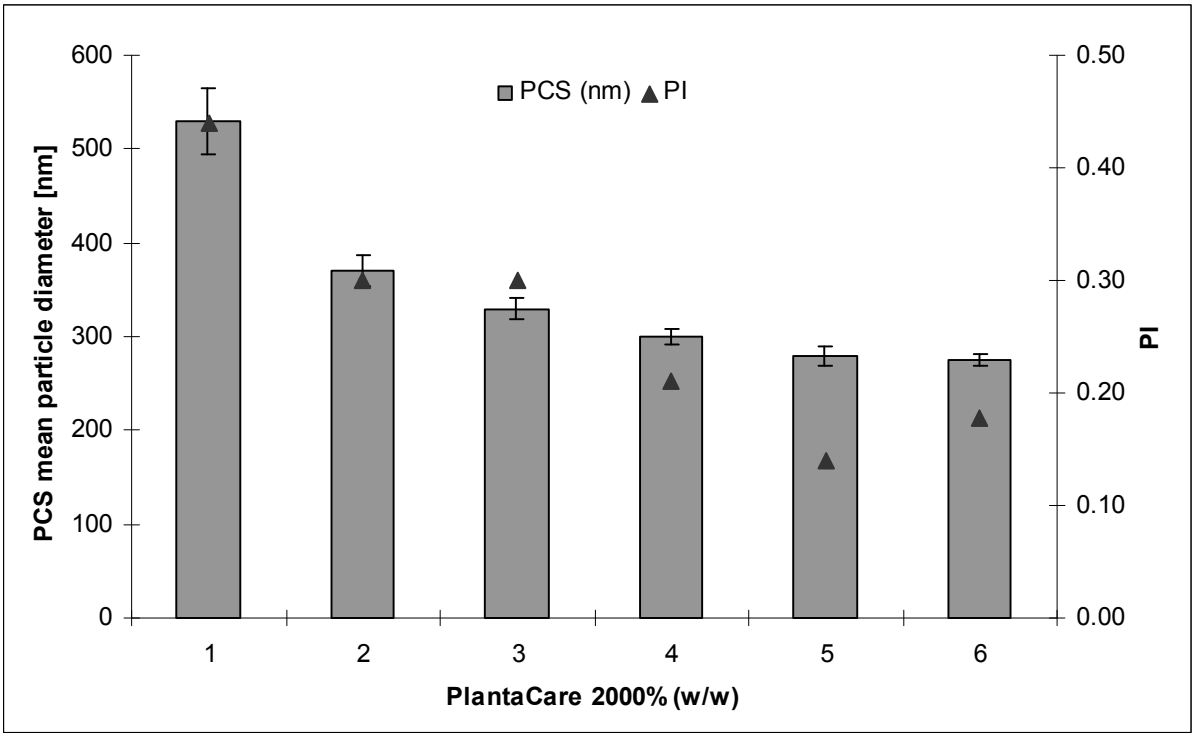

Figure 4-4: PCS particle size and PI of the NLC formulations produced using PlantaCare 2000 at different concentrations (lipid phase 45% (w/w), carnauba wax:BCO 60:40). No change in the particle size above 5% (w/w) PlantaCare 2000 was observed.

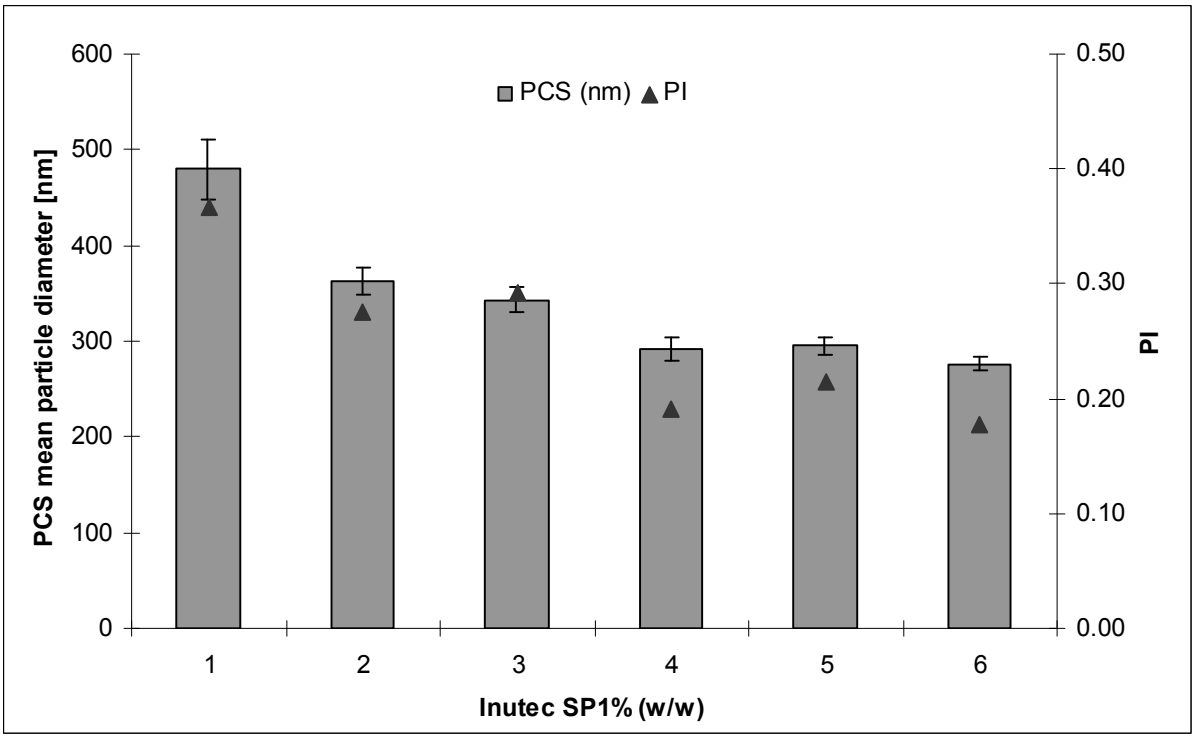

Figure 4-5: PCS particle size and PI of NLC formulations produced using Inutec SP1 at different concentrations (lipid phase 45% (w/w), carnauba wax:BCO 60:40). No change in the particle size above 4% (w/w) Inutec SP1 was observed.

4.2.2 Physical stability of the Q10 and BCO loaded NLC

After adjusting the production parameters and the composition of the BCO-loaded NLC, Q 10 was successfully added to the formula. Due to the high lipophilicity of the Q10 it could be easily dissolved in the lipid phase during production. The 27% (w/w) BCO in the total formula were reduced to 25% (w/w) and Q10 was instead added (2% (w/w) to the total formula). For the physical stability study the so called "master formula" was produced and stored at four different temperatures (4°C, RT, 40°C and 50°C). The composition of the master formula is shown in Table 4-5.

Table 4-5: The composition of the "master formula" of the Q10 and BCO loaded NLC.

Composition	% (w/w)
carnauba wax	18
BCO	25
coenzyme Q 10	2
PlantaCare 2000	5
water	50

4.2.2.1 Particle size analysis by PCS and LD

The particle size analysis results for the samples stored at the four different temperatures on day 0 and after 14 days, 1, 3, 9 and 13 months are depicted in Figure 4-6 and Figure 4-7.

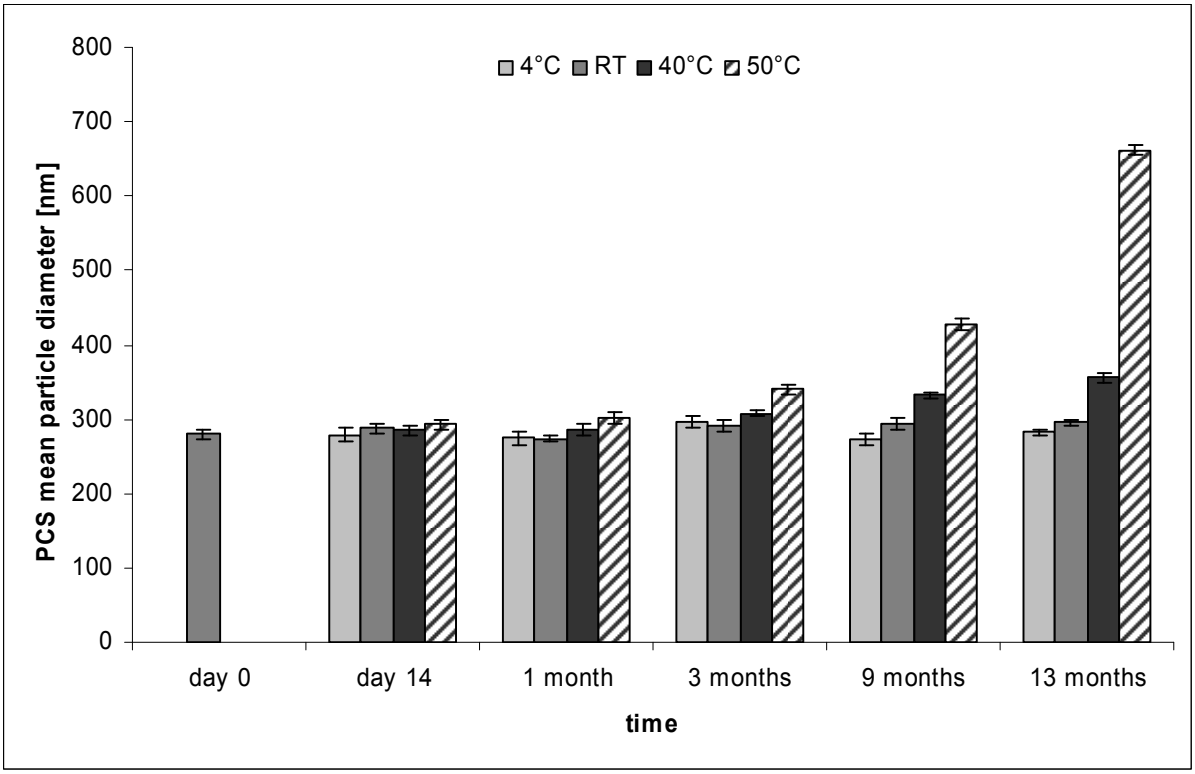

Figure 4-6: The PCS particle size of the Q10 and BCO loaded NLC (master formula) at day 0 and after 14 days, 1, 3, 9 and 13 months at 4ºC, RT, 40ºC and 50ºC.

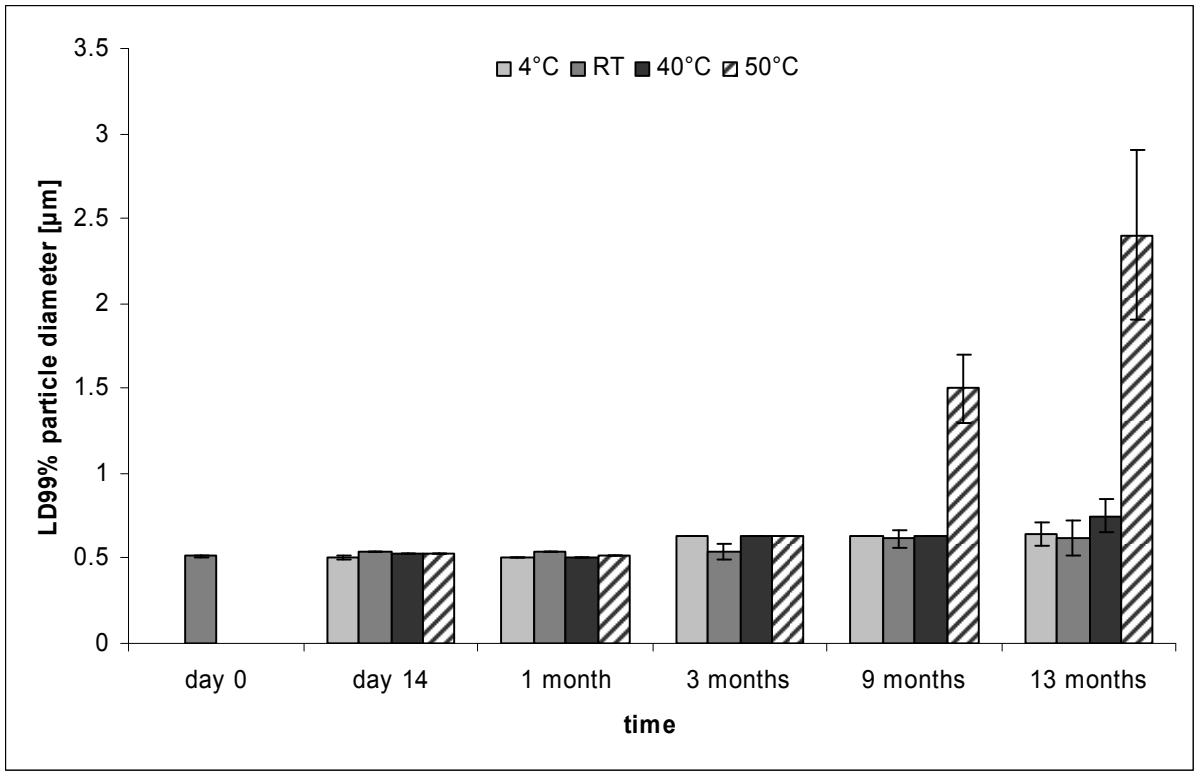

Figure 4-7: The LD99% particle size of the Q10 and BCO loaded NLC (master formula) at day 0 and after 14 days, 1, 3, 9 and 13 months at 4ºC, RT, 40ºC and 50ºC.

No or very little change in the particle size after 13 months could be recorded at the three lower storage temperatures. An increase in particle size was measured for the sample stored at 50°C after 9 months. The high temperature condition led to particle aggregation. The formula is considered to be physically stable according to the cosmetic industry requirements where the stability is monitored for only one month when the sample is stored at 45ºC [249, 250].

4.2.2.2 Zeta potential analysis

The analysis of the zeta potential, which is the electric potential at the plan of shear, is a useful tool to predict the physical stability of colloidal systems. Nanoparticles representing a high zeta potential value indicate good physical stability [210]. The zeta potential of the master formula after production was -55.0 mV ± 0.9 indicating good physical stability since particles aggregation was not likely to occur due to the electrostatic repulsion between the particles. The surfactant PlantaCare 2000 is a nonionic surfactant and the chain length of the decyl glucoside provides a steric hindrance that gives additional particle stabilization. The zeta potential values of the samples stored at the four different storage temperatures have been measured after one and 13 months (Table 4-6).

Table 4-6: The zeta potential values after 1 and 13 months of the "master formula" samples stored at 4ºC, RT, 40ºC and 50ºC.

Storage temperature	1 month	13 months
4°C	-56.0±2.1	-52.0±2.0
RT	-53.8±1.2	-53.0±2.0
40°C	-55.8±1.4	-56.7±2.0
50°C	-54.4±1.6	-48.7±0.3

No change in the zeta potential values of the samples stored at 4°C, RT and 40°C occurred after one month or 13 months. There was a decrease in the zeta potential value of the sample stored at 50°C after 13 months indicating a change in the particles. This can be confirmed by the LD and PCS measurements where particle size growth was observed (Figure 4-6 and Figure 4-7).

4.2.3 Chemical stability of BCO and Q10 in the loaded NLC

4.2.3.1 BCO stability: determination of the peroxide value

The chemical stability of the BCO was determined by employing an "oxidative stress test" on different samples (the NLC master formula, an o/w reference emulsion and the BCO) and then measuring the peroxide number of the BCO (see chapter 2). The amount of BCO in all samples was the same. The lower the peroxide number is the higher is the protective ability of the system against the oxidation of BCO. The NLC master formula showed a higher protection against the oxidation of BCO than the reference emulsion, where the carnauba wax was substituted by Mygliol 812 (Figure 4-8). This is due to the solid matrix of the nanoparticles that hinders the oxygen from reaching to the BCO and oxidizing it.

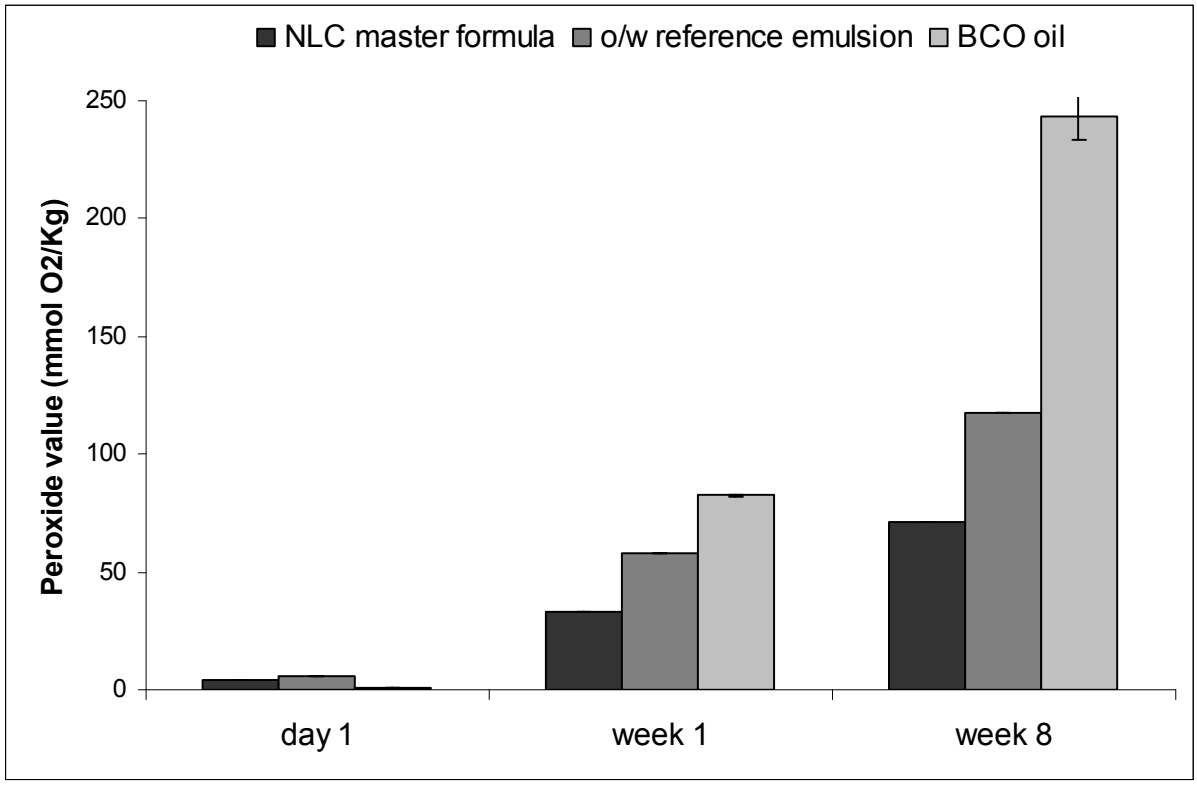

Figure 4-8: The peroxide values of the NLC master formula, the reference emulsion and the BCO after employing the "oxidation stress test" for 8 weeks. The BCO in the NLC sample had lower peroxide number indicating higher protection against oxidation than in the reference emulsion (n=3).

4.2.3.2 Q10 stability

The chemical stability of Q10 in the NLC master formula and a reference emulsion prepared by substituting the carnauba wax by Miglyol 812 has been assessed by HPLC analysis. Figure 4-9 depicts the percentage of Q10 recovered from the NLC during one year of storage at four different storage temperatures. Those values have been determined against a calibration curve. During storage, the amount of Q10 recovered has decreased. 75% of the incorporated Q10 has been measured in the NLC samples stored at 40°C after 12 weeks, and about 80% Q10 after one year in the samples stored at RT.

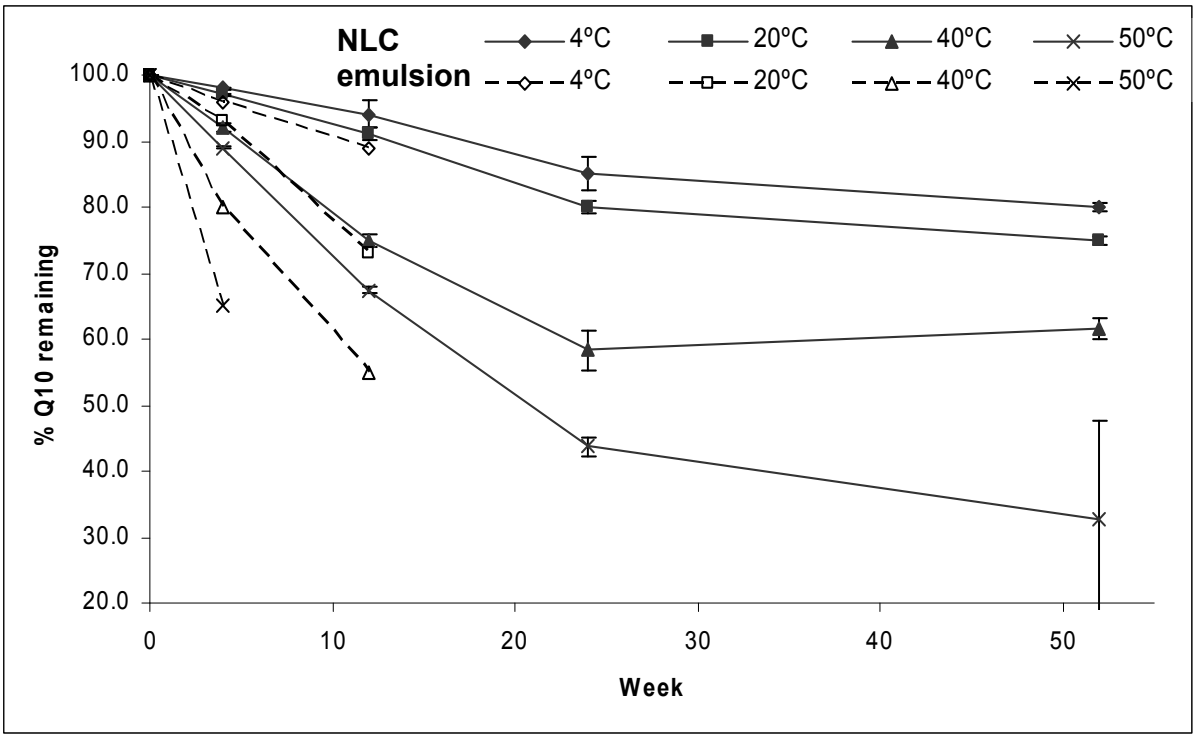

Figure 4-9: Remaining % age Q10 in the NLC master formula and in the reference emulsion at 4ºC, RT, 40ºC and 50ºC storage temperature during one year (emulsion samples measurements were terminated after three months). The Q10 concentration in the NLC was 80% after one year in the sample stored at RT, and 75% at 40ºC after three months (n=4).

The remaining concentration of the Q10 in the reference emulsion was about 65% in the sample stored at 50°C after four weeks with a thin orange layer on the surface. The sample stored at 40°C had a Q10 remaining concentration of about 55% after three months. Moreover, a phase separation occurred in this sample after three months. Recrystallized Q10 was observed on the vials walls of the reference emulsion at the lower storage temperatures (4°C and RT). This caused inhomogeneous distribution of the Q10 in the emulsion and therefore, the HPLC analysis of all reference emulsion samples was terminated after three months. The recrystallization of the Q10 on the vials walls can be explained by the fact that Q10 can freely move from the oil droplets to the aqueous phase and hence precipitate on the container wall. This phenomenon did not happen in the NLC system. Therefore, the NLC developed master formula is an optimal carrier system for the Q10. After one year storage at 50°C the emulsions stabilized with Inutec SP 1 showed a change in color (dark brown) while the emulsions stabilized with PlantaCare 2000 were still orange (Figure 4-10). This can be a result of a chemical incompatibility between the Q10 and Inutec SP1.

Figure 4-10: The reference emulsion samples after 1 year storage at 50°C. A change in the Q 10 color from orange to dark brown was observed in the sample stabilized using Inutec SP1 (the vial at the left). The sample stabilized using PlantaCare 2000 had a normal color (the vial at the right).

4.3 Retinol-loaded NLC

Retinol is highly susceptible to oxidative and light degradation [130]. This high instability makes it hard to produce long-term stable products containing retinol (e.g. creams) due to the loss of activity. Many trials have been performed to stabilize retinol, e.g. incorporation in cyclodextrins [251], liposomes [173], SLN or NLC [130, 252] and adding lipophilic antioxidant to the SLN matrix [253]. In this work different NLC suspensions with higher retinol loading were produced. The physical stability of these suspensions as well as the chemical stability of the incorporated retinol were studied.

4.3.1 Production of retinol-loaded NLC

4.3.1.1 Retinol-loaded NLC based on Retinol 15 D

Retinol was incorporated in NLC formulations using Retinol 15 D, which is a 15% (w/w) retinol solution in medium chain triglycerides (caprylic/capric triglycerides). Based on previous work [130, 252] these NLC formulations were produced from different lipids and stabilized by different surfactants. The concentration of the retinol in these formulations was 0.5% (w/w) to the total formula, the composition is listed in Table 4-7.

Table 4-7: The composition of the formulations containing 0.5% (w/w) retinol. The lipid was either Compritol 888, Elfacos C 26 or Imwitor 900, the surfactant either Tween 80, Inutec SP1 or Miranol 32.

Composition	% (w/w)
lipid	10.0
Mygliol 812	1.7
Retinol 15 D	3.3
surfactant	1.5
water	83.5

The NLC suspensions produced using Imwitor 900 were excluded from further investigations because of chemical instability (data not shown). Elfacos and Compritol NLCs were selected for further investigations whereby the concentration of the retinol in the formulation was increased to 0.75% and 1.0% (w/w). The compositions of these formulations are listed in next two tables.

Table 4-8: The composition of the formulations containing 0.75% (w/w) retinol. The lipid was either Compritol 888 or Elfacos C 26, the surfactant either Tween 80, Inutec SP1 or Miranol 32.

Composition	% (w/w)
lipid	10.0
Retinol 15 D	5.0
surfactant	1.5
water	83.5

Table 4-9: The composition of the formulations containing 1.0% (w/w) retinol. The lipid was either Compritol 888 or Elfacos C 26, the surfactant either Tween 80 or Miranol 32.

Composition	% (w/w)
lipid	10.0
Retinol 15 D	6.7
surfactant	1.5
water	82.8

During the NLC production the retinol (Retinol 15 D) was always added after melting the lipid to avoid the contact between retinol and air at high temperature for a longer time and hence the retinol oxidation.

4.3.1.2 Retinol-loaded NLC based on Retinol 50 C

In this part of the work retinol was incorporated in NLC formulations using Retinol 50 C, which is a 50% retinol solution in polysorbate 20. The retinol concentration was 3% (w/w) to the total formula and the solid lipid was carnauba wax. The detailed composition of these NLC formulations is listed in Table 4-10.

Table 4-10: The composition of the formulations containing 3.0% (w/w) retinol in the total formula.

Formula	Composition	% (w/w)
Retinol C1	carnauba wax	6.0
	Retinol 50 C	6.0
	Miranol 32	2.0
	water	86.0
Retinol C2	carnauba wax	12.0
	Retinol 50 C	6.0
	Miranol 32	2.0
	water	80.0

4.3.2 Physical stability of the retinol-loaded NLC

For the physical stability study all samples were stored at room temperature and at 40ºC. The particle size was measured using PCS and LD one day after production and up to nine months. The following nine figures show the particle size of the different formulations produced based on Retinol 15D. Remarkably the particle size of the higher retinol loading formulations (1.0% (w/w)) was smaller than the lower retinol loading ones (0.5% and 0.75% (w/w)). This might be due to the increase in the homogenization efficacy when the viscosity of the lipid phase is decreased, maintaining all homogenization conditions constant for all formulations (see chapter 2). This occurred when the amount of the liquid lipid (Mygliol 812 as Retinol 15 D) was increased in the formulations of the higher retinol loading (1.0% (w/w)) and the amount of the solid lipid was maintained the same (see Table 4-7, Table 4-8 and Table 4-9). Although the total amount of the lipid phase in these formulations is more than the

total amount of the lipid phase in the formulations of the lower retinol loading (16.7 % and 15.0% (w/w) respectively), but the ratio of the liquid lipid to the solid lipid is also higher. That means, each droplet of the lipid phase in the emulsion (the NLC during homogenization) contains a higher amount of Mygliol 812. That makes it less viscous and hence easier to homogenize [234].

The NLC formulations produced using carnauba wax had a particle size below 0.6 µm (Figure 4-20). The formulation Retinol C1 contains only 6.0% (w/w) carnauba wax, while the formulation Retinol C2 contains 12% (w/w) carnauba wax, i.e. the total lipid phase is less in the first formulation. This makes it easier to homogenize in compare to the second formulation and hence, smaller particle size is obtained.

The formulations with the highest retinol loading were physically the most stable, i.e. no remarkable change in particle size was recorded after nine months. This is due to the increased amount of the liquid lipid too. It inhibits the crystallization of the most stable, more ordered polymorph of the solid lipid and hence the aggregations and particle size growth [214].

Aggregations and increase in particle size were noticed in the formulations which were produced using Inutec SP1. This can be due to the insufficient stabilization achieved by using Inutec SP1 alone as surfactant.

The zeta potential values were determined for the formulations based on Retinol 15 D one day after production and after nine months (Table 4-11). It can be noticed that the formulations stabilized by Miranol 32 had zeta potential values between -30 mV and -50 mV indicating good physical stability. The formulations stabilized by Tween 80 had lower zeta potential values (between -10 mV and -20 mV). Due to the steric stabilization of this surfactant, these zeta potential values are sufficient to stabilize the particles and prevent aggregation. The formulations stabilized by Inutec SP1 had relatively lower zeta potential values. After nine month a decrease in the zeta potential value could be noticed indicating changes in the particles structure (aggregation).

Table 4-11: The zeta potential values of the Retinol 15 C based formulations stored at RT and 40ºC one day after production and after nine months.

Retinol conc. (w/w)	Lipid	Surfactant	Day 1	9 months	
			RT	RT	40°C
0.5%	Compritol 888	Inutec SP1	-17.5±0.7	-9.5±0.9	-5.4±0.2
		Tween 80	-16.0±0.6	-15.0±0.2	-17.0±0.6
		Miranol 32	-36.4±0.4	-37.1±0.3	-31.2±0.4
	Elfacos C 26	Inutec SP1	-27.5±0.6	-25.7±0.5	-22.1±0.6
		Tween 80	-23.2±0.3	-24.1±0.5	-25.0±0.7
		Miranol 32	-49.2±0.2	-50.4±0.1	-43.2±0.8
0.75%	Compritol 888	Inutec SP1	-12.0±0.7	-8.0±0.3	-7.5±0.6
		Tween 80	-12.4±0.1	-11.3±0.1	-18.0±0.1
		Miranol 32	-31.2±0.3	-39.1±0.2	-46.9±2.0
	Elfacos C 26	Inutec SP1	-23.3±1.3	-18.7±0.2	-16.1±0.9
		Tween 80	-17.9±2.1	-18.9±0.4	-14.5±0.5
		Miranol 32	-51.6±2.3	-43.8±1.0	-35.0±0.2
1.0%	Compritol 888	Miranol 32	-42.0±0.2	-40.1±0.7	-39.3±0.2
		Tween 80	-10.1±0.1	-11.2±0.4	-9.7±0.6
	Elfacos C 26	Miranol 32	-48.8±0.6	-48.8±0.6	-48.8±0.6
		Tween 80	-14.1±0.3	-15.5±0.7	-15.1±0.3

The zeta potential values of the two formulations based on Retinol 50 C and carnauba wax were also determined one day after production and after nine months. These values were -54.2 mV ± 0.7 and -49.3 mV ± 0.8 one day after production and -52.1 mV ± 0.8 and -48.5 mV ± 0.4 after nine months for the Retinol C1 and Retinol C2 formulations, respectively. The zeta potential values one day after production indicate a very good physical stability for the two formulations. These values did not change after nine months of storage indicating long-term physical stability of the formulations.

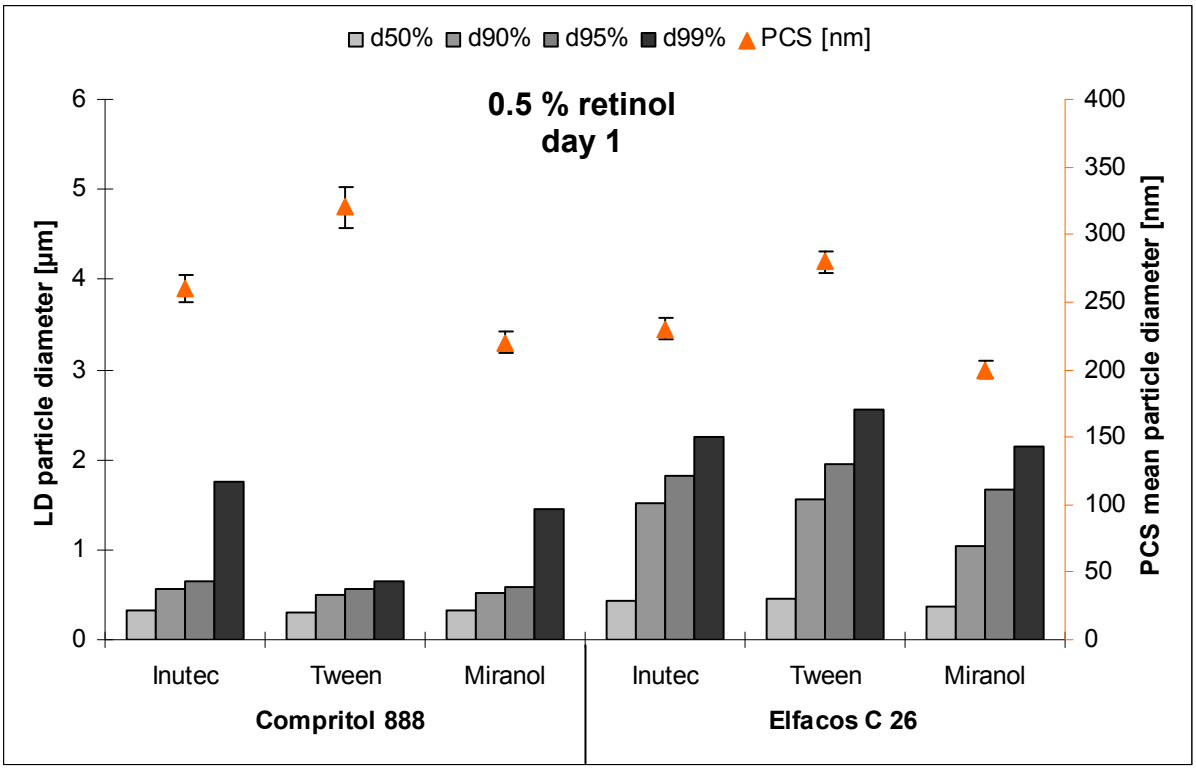

Figure 4-11: Day 1 PCS and LD particle size of the NLC formulations containing 0.5% (w/w) retinol, all particle sizes were below 2.5 µm (d99%).

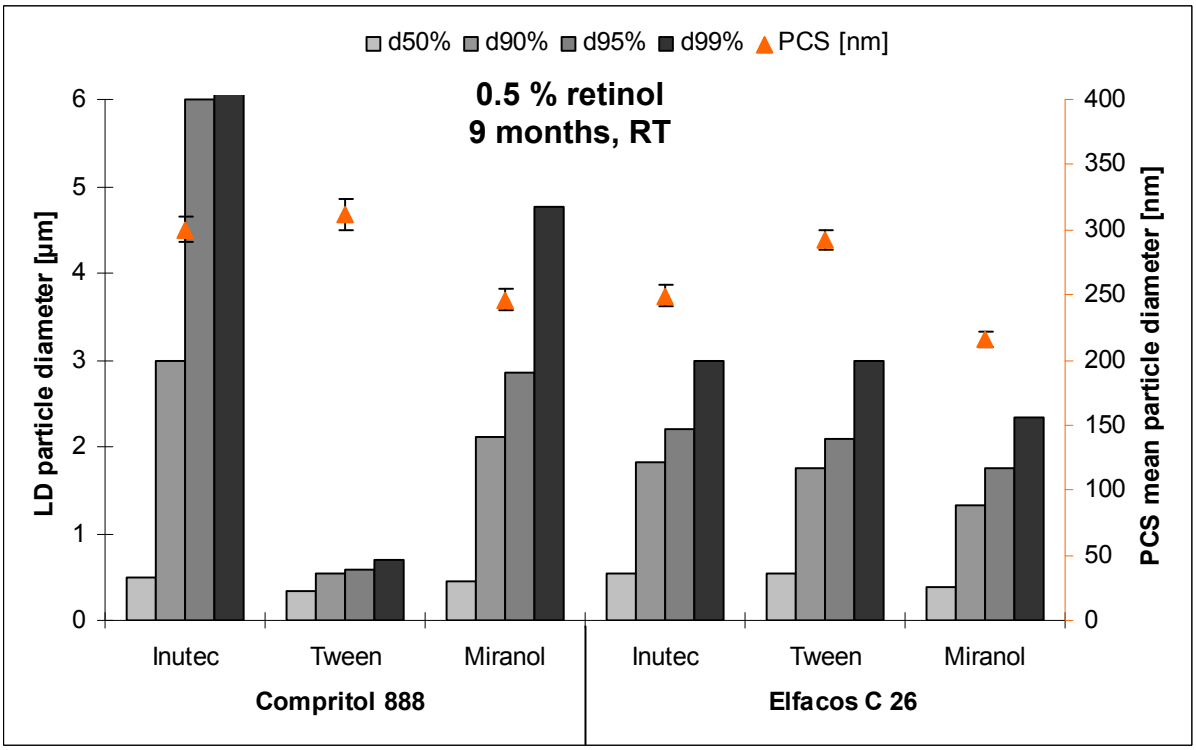

Figure 4-12: Month 9 (RT) PCS and LD particle size of the NLC formulations containing 0.5% (w/w) retinol. An increase in the particle size of the sample produced using Compritol and Inutec was measured.

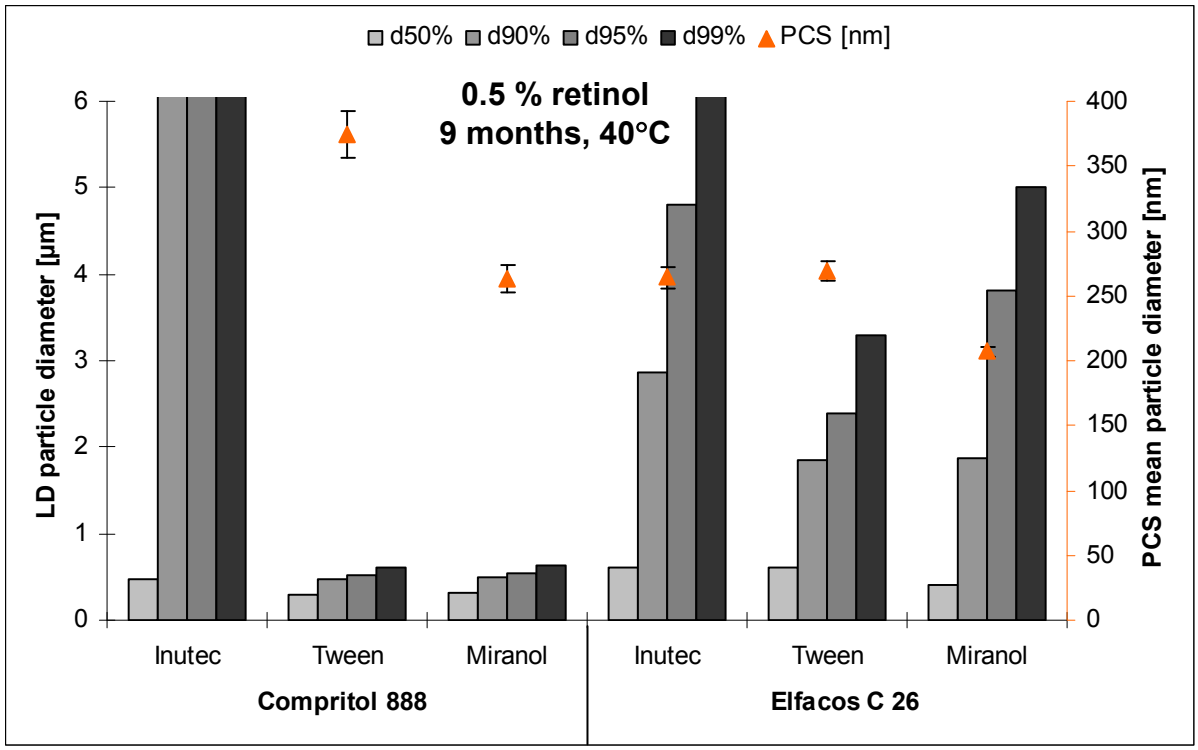

Figure 4-13: Month 9 (40ºC) PCS and LD particle size of the NLC formulations containing 0.5% (w/w) retinol. The samples produced using Inutec had an increase in particle size.

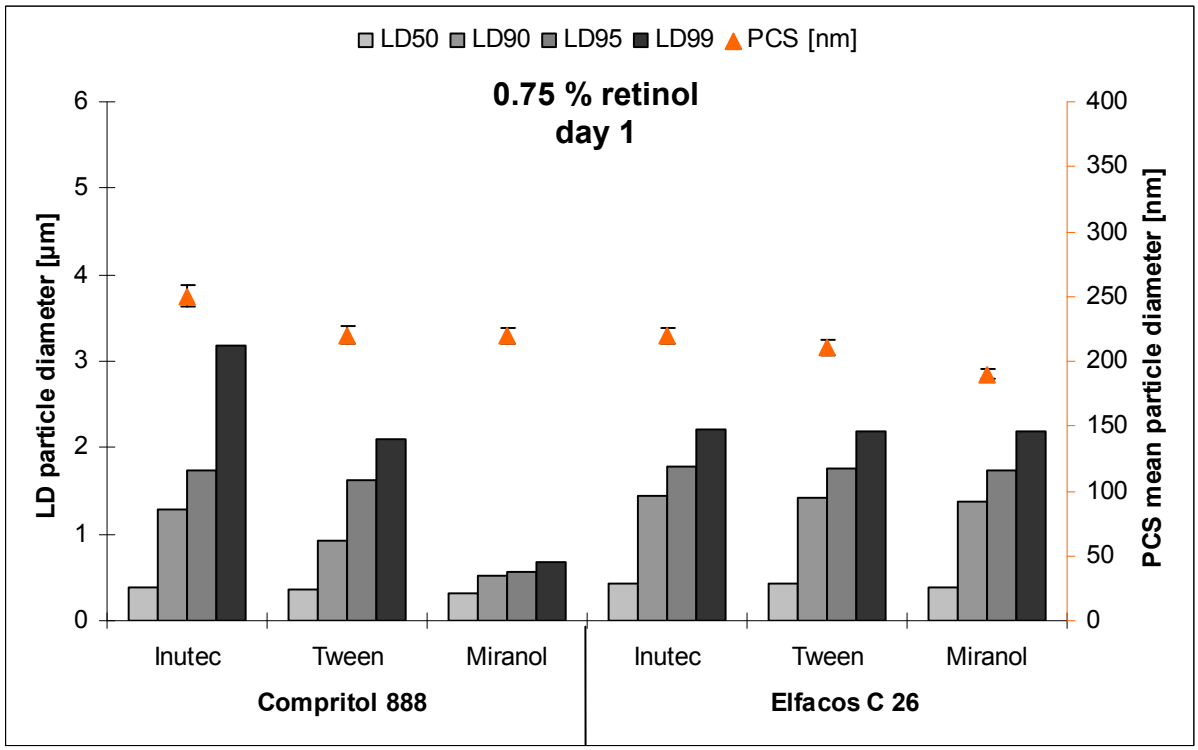

Figure 4-14: Day 1 (RT) PCS and LD particle size of the NLC formulations containing 0.75% (w/w) retinol, all particle sizes were below 2.0 µm (d99%) except the Compritol Inutec formula.

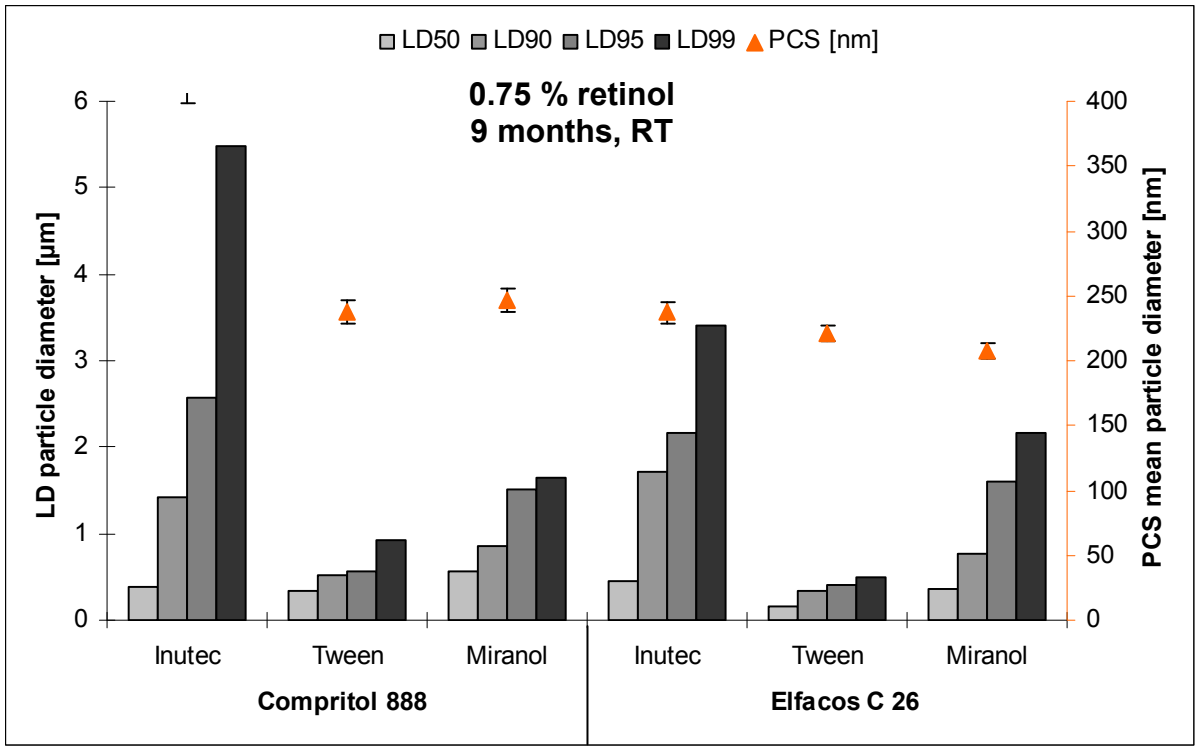

Figure 4-15: Month 9 (RT) PCS and LD particle size of the NLC formulations containing 0.75% (w/w) retinol. The samples produced using Inutec had an increase in particle size.

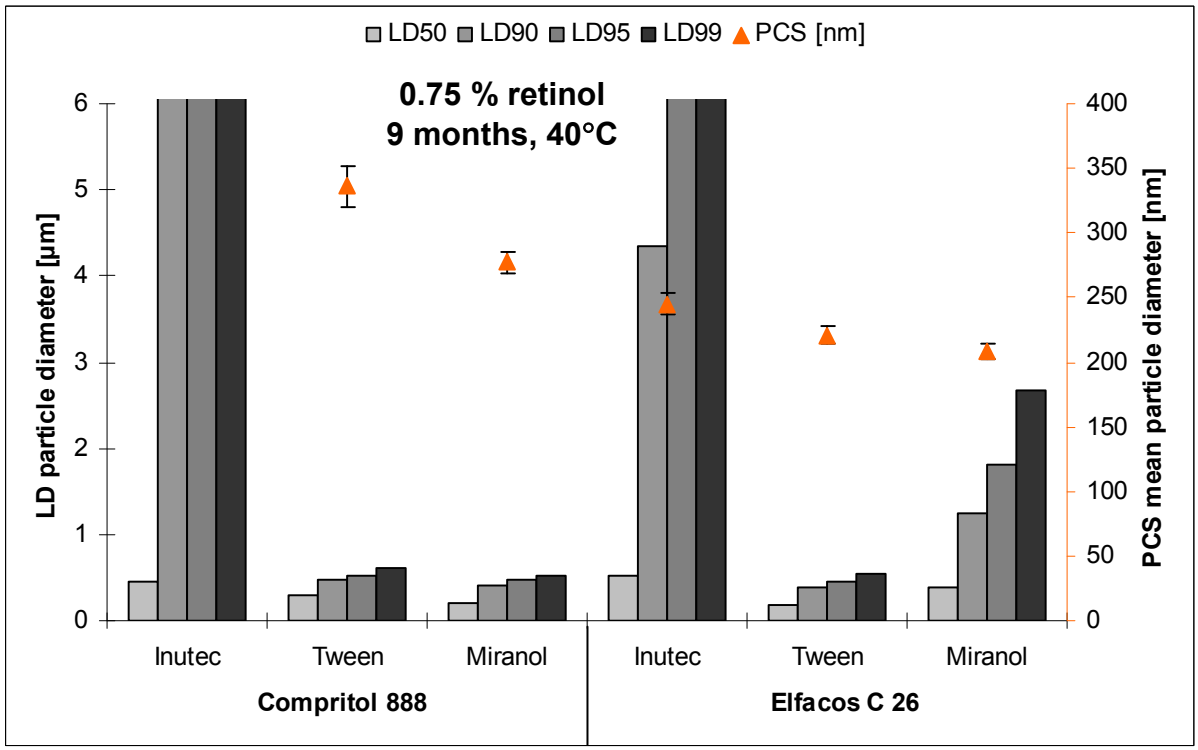

Figure 4-16: Month 9, (40°C) PCS and LD particle size of the NLC formulations containing 0.75% (w/w) retinol. The samples produced using Inutec had an increase in particle size.

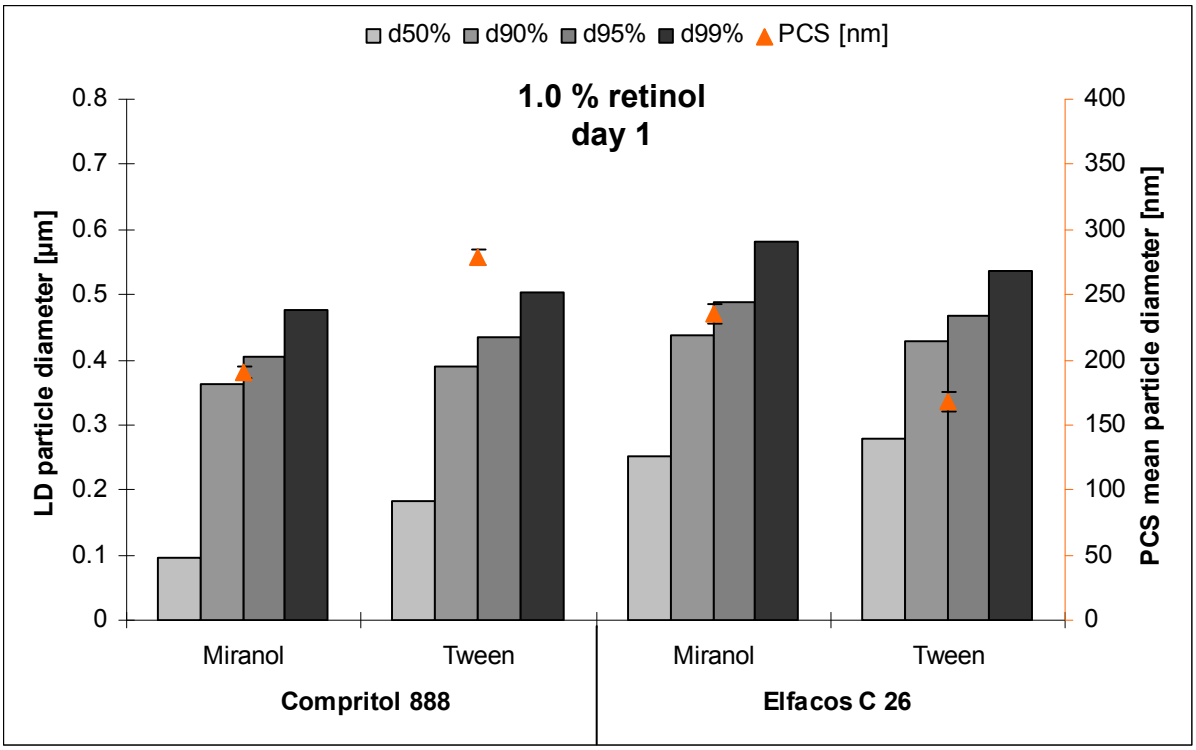

Figure 4-17: Day 1 (RT) PCS and LD particle size of the NLC formulations containing 1.0% (w/w) retinol, all particle sizes were below 0.6 µm (d99%).

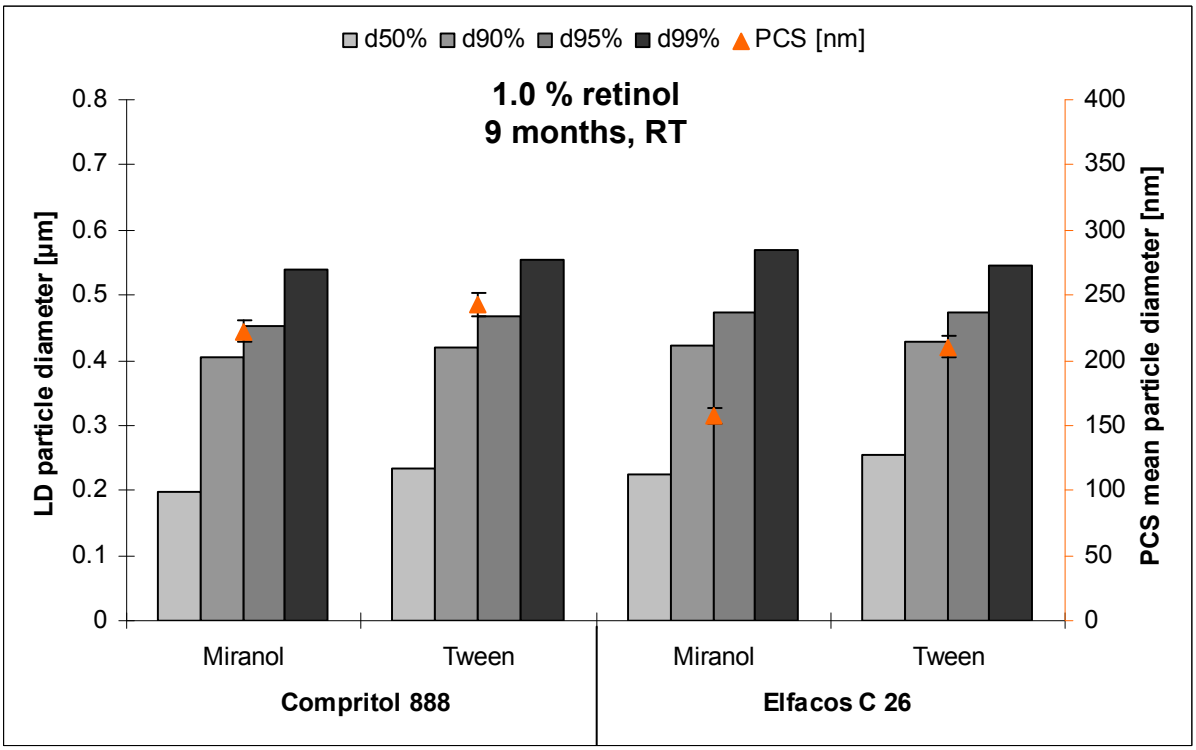

Figure 4-18: Month 9 (RT) PCS and LD particle size of the NLC formulations containing 1.0% (w/w) retinol. The particle size of all samples stayed below 0.6 µm (d99%).

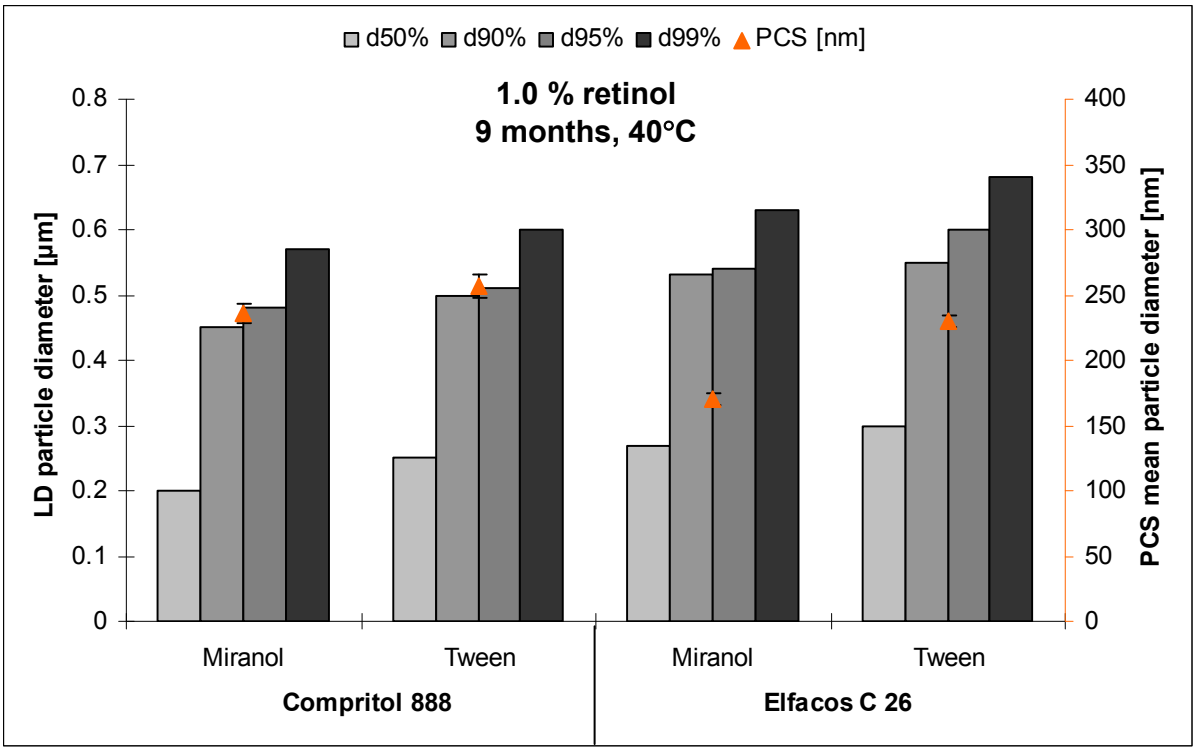

Figure 4-19: Month 9, (40°C) PCS and LD particle size of the NLC formulations containing 1.0% (w/w) retinol. The particle size of all samples stayed below 0.6 µm (d99%).

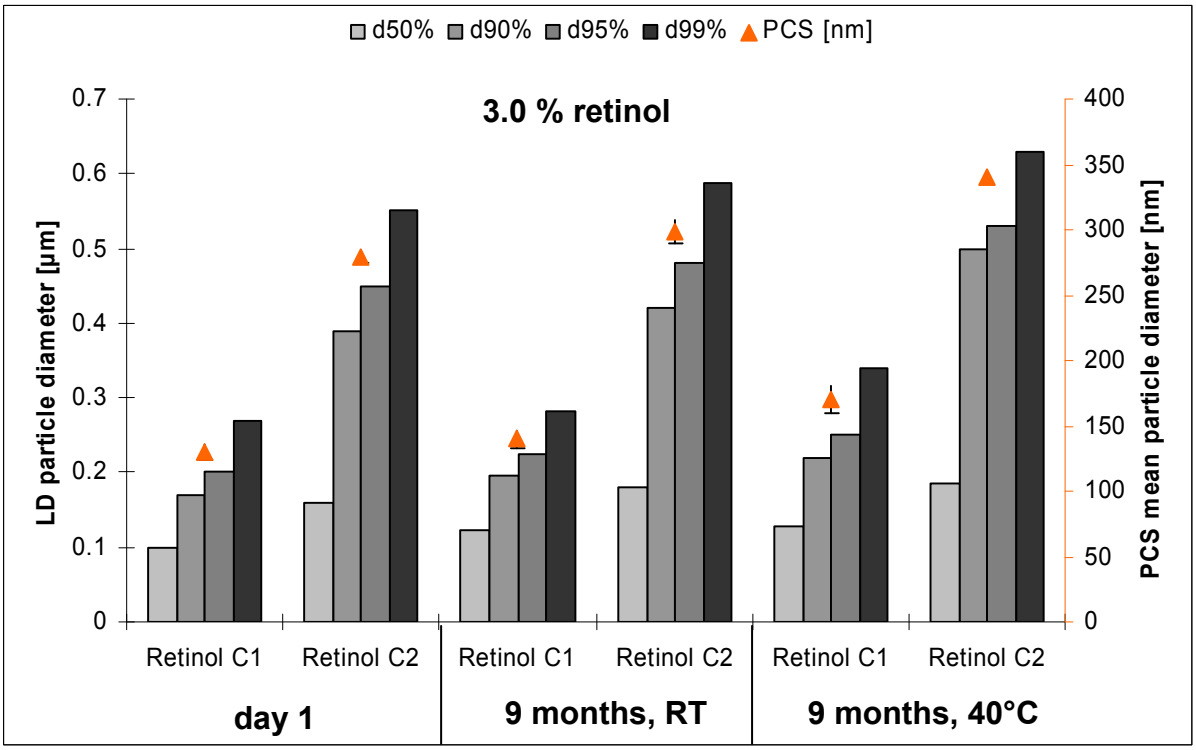

Figure 4-20: Day 1 and month 9 (RT and 40°C) PCS and LD particle size of the NLC formulations containing 3.0% (w/w) retinol. The particle sizes were below 0.6 µm (d99%) at day 1 and after 9 months.

4.3.3 Chemical stability of retinol in the retinol-loaded NLC

The retinol-loaded NLC formulations were stored at room temperature and at 40ºC and the chemical stability of retinol was investigated. Over one year the remaining retinol concentration was assessed using HPLC. The next seven figures show the %age remaining of retinol in the different formulations. The samples with the highest %age remaining retinol were considered the most stable. Retinol was more stable in the higher retinol loading formulations than in the lower retinol loading formulations. Comparing the %age retinol remaining in the formulations based on Retinol 15 D with 0.5%, 0.75% and 1.0% (w/w) retinol loading stored at room temperature, the retinol in the formulations with 1.0% (w/w) retinol loading was clearly the most stable. The %age retinol remaining in the 1.0% (w/w) retinol loading formulations was about 80% while in the 0.75% (w/w) formulations it was between 60% and 70%, and in the 0.5% (w/w) retinol loading formulations it was between 40% and 65% (Figure 4-21, Figure 4-23 and Figure 4-25). This is due to the increased amount of the oil in which the retinol is dissolved (Retinol 15 D). It inhibits the crystallization of the most stable, more ordered polymorph of the lipid. Due to the increased number of imperfections in the crystal lattice, a higher amount of retinol can be incorporated in the inner core of the particles. This inclusion enhances the chemical stability.

The retinol in the formulation composed of Compritol 888 and Inutec SP1 (both 0.5% and 0.75% (w/w) retinol loading) showed the lowest stability (Figure 4-22 and Figure 4-24). This is because of the expulsion of the retinol from the lipid matrix of the nanoparticles. This was accompanied with particle size growth and lipid aggregations (physical instability).

The retinol in the formulations composed of Compritol 888 and Tween 80, Elfacos C 26 and Tween 80 and Elfacos C 26 and Miranol 32 and with a 1.0% (w/w) retinol loading showed the highest retinol stability in comparison to the same formulations with the lower retinol loading (0.5% and 0.75% (w/w)) (Figure 4-22, Figure 4-24 and Figure 4-26).

Figure 4-27 shows the %age retinol remaining of the retinol in the two formulations based on the Retinol 50 C and stored at room temperature and at 40ºC. At room temperature after one year the %age retinol remaining in the formulation Retinol C1 was 77% while in the formulation Retinol C2 the %age retinol remaining was only 68%. This can be explained by the inhibition of the crystallization of the most stable, more ordered carnauba wax polymorph duo to the high polysorbate 20:carnauba wax ratio (1:1 in the Retinol C1 formulation and 1:2 in the Retinol C2 formulation). The increased number of imperfections in the crystal lattice of the carnauba wax in C1 causes the retinol to be more incorporated in the inner core of the particles and hence more protected and more chemically stable.

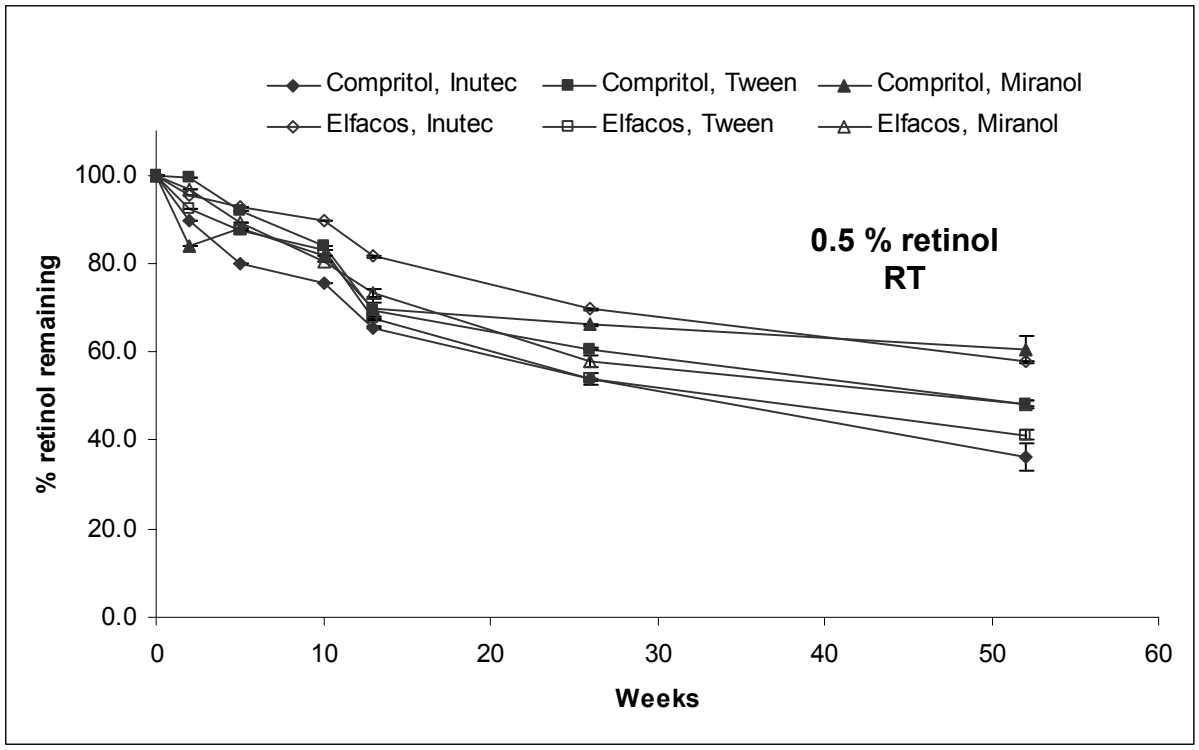

Figure 4-21: The %age remaining retinol in the NLC with 0.5% (w/w) retinol loading stored at RT for one year. After one year the %age remaining retinol was between 40% and 65% (n=4).

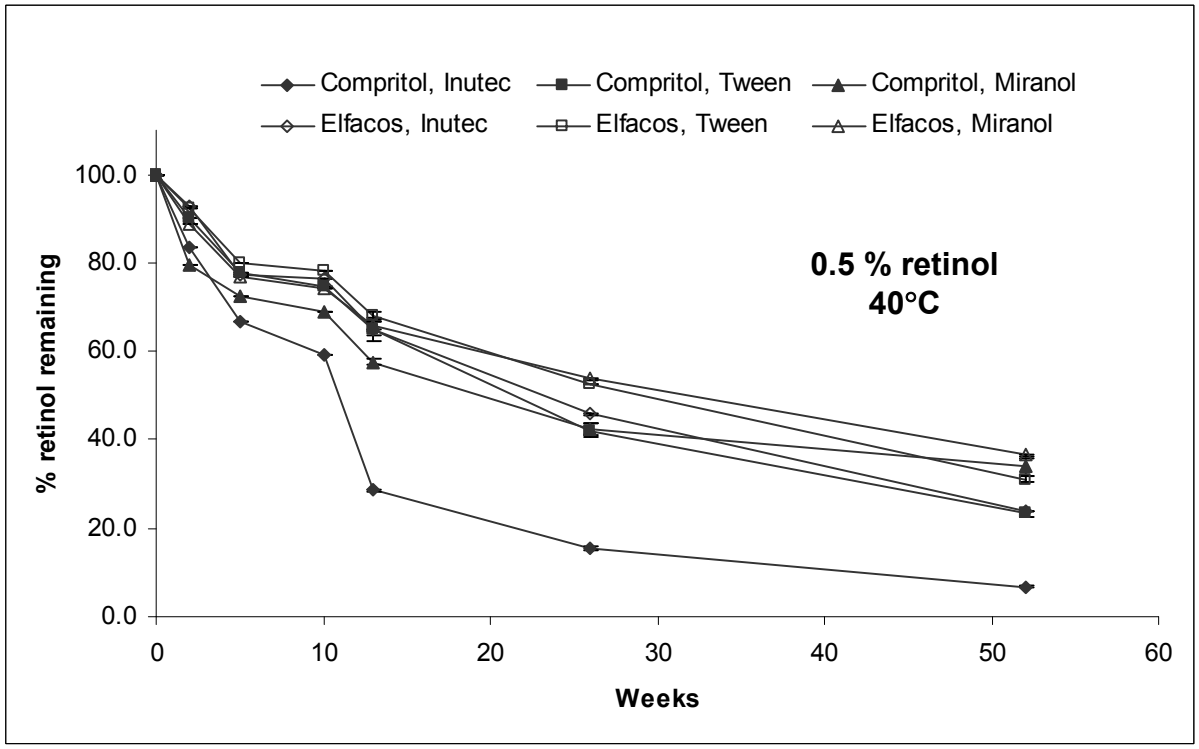

Figure 4-22: The %age remaining retinol in the NLC with 0.5% (w/w) retinol loading stored at 40ºC for one year. The NLC formulation produced using Compritol 888 and Inutec SP1 is clearly chemically not stable (n=4).

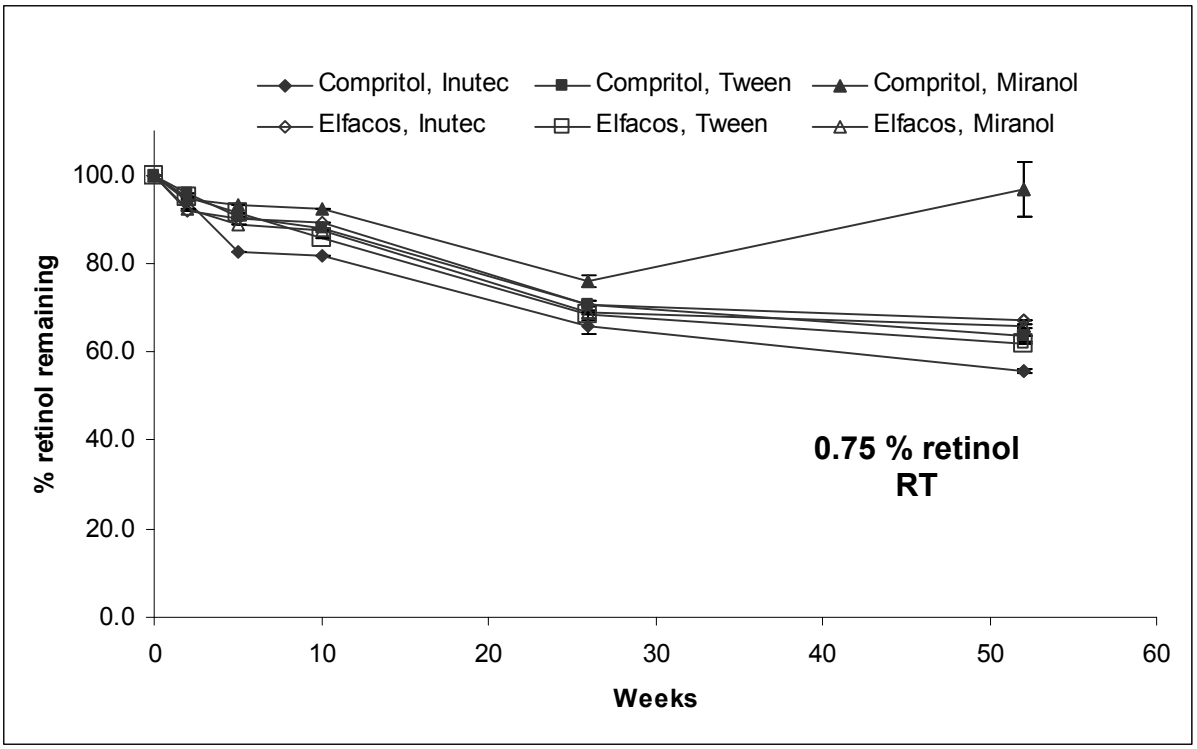

Figure 4-23: The %age remaining retinol in the NLC with 0.75% (w/w) retinol loading stored at RT for one year. After one year the retinol %age remaining was between 60% and 70%. The formulation produced using Compritol 888 and Miranol 32 has a high %age remaining retinol due to water loss (n=4).

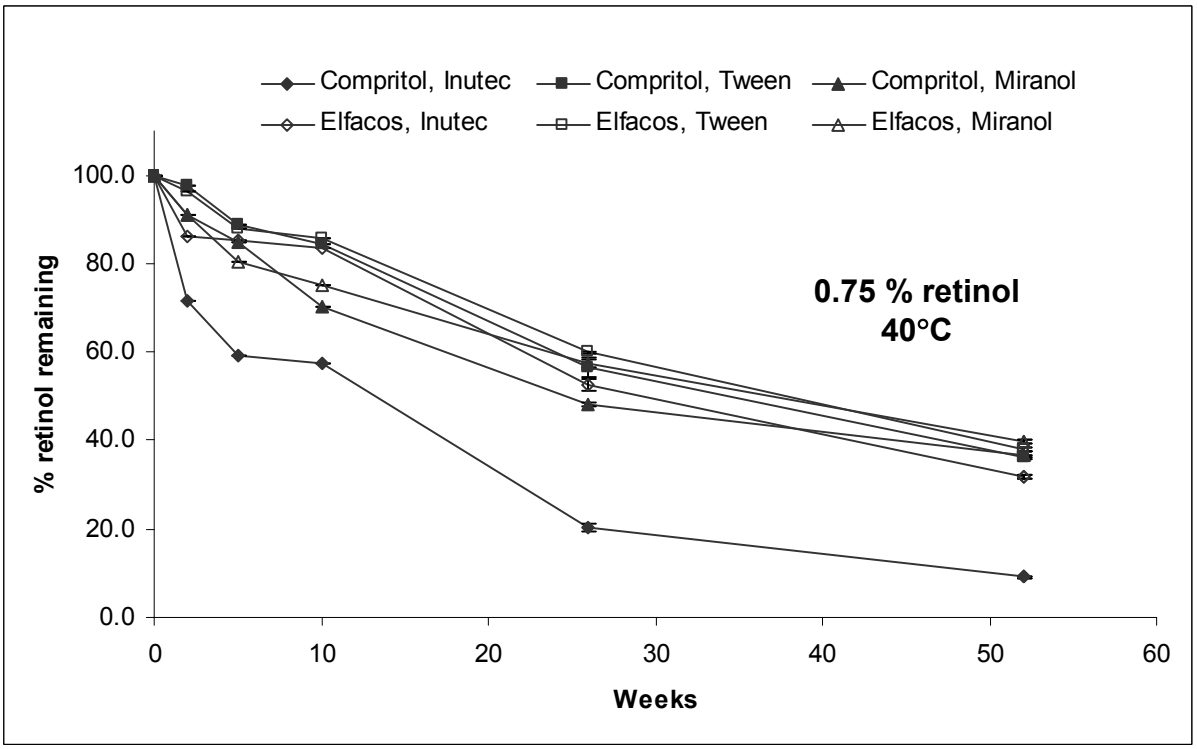

Figure 4-24: The %age remaining retinol in the NLC with 0.75% (w/w) retinol loading stored at 40ºC for one year. The NLC formulation produced using Compritol 888 and Inutec SP1 is clearly chemically not stable (n=4).

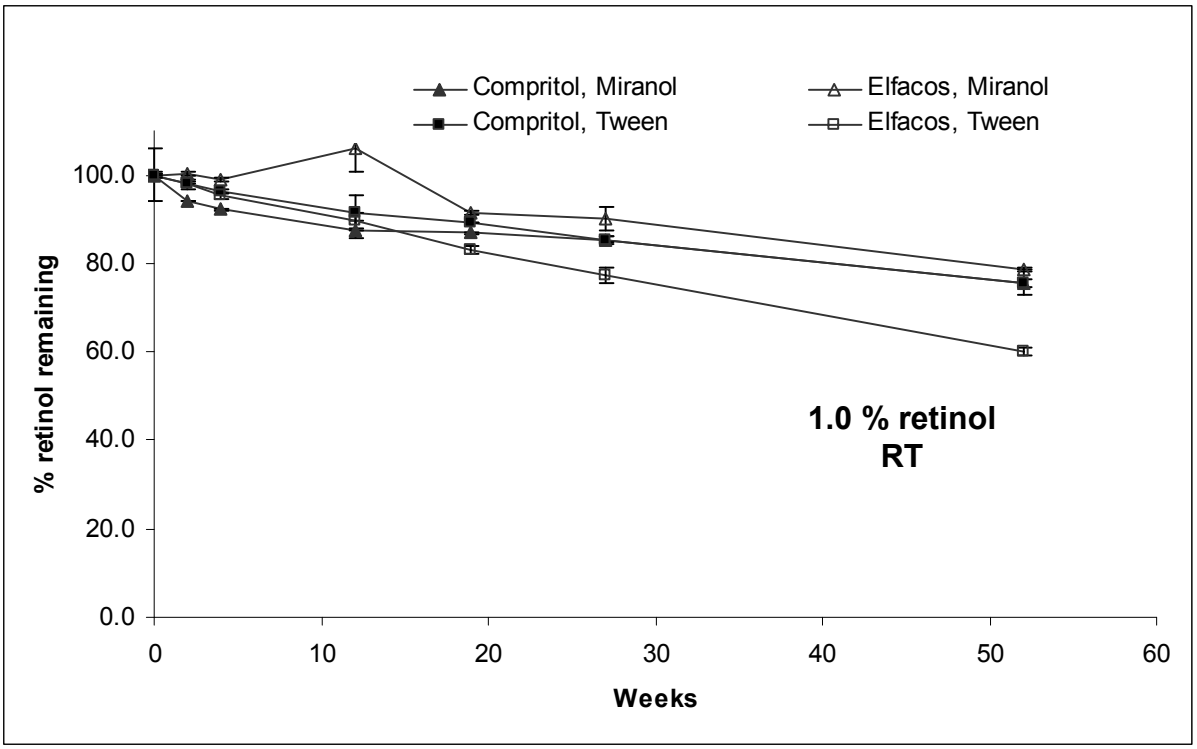

Figure 4-25: The %age remaining retinol in the NLC with 1.0% (w/w) retinol loading stored at RT for one year. After one year the retinol %age remaining in the NLC produced using Elfacos C 26 and Tween 80 was 60%. While the NLC produced using Elfacos C 26 and Miranol 32 contained 79% retinol (n=4).

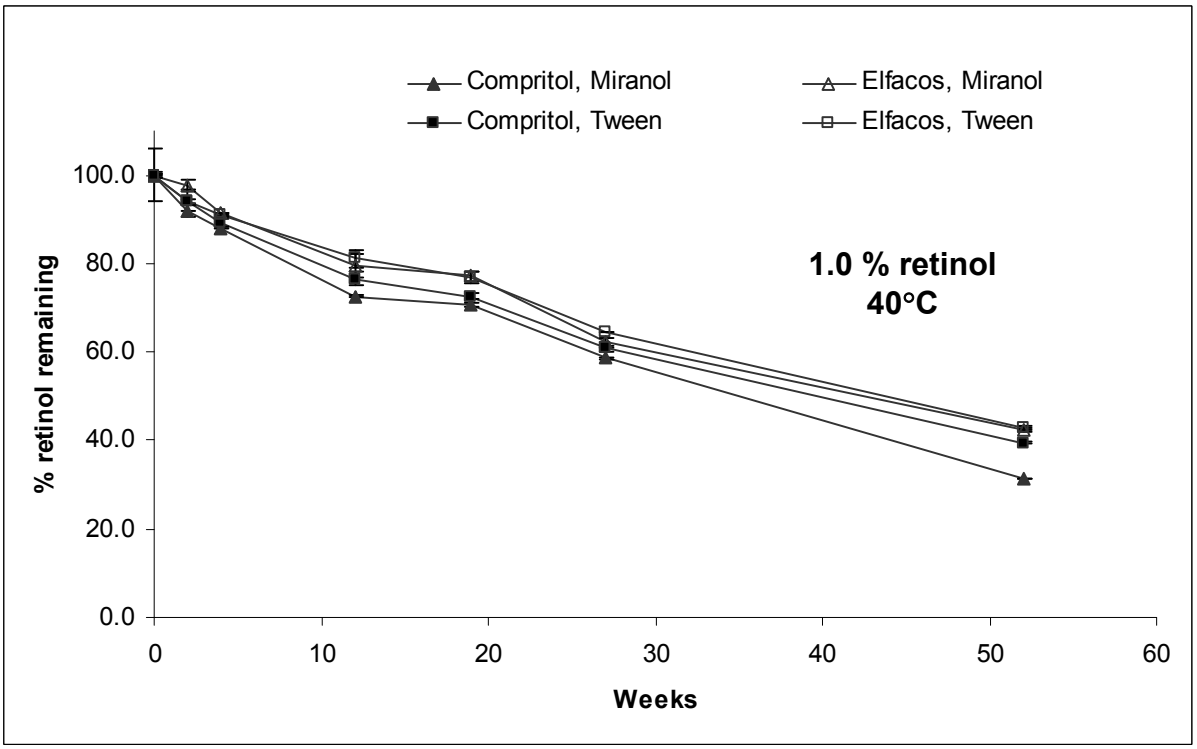

Figure 4-26: The %age remaining retinol in the NLC with 1.0% (w/w) retinol loading stored at 40ºC for one year. After three months the NLC formulation made using elfacos C 26 and Miranol 32 was the most stable one with 80% retinol remaining. After one year the NLC sample made using Compritol 888 and Miranol 32 was the less stable one (n=4).

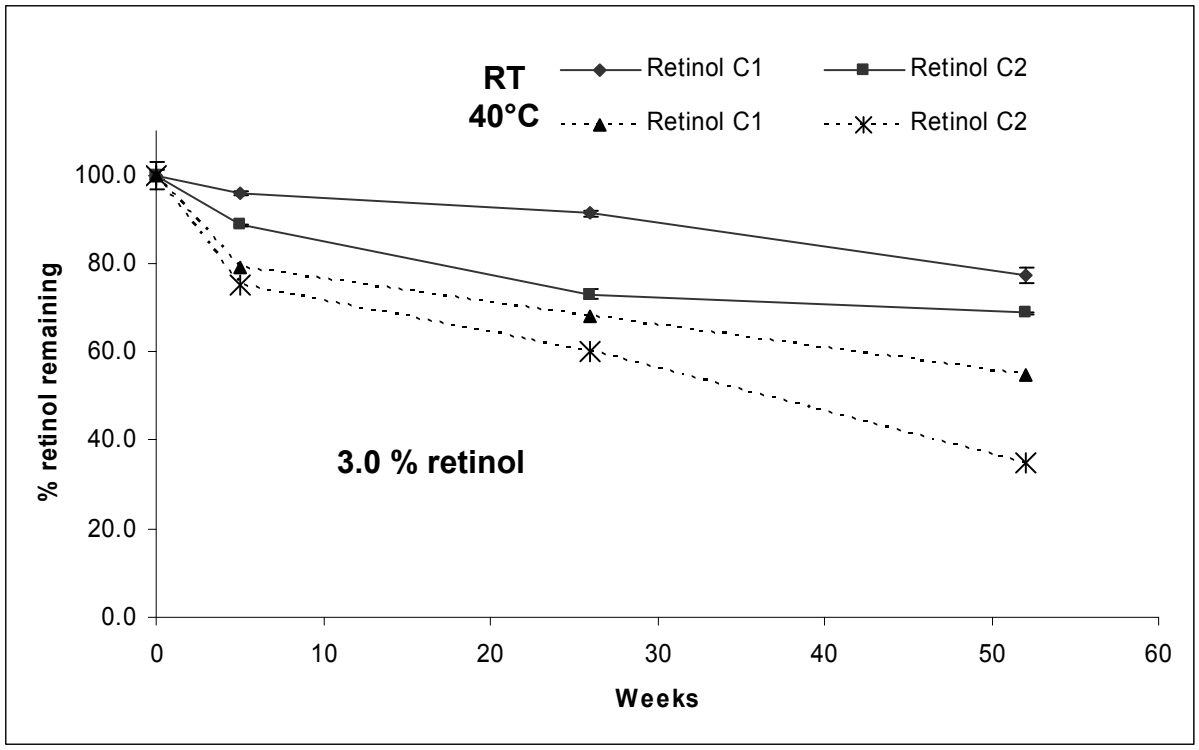

Figure 4-27: The %age remaining retinol in the NLC with 3.0% (w/w) retinol loading stored at RT and 40°C for one year. After one year the %age remaining retinol in the Retinol C1 formulation was 77% while the remained retinol in the Retinol C2 formulation was only 68% (n=4).

From this study it can be concluded that by increasing the retinol loading in the lipid matrix of the NLC an enhanced chemical stability can be achieved.

4.4 Conclusion

In this part of the work coenzyme Q 10 and black currant seed oil-loaded NLC and retinol-loaded NLC were produced and the physicochemical properties of these formulations were evaluated. The production of physically stable formulations, in terms of particle size, was successful for both systems. The chemical stability of Q10, BCO and retinol was improved when they were incorporated in NLC. The chemical stability of these materials in their NLC formulations was better than in their nanoemulsions. The developed formulations can be used in final topical products to achieve improved chemical stability in addition to the positive effects of the lipid nanoparticles on the skin. Concerning the Q10 and BCO loaded NLC, the formulation based on carnauba wax and PlantaCare 2000 showed the best physical and chemical stability. The best retinol formulations based on Retinol 15 D were the formulations containing 1% (w/w) retinol and formulated with Compritol 888 and Tween 80 and with Elfacos C 26 and Miranol 32. Moreover, the formulation based on Retinol 50 C (Retinol C1) showed a very good physical and chemical stability (77%).

5 NLC FOR ULTRAVIOLET (UV) RADIATION PROTECTION

5.1 Introduction

Ultraviolet radiation reaching the surface of the earth contains about 95% of UV-A (320-400 nm) and 5% of UV-B (290-320 nm), while UV-C (200-290 nm) does not reach the surface of the earth because it is absorbed by the ozone layer [174, 254]. This UV load leads to a range of acute and chronic types of skin damage. UV-A, UV-B and UV-C can all damage the collagen fibers and thereby accelerate the aging of the skin. UV-A, also called near ultraviolet region, possesses less energy than UV-B or UV-C radiations and a longer wavelength. Therefore, it penetrates into the skin and reach the dermis provoking several damages such as skin aging, DNA damage and possibly skin cancer [255]. It might cause immediate and delayed tanning reactions but does not cause sunburn because it does not cause reddening of the skin (erythema) and therefore, it can not be measured in the SPF testing. UV-A is considered to be an essential cause of wrinkles [256]. The acute sunburn is mainly caused by the UV-B radiation fraction [174]. This UV radiation fraction can cause skin cancer. It can also excite the DNA molecules in the skin cells, causing the formation of covalent bonds between adjacent thymine bases producing thymidine dimers. To avoid all these harmful effects during the exposure to sunlight, the use of topical sunscreens (UV blockers) became a routine by a large percentage of the population [257]. Sunscreens can be divided into three types, organic sunscreens, inorganic sunscreens and what so called photoprotectors like antioxidants, enzymes and free radical scavengers.

5.1.1 Organic sunscreens

The principle of photoprotection of organic sunscreens is the absorption of UV radiation attributed to the conjugated double bonds of their chemical structures. In general, their chemical structure consists of aromatic compounds and two functional groups acting as “electron releasers” and “electron acceptors”. Upon exposure to UV radiation the molecule tends to delocalize the electrons to reach a higher state of energy. The excitation caused by the absorption of UV light is the favored state of the molecule [258].

PABA (*p* -aminobenzoic acid) was introduced as one of the first organic sunscreens in the 1920s. It had the advantage of being water resistant. However, there was an increasing evidence that PABA can elicit photocontact allergies and possibly autoimmune diseases such as systemic lupus erythematosus [259]. Moreover, there were reports that the decomposition of PABA could produce a potentially carcinogenic nitrosamine degradation product [260]. Benzophenone-3 (oxybenzone) became in the 1980s the most frequently used component of sunscreen formulations.

In general, organic sunscreen products can induce photocontact allergic reactions [261]. In contrast to the acute toxic effects of organic sunscreens, their chronic toxicity has not yet been extensively studied. The systemic absorption of sunscreens after topical application is also an important point, it has been reported for some organic UV blockers [262, 263]. It has been shown that 0.5% of the total amount of benzophenon-3 (oxybenzone), which was applied topically onto the skin, could be detected in the urine of human volunteers for up to 48 hrs [264]. Organic sunscreens, including oxybenzone, have also been found in human breast milk [265]. Moreover, the user demand for water-resistant sunscreens encourages the production of more lipophilic sunscreens, which could increase their dermal absorption. The postulated *in vivo* estrogenicity of organic sunscreens has been recently studied [266]. Six frequently used UV-A and UV-B organic sunscreens, including oxybenzone, were administered orally (median effective dose 1.000–1.500 mg/kg/day) to rats over a period of four days. A significant increase of the uterine weight was induced by three out of the six sunscreens. It was, therefore, hypothesized that the oral intake of sunscreens might be a potential risk for humans via bioaccumulation. But also dermal application could induce a significant increase in the uterotrophic testing. This report caused a broad public discussion on the safety of organic sunscreens. Some European countries have banned the suspected products from the market for some time. Therefore, the European Union cosmetics advisory committee stated that there are no estrogenic effects of organic sunscreen products allowed in the EU market. Although the estrogenicity of organic sunscreens is an interesting aspect worth studying, the clinical relevance of these findings is not high because at this time the benefits of using organic sunscreens outweighs the risks of possible estrogenicity [174].

When the contribution of UV-A to photocarcinogenesis and photoaging became apparent, the sunscreens absorbing the longer UV-A range have been introduced in the late 1990s. Examples of these UV-A sunscreens are butyl methoxydibenzoylmethane, terephthalidene dicamphor sulfonic acid (e.g. Mexoryl SX®) and drometrizole trisiloxane. Micronized organic pigments such as methylene bis-benzotriazolyl tetramethylbutylphenol (Tinosorb M®) have been introduced as broad spectrum sunscreens. Table 5-1 gives an overview of some organic UV filters permitted in Europe. With all the different products in the market new problems arose. Interaction between some solar UV-A and UV-B filters has been proven, which leads to a consequent loss of UV protection [182].

Preparation of oxybenzone-loaded gelatin microspheres increased the efficacy of the sunscreen more than four times and provided the advantage of overcoming solubility and skin

irritation problems. The SPF increase could be due to the microsphere film formation over the skin which acts as a physical sunscreen [267].

Nanoparticles have been investigated as a delivery system for labile organic sunscreens. PLGA (poly- *D, L*-lactide-co-glycolide), a biocompatible polymer, nanoparticles were produced as vehicles for organic sunscreens for the prevention of photodegradation of the sunscreens [268]. The latest development of a carrier system for organic UV blockers was the sol-gel glass microcapsules. The organic UV blocker is encapsulated within a silica shell of a diameter ranging from 0.3 to 3 μm [269]. This new system reduces the contact between the UV blocker and skin, and hence the undesired effects related to this contact e.g. photoallergy and systemic absorption. Based on this technique the company Sol-Gel Technologies Ltd. is now manufacturing the product "UV-Pearls".

Table 5-1: A selection of the organic UV blockers permitted for use in Europe.

UV blocker group	UV blocker chemical name	Trade name	Protection range
p-Aminobenzoic acid and its esters	ethylhexyl dimethyl PABA	Escalol 507	UV-B
Salicylates	ethylhexyl salicylate	Eusolex OS	UV-B
	ethyl triazone	Uvinul T 150	UV-B
	homosalate	Eusolex HMS	UV-B
Cinnamates	ethylhexyl methoxycinnamate	Parsol MCX	UV-B
	octocrylene	Uvinul N539	UV-B
Benzophenones	benzophenone-3, oxybenzone	Eusolex 4360	UV-B/UV-A
Dibenzoylmethanes	butyl methoxydibenzoylmethane	Parsol 1789/ Eusolex 9020	UV-A
Camphor derivatives	3-benzylidene camphor	Mexoryl SD	UV-B
	4-methylbenzylidene camphor	Eusolex 6300	UV-B
Phenols	bis-ethylhexyloxyphenol methoxyphenyl triazine	Tinosorb S	UV-B/UV-A
	drometrizole trisiloxane	Mexoryl XL	UV-A

5.1.2 Inorganic sunscreens

The most used inorganic (physical) sunscreens (UV blockers) are zinc oxide (ZnO), titanium dioxide (TiO_2), silicates and ferric oxide. The UV radiation blocking by these inorganic sunscreens is attributed to three mechanisms namely reflection, scattering, and in some cases absorption [255, 270]. The UV blocking properties of inorganic sunscreens are attributed to many factors such as particle size, number of particles (concentration), refraction index, crystalline form, dispersion media and semiconductor properties [179]. The advantages of the inorganic sunscreens are in general their stability, the broad spectrum of UV radiation protection, the lack of photosensitization and their low toxicity compared to the organic UV blockers [174]. But on the other hand inorganic UV blockers have some disadvantages. They have a visual appearance because of their solid consistency, they also leave white

pigmentation residues on the skin. In the last two decades preparations of improved quality were produced. The particles of zinc oxide and titanium dioxide were micronized or nanosized to reduce the reflection of the visible light and to give these inorganic sunscreens a more transparent appearance and a better skin feeling [271]. The micronization of the particles transforms the inorganic substances into reflectors and absorbents at the same time.
Electrons of the metallic oxides are mobilized by the absorption of UV radiation and hence, forming either free radicals and/or reactive oxygen species by reducing the oxygen molecules (O_2). It has been reported that the photocatalytic activity (the acceleration of a photoreaction in the presence of a catalyst) of TiO_2 may alter cellular homoeostasis and damage cellular RNA and DNA [272]. In cosmetic preparations the TiO_2 is coated to reduce the photocatalytic activity and skin penetration [174]. Coating materials can be organic such as stearic acid, PVP, methicone, dimethicone and glycin, or inorganic such as alumina, silica or aluminium phosphate [273].

Penetration of intact skin dependents partially on particle size, but there are also other key factors that influence skin penetration. These factors include the physicochemical properties of nanomaterials (e.g. shape, surface coatings, surface charge, composition and solubility), the presence of other substances or solvents that act as penetration enhancers and the condition of the skin (e.g. abrasions, blemishes, age) [274].
The potential of solid nanoparticles, size of 100 nm or less, to penetrate the stratum corneum and diffuse into underlying structures is at the center of the debate concerning their safety for topical use. The European Scientific Committee on Consumer Products has issued a number of opinions on the subject, but still believes that there is till now insufficient information for a proper safety evaluation of microfine (or nanosized) TiO_2 and ZnO.
Many studies have been performed and there is still a lack of available data demonstrating whether nanoparticles can gain access to the epidermis after topical application [275]. Nanoparticles administered on the skin are known to localize to regional lymph nodes, potentially via skin macrophages and Langerhans cells [276]. Observing that endothelial cells have a capacity to internalize nanoparticles more than larger particles of the same material increased the concerns of potential pro-inflammatory or cytotoxic potential of these nanomaterials [277].
Lademann et al. did not detect any absorption of nanosized TiO_2 particles (crystal size approximately 17 nm) into the epidermis following repeated application of an o/w emulsion to

the forearms of volunteers over several days. Only the upper stratum corneum and hair follicles showed evidence of particle penetration [278].

Although nanoparticles of physical sunscreens do not appear to penetrate into the viable epidermis, there is a potential systemic exposure to the nanoparticulate inorganic sunscreens which may partially diffuse following topical application [279]. Penetration of nanosized TiO_2 into human skin seems to be possible because of the mean particle size of 20 nm. A pilot study suggested that skin absorption of TiO_2 nanomaterials took place [280]. Another pilot study that has been performed on selected patients scheduled to have skin surgery showed that the levels of TiO_2 in the epidermis and dermis of subjects who applied the microfine TiO_2 to their skin were higher than the level of TiO_2 found in the controls [180]. Müller-Goymann investigated the *in vivo* and *in vitro* penetration behaviour of the nanosized TiO_2 particles into human skin. Results showed that nanosized TiO_2 penetrates deeper into human skin from an oily dispersion than from an aqueous one. The encapsulation of the micropigment into liposomes causes a higher penetration depth of the particles into the skin [281].

In a memorandum from Bergeson and Campbell sent to their firm clients it was cited that there is no evidence for skin penetration into viable tissues for nanoparticles of about 20 nm. On the other hand, there are less studies regarding skin with impaired barrier function e.g. atopic skin, acne, eczema or sunburned skin. Also mechanical effects on skin, e.g. flexing or shaving, might have an effect on nanoparticles penetration [282]. Actually it is knows that broken skin is an ineffective barrier and enables particles up to 7000 nm in size to reach the living tissues [283]. The European Union has also launched a research project called "Nanoderm" to investigate the quality of the skin as a barrier to formulations containing nanoparticles [181].

Studying the toxic effects of TiO_2 to cellular components, some studies showed that TiO_2 does not penetrate the stratum corneum in viable skin. This was proven by investigating the dermal absorption of TiO_2 by light and electron microscopy. The TiO_2 particles were of different surface characteristics (hydrophobic or amphiphilic), sizes (from 20 nm to 100 nm) and shapes (cubic or needle). Non of the TiO_2 pigments was detected in the deeper stratum corneum layers or epidermis [284].

On the other hand, other studies found that TiO_2 could penetrate from dermal fibroblasts to skin tissue and cause damage to the cell structure and function [285]. It has been also reported that topical zinc ions cross the skin and can be found in dermis and blood [286].

Comparing micronized ZnO and micronized TiO_2, ZnO was more efficient in the absorption of UV light, especially in the UV-A range. ZnO was also non-photoreactive and has a more

aesthetic appearance than micronized TiO_2. This is because of its low reflection of visible light in this particular particle size range [287]. Nevertheless, the comparison depends on the particle size of the substances. ZnO is used as both UV-A and UV-B blocker while TiO_2 is used mainly as a UV-B blocker, but the bigger a TiO_2 particle is, the more UV-A protection is achieved [287]. ZnO is currently used in sunscreens but not permitted as a UV filter in Europe. Moreover, many sunscreen products contain organic UV blockers in addition to the inorganic UV blockers to achieve a higher SPF [288]. On the other hand, it has been reported that inorganic UV blockers can decrease the activity of the organic ones when they are together in one formulation [182]. Current FDA rules do not allow formulators to combine the organic UV-A blocker avobenzone with the titanium dioxide [289].

5.1.2.1 Placebo NLC

Solid lipid nanoparticles (SLN) showed a UV blocking potential, i.e. they act as physical sunscreens on their own [290]. The crystalline lipid of the nanoparticles has the ability to scatter the UV radiation on its own leading to photoprotection without the need of molecular sunscreens [125].

Müller-Goymann et al. have incorporated different pigments including TiO_2 into different lipid nanoparticles and studied the enhancement of the sun protection factor of these formulations. They also investigated the physical stability of these formulations and the entrapment efficacy of the TiO_2 in the lipid nanoparticles [128, 291, 292].

5.1.3 Photoprotectors

Antioxidants present in the skin neutralize the harmful chemical reactions occurred upon exposure to UV radiation. Hence, these antioxidants protect the skin and reduce its damages such as reduction of elasticity and formation of age spots [293]. Upon skin exposure to UV radiation the skin content of antioxidant enzymes and other small molecular weight antioxidants diminishes [294]. Therefore, and to re-establish the proantioxidant balance that was disturbed by the skin exposure to UV radiation, diverse chelating agents, excited state quenchers, free radicals scavengers and enzymes are applied [295]. Ethylenediamine triacetic acid and vitamin C can be mentioned as examples for chelating agents. Xanthine, melanin and β-carotenes are among the quencher molecules, whereas vitamin E (D α-tocopherol) and coenzyme Q 10 are considered to be free radical scavengers [296, 297].

All in all, to overcome the disadvantages of the organic and inorganic sunscreens previously mentioned, e.g. systemic absorption, interaction with other sunscreens in the same formulation and undesired appearance or skin feeling, the encapsulation of these sunscreens might be an approach. Reduction of the skin penetration, improved photostability of the sunscreen, lowering the allergy potential, better appearance and skin feeling and avoiding incompatibility with other sunscreens are expected [269].

Based on this concept, the NLC can also be considered as a carrier system for some sunscreens. The UV blocking activity of placebo NLC and sunscreen-loaded NLC formulations has been studied [125, 252]. In this chapter further studies and tests have been performed on placebo NLC formulations and on different sunscreen-loaded NLC formulations.

5.2 Placebo (Non-loaded) NLC

Placebo NLC suspensions were produced and the UV absorption properties and the factors affecting them were studied. Furthermore, placebo NLC were admixed to a conventional cream and the UV protection activity of this cream containing placebo NLC was determined.

5.2.1 Production of placebo NLC

The production of the placebo NLC was performed as described in chapter 2. Shortly, the lipid blend is heated to 5-10ºC above the melting point of the solid lipid, and subsequently dispersed by high speed stirring at 8000 rpm for 20-30 sec in a hot aqueous surfactant/stabilizer solution of a same temperature. The obtained preemulsion is homogenized with a high pressure homogenizer applying a pressure of 800 bar and two homogenization cycles yielding a hot o/w nanoemulsion. The obtained nanoemulsion was filled in silanized glass vials, which were immediately sealed. A thermostated water bath adjusted to 15ºC has been used as cooling system to control the cooling rate of the obtained formulations. After cooling, the emulsion droplets crystallize forming lipid nanoparticles with solid particle matrix [196]. Nanoemulsions served as references and were produced in the same way after substituting the solid lipid with Miglyol 812.

5.2.2 UV absorption properties of placebo NLC

As an *in vitro* method to determine the UV absorption of the placebo NLC, the spectral absorption between 400 and 200 nm has been measured (UV radiation range) [298]. The NLC suspensions and the reference nanoemulsions were diluted with the same dilution factor to have an absorbance around 1, i.e. the lipid phase concentration (solid lipid or oil) was the

same in the measured samples of the NLC suspensions and the reference nanoemulsions. To develop an NLC formulation which has a high UV absorbance the effects of the lipid matrix and the particle size were investigated.

5.2.2.1 Effect of placebo NLC lipid matrix on the UV absorption

The UV absorption of an NLC suspension (consisting of 40% cetyl palmitate, 10% Cetiol MM, 3% PlantaCare 2000 and 47% water) was compared to a conventional nanoemulsion (consisting of 50% Miglyol 812, 3% PlantaCare 2000 and 47% water). The particle size distribution of both formulations was in the same range (PCS mean particle size 343±6 nm for the NLC and 332±7 nm for the emulsion). The samples were diluted so that the UV absorbance range is between 0.5 and 2. The lipid phase concentration was 0.1 µg/ml. It was observed that within the UV region the absorbance of the NLC is twice higher than the absorbance of the emulsion (Figure 5-1). This is due to the fact that the NLC suspension decreases spectral transmission to a greater extent than the droplets of the oil in the reference nanoemulsion. This decrease in spectral transmission is due to scattering of the UV light.

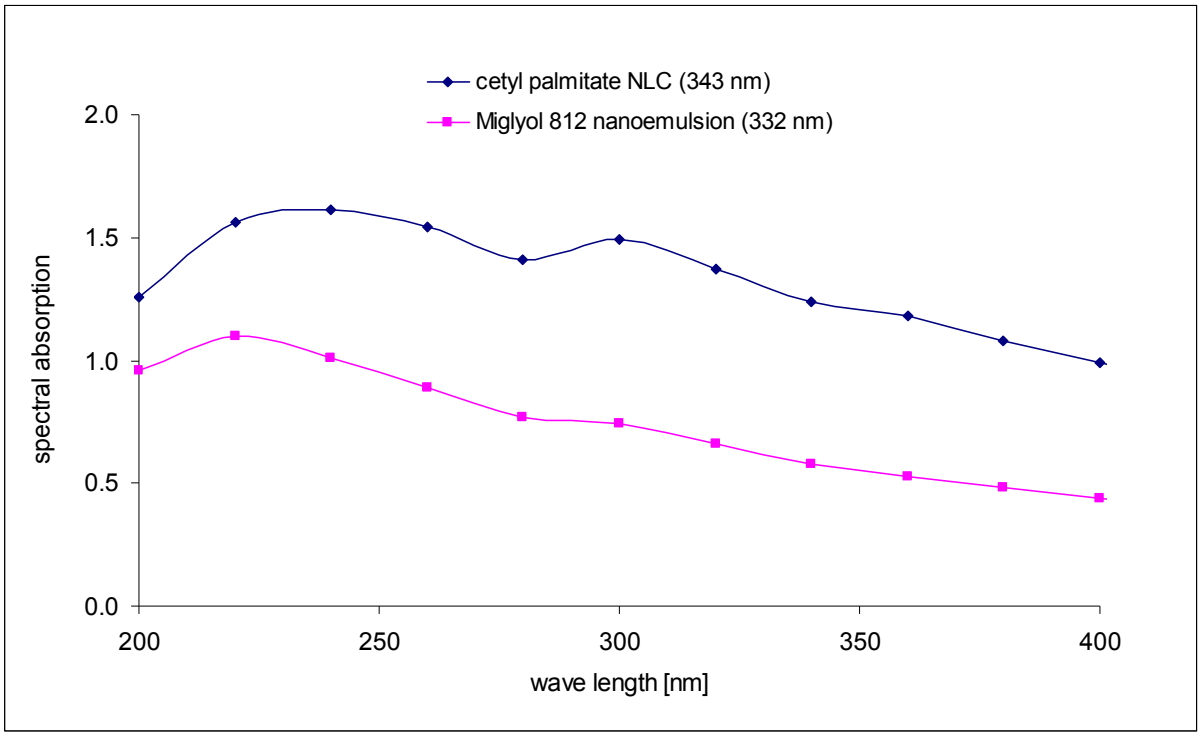

Figure 5-1: The absorption spectra of a placebo NLC suspension and a conventional nanoemulsion. The absorbance of the NLC is approximately twice higher than the absorbance of the emulsion, lipid phase concentration= 0.1 µg/ml (n=3).

To determine if there is an influence of the solid lipid type on the UV absorption, the absorption spectra of 2 NLC formulations (consisting of 19% carnauba wax or cetyl

palmitate, 1% Miglyol 812, 1.8% TegoCare 450 and 78.2% water) were compared. The absorption spectrum of a conventional nanoemulsion (consisting of 20% Miglyol 812, 1.8% TegoCare 450 and 78.2% water) was also measured. The particle size distribution of the three formulations was in the same range (PCS mean particle size 302±5 nm for the carnauba wax NLC, 291±8 nm for the cetyl palmitate NLC and 297±3 nm for the nanoemulsion). The samples were diluted so that the UV absorbance range is below 1. The lipid phase concentration was 0.04 µg/ml. It was observed that the two NLC formulations have almost the same spectral absorption which is twice higher than the absorption of the nanoemulsion (Figure 5-2).

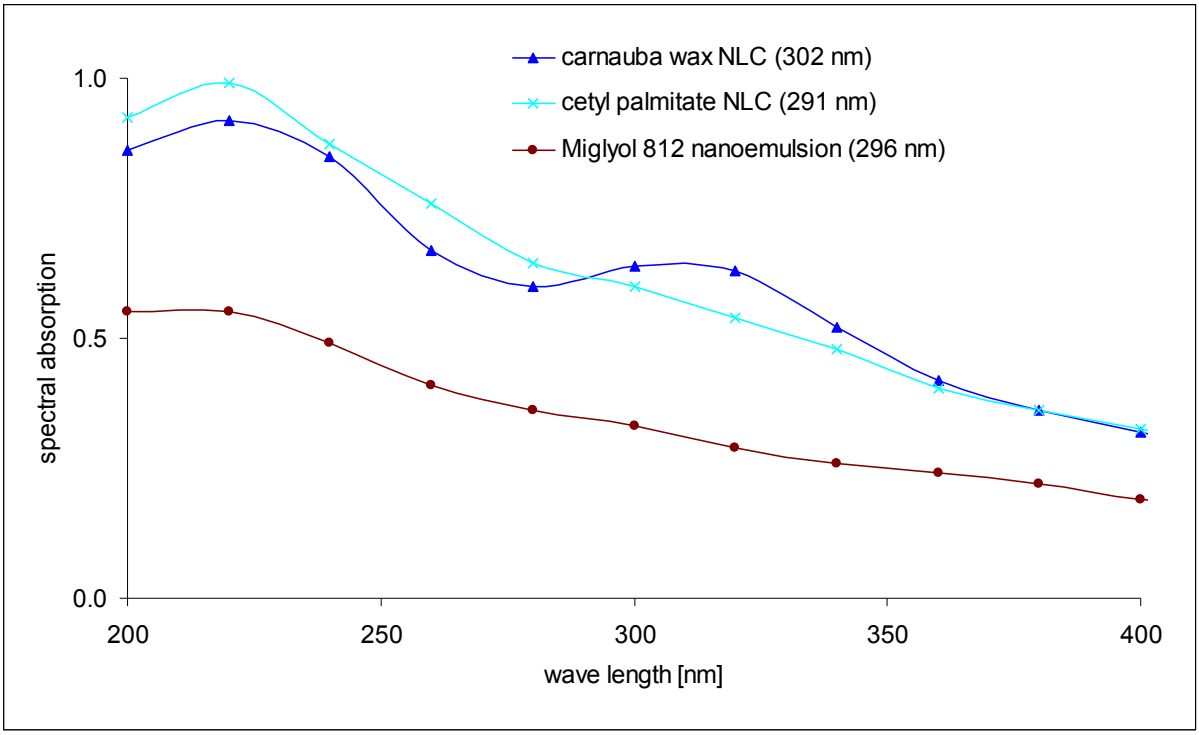

Figure 5-2: The absorption spectra of 2 NLC formulations (carnauba wax or cetyl palmitate) and a conventional nanoemulsion (Miglyol 812). The absorbance of the NLC samples is approximately twice higher than the absorbance of the nanoemulsion, lipid phase concentration= 0.04 µg/ml (n=3).

5.2.2.2 Effect of placebo NLC particle size on the UV absorption

To study the effect of the particle size of the placebo NLC on the UV absorption two NLC formulations were produced using two different solid lipids (carnauba wax and cetyl palmitate). Each formulation was produced four times, each time with a different homogenization pressure and number of homogenization cycles, to obtain different particle sizes. The UV absorbance of these NLC formulations was measured. The composition of these NLC formulations, their PCS mean particle size, the homogenization pressure and the number of homogenization cycles are shown in Table 5-2.

Table 5-2: Composition, PCS mean particle size, homogenization pressure and number of cycles of the two NLC formulations produced to study the effect of particle size on the UV absorption.

Formulation	Composition		PCS size (nm)	Homogenization pressure and cycle no.
carnauba wax NLC	carnauba wax	30.0%	652±8	250 bar, 2 cycles
	Miglyol 812	5.0%	533±7	400bar, 2 cycles
	Inutec SP1	2.5%	378±4	500bar, 2 cycles
	water	62.5%	324±5	500bar, 3 cycles
cetyl palmitate NLC	cetyl palmitate	24.0%	717±9	200 bar, 2 cycles
	Cetiol MM	6.0%	533±8	300bar, 2 cycles
	Miglyol 812	5.0%	373±6	500bar, 2 cycles
	Inutec SP1	2.5%	353±6	500bar, 3 cycles
	water	62.5%		

From the absorption spectra of these NLC samples it was observed that there is an optimal size for the maximum UV absorption. This size was the same for both NLC formulas (about 375 nm PCS mean particle size) (Figure 5-3, Figure 5-4). This can be explained as follows, when the particles become smaller the surface/volume ratio becomes higher, i.e. there are more surfaces where the light is reflected, absorbed, or refracted. But when the particles are smaller than a definite particular size (smaller that 370 nm) they become transparent, and hence the absorption of UV radiation decreases. Moreover, when the particle size is comparable to the wavelength of the UV radiation, the destructive interference of the particles with the radiation beam becomes very small, i.e. these very small particles do not absorb, refract or reflect the light as the relatively bigger ones [203, 299].

Figure 5-5 shows the possible interferences between a light beam and a spherical particle. The light can be either reflected, absorbed or refracted. The diameter of the particle in this drawing is significantly bigger than the incident light wavelength.

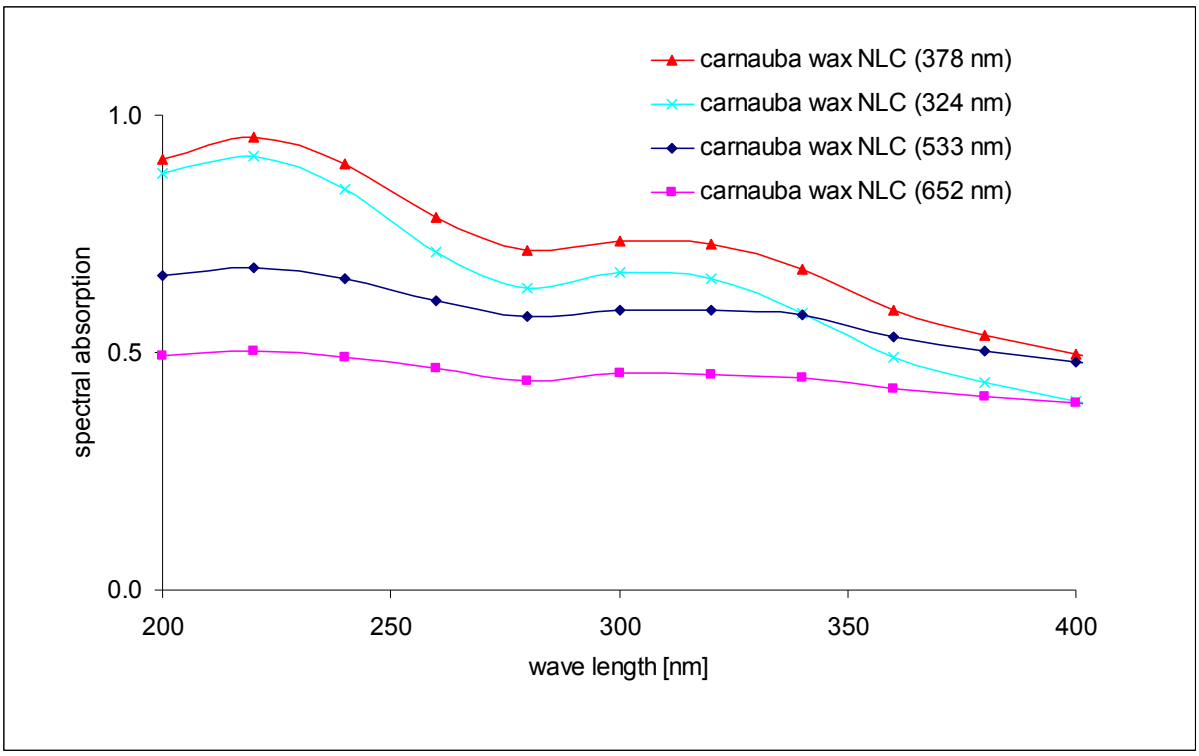

Figure 5-3: The absorption spectra of the carnauba wax NLC formulation with four different particle sizes. The UV absorption of the NLC sample having 378 nm mean particle size was the highest among the four samples, lipid phase concentration= 0.0525µg/ml (n=3).

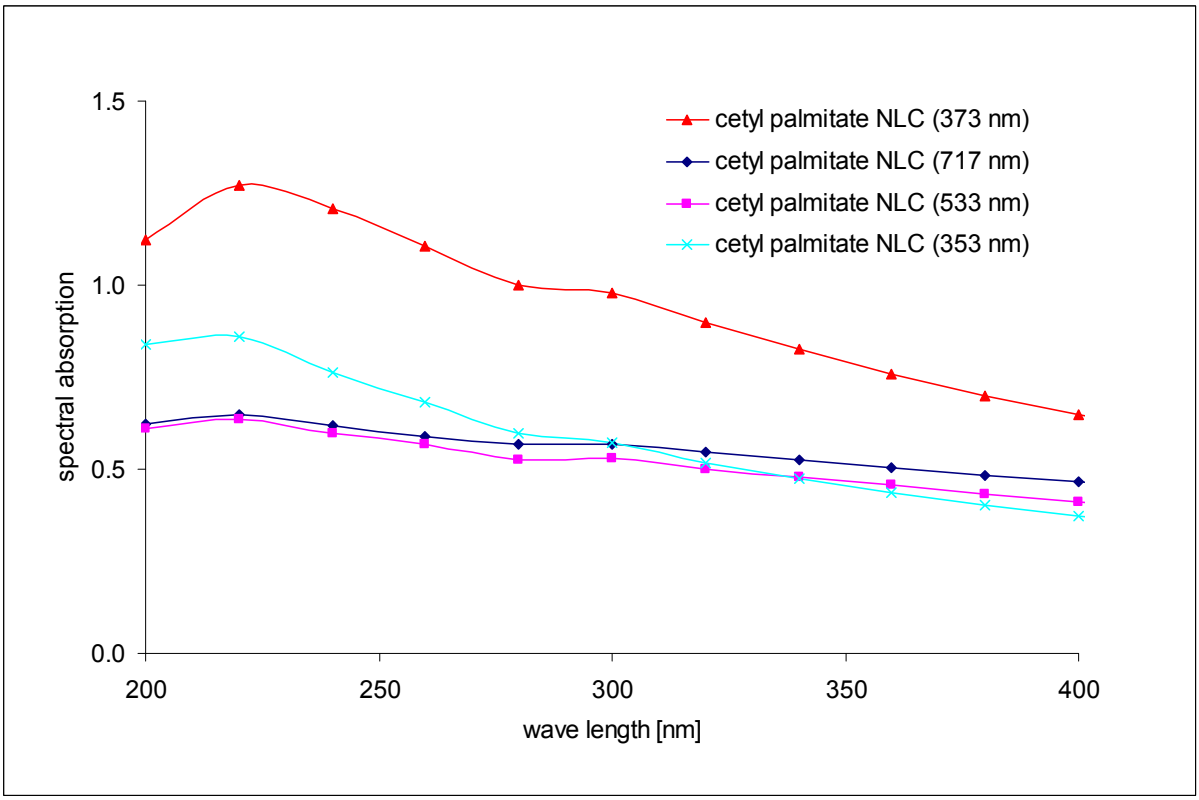

Figure 5-4: The absorption spectra of the cetyl palmitate NLC formulation with four different particle sizes. The UV absorption of the NLC sample having 373 nm mean particle size was the highest among the four samples, lipid phase concentration= 0.035µg/ml (n=3).

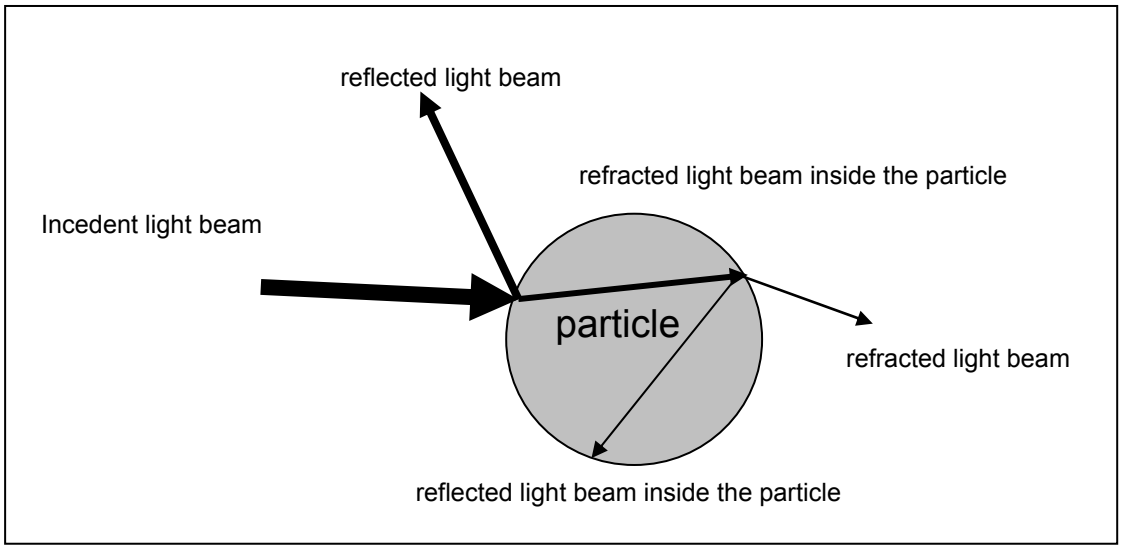

Figure 5-5: The possible interferences between a light beam and a spherical particle. Light can be either reflected, absorbed or refracted, light absorption is expressed as a decrease in light intensity (thinner arrow) (modified after [299]).

5.2.3 UV blocking activity of creams containing placebo NLC

NLC cream and NLC emulsion were prepared by admixing the placebo cetyl palmitate NLC formulation to a conventional cream or a conventional emulsion respectively. 5 g NLC dispersion were added to 95 g cream or emulsion. The UV blocking activity of these placebo cetyl palmitate NLC cream and emulsion and a conventional cream and conventional emulsion (without NLC) was compared. This was performed by measuring the concentration of a β-carotene solution in a quartz Petri dish covered with 0.3 g evenly spread layer of one of these creams or emulsions. The Petri dishes were exposed to artificial sun light containing UV radiation inside an artificial sunlight chamber Suntest (Heraeus GmbH, Hanus, Germany) and were irradiated with a radiation intensity of about 830 W/m^2 (between 300 and 830 nm) for 60 min (see chapter 2). The β-carotene concentration was assessed after 30 and 60 min of exposure. After 30 min of exposure to the artificial sun light the remaining β-carotene concentration for the two preparations (cream and emulsion) containing 5% placebo NLC dispersion was twice higher than the remaining β-carotene concentration for the conventional cream and emulsion. After 60 min the difference between the remaining β-carotene concentration of the NLC preparations and the conventional ones increased to be six times higher for the NLC cream in comparison to the conventional cream and 4 times higher for the NLC emulsion in compare to the conventional emulsion (Figure 5-6 and Figure 5-7). After 60 min the color of β-carotene can still be detected in the Petri dishes covered with the placebo NLC cream (yellowish color), while no β-carotene could be detected in the Petri dishes covered with the conventional cream (Figure 5-8).Therefore, it can be concluded that the UV

blocking activity of the preparations containing 5% placebo NLC is clearly higher than the same cream or emulsion without the placebo NLC (conventional cream and emulsion).

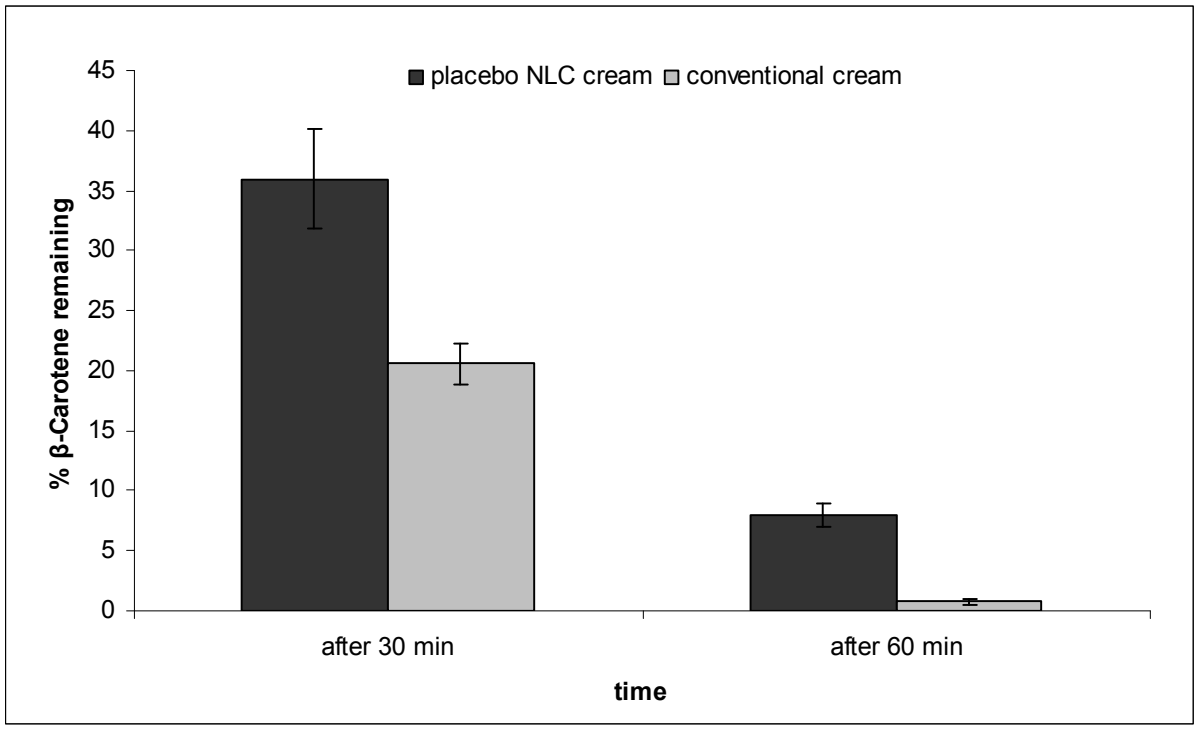

Figure 5-6: The remaining concentration of β-carotene after 30 and 60 min of exposure to artificial sun light. After 30 min the placebo NLC cream showed twice higher remaining β-carotene concentration than the conventional cream (n=3).

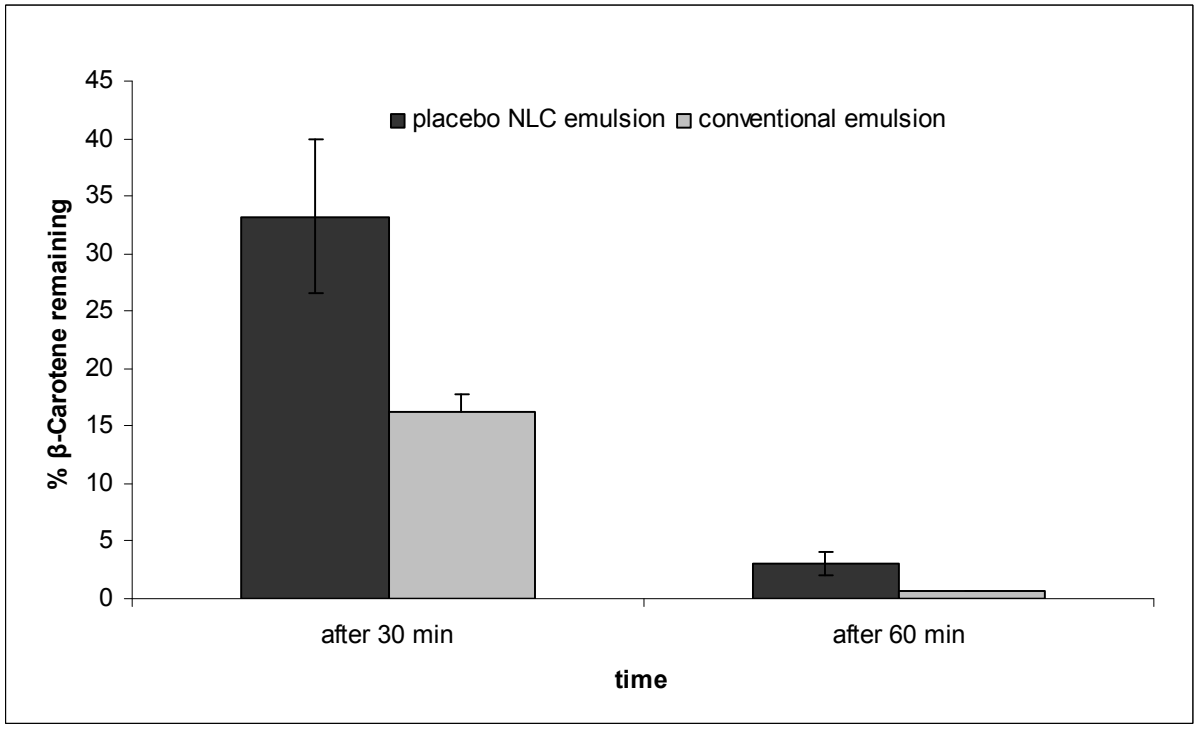

Figure 5-7: The remaining concentration of β-carotene after 30 and 60 min of exposure to artificial sun light. After 30 min the placebo NLC emulsion showed twice higher remaining β-carotene concentration than the conventional emulsion (n=3).

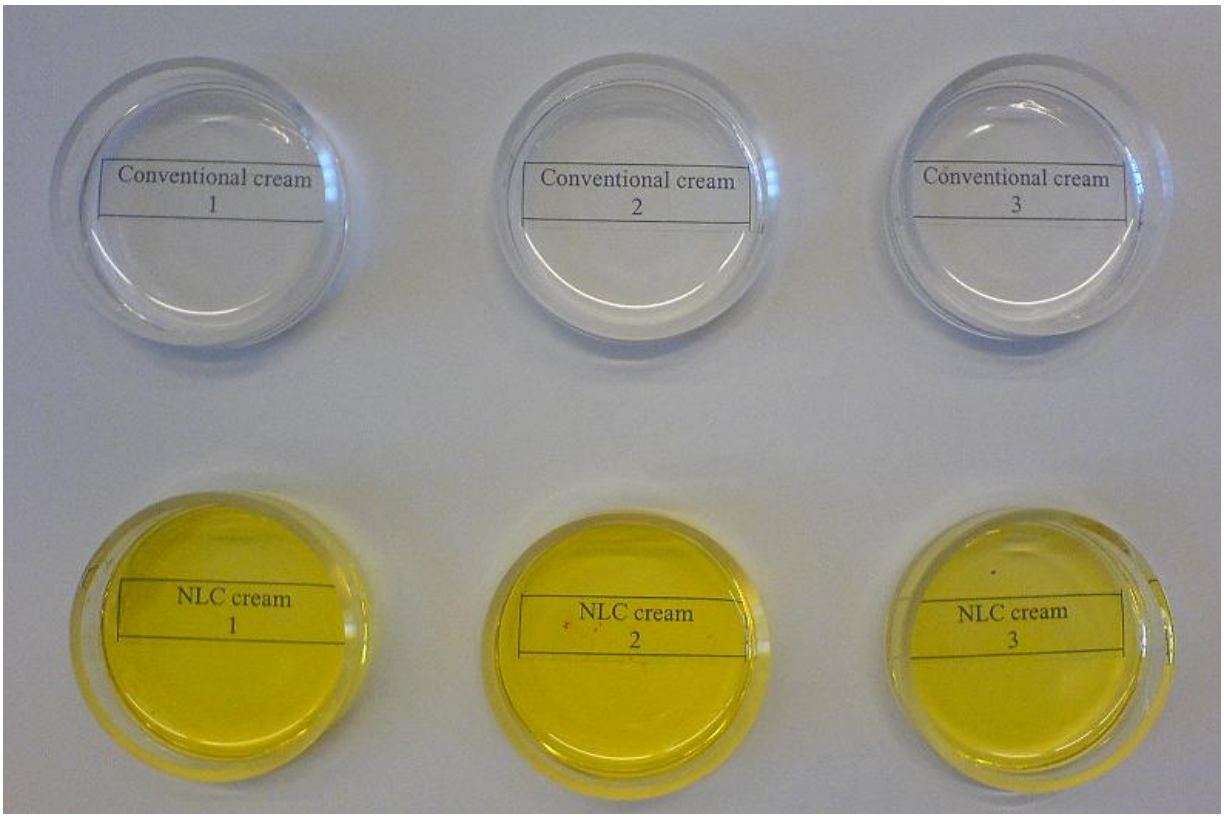

Figure 5-8: β-carotene solution in Petri dishes after 60 min of exposure to the artificial sun light. No β-carotene color can be seen in the upper three dishes (covered with conventional cream), while in the three lower dishes (covered with the placebo NLC cream) the β-carotene yellowish color can still be seen.

5.2.4 Conclusion

Placebo NLC suspensions are able to block the UV radiation on their own. This gives a chance to produce cosmetic products that have photoprotection properties without the need of using any sunscreens in the formulation. This is an advantage when there are tolerability problems with the conventional sunscreens. To achieve a maximum UV blocking activity the particle size of the NLC should be optimized.

5.3 BMBM-loaded NLC

Avobenzone or butyl methoxydibenzoylmethane (BMBM) is an organic UV blocker used in sunscreen products to absorb the full spectrum of the UV-A rays. The most effective sunscreens contain BMBM and titanium dioxide. Therefore, BMBM has been used in combination with titanium dioxide and/or zinc oxide in many countries. However, in the USA combinations of BMBM and physical (inorganic) sunscreens are not permitted. BMBM has been reported to be unstable when contained in formulations with inorganic sunscreens [182]. Enclosing the BMBM in the NLC might have many advantages. It is expected to increase the UV blocking activity of BMBM and it will separate the BMBM from the physical blockers, this will make it possible to combine the two blockers in one product without having interaction between them, which might lead to BMBM instability. Also it might prevent the photodegradation of the BMBM and decrease or prevent its dermal absorption.

5.3.1 Development of BMBM-loaded NLC

5.3.1.1 Lipid screening

The solubility of BMBM in 20 solid lipids (at 80ºC) has been assessed. The starting concentration of BMBM was 20% (w/w) and the concentration was increased to 30% (w/w) if the 20% (w/w) BMBM were soluble in the screened lipid (Table 5-3).

Table 5-3: Results of BMBM lipid screening (solubility in the melted lipid at 80ºC), "-" means no mixture was prepared.

Lipid	Melting point °C	20% (w/w) BMBM	30% (w/w) BMBM
Apifil	73	soluble	partially soluble
Atowax	65	soluble	partially soluble
bees wax	66	soluble	partially soluble
cetyl alcohol	56	not soluble	-
Compritol HD5	69	soluble	partially soluble
Compritol 888	74	partially soluble	-
Dynasan 114	58	soluble	**soluble**
Dyansan 116	63	partially soluble	-
Dyansan 118	73	soluble	not soluble
Geleol	58	not soluble	-
glyceryl monostearate	67	not soluble	-
Inwitor 191	71	not soluble	-
Inwitor 900	64	not soluble	-
Precifac ATO	52	soluble	**soluble**
Softisan 134	36	soluble	**soluble**
Softisan 142	44	not soluble	-
Softisan 154	58	soluble	partially soluble
Syncrowax	73	not soluble	-
Witipsol S 58	33	not soluble	-
Witipsol E 85	44	soluble	partially soluble

The results obtained from this lipid screening showed that the solubility of BMBM is the highest in Dynasan 114, Precifac ATO and Softisan 134 (30% (w/w)) among the investigated solid lipids. Therefore, these three lipids were selected for the production of the BMBM-loaded NLC. Miglyol 812 was selected as oil for the production of the NLC because 30% (w/w) BMBM could be dissolved in it.

5.3.1.2 BMBM-loaded NLC production and stability

The BMBM-loaded NLC formulations were produced using the three selected lipids after the lipid screening (Dynasan 114, Precifac ATO and Softisan 134). The BMBM concentration in the lipid phase was either 30% (w/w), which is the concentration that could be dissolved in the selected three lipid according to the results of the lipid screening or half of this concentration (15% (w/w)). The concentration of the lipid phase was 20%, 30% or 40% (w/w) to the total formulation (Table 5-4). The aim of increasing the lipid phase concentration was to have a higher concentration of BMBM in the total formulation. The surfactant used was TegoCare 450 with a concentration of 1.8% (w/w). The homogenization conditions were 800 bar and two homogenization cycles at 85ºC.

Table 5-4: The composition of the BMBM-loaded NLC formulations.

Lipid phase % (w/w)	Composition % (w/w)			
	BMBM concentration in the lipid phase % (w/w)			
	15%		30%	
20%	lipid	11.9%	lipid	9.8%
	Miglyol 812	5.1%	Miglyol 812	4.2%
	BMBM	3.0%	BMBM	6.0%
	TegoCare 450	1.8%	TegoCare 450	1.8%
	water	78.2%	water	78.2%
30%	lipid	17.9%	lipid	14.7%
	Miglyol 812	7.6%	Miglyol 812	6.3%
	BMBM	4.5%	BMBM	9.0%
	TegoCare 450	1.8%	TegoCare 450	1.8%
	water	68.2%	water	68.2%
40%	lipid	23.8%	lipid	19.6%
	Miglyol 812	10.2%	Miglyol 812	8.4%
	BMBM	6.0%	BMBM	12.0%
	TegoCare 450	1.8%	TegoCare 450	1.8%
	water	58.2%	water	58.2%

The BMBM-loaded NLC formulations were stored at three different temperatures (4ºC, 25ºC and 40ºC) and the formation of BMBM crystals, i.e. expulsion of the BMBM from the matrix of the lipid nanoparticles and recrystallization in the aqueous phase, was monitored using polarized light microscopy. The particle size was assessed using PCS and LD at defined time points during a period of three months.

After three months BMBM crystals could be seen by light microscopy (LM) in all the samples except the Precifac ATO NLC formulations. The BMBM crystals formed faster when the BMBM concentration in the lipid phase was higher (30% (w/w)), and it formed faster in the NLC samples produced using Softisan 134 (Figure 5-9).

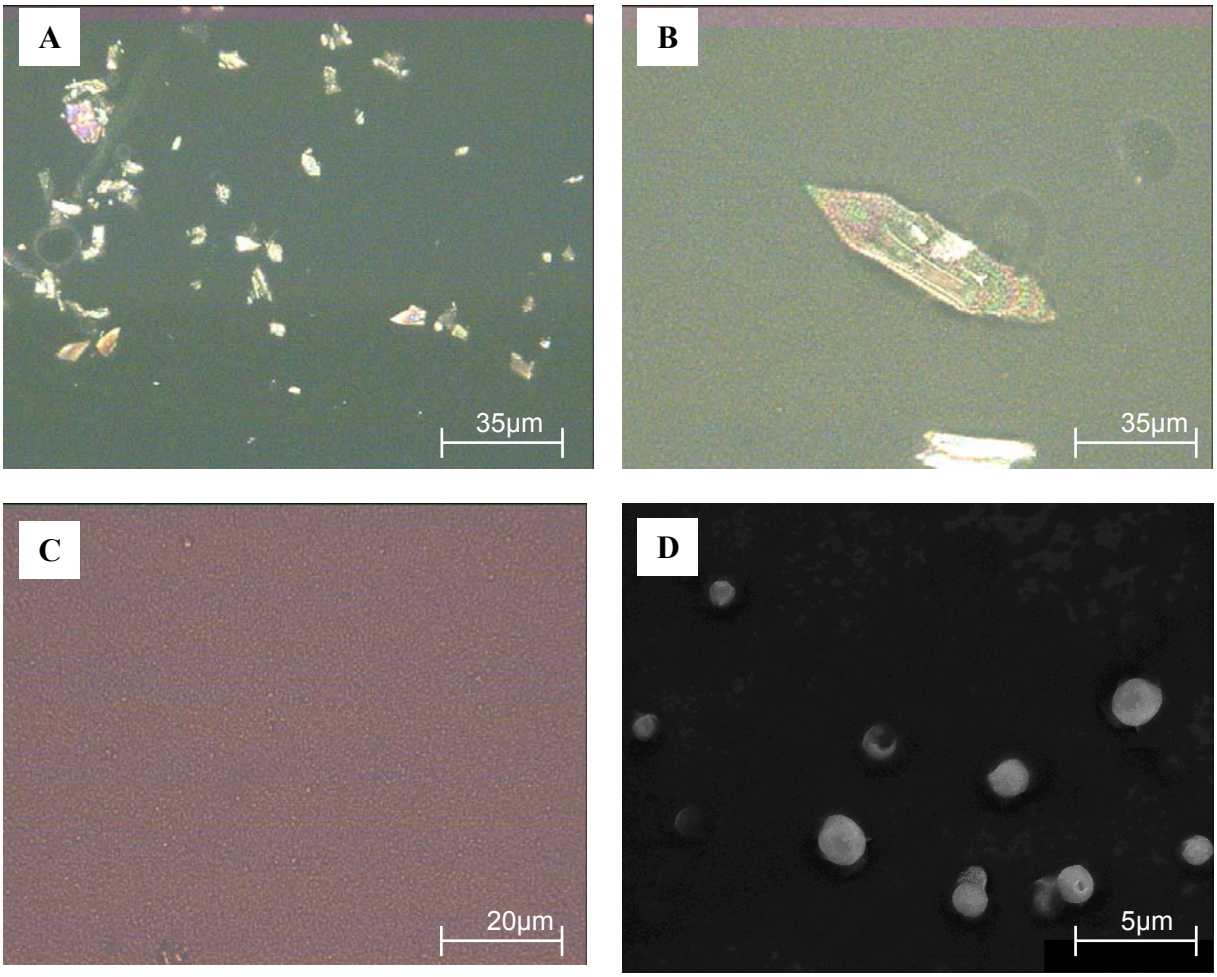

Figure 5-9: LM and SEM pictures of samples stored at RT containing 40% lipid phase of 30% (w/w) BMBM loading.
A- LM picture of Dynasan 114 NLC, crystals of BMBM formed after six weeks, (magnification 63X10).
B- LM picture of Softisan 134 NLC, crystals of BMBM formed after four weeks, (magnification 63X10).
C- LM picture of Precifac ATO NLC, no crystals of BMBM were detected after three months, (magnification 100X10).
D- SEM picture of Precifac ATO NLC. Lipid particles size is around 2 µm. No BMBM crystals were seen.

The BMBM crystals formation in the NLC samples stored at 4ºC was faster than in the NLC samples stored at higher temperatures. This is because the lower temperature (4ºC) promotes the formation of the more stable crystal form of the solid lipid and the BMBM in a shorter time due to the faster energy loss from the solid matrix. The formation of the more stable more ordered polymorph of the solid lipid (β polymorph) results in the expulsion of the BMBM from the lipid matrix to the aqueous phase. Because BMBM is a lipophilic compound the saturation solubility is easily reached and supersaturation occurs (also faster at lower

temperatures). Because of this supersaturation, the BMBM starts to crystallize and the crystals grow larger with time. The formation of the crystals and their growth depend on many external factors like supersaturation, the solvent, the temperature, the presence of impurities, the range of interaction between the molecules and the concentration of the surfactant. They also depend on internal factors like the structure of the molecules and the bonds between the atoms of the molecules [300]. This explains the differences in the BMBM crystals which were detected in the Dynasan 114 and Softisan 134 NLC samples. The different solubility of the BMBM in the solid lipid matrix and the rate of reaching the supersaturation by the BMBM in the aqueous phase (depending on the formation of the solid lipid more stable polymorph and hence the BMBM expulsion) resulted in different crystal forms of BMBM. Because of the formation of BMBM crystals in the Dynasan 114 and Softisan 134 NLC samples, the particle size analysis of these samples was terminated.

The particle size of the BMBM-loaded NLC formulations produced using Precifac ATO (30% (w/w) BMBM loading in the lipid phase) and stored at room temperature was measured at day 0 and up to three months using PCS and LD (Figure 5-10 and Figure 5-11). From the PCS and LD results it is clear that when the lipid phase concentration was increased from 20% to 40% (w/w) the particle size had consequently increased. This is because by increasing the lipid phase concentration the homogenization efficacy decreases, while maintaining all homogenization conditions (homogenization pressure, number of homogenization cycles and temperature) the same. The increase of the lipid phase concentration means that there are more droplets of the melted lipid and larger surfaces to be formed between the lipid phase and the aqueous phase by the high pressure homogenization. Therefore, the same input of energy (homogenization pressure and number of homogenization cycles) to a larger amount of lipid phase will result in a larger particle size.

The particle size of the formulations containing 20% and 30% (w/w) lipid phase remained unchanged, while a remarkable growth in the particle size was seen in the 40% (w/w) lipid phase formulation. This growth in particle size is because of the particle aggregation, which occurred due to the high lipid concentration. This is because the increase of the lipid phase concentration increases the probability of the particles to collide and hence to aggregate [214]. Moreover, gelation occurred to the Precifac ATO formulation with 40% (w/w) lipid phase and it became semisolid. This is due to the aggregation of the lipid particles and the recrystallization of the solid lipid to the more stable β modification [214]. The other two formulations of the BMBM-loaded NLC produced using Precifac ATO (20% and 30% (w/w)

lipid phase) did not become semisolid. Therefore the formulation with 30% (w/w) lipid phase was chosen to be incorporated in creams for the UV blocking activity test.

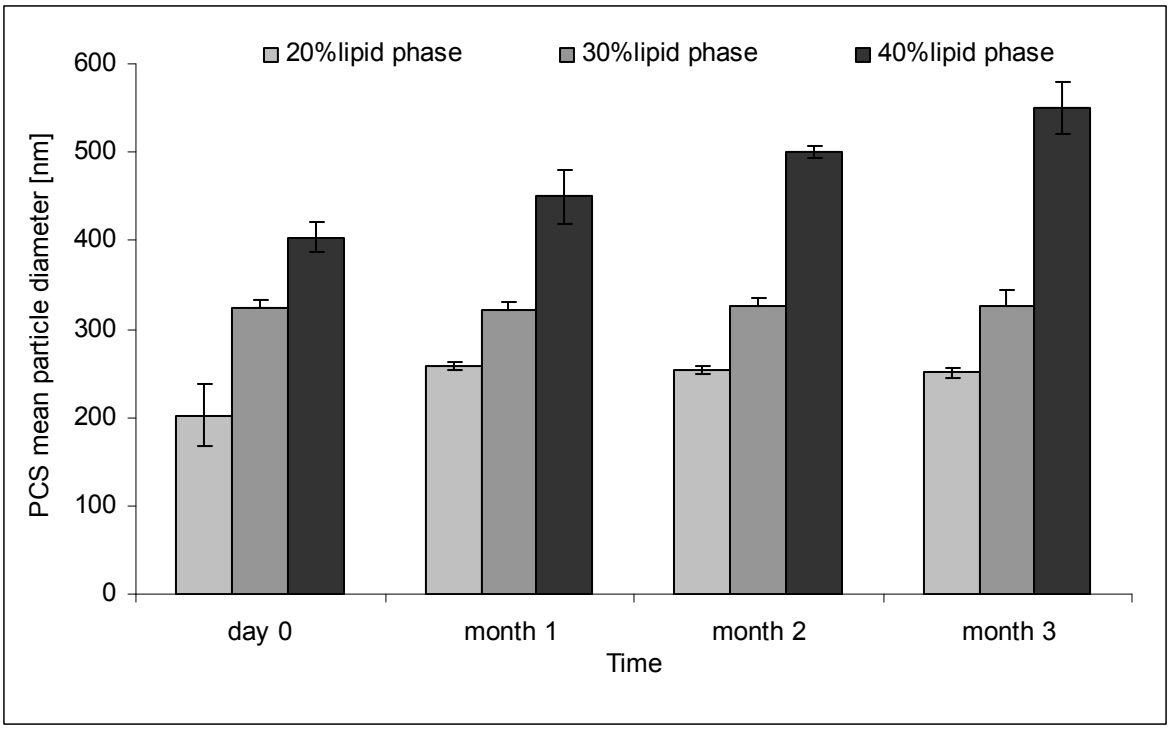

Figure 5-10: The PCS mean particle size of the BMBM-loaded NLC produced using Precifac ATO. The 20% and 30% (w/w) lipid phase formulations were physically stable, while the mean particle diameter of the 40% (w/w) lipid phase formulation increased (n=10).

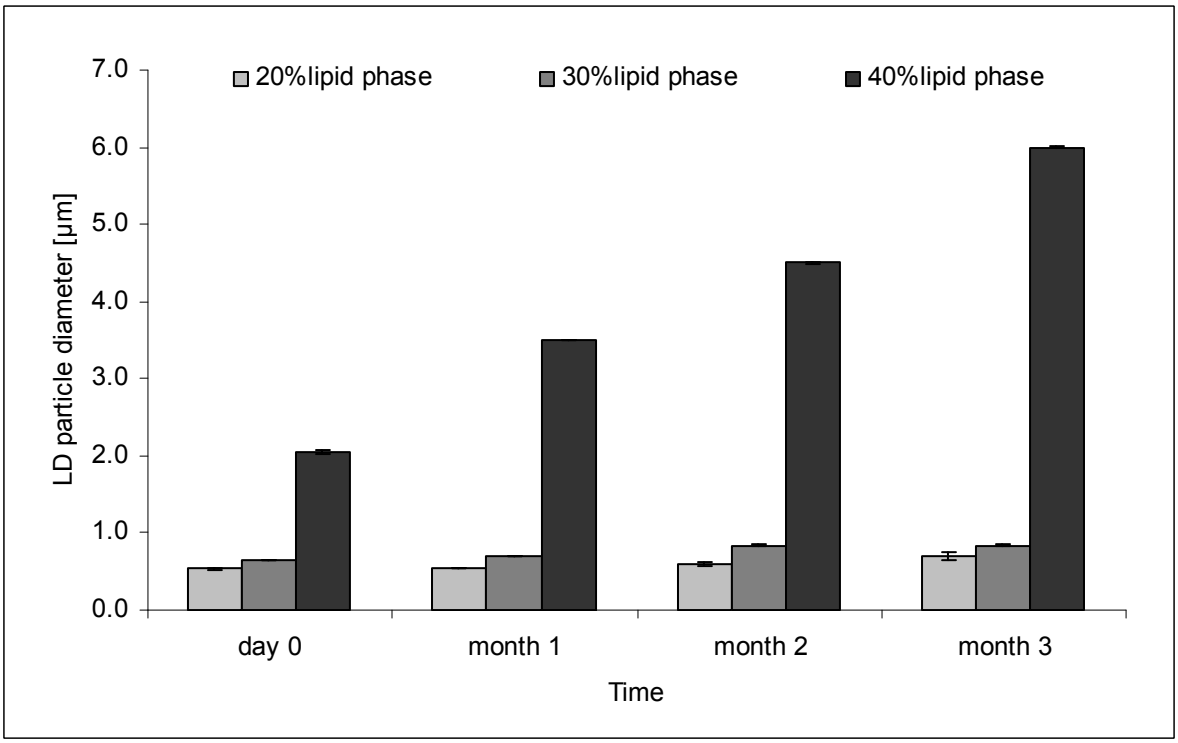

Figure 5-11: The LD 99% particle size of the BMBM-loaded NLC produced using Precifac ATO. The 20% and 30% (w/w) lipid phase formulations were physically stable, while the particle size of the 40% (w/w) lipid phase formulation increased (n=3).

5.3.2 UV absorption properties of BMBM-loaded NLC

The spectral absorption between 400 and 200 nm has been measured for a BMBM-loaded Precifac ATO NLC and a BMBM-loaded Miglyol 812 nanoemulsion and also for a placebo Precifac ATO NLC and a placebo Miglyol 812 nanoemulsion. All samples contained 30% (w/w) lipid phase (Table 5-5). The particle size of all the samples was the same (320-340 nm PCS mean particle diameter). All samples were diluted with the same dilution factor and the lipid phase concentration was 0.1μg/ml. Figure 5-12 shows that the BMBM-loaded Precifac ATO NLC has a twice higher UV absorption than the BMBM-loaded Miglyol 812 nanoemulsion. The placebo Miglyol 812 nanoemulsion has no remarkable UV absorption while the placebo Precifac ATO NLC has a detectable UV absorption but less than the BMBM-loaded formulations (NLC and nanoemulsion).

Table 5-5: The composition of placebo NLC, placebo nanoemulsion, BMBM-loaded NLC and BMBM-loaded nanoemulsion.

Composition % (w/w)							
Placebo				BMBM-loaded			
NLC		nanoemulsion		NLC		nanoemulsion	
Precifac ATO	23.7%			Precifac ATO	14.7%		
Miglyol 812	6.3%	Miglyol 812	30.0%	Miglyol 812	6.3%	Miglyol 812	21.0%
				BMBM	9.0%	BMBM	9.0%
TegoCare 450	1.8%	TegoCare 450	1.8%	TegoCare 450	1.8%	TegoCare 450	1.8%
water	68.2%	water	68.2%	water	68.2%	water	68.2%

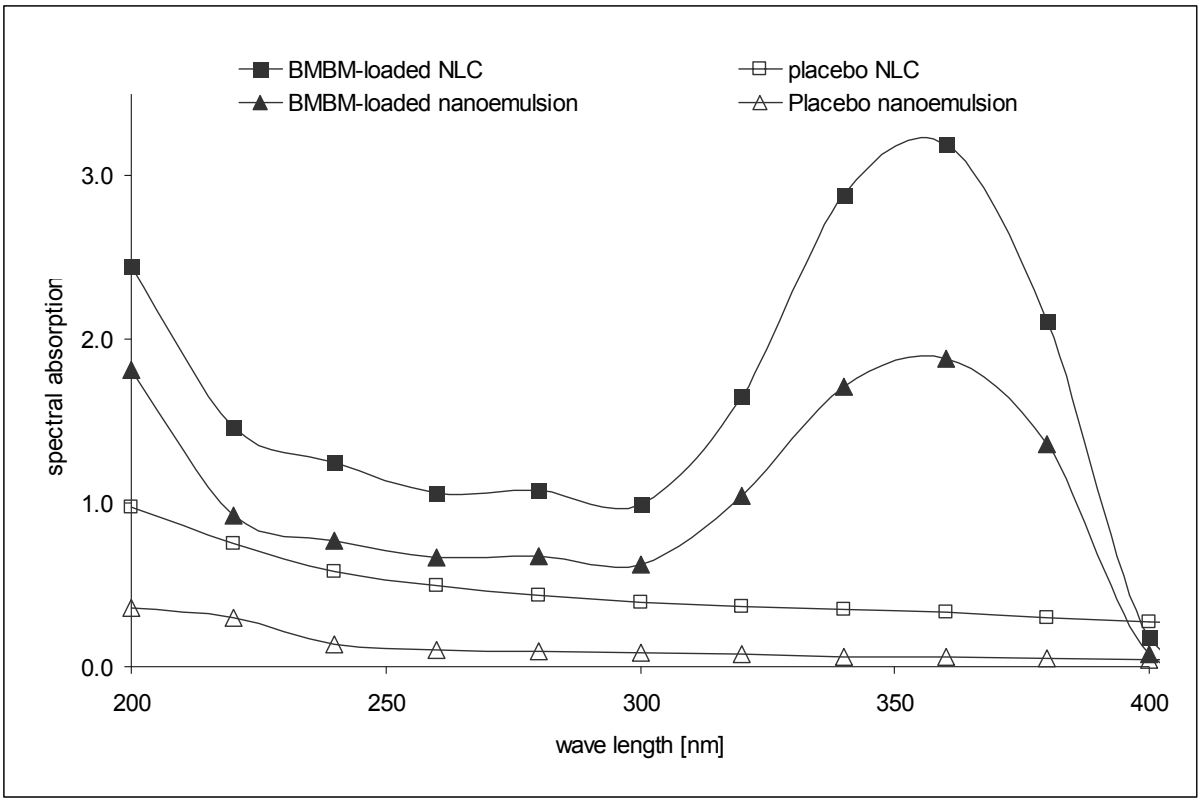

Figure 5-12: Absorption spectra of BMBM-loaded Precifac ATO NLC, BMBM-loaded Miglyol nanoemulsion, placebo Precifac ATO NLC and placebo Miglyol nanoemulsion. The BMBM-loaded NLC has the highest UV absorption, lipid phase concentration= 0.1µg/ml (n=3).

5.3.3 UV blocking activity of creams containing BMBM-loaded NLC

The UV blocking activity of four different creams was assessed. These four creams were BMBM-loaded Precifac ATO NLC cream, BMBM conventional cream, Placebo Precifac ATO NLC cream and conventional cream (compositions are listed in Table 5-5 and Table 5-6).

Table 5-6: The composition of the four creams prepared for the UV blocking activity test (all amounts are in % (w/w), "-" means substance was not added).

Substance	Formulation			
	BMBM-loaded NLC cream	**BMBM conventional cream**	**Placebo NLC cream**	**Conventional cream**
BMBM-loaded NLC suspension	10.00	-	-	-
Placebo NLC suspension	-	-	10.00	-
Precifac ATO	-	1.47	-	2.37
Miglyol 812	-	0.63	-	0.63
TegoCare 450	-	0.18	-	0.18
BMBM	-	0.90	-	-
TegoSoft DO	4.00	4.00	4.00	4.00
Montanov 202	7.00	7.00	7.00	7.00
glycerol	5.00	5.00	5.00	5.00
Inutec SP1	0.50	0.50	0.50	0.50
water	add 100	add 100	add 100	add 100

This was performed by measuring the concentration of a β-carotene solution in a quartz Petri dish covered with 0.3 g evenly spread layer of one of these creams or emulsions. The Petri dishes were exposed to artificial sun light containing UV radiation inside an artificial sunlight chamber Suntest (Heraeus GmbH, Hanus, Germany) and were irradiated with a radiation intensity of about 830 W/m^2 (between 300 and 830 nm) for 120 min (see chapter 2). The β-carotene concentration was assessed after 60 and 120 min of exposure (Figure 5-13).

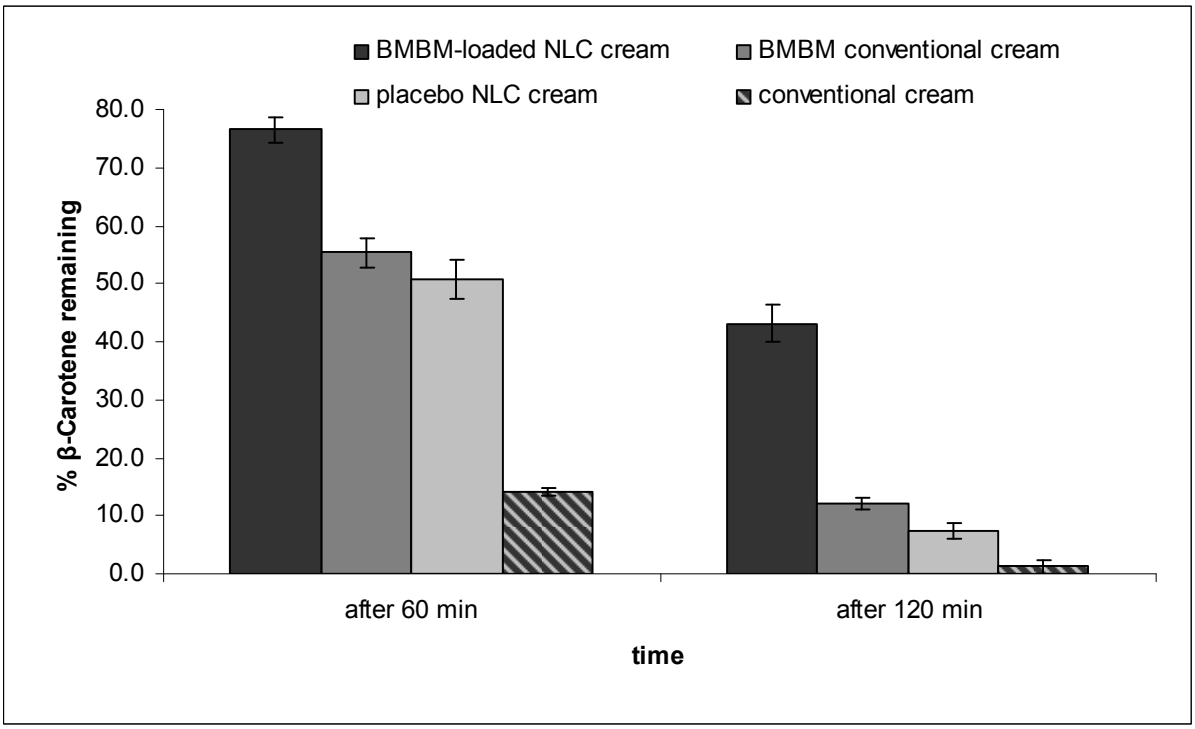

Figure 5-13: The remaining concentration of β-carotene after 60 and 120 min of exposure to artificial sunlight. After 120 min the BMBM-loaded NLC cream showed about four times higher UV blocking activity than the conventional BMBM cream, (n=3).

After 120 min of exposure to the artificial sun light the remaining β-carotene concentration of the BMBM-loaded NLC cream was about four times higher than the β-carotene concentration of the conventional BMBM cream. This is an indication that the cream containing the BMBM-loaded NLC has about four times higher UV blocking activity than the conventional BMBM cream. This can be contributed to the synergistic effect achieved when the BMBM is incorporated in NLC.

In the same way it can be concluded that the placebo NLC cream has about five times higher UV blocking activity than the conventional cream. Interesting is, the BMBM conventional cream and the placebo NLC cream, these two formulations have a comparable UV blocking activity. That means, with a cream containing 3% (w/w) placebo lipid nanoparticles (10% NLC suspension containing 30% (w/w) lipid phase) a UV blocking activity could be reached

that is comparable to the UV blocking activity of a cream containing 0.9% BMBM. This gives a chance of producing sunscreen formulations with low SPF which are free of organic sunscreens and have a remarkable UV blocking activity. These formulations will not have the disadvantages that the conventional sunscreen products containing organic UV blockers have.

5.3.4 Conclusion

BMBM, as a model for organic UV blockers, could be successfully incorporated in an NLC formulation. Enclosing this organic UV blocker in NLC increased the UV blocking activity of this blocker. This will give a chance to reduce the concentration of the organic UV blocker in the finished products while maintaining the desired high UV blocking activity. Using lower concentrations of the organic UV blockers will decrease the possibility of having the allergic reactions caused by these substances, and will also reduce the skin absorption of these organic UV blockers due to their inclusion inside the lipid particles and the lower total concentration applied to the skin.

5.4 Titanium dioxide (TiO_2) loaded NLC

TiO_2 can be an optimal inorganic sunscreen if it is contained in an optimal formulation that prevents any undesired interaction or side effect. In this part of the work nanosized TiO_2 particles were incorporated in NLC and the UV blocking activity of these new formulations was compared with conventional preparations.

5.4.1 Development of TiO_2-loaded NLC

Many types of TiO_2 with different surface coatings are available in the market as it was mentioned previously. To incorporate the TiO_2 in the lipid matrix of the NLC different types of lipophilic nanosized TiO_2 pigments were selected and various solid lipids and oils were screened for the production of the NLC (Table 5-7).

Table 5-7: The different nanosized TiO_2 pigments, solid lipids, oils and surfactants used for the development of the TiO_2-loaded NLC.

TiO_2			Solid lipid	Oil	Surfactant
Trade name	Surface coating	Size (nm)			
UV-Titan M 160	alumina, stearic acid	17	Dynasan 118	Miglyol 812	Tween 80
UV-Titan M 170	alumina, silicone	14	Dynasan 114	Decyl oleate	PlantaCare 2000
UV-Titan X 195	silica, silicon	14	cetyl palmitate		TegoCare 450
			Compritol 888		
			carnauba wax		

Not all formulations were successful, agglomerates of TiO_2 particles were detected in some formulations, sediments of agglomerated TiO_2 or TiO_2 loaded lipid particles as well as phase separation occurred. This is mainly due to the affinity between the nanosized TiO_2 particles from one side and the lipid and the surfactant used from the other side. When the affinity of the nanosized TiO_2 particles to the surfactant is higher than the affinity to the lipid phase (solid lipid-oil blend), the TiO_2 particles tend to agglomerate inside the surfactant micelles and hence, agglomerates of the TiO_2 are formed. Moreover the surfactant is consumed forming these micelles and the lipid particles (oil droplets at high temperature) are left without a sufficient amount of surfactant. This leads to either larger droplets or insufficiently stabilized droplets. Hence, phase separation occurs shortly after homogenization (while the emulsion is still hot) or agglomerates of the lipid particles occur after short time (when the suspension is in storage). The phase separation was seen in the formulations containing Dynasan 114 and Dynasan 118. In these formulations the nanosized TiO_2 particles agglomerated inside the micelles and the lipid phase was not sufficiently stabilized, hence phase separation occurred and it was not even possible to form a stable preemulsion (using

ultraturax) to be homogenized. Aggregates of the lipid particles were detected two days after production in the formulations containing cetyl palmitate. In this case the nanosized TiO_2 particles were, most likely, on the surface of the lipid particles and this led to particles aggregation due to insufficient stabilization. Micronized and nanosized TiO_2 coated particles can form an interfacial film of densely packed solid particles between the lipid phase and the water phase (so called pickering emulsions). This has happened in the case of the cetyl palmitate formulations and therefore, the TiO_2 particles were on the surface of the lipid particles after cooling down the homogenized emulsion. Moreover, these cetyl palmitate emulsions had a relatively large particle size and when the emulsions are cooled down the suspended lipid particles were bigger that 10 μm and due to their low density (less that the density of water) they tended to float.

Carnauba wax and Compritol 888 were able to be successfully formulated with the nanosized TiO_2 particles coated with alumina (UV-Titan M 160) and their NLC were physically stable. Table 5-8 shows the NLC formulations of these two lipids with different TiO_2 loads.

The lipid phase was heated to about 10°C above the melting point of the lipid and the TiO_2 powder was dispersed in it. Because the TiO_2 powders were "ultrafine" (particle size around 14-17 nm) the handling of these powders was tedious. To avoid agglomeration of the TiO_2 particles in the melted lipid phase, longer time of stirring using a magnet stirrer was necessary (around 20 min) to have a very well dispersed particles of TiO_2. The surfactant solution was added to the lipid phase and the lipid phase was dispersed in the aqueous phase using an ultraturax at 10000 rpm. The homogenization conditions were two homogenization cycles and 800 bar.

Table 5-8: The composition of the TiO_2-loaded NLC formulations produced.

Carnauba wax NLC		**Compritol 888 NLC**	
carnauba wax	10.0 %	Compritol 888	10.0 %
decyl oleate	5.0 %	Miglyol 812	5.0 %
UV-Titan M 160	**2.0, 4.0, 6.0 %**	**UV-Titan M 160**	**2.0, 4.0 %**
PlantaCare 2000	3.0 %	PlantaCare 2000	3.0 %
water	add 100.0 %	water	add 100.0 %

5.4.2 Characterization of TiO_2-loaded NLC

The particle size of the TiO_2-loaded NLC was measured one day after production and up to six months using PCS and LD (Figure 5-14 and Figure 5-15). After six months no remarkable particle size growth was seen. It is noticeable that, the higher the TiO_2 loading the bigger is the particle size. The increase in the size of the lipid particles can be attributed to the increase of the lipid phase viscosity due to the increasing amount of the TiO_2 particles suspended in

the melted lipid phase. Hence, the energy input during the homogenization process needs to be higher to get the same particle size of the NLC with the lower TiO_2 loading. By maintaining the homogenization conditions constant for all the samples, bigger particle size resulted for the formulations with the higher TiO_2 loading.

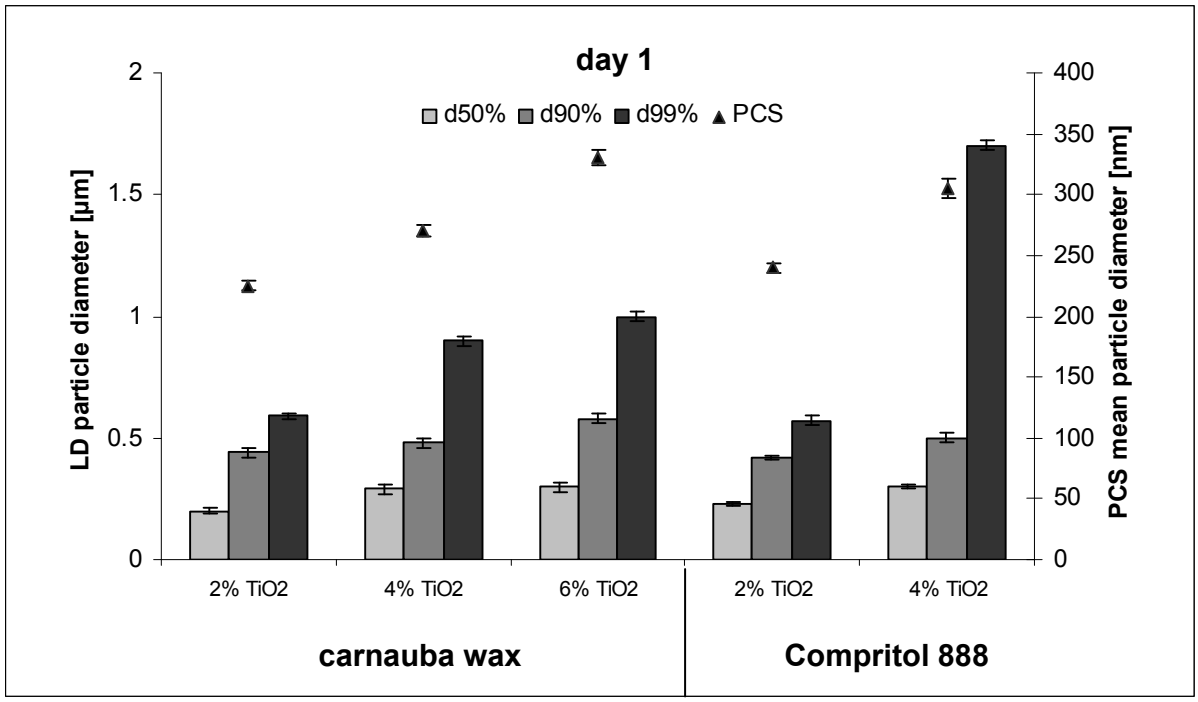

Figure 5-14: PCS and LD particle size measurements of the TiO_2-loaded NLC at day one. By increasing the TiO_2-loading the particle size was bigger (n=3).

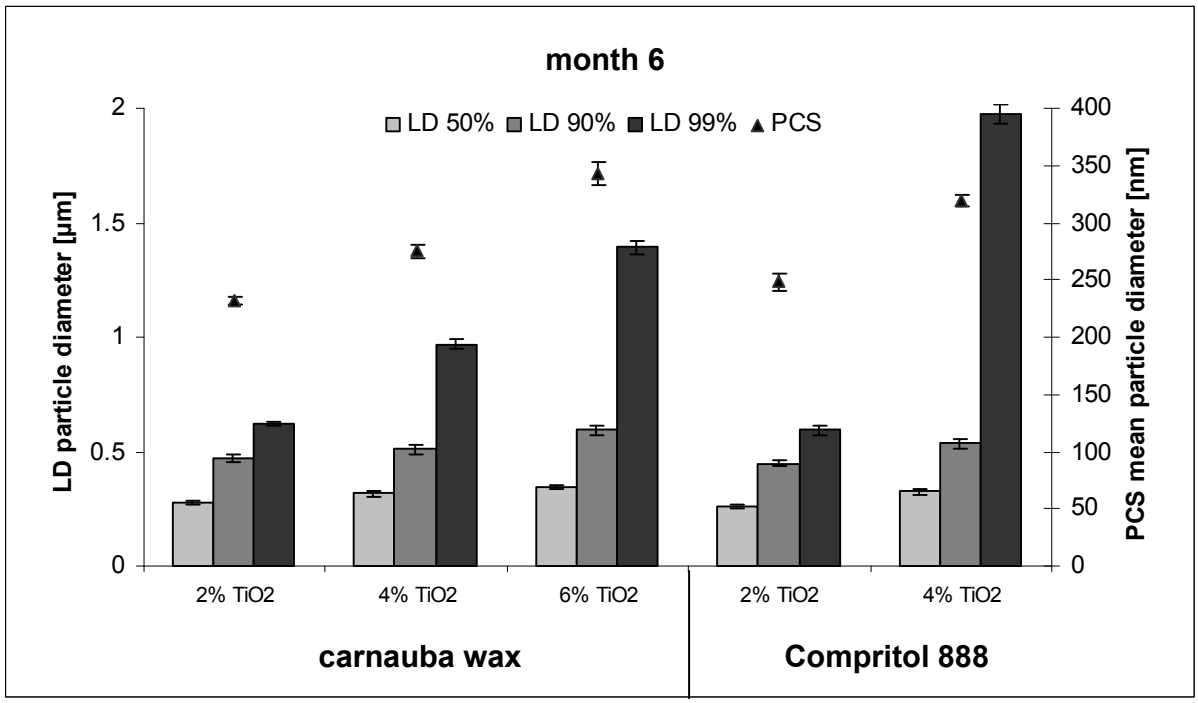

Figure 5-15: PCS and LD particle size of the TiO_2-loaded NLC after six months. No remarkable increase in particle size was seen (n=3).

The morphological characterization performed by scanning electron microscopy (SEM) confirmed the information obtained from the particle size measurements (Figure 5-16). The TiO_2-loaded carnauba wax lipid particles are spherical and the mean size of the particles is about 1 µm. Figure 5-17 is a zoomed picture where the TiO_2 nanoparticles can be seen as shiny points inside the lipid particle.

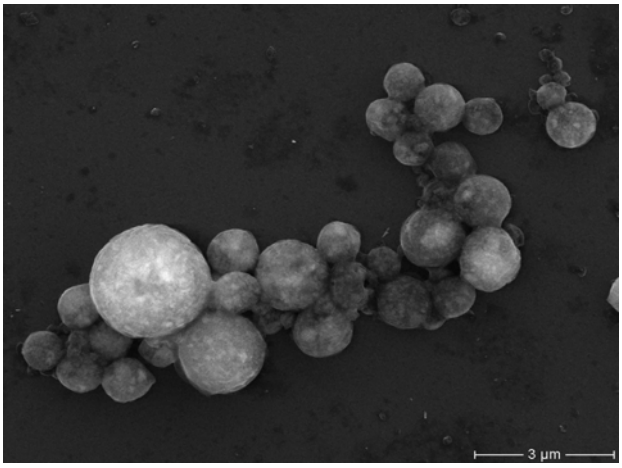

Figure 5-16: SEM picture of TiO_2-loaded carnauba wax NLC (6% loading).

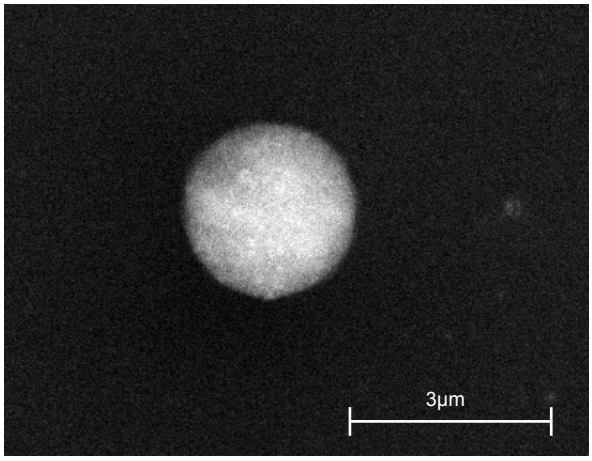

Figure 5-17: SEM picture (zoomed) of TiO_2-loaded carnauba wax NLC (6% loading). The TiO_2 particles can be seen inside the lipid particle.

Energy Dispersive X-ray (EDX) analysis was used to identify which elements are actually present in the specimen under the electrons probe, which is in this instance the lipid nanoparticle in Figure 5-17. The EDX spectrum (Figure 5-18) shows that the TiO_2 nanoparticles are present on the surface of the NLC. The titanium (Ti) and aluminium (Al) peaks are coming surely from the TiO_2 particles. The Al peak is coming from the alumina (Al_2O_3) coating the nanosized TiO_2 particles.

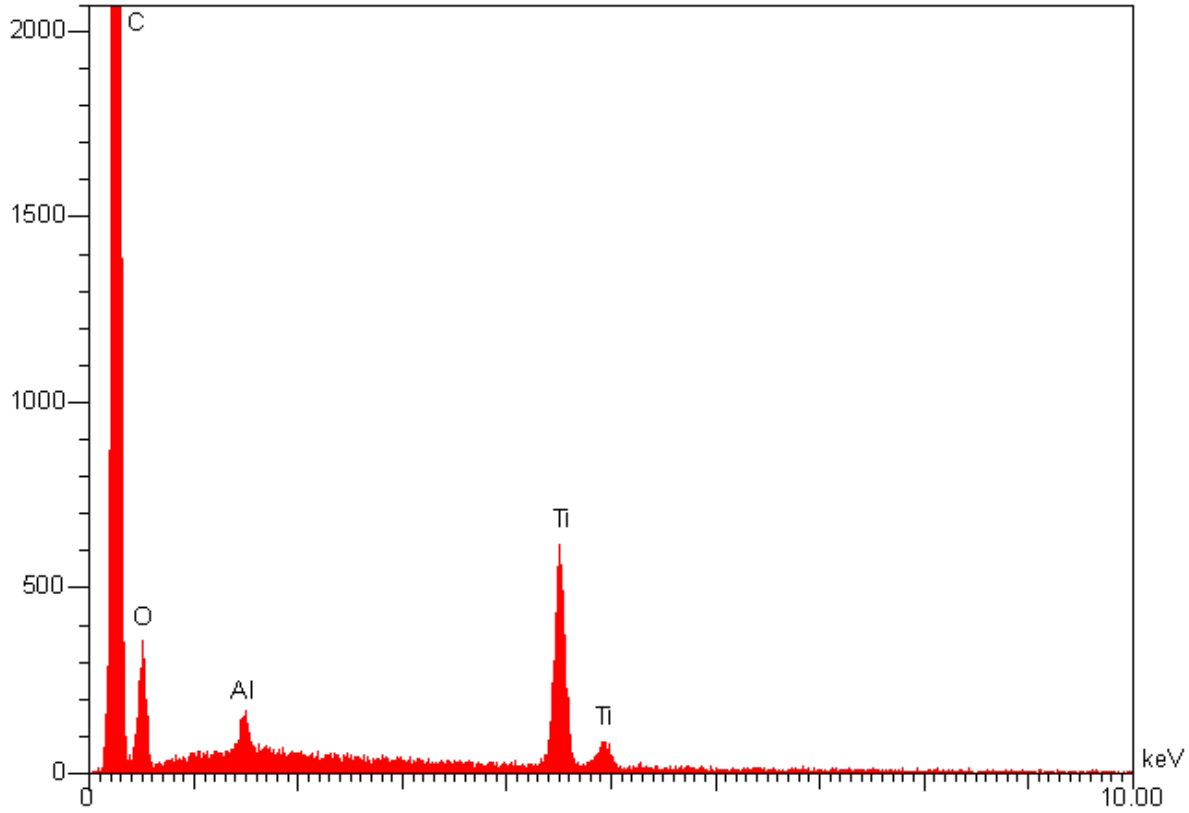

Figure 5-18: The EDX spectrum obtained from scanning the lipid nanoparticle in Figure 5-17.

5.4.3 UV absorption properties of TiO_2-loaded NLC

The spectral absorption between 400 and 200 nm has been measured for two TiO_2-loaded NLC (carnauba wax and Compritol 888, 2% TiO_2 loading) and a 2% TiO_2 nanoemulsion (decyl oleate). The particle size of all samples was comparable. All samples were diluted with the same dilution factor and the lipid phase concentration was 0.272 µg/ml. Figure 5-19 shows that the TiO_2-loaded carnauba wax NLC formulation has approximately three times higher UV absorption than the TiO_2-loaded decyl oleate nanoemulsion. The TiO_2-loaded Compritol 888 NLC formulation has approximately twice higher UV absorption than the TiO_2-loaded decyl oleate nanoemulsion.

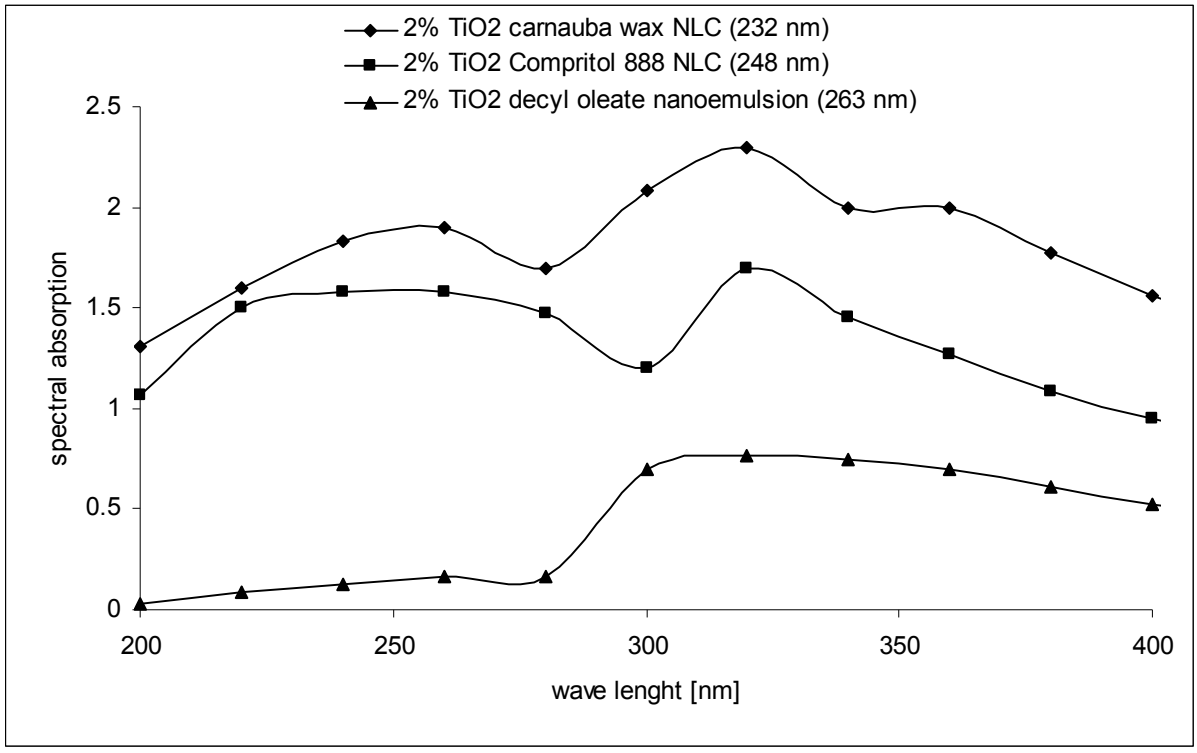

Figure 5-19: Absorption spectra of 2% TiO_2-loaded carnauba wax NLC, 2% TiO_2-loaded Compritiol 888 NLC and 2% TiO_2 decyl oleate nanoemulsion. The UV absorption of the NLC formulations was remarkably higher than the UV absorption of the nanoemulsion, lipid phase concentration= 0.272 µg/ml (n=3).

The two NLC formulations have a higher UV absorption because of the increase of the UV scattering and absorption. This is because of the larger particle sizes in the nanometric scale (the NLC particles) enabling to reach upper wavelengths in the UV spectrum. It must be also considered that the type of the lipid matrix contributes to obtain a better UV blocking. The carnauba wax is partially composed of cinnamates, which by the combination with TiO_2 shows a synergistic effect to improve the UV blocking activity [291].

To study the effect of increasing the TiO_2 loading in the lipid matrix of the nanoparticles on the UV absorption of the formulation, the spectral absorption of the different TiO_2-loaded carnauba wax NLC formulations was measured. All samples were diluted with the same dilution factor and the lipid phase concentration was about 0.04 µg/ml. A higher spectral absorption was measured when the TiO_2 loading was increased in the NLC. The formulation with 6% TiO_2 loading has the highest spectral absorption compared to the 4% TiO_2 loading and the 2% TiO_2 loading. All NLC formulations had a higher spectral absorption than the emulsion (Figure 5-20). This is because of the presence of a higher amount of the UV absorbing substance per unit weight (TiO_2).

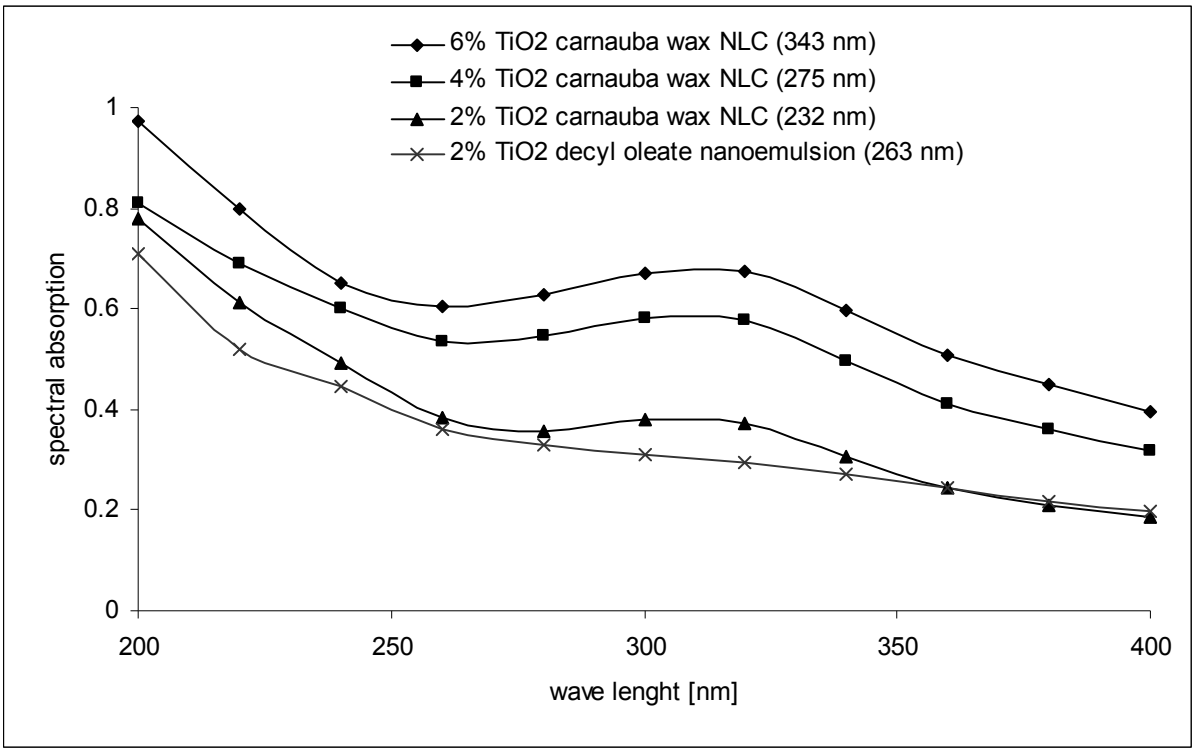

Figure 5-20: Absorption spectra of 2%, 4%, 6% TiO_2-loaded carnauba wax NLC and a 2% TiO_2 decyl oleate nanoemulsion. The spectral absorption of the NLC formulations increased as the TiO_2 loading increased, lipid phase concentration≅ 0.04 µg/ml (n=3).

5.4.4 UV blocking activity of creams containing TiO2-loaded NLC

The UV blocking activity of four different creams was assessed. These four creams were TiO_2-loaded carnauba wax NLC creams with 2%, 4% and 6% TiO_2 loading in the NLC suspension and a 2% TiO_2 conventional cream (Table 5-9). This was performed by measuring the concentration of a β-carotene solution in a quartz Petri dish covered with 0.3 g evenly spread layer of one of these creams. The Petri dishes were exposed to artificial sun light containing UV radiation inside an artificial sunlight chamber Suntest (Heraeus GmbH, Hanus, Germany) and were eradiated with a radiation intensity of about 830 W/m^2 (between 300 and

830 nm) for 60 min (see chapter 2). The β-carotene concentration was assessed after 15, 30 and 60 min of exposure (Figure 5-21).

Table 5-9: The composition of the four creams prepared for the UV blocking activity test (all amounts are in % (w/w), "-" means substance was not added).

	Formulation	
Substance	**TiO_2-loaded NLC cream**	**Conventional cream**
TiO_2-loaded NLC (TiO_2 loading is 2%, 4% or 6% (w/w))	10.0	-
carnauba wax	-	10.00
decyl oleate	-	5.00
PlantaCare 2000	-	3.00
UV-Titan M 160	-	2.00
TegoSoft DO	4.00	4.00
Montanov 202	7.00	7.00
glycerol	5.00	5.00
Inutec SP1	0.50	0.50
water	add 100	add 100

The remaining concentration of the β-carotene in the different solutions showed that the TiO_2 -loaded NLC creams had a higher UV blocking activity than the conventional TiO_2 cream. That was clearly seen after 60 min when the remaining β-carotene concentration of the 2% TiO_2-loaded NLC cream was approximately three times higher than the remaining β-carotene concentration of the conventional TiO_2 cream. By increasing the TiO_2 concentration in the NLC (4% and 6%) a higher β-carotene concentration was measured indicating a higher UV blocking activity.

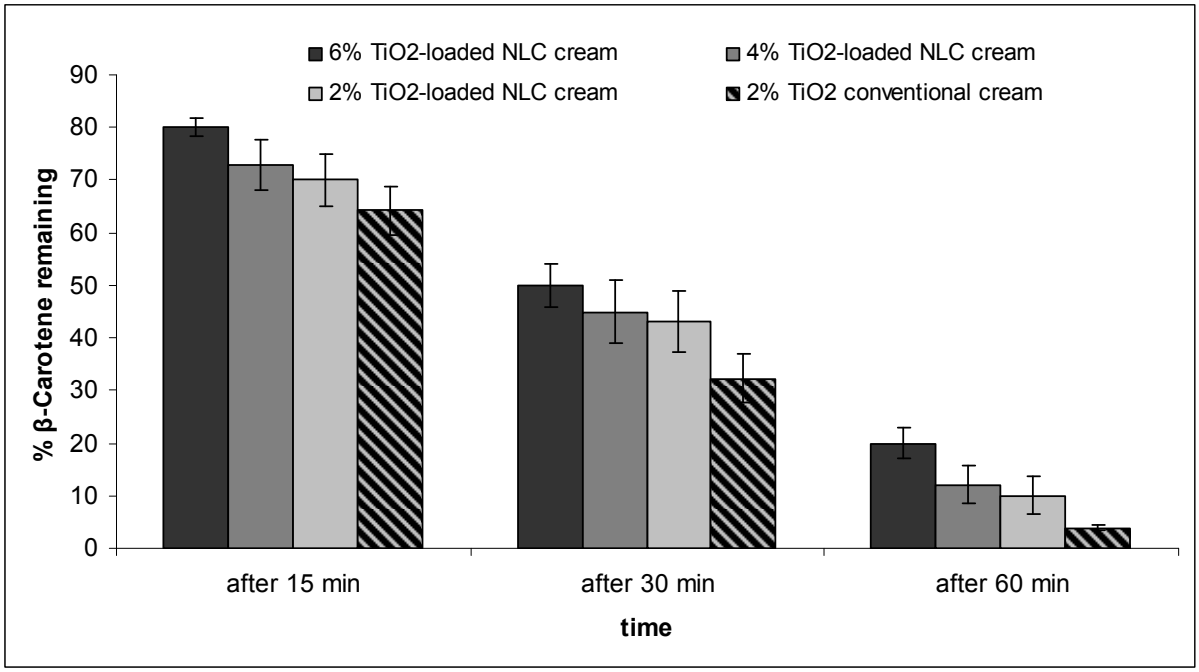

Figure 5-21: The remaining concentration of β-carotene after 15, 30 and 60 min of exposure to the artificial sun light (n=3).

Figure 5-22 shows the cuvettes filled with β-carotene solution to be analysed spectrophotometrically after 60 min exposure to artificial sun light.

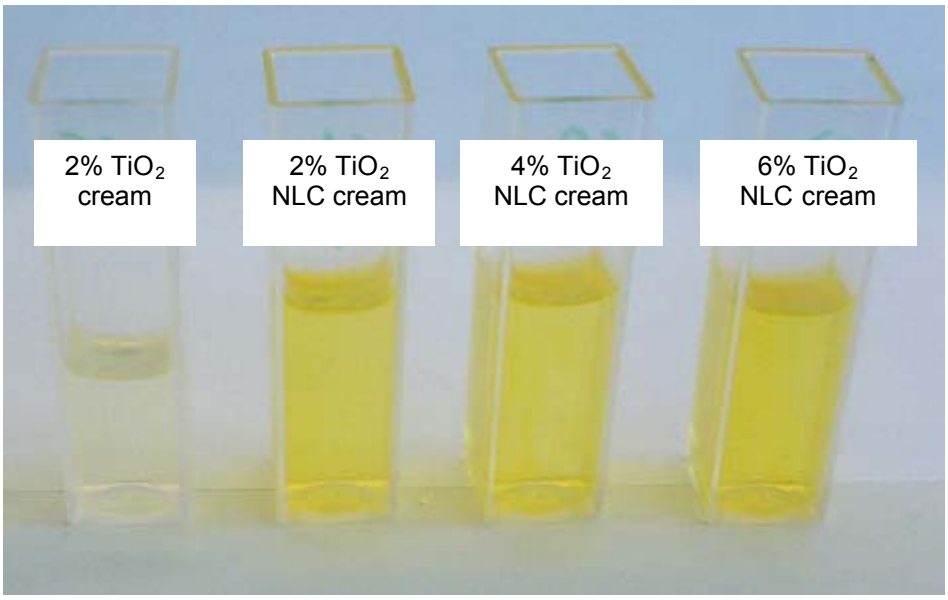

Figure 5-22: Four cuvettes containing β-carotene solution collected from four different Petri dishes after 60 min exposure to the artificial sun light.

5.4.5 Conclusion

TiO_2, as inorganic UV blocker, could be successfully incorporated in NLC formulations. Enclosing TiO_2 in NLC increased the UV blocking activity of this blocker. This will give a chance to reduce the concentration of the TiO_2 in the finished products while maintaining the desired high UV blocking activity. Using lower concentrations of TiO_2 and having it enclosed in the lipid matrix of the NLC will prevent or at least minimize the possible skin penetration. Also because the TiO_2 is enclosed inside the NLC it can be formulated with organic UV blockers in the oil droplets of the cream or lotion without having the possibility of losing the organic UV blockers activity due to the direct interaction between the TiO_2 and the these blockers.

6 PERFUME-LOADED NLC

6.1 Introduction

A perfume is a mixture of fragrant essential oils (etheric oils) and aroma compounds, fixatives and solvents used to give the human body, objects and spaces a pleasant smell [301]. In many applications of perfumes it is desired to have a prolonged release. From ethanolic solutions (eau de toilettes) the ethanol evaporates very fast, the perfume oil remaining on the skin also evaporates relatively fast as a function of its vapor pressure. One approach to obtain a prolonged release of perfumes is to incorporate them into oils and emulsions. After evaporation of the water phase of the emulsion, the oil droplets containing the perfume remain on the skin. In contrast to ethanol, the oil (e.g. olive oil, castor oil) has a very low vapor pressure (around 0 kPa at 20ºC). Therefore the oil droplets remain on the skin, and the evaporation of the perfume is hindered. This can be explained by *Raoult's law* which gives an approximation to the vapor pressure of mixtures of liquids. It states that the vapor pressure of a single phase mixture is equal to the mole fraction weighted sum of the components vapor pressures:

$$P_{a+b} = p_a x_a + p_b x_b$$

where p is the vapor pressure and x is the mole fraction.

The term $p_i x_i$ is the vapor pressure of a component i in the mixture. *Raoult's Law* is applicable only to non-electrolytes (uncharged species) and it is most appropriate for non-polar molecules with only weak intermolecular attractions, which is the case with perfumes and oils [302]. The perfume molecules need to diffuse first through the oil phase before they evaporate into the air. Figure 6-1 (left and middle) shows schematically the mechanisms of perfume evaporation from an ethanolic solution and from an emulsion. The rate-controlling factor of perfume release from emulsions is the vapor pressure of the oil. Thus, by decreasing the oil vapor pressure, the release can be prolonged. Ideally the liquid oil is replaced by a lipid, which is solid at room temperature and also at skin temperature. This was set forth in the concept of the NLC. The liquid lipid (oil) of o/w emulsions was replaced by a lipid blend, leading to nanoparticles which have a solid matrix at room temperature. The solid state of the matrix where the perfume is enclosed should theoretically lead to a further slower release in compare to emulsions (Figure 6-1 right), presumed the NLC structure is a solid matrix one.

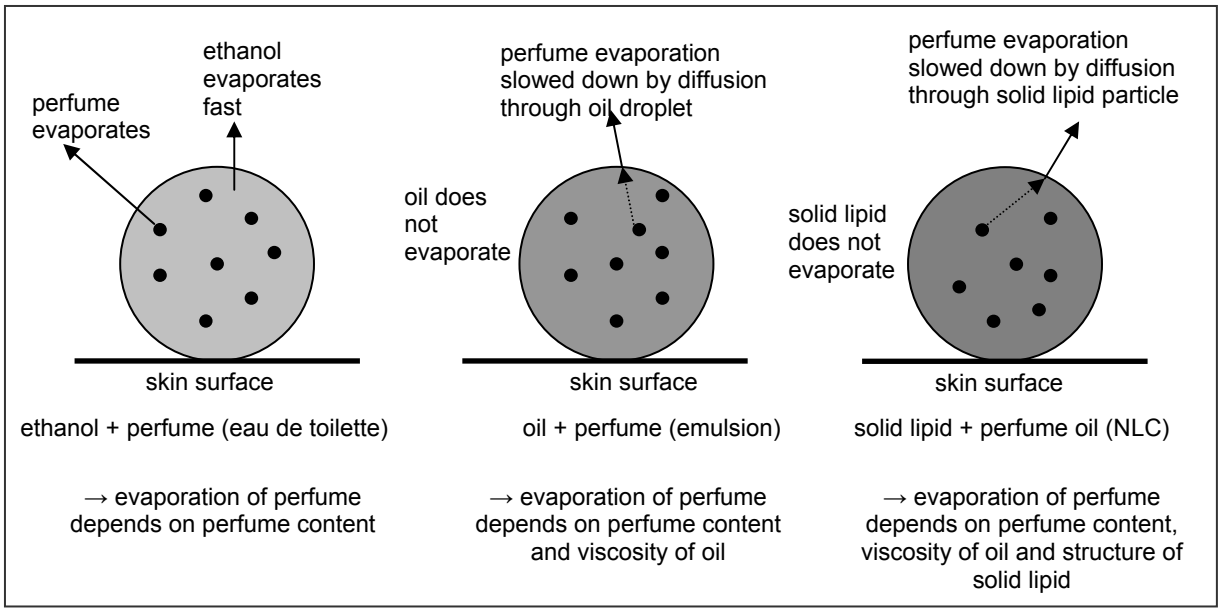

Figure 6-1: Mechanisms of evaporation of perfume from an eau de toilette, an o/w emulsion droplet and NLC (from left to right).

Former trials have been performed to incorporate volatile substances (perfumes, insects repellents) in solid lipid nanoparticles or nanostructured lipid carriers and their release from these matrices has been investigated [30, 90, 303, 304]. The sustainability of the perfume depends on many factors that have been further studied in this part of the work.

6.2 Development of perfume-loaded NLC

Many formulations were produced to monitor the different factors that might affect the stability of the formulation and the release profile of the perfume. Different solid lipids, surfactants (TegoCare 450, PlantaCare 2000 and Tween 80) and perfumes (CA, CT and Kenzo) were required for this study.

6.2.1 Lipid screening

The lipid screening was performed as described in chapter 2. More than ten solid lipids have been screened to determine which lipid has the highest perfume incorporation capacity (perfume CA). Turbidity or immiscibility of the melted solid lipid/perfume mixture indicated that the solid lipid is not suitable for perfume incorporation. After that the lipid/perfume mixtures were cooled down and the hardness of these solidified mixtures was investigated along with the inclusion of the perfume inside the lipid matrix. That was performed by simply putting a piece of the solidified mixture on a filter paper and observing if any oily spot is formed. Absence of oil means good inclusion of the perfume. Some screened lipids were chosen for a further lipid screening with higher amounts of perfume. Table 6-1 contains the lipids which have been screened.

Concerning the perfumes CT and Kenzo, the lipid screening was performed with the lipids of concern. Apifil showed a very good inclusion for both perfumes, while the lipid carnauba wax showed a lower inclusion for the perfume Kenzo.

Table 6-1: Lipid screening results of some solid lipids with different concentrations of the perfume CA.

Lipid	% Perfume	Miscibility with melted lipid	Filter paper test
Apifil	5	miscible	no spot
	10	miscible	no spot
	20	miscible	no spot
	30	miscible	no spot
	40	miscible	no spot
Atowax	5	miscible	no spot
Bees wax	5	miscible	no spot
Compritol ATO 888	5	miscible	no spot
	10	miscible	no spot
	20	miscible	no spot
	30	miscible	spot
	40	miscible	spot
Dynasan 114	5	miscible	no spot
Dynasan 116	5	miscible	no spot
	10	miscible	no spot
	20	miscible	no spot
	30	miscible	no spot
	40	miscible	spot
Dynasan 118	5	miscible	no spot
Hydrine	5	immiscible	spot
Imwitor 900	5	miscible	no spot
Precifac ATO	5	miscible	no spot
	10	miscible	no spot
	20	miscible	no spot
	30	miscible	no spot
	40	miscible	spot
Syncrowax	5	miscible	no spot
Witepsol S 58	5	turbid	spot

6.2.2 Production of perfume-loaded NLC

Production was performed as described in chapter 2. Homogenization was performed at 5°C above the melting point of the solid lipid applying two homogenization cycles at 800 bars (unless otherwise mentioned). To prevent perfume loss through fast volatilization (due to high temperature of the lipid melt) the perfume was added just before homogenization when the lipid melt reached the required temperature. The same procedure was followed with all the perfumes used.

6.3 Characterization of perfume-loaded NLC

The shape and the physical properties of the perfume-loaded NLC have a great influence on the perfume release. Therefore, the following methods have been utilized to characterize the produced NLC suspensions.

6.3.1 Light microscopy (LM)

All produced samples were examined by light microscopy to determine roughly the particles size and most important to detect any presence of crystals. The samples that showed lipid crystals were excluded and no further measurements were performed. The four following figures show exemplarily some of the samples investigated.

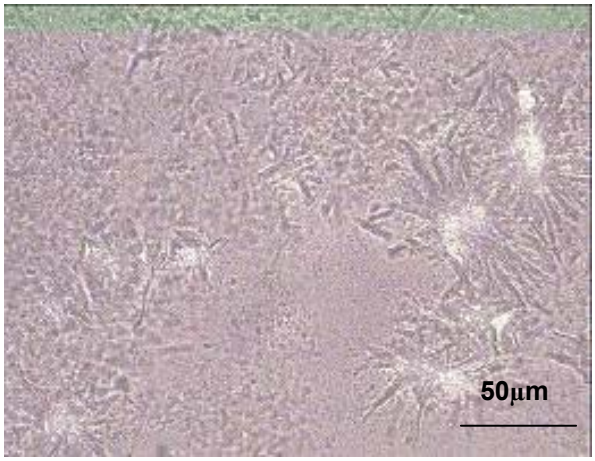

Figure 6-2: LM picture of NLC (Compritol ATO 888, CA). Crystals of the lipid could be detected after 30 days of storage at RT (magnification 63X10).

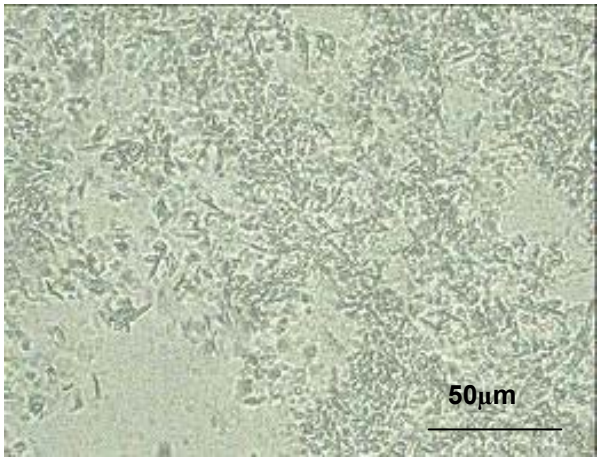

Figure 6-3: LM picture of NLC (Witepsol S 58, CA). Crystals of the lipid could be already detected after 15 days of storage at RT (magnification 63X10).

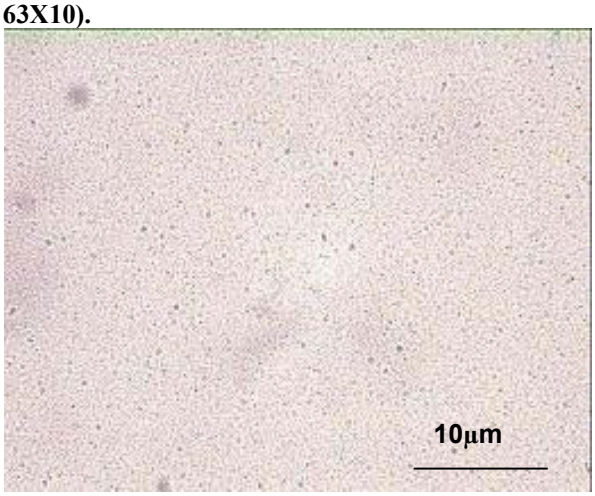

Figure 6-4: LM picture of NLC (Apifil, CA) (2% (w/w) CA). No crystals could be detected after three months of storage at RT. Lipid particles size is below 1 µm (magnification 100X10).

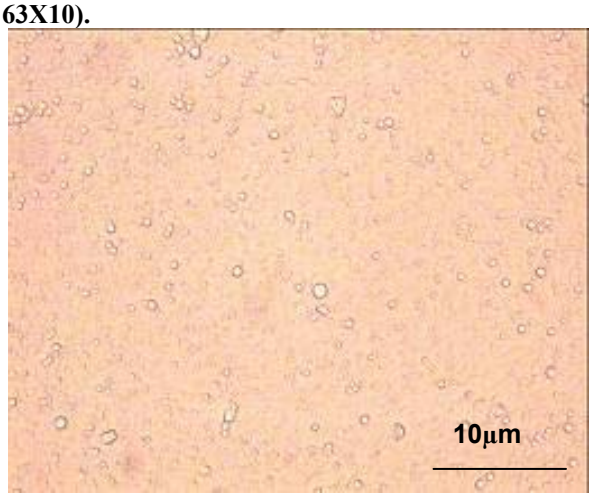

Figure 6-5: LM picture of NLC (Dynasan 116, CA) (2% (w/w) CA). No crystals could be detected after three months of storage at RT. Lipid particles size is below 3µm (magnification 100X10).

In the first two figures lipid crystals can be clearly seen. The appearance of these crystals might be because of the formation of the more stable β-modification of the solid lipid during the storage time. The other two figures show the perfume-loaded NLC which are homogeneous in particle size and contain no crystals.

6.3.2 Scanning electron microscopy (SEM)

As described in chapter 2, some selected perfume-loaded NLC samples were investigated using SEM. Figure 6-6 shows some lipid particles of a diameter between 1-2 µm produced using the lipid Precifac ATO 888 and loaded with the perfume CA (2% (w/w)). The smaller particles were melted and could be seen as dark spots due to the high temperature generated by the electrons beam focused on the sample. Because of this phenomenon higher magnification pictures could not be made for the NLC samples produced using relatively low melting point lipids.

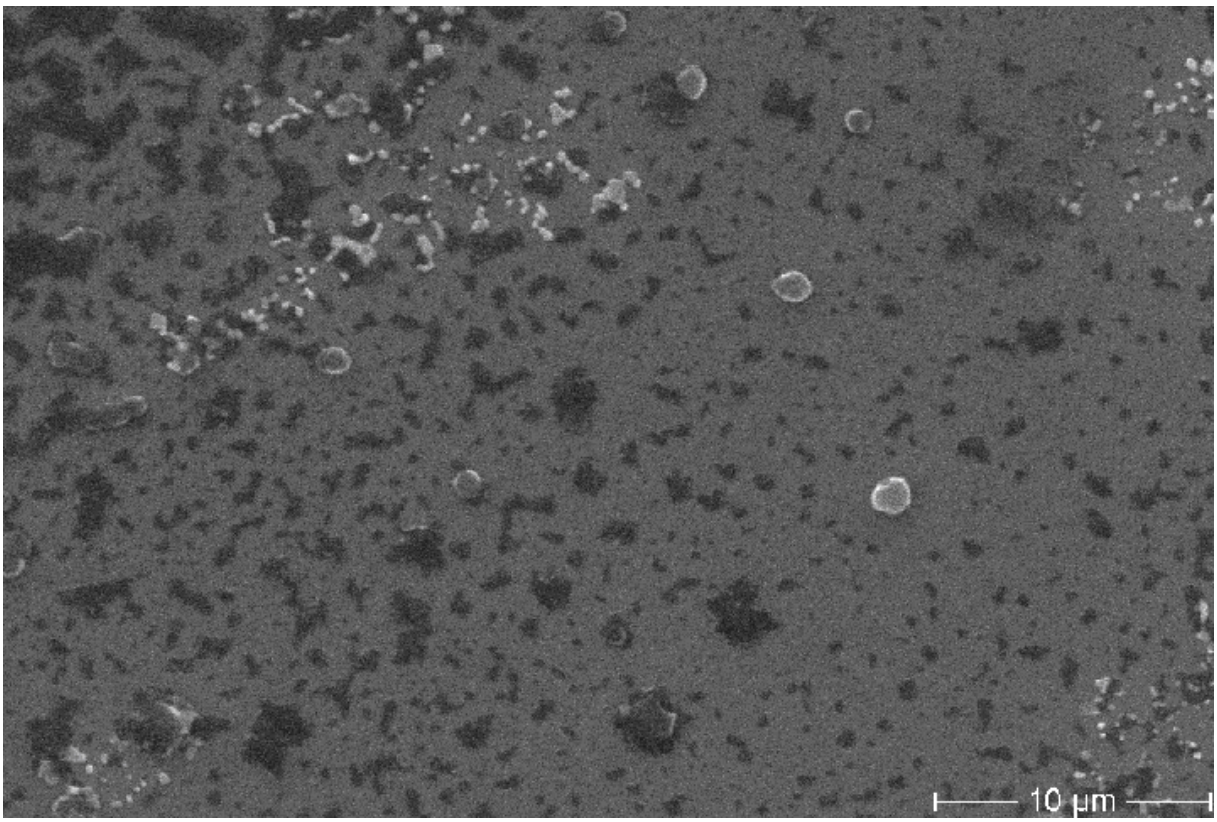

Figure 6-6: Electron microscopy picture of NLC (Precifac ATO 888, CA). Lipid particles of 2 µm size can be clearly seen. The dark spots are the smaller lipid particles which have melted by the heat generated from the electrons beam.

6.3.3 Particle size investigation

The particle size of the produced perfume-loaded NLC samples was measured using LD and PCS as described in chapter 2.

6.3.4 DSC analysis

The produced perfume-loaded NLC formulations were also analysed using DSC to determine the melting point and the recrystallization index (RI) of the lipid matrix of the nanoparticles. The samples listed below (Table 6-2) were analysed using DSC on day 1 and after 10 weeks (Table 6-3). An unchanged melting point and RI during storage prove the physical stability of the NLC (samples containing Precifac ATO 888 and Dynasan 116). The melting point and RI of the two samples produced using Apifil and TegoCare 450 or Tween 80 increased after ten weeks. This indicates changes in the lipid matrix to the more stable lipid polymorph (β-modification). This might cause changes in the perfume release profile.

Table 6-2: The composition of the perfume-loaded NLC samples analysed using DSC.

Sample name	Composition % (w/w)	
Precifac TegoCare	Precifac ATO 888	8.8%
	Miglyol 812	1.0%
	CA	0.2%
	TegoCare450	3.0%
	water	87.0%
Precifac Tween	Precifac ATO 888	8.8%
	Miglyol 812	1.0%
	CA	0.2%
	Tween 80	3.0%
	water	87.0%
Dynasan TegoCare	Dynasan 116	8.8%
	Miglyol 812	1.0%
	CA	0.2%
	TegoCare450	3.0%
	water	87.0%
Dynasan Tween	Dynasan 116	8.8%
	Miglyol 812	1.0%
	CA	0.2%
	Tween 80	3.0%
	water	87.0%
Apifil TegoCare CA	Apifil	12.0%
	CA	2.0%
	TegoCare450	1.2%
	water	84.8%
Apifil Tween CA	Apifil	13.0%
	CA	2.0%
	Tween 80	1.2%
	water	84.8%

Table 6-3: The DSC analysis results of three bulk solid lipids and the perfume-loaded NLC samples produced using these lipids.

Sample name	Measurement point	Onset ºC	Melting point ºC	Enthalpy J/g	Recrystallization index %
Precifac ATO 888 bulk lipid	day 1	48.0	52.0	222	100
	week 10	47.9	52.1	227	100
Dynasan 116 bulk lipid	day 1	62.0	63.0	194	100
	week 10	62.1	63.0	191	100
Apifil bulk lipid	day 1	59.0	70.0	127	100
	week 10	59.2	70.2	126	100
Precifac TegoCare	day 1	41.3	46.1	99	53
	week 10	40.9	46.4	94	51
Precifac Tween	day 1	42.2	46.1	21	11
	week 10	42.1	46.6	53	28
Dynasan TegoCare	day 1	52.3	59.6	132	54
	week 10	52.6	59.3	133	54
Dynasan Tween	day 1	54.9	57.6	18	7
	week 10	54.9	57.6	43	18
Apifil TegoCare CA	day 1	37.1	55.5	69	23
	week 10	36.2	57.3	148	50
Apifil Tween CA	day 1	36.1	51.9	75	25
	week 10	50.2	55.4	94	32

6.4 Stability of perfume-loaded NLC

The stability of the perfume-loaded NLC was monitored by assessing the physical appearance of the suspensions (by eye and light microscopy), measuring the particle size after definite periods of time using LD and PCS and by investigating the crystallization using DSC.

Some samples were stable over a year. Others showed an increase in viscosity and their consistency became gel-like, this was coupled with a significant increase in the recrystallization index. A simple explanation is that the lipids of these unstable samples were transforming from the metastable crystal modification to the stable one, causing the particle size to grow and the viscosity to increase [214]. For instance, the sample produced using Apifil as solid lipid, the perfume CA and TegoCare 450 as surfactant (Apifil TegoCare) showed a change in viscosity after ten weeks, and an increase in particle size along with the increase in RI (from 23% to 50%) (c.f. 6.3).

6.5 Factors affecting the perfume release

The release study was performed as described in chapter 2 to compare the capacity of different samples to retain the perfume incorporated for a longer time and release it slowly from the lipid matrix of the nanoparticles. Reference emulsions were also produced to compare the NLC samples with them concerning the release profile of the incorporated perfume. Many factors that could affect the release profile of the perfume from the NLC system were considered during this study. The effect of the particle size, the lipid matrix, the surfactant, the perfume concentration in the lipid matrix and the perfume type were studied.

6.5.1 Particle size

The particle size of a colloidal system (e.g. NLC) is a crucial factor for the release of the material(s) incorporated inside the particles. The perfume-loaded NLC matrix is considered to be a solid solution. This makes *Higuchi equation* ideal for the description of the perfume release from the system [305-309]. In *Higuchi equation* the released amount per unit surface area is proportional to the square-root time, and expressed as:

$$Q = \sqrt{D(C_0 - C_s)t} \qquad \text{eq.1}$$

$$Q = m_t / A \qquad \text{eq.2}$$

Where Q is the amount of incorporated perfume released after time t per unit of exposed area A, D is the diffusion coefficient of the perfume in the permeating fluid, C_0 is the initial

amount of perfume in the matrix per unit volume, C_s is the solubility of the perfume in the permeating fluid, m_t is the amount of perfume released after time t and A is the surface area of the matrix exposed to the fluid.

$$m_t = \%rel.C_0 \quad \text{eq.3}$$

From eq.1, eq.2 and eq.3 the % released can be expressed as:

$$\%rel = \frac{A}{C_0}\sqrt{D(C_0 - C_s)t} \quad \text{eq.4}$$

The surface area of a sphere is expressed as:

$$A = 4\pi r^2 \quad \text{eq.5}$$

where r is the sphere radius.

The volume of a sphere is expressed as:

$$V = \frac{4}{3}\pi r^3 \quad \text{eq.6}$$

From eq.5:

$$\frac{A}{4} = \pi r^2 \quad \text{eq.7}$$

From eq.6:

$$\frac{3V}{4r} = \pi r^2 \quad \text{eq.8}$$

That leads to:

$$A = \frac{3V}{r} \quad \text{eq.9}$$

Because V is constant for a given amount of lipid in the formulation

$$A = K_1\frac{1}{r} \quad \text{eq.10}$$

That means when the particle size decreases, the total surface area of the particles increases.

From eq.4 the slope of the release line is expressed as:

$$Slope = \frac{A}{C_0}\sqrt{D(C_0 - C_s)} \quad \text{eq.11}$$

In other words:

$$Slope = K_2 A \qquad \text{eq.12}$$

From eq.10 the slope can be expressed as:

$$Slope = K\frac{1}{r} \qquad \text{eq.13}$$

It means when the particle size decreases, the slope of the release line will increase, in other words the smaller the particles, the faster the release.

Three samples were chosen to investigate the role of the particle size on the release profile. These samples and their PCS mean particle sizes were as follow: L (263 nm), M (200 nm) and S (190 nm). All samples had the same lipid, lipid concentration, perfume load and surfactant type and concentration (Table 6-4). The difference between them was only the particle size. This was achieved by using different homogenization pressures during the production. The release of the perfume from these three samples was plotted against time and against the square root of time (Figure 6-7 and Figure 6-8 respectively). The slopes and R^2 of the release lines plotted against the square root of time were also calculated (Table 6-5). From Figure 6-8 it can be clearly seen that the release of the perfume follows Higuchi equation for release from a matrix. This is because the relation between the % released and the square root of time is linear. Also it can be concluded that the smaller the particle size the faster the release of the perfume from the matrix of the lipid particles. This is confirmed by the slopes of the different release graphs. The slope of the release line increases as the particle size decreases.

Table 6-4: The composition and the particle size of the perfume-loaded NLC samples used to study the effect of the particle size on the release profile.

Sample name	Composition % (w/w)		Particle size analysis		
S	Apifil	13.0%	PCS (nm)	190	± 1
	CA	2.0%	PI	0.14	± 0.00
	TegoCare450	1.2%	d 50% (µm)	0.120	± 0.007
	water	83.8%	d 90% (µm)	0.310	± 0.006
			d 95% (µm)	0.374	± 0.004
			d 99% (µm)	0.476	± 0.003
M	Apifil	13.0%	PCS (nm)	200	± 3
	CA	2.0%	PI	0.14	± 0.00
	TegoCare450	1.2%	d 50% (µm)	0.120	± 0.007
	water	83.8%	d 90% (µm)	0.310	± 0.006
			d 95% (µm)	0.374	± 0.004
			d 99% (µm)	0.476	± 0.003
L	Apifil	13.0%	PCS (nm)	263	± 3
	CA	2.0%	PI	0.18	± 0.00
	TegoCare450	1.2%	d 50% (µm)	0.230	± 0.004
	water	83.8%	d 90% (µm)	0.457	± 0.017
			d 95% (µm)	2.704	± 2.111
			d 99% (µm)	32.603	± 9.037

Table 6-5: .The release lines equations, slopes and R^2 of the perfume-loaded NLC formulas with different particle size plotted against the square root of time.

Sample	Equation	Slope	R^2
Pf14c L	y=2.04x – 0.26	2.04	0.9996
Pf14c M	y=2.15x + 0.059	2.15	0.9953
Pf14c S	y=2.45x + 0.21	2.45	0.9987

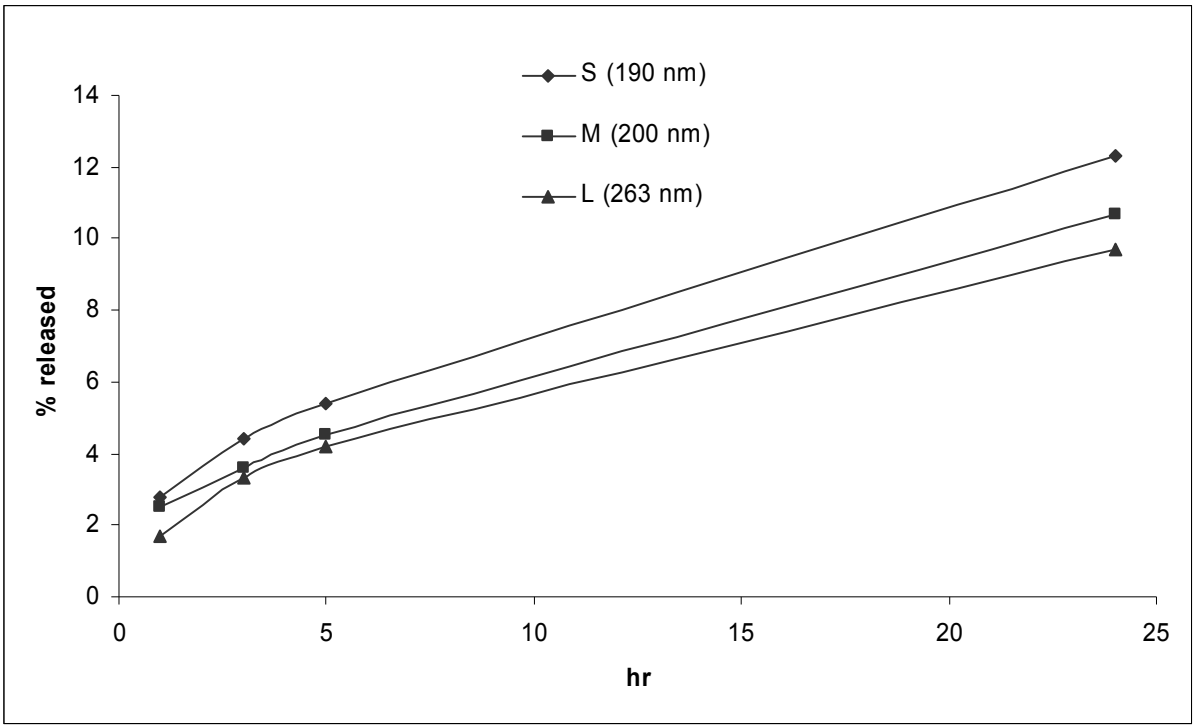

Figure 6-7: The release profiles of three perfume-loaded NLC samples having different particle size and produced using Apifil as solid lipid, CA as perfume and TegoCare 450 as surfactant (n=3).

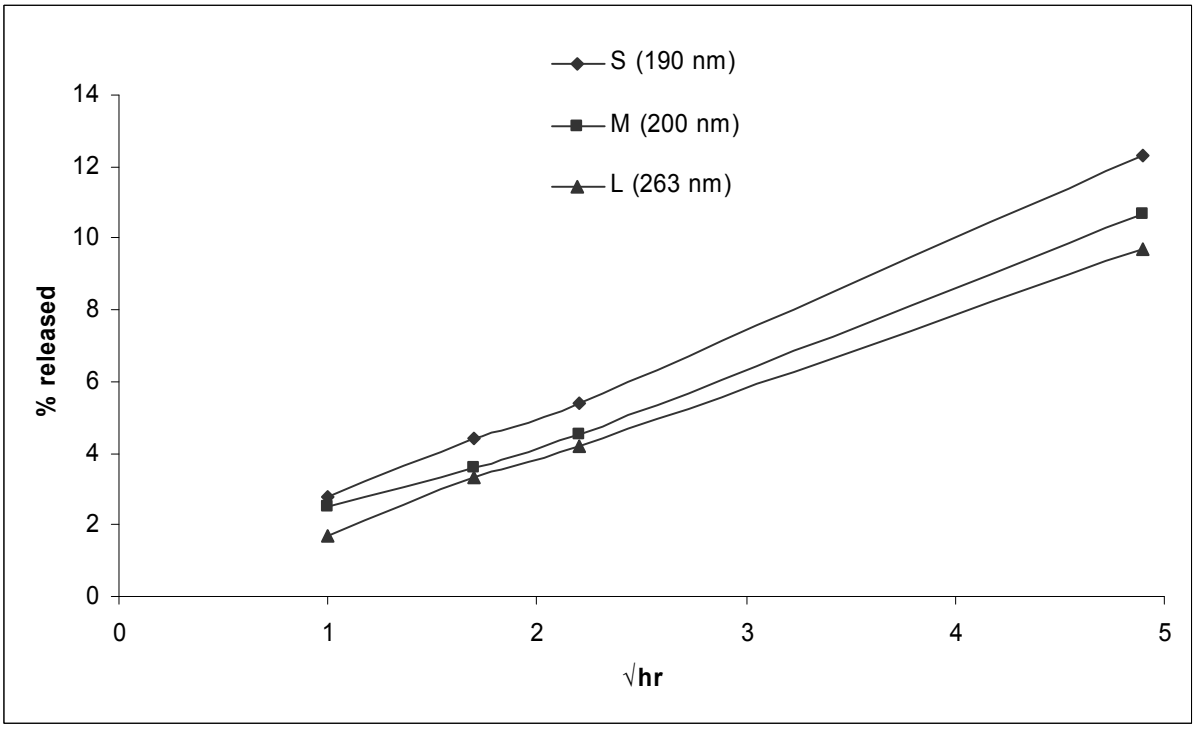

Figure 6-8: The Higuchi plot of the release profiles of three perfume-loaded NLC samples having different particle size and produced using Apifil, the perfume CA and TegoCare 450 as surfactant (n=3). The % releases is plotted against the square root of time.

6.5.2 Lipid matrix

Different lipid matrices lead to different release profiles. The lipids have different crystals order and crystallization modification, different melting points and different hydrophilic lipophilic balance (HLB) values, e.g. Apifil HLB = 9.4, Compritol 888 HLB = 2 [130, 144]. This makes the affinity of the perfume to be entrapped within the lipid matrix different from one lipid to another. A release study comparing between different perfume-loaded NLC formulations made from three different lipids (Apifil, Dynasan 116 and Precifac ATO 888) was performed. The particle size of the different samples was comparable (Table 6-6). Figure 6-9 shows that by changing the lipid (while maintaining the other factors constant) the release profile of the perfume from the NLC system changes.

Table 6-6: The composition and the particle size of the perfume-loaded NLC samples used to study the effect of the lipid matrix and the surfactant type on the release profile.

Sample name	Composition % (w/w)		Particle size analysis			
Dynasan TegoCare	Dynasan 116	8.8%	PCS (nm)	243	±	4
	Miglyol 812	1.0%	PI	0.15	±	0.06
	CA	0.2%	d 50% (µm)	0.170	±	0.091
	TegoCare450	3.0%	d 90% (µm)	0.409	±	0.037
	water	87.0%	d 95% (µm)	0.459	±	0.041
			d 99% (µm)	0.548	±	0.050
Dynasan Tween	Dynasan 116	8.8%	PCS (nm)	177	±	14
	Miglyol 812	1.0%	PI	0.28	±	0.10
	CA	0.2%	d 50% (µm)	0.105	±	0.001
	Tween 80	3.0%	d 90% (µm)	0.205	±	0.008
	water	87.0%	d 95% (µm)	0.274	±	0.024
			d 99% (µm)	0.731	±	0.330
Precifac TegoCare	Precifac ATO 888	8.8%	PCS (nm)	216	±	4
	Miglyol 812	1.0%	PI	0.16	±	0.05
	CA	0.2%	d 50% (µm)	0.181	±	0.004
	TegoCare450	3.0%	d 90% (µm)	0.388	±	0.002
	water	87.0%	d 95% (µm)	0.455	±	0.003
			d 99% (µm)	0.584	±	0.008
Precifac Tween	Precifac ATO 888	8.8%	PCS (nm)	179	±	6
	Miglyol 812	1.0%	PI	0.17	±	0.04
	CA	0.2%	d 50% (µm)	0.144	±	0.000
	Tween 80	3.0%	d 90% (µm)	0.968	±	0.034
	water	87.0%	d 95% (µm)	8.201	±	0.103
			d 99% (µm)	24.370	±	0.378
Apifil TegoCare	Apifil	8.8%	PCS (nm)	269	±	6
	Miglyol 812	1.0%	PI	0.23	±	0.04
	CA	0.2%	d 50% (µm)	0.534	±	0.009
	TegoCare450	3.0%	d 90% (µm)	2.029	±	0.007
	water	87.0%	d 95% (µm)	2.256	±	0.011
			d 99% (µm)	2.585	±	0.011

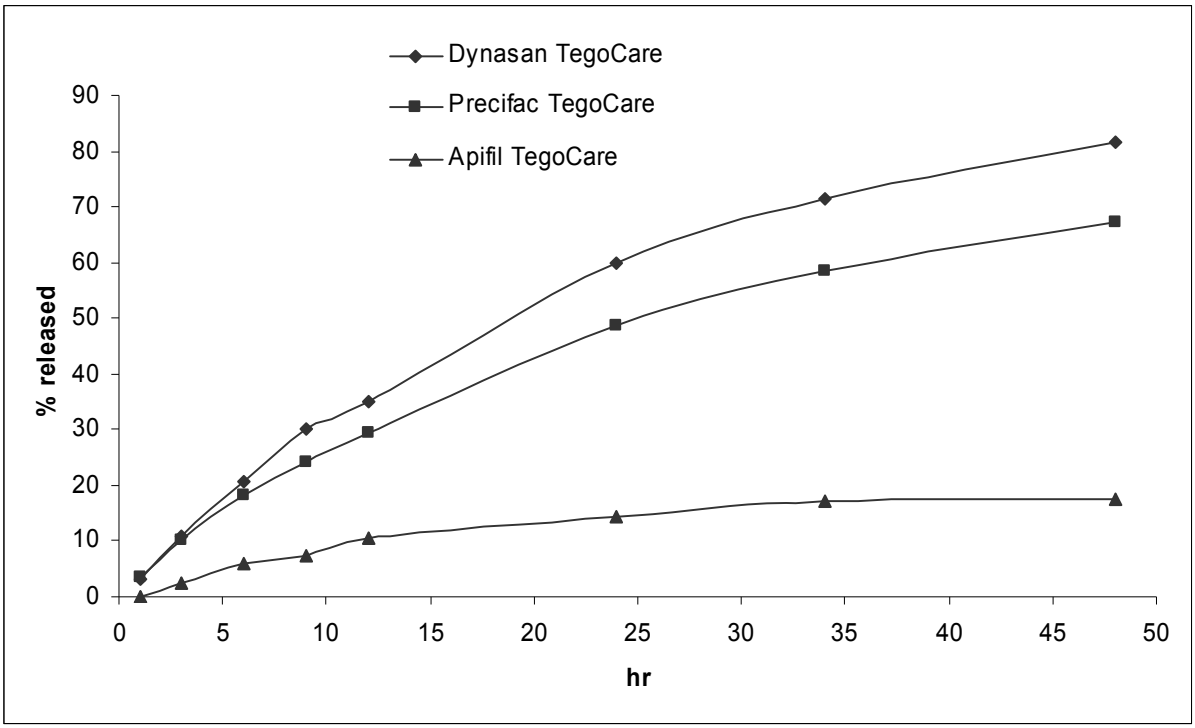

Figure 6-9: The release profiles of three perfume-loaded NLC samples with different lipid matrices. The NLC samples are produced using different solid lipids while keeping the same perfume (CA) and surfactant (TegoCare 450) (n=3).

6.5.3 Surfactant

Surfactants as they are used to stabilize the particles in the dispersion media (or emulsify the oil in water) may affect the structure of the lipid nanoparticles. This happens because of the interaction between the emulsifying agent molecules and the lipid molecules. Depending on the HLB of the surfactant and the molecular weight of the surfactant molecules, the affinity of the surfactant to the lipid differs. Having the surfactant molecules embedded in the lipid matrix might dramatically affect the crystallization of the lipid, and leave spaces in the lipid lattice. These spaces will give rise to higher loading capacity of perfume, incorporation in imperfections inside the particle matrix and eventually a slower release profile. Moreover, the ability of the surfactant to stabilize the oil droplets (in the lipid melted state during homogenization) and form smaller NLCs gives the surfactant also a role through the size of the formed lipid particles. Figure 6-10 shows the change in the release profile of the perfume when the surfactant is changed (detailed composition and particle size in Table 6-6). The Tween 80 stabilised samples had a slower release than the TegoCare 450 samples. The samples produced using TegoCare 450 as surfactant (Precifac TegoCare and Dynasan TegoCare) have a significantly higher recrystallization index in comparison to the samples produced using Tween 80 (Precifac Tween and Dynasan Tween), comparing the samples containing the same solid lipid with each other, c.f. Table 6-3. This indicates that the crystals

of the lipid matrix of the first two samples (with TegoCare 450) are more ordered and leaving less spaces in between. Therefore, the incorporated perfume is less enclosed and is faster released from the matrix of the particles.

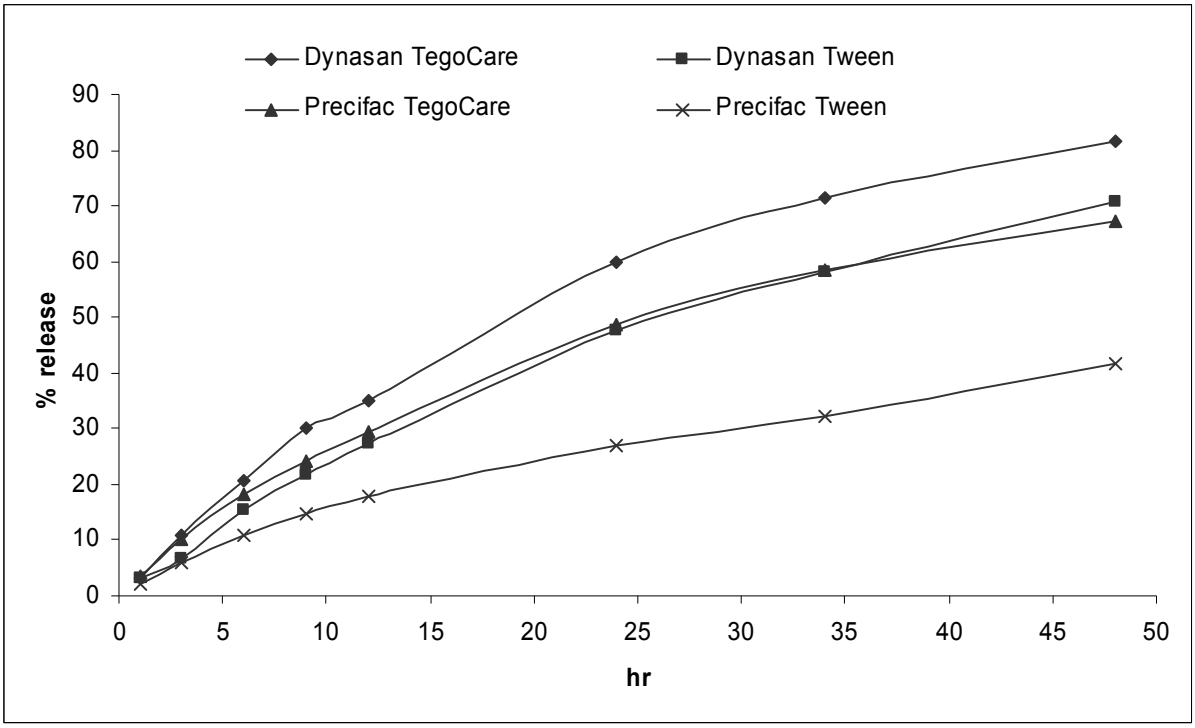

Figure 6-10: The release profiles of four perfume-loaded NLC samples (perfume CA) made using Precifac ATO 888 and Dynasan 116 as solid lipids and TegoCare 450 and Tween 80 as surfactants (n=3).

6.5.4 Perfume loading

Perfume loading might affect the release profile. It depends on the affinity of the perfume to mix with the lipid and be enclosed in the matrix. It can be seen clearly by comparing the samples produced using the perfume Kenzo and the two lipids Apifil and carnauba wax. Table 6-7 shows the detailed composition and the particle size of the different samples. With Apifil a slower perfume release was achieved by decreasing the perfume concentration in the lipid phase (Figure 6-11). While with carnauba wax the release rate was the same in all the samples with different perfume loading (Figure 6-12).

This is because the perfume was not enclosed in the carnauba wax lipid matrix while it was very well incorporated in the Apifil. When the perfume enclosing capacity of Apifil was exceeded a faster release of the perfume occurred. In the carnauba wax NLC samples the perfume was already outside the lipid matrix, and changing the concentration did not change the release profile.

Table 6-7: The composition and the particle size of the perfume-loaded NLC samples used to study the effect of the perfume loading on the release profile.

Sample name	Composition % (w/w)		Particle size analysis		
Apifil Kenzo 2%	Apifil	13.0%	PCS (nm)	182	± 2
	Kenzo	2.0%	PI	0.23	± 0.04
	TegoCare450	1.5%	d 50% (μm)	0.120	± 0.000
	water	83.5%	d 90% (μm)	0.214	± 0.001
			d 95% (μm)	0.246	± 0.002
			d 99% (μm)	0.303	± 0.005
Apifil Kenzo 4%	Apifil	11.0%	PCS (nm)	180	± 3
	Kenzo	4.0%	PI	0.20	± 0.04
	TegoCare450	1.5%	d 50% (μm)	0.126	± 0.001
	water	83.5%	d 90% (μm)	0.256	± 0.010
			d 95% (μm)	0.393	± 0.007
			d 99% (μm)	1.405	± 0.017
Apifil Kenzo8%	Apifil	7.0%	PCS (nm)	193	± 4
	Kenzo	8.0%	PI	0.19	± 0.04
	TegoCare450	1.5%	d 50% (μm)	0.130	± 0.002
	water	83.5%	d 90% (μm)	0.293	± 0.004
			d 95% (μm)	0.482	± 0.005
			d 99% (μm)	1.561	± 0.001
Apifil Kenzo 10%	Apifil	5.0%	PCS (nm)	195	± 4
	Kenzo	10.0%	PI	0.20	± 0.03
	TegoCare450	1.5%	d 50% (μm)	0.134	± 0.001
	water	83.5%	d 90% (μm)	0.217	± 0.004
			d 95% (μm)	0.242	± 0.007
			d 99% (μm)	0.285	± 0.097
Carnauba wax Kenzo 2%	carnauba wax	13.0%	PCS (nm)	743	± 50
	Kenzo	2.0%	PI	0.70	± 0.32
	TegoCare450	1.5%	d 50% (μm)	4.275	± 0.142
	water	83.5%	d 90% (μm)	7.686	± 0.226
			d 95% (μm)	8.703	± 0.214
			d 99% (μm)	10.453	± 0.239
Carnauba wax Kenzo 4%	carnauba wax	11.0%	PCS (nm)	605	± 35
	Kenzo	4.0%	PI	0.45	± 0.27
	TegoCare450	1.5%	d 50% (μm)	3.636	± 0.089
	water	83.5%	d 90% (μm)	7.414	± 0.182
			d 95% (μm)	10.051	± 0.415
			d 99% (μm)	22.980	± 0.885
Carnauba wax Kenzo8%	carnauba wax	7.0%	PCS (nm)	434	± 98
	Kenzo	8.0%	PI	0.80	± 0.25
	TegoCare450	1.5%	d 50% (μm)	7.599	± 0.113
	water	83.5%	d 90% (μm)	247.50	± 15.98
			d 95% (μm)	316.15	± 30.05
			d 99% (μm)	456.35	± 27.65
Carnauba wax Kenzo 10%	carnauba wax	5.0%	PCS (nm)	275	± 6
	Kenzo	10.0%	PI	0.15	± 0.04
	TegoCare450	1.5%	d 50% (μm)	0.293	± 0.001
	water	83.5%	d 90% (μm)	0.700	± 0.004
			d 95% (μm)	1.458	± 0.007
			d 99% (μm)	2.120	± 0.097

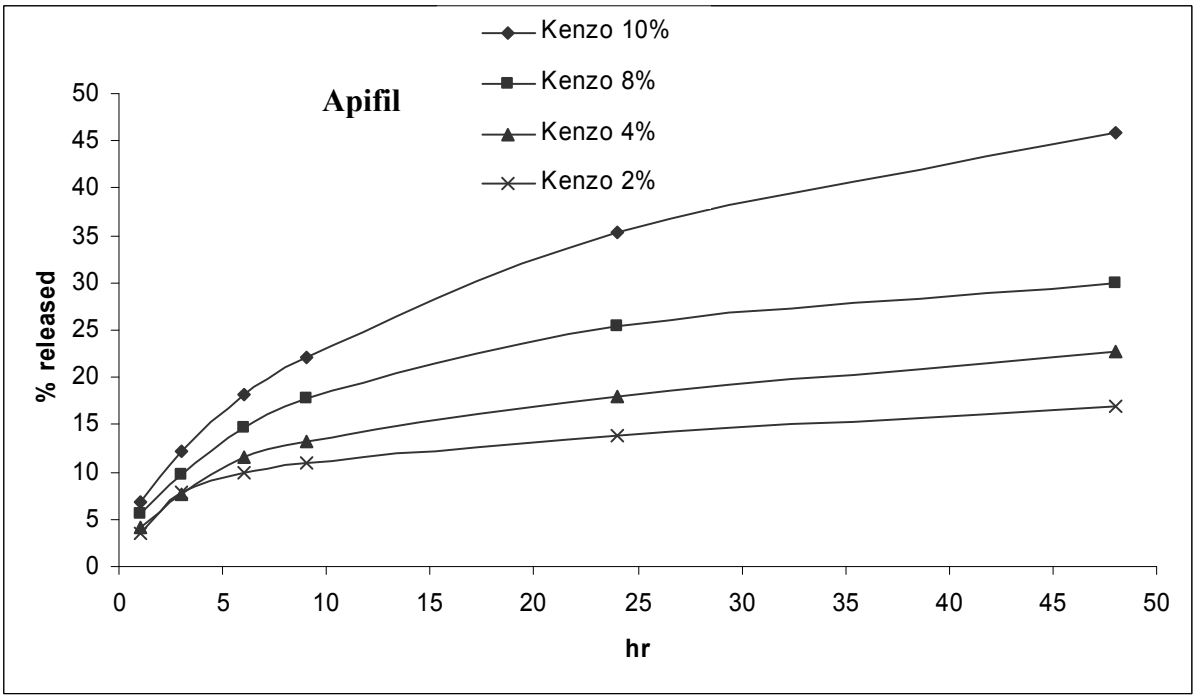

Figure 6-11: The release profiles of four perfume-loaded NLC samples produced using Apifil as solid lipid and the perfume Kenzo with different perfume loads (2, 4, 8 and 10% (w/w)) (n=3).

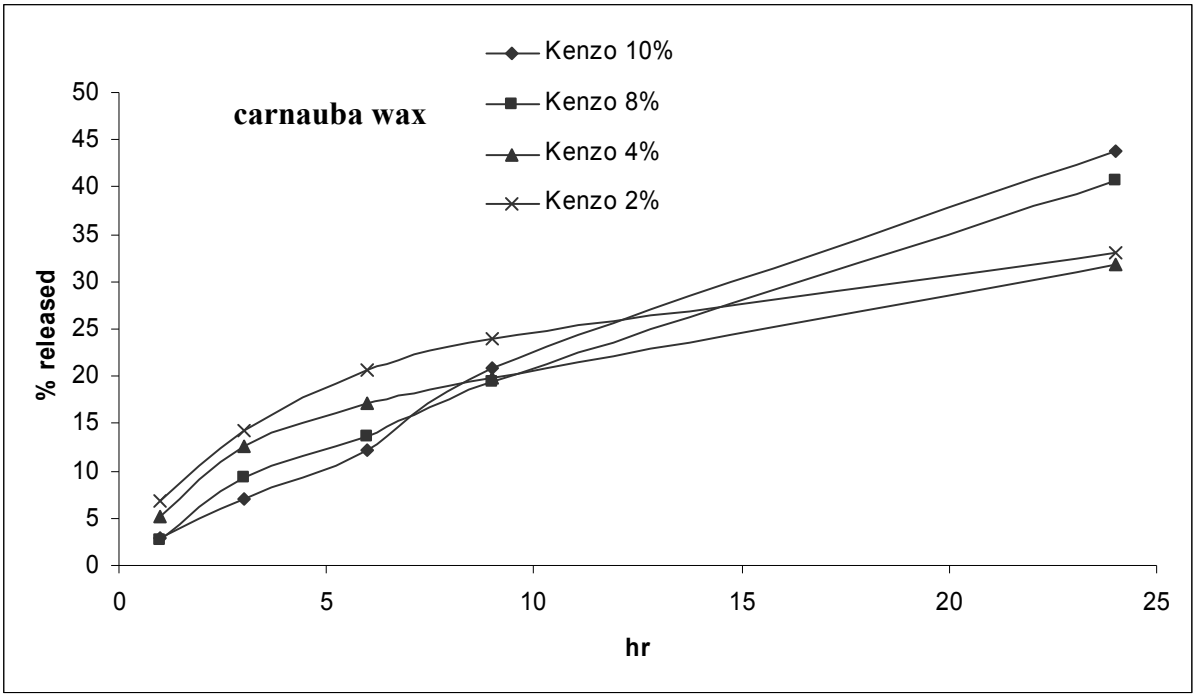

Figure 6-12: The release profiles of four perfume-loaded NLC samples produced using carnauba wax as solid lipid and the perfume Kenzo with different perfume loads (2, 4, 8 and 10% (w/w)) (n=3).

6.5.5 Perfume type

The perfume type affects the release profile because with the different compositions of perfumes there are different affinities to the lipid matrix. But in the studies performed in this work no differences were noticed when the perfume was changed. Figure 6-13 and Figure 6-14 show the release profile of the perfumes CA and CT from the same formulations. The perfume concentration was always 2% (w/w). Table 6-8 shows the detailed composition and the particle size of the different samples.

Table 6-8: The composition and the particle size of the perfume-loaded NLC samples used to study the effect of the perfume type on the release profile.

Sample name	Composition % (w/w)		Particle size analysis		
Dynasan Tween CA	Dynasan 116	12.0%	PCS (nm)	444	± 6
	CA	2.0%	PI	0.29	± 0.05
	Tween 80	3.0%	d 50% (µm)	0.271	± 0.002
	water	83.0%	d 90% (µm)	0.449	± 0.005
			d 95% (µm)	0.497	± 0.008
			d 99% (µm)	0.587	± 0.010
Dynasan Tween CT	Dynasan 116	13.0%	PCS (nm)	248	± 4
	CT	2.0%	PI	0.26	± 0.16
	Tween 80	3.0%	d 50% (µm)	0.143	± 0.001
	water	83.0%	d 90% (µm)	0.383	± 0.003
			d 95% (µm)	0.425	± 0.003
			d 99% (µm)	0.493	± 0.001
Precifac Tween CA	Precifac ATO	12.0%	PCS (nm)	450	± 4
	CA	2.0%	PI	0.16	± 0.03
	Tween 80	3.0%	d 50% (µm)	0.235	± 0.003
	water	83.0%	d 90% (µm)	0.419	± 0.003
			d 95% (µm)	0.466	± 0.003
			d 99% (µm)	0.548	± 0.004
Precifac Tween CT	Precifac ATO	13.0%	PCS (nm)	334	± 11
	CT	2.0%	PI	0.18	± 0.03
	Tween 80	3.0%	d 50% (µm)	0.229	± 0.004
	water	83.0%	d 90% (µm)	0.432	± 0.002
			d 95% (µm)	0.486	± 0.001
			d 99% (µm)	0.585	± 0.001
Apifil TegoCare CA	Apifil	12.0%	PCS (nm)	250	± 1
	CA	2.0%	PI	0.30	± 0.05
	TegoCare450	1.2%	d 50% (µm)	0.120	± 0.007
	water	84.8%	d 90% (µm)	0.310	± 0.006
			d 95% (µm)	0.374	± 0.004
			d 99% (µm)	0.476	± 0.003
Apifil TegoCare CT	Apifil	13.0%	PCS (nm)	248	± 6
	CT	2.0%	PI	0.30	± 0.26
	TegoCare450	1.2%	d 50% (µm)	0.215	± 0.002
	water	84.8%	d 90% (µm)	0.418	± 0.007
			d 95% (µm)	0.469	± 0.011
			d 99% (µm)	0.553	± 0.021

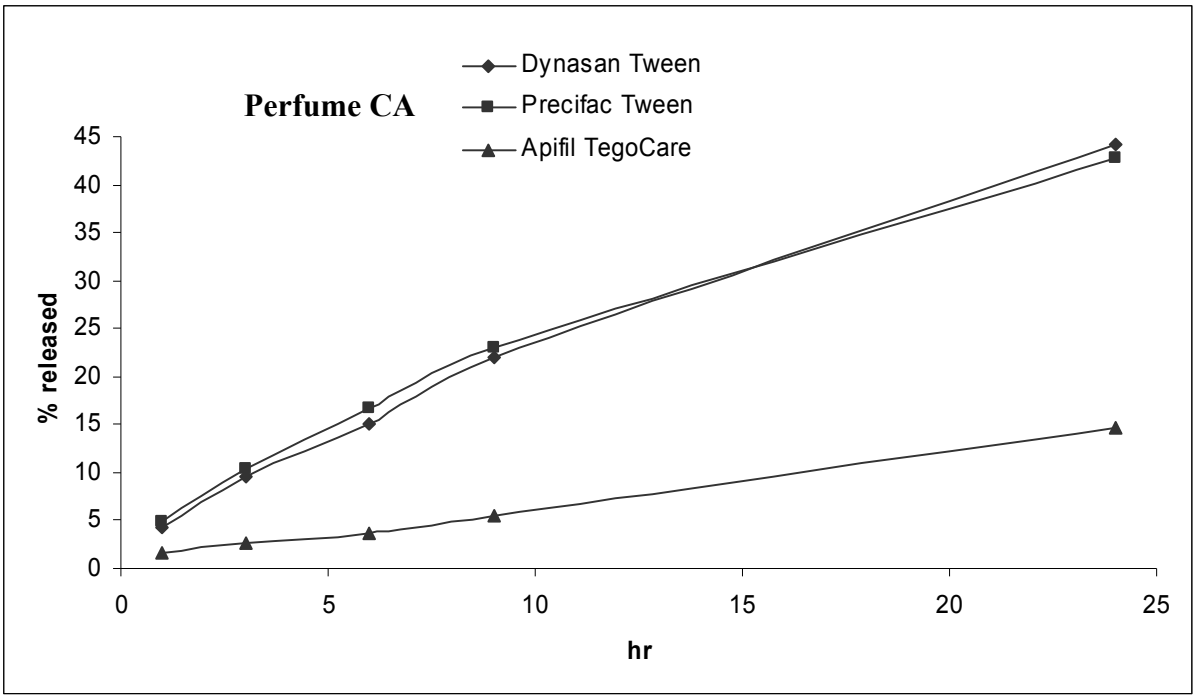

Figure 6-13: The release profiles of three different perfume loaded NLC samples produced using the perfume CA (n=3).

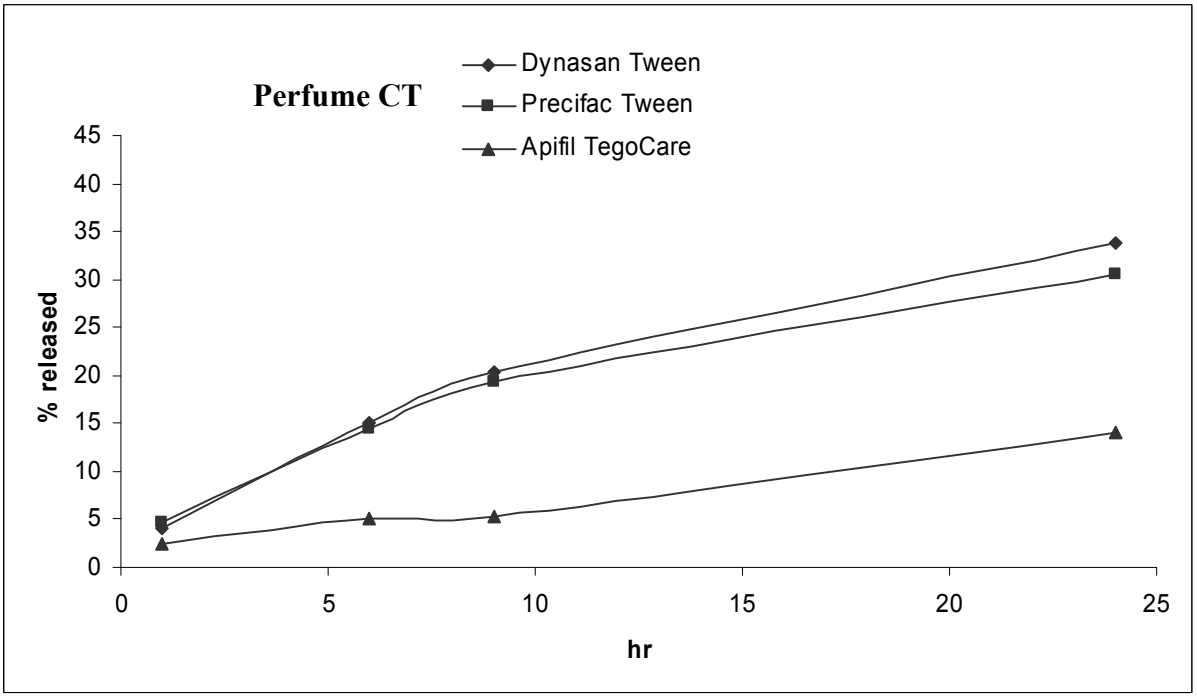

Figure 6-14: The release profiles of three different perfume-loaded NLC samples produced using the perfume CT (n=3).

6.6 Positively charged perfume-loaded NLC

Preparing positively charged perfume-loaded NLC has the advantage that the nanoparticles can adhere to the biological surfaces like hair and skin, as well as to textiles [310]. These charged particles can be admixed to shampoos, body care preparations and even to washing materials and softeners to have a more sustainable perfume after using these preparations. In this part of the work two formulations were produced containing different positively charged surfactants: Kenzo 1 and Kenzo 2 (Table 6-9). These formulas were admixed to a smell-neutral fabric softener and tested for the perfume sustainability.

Table 6-9: The composition and the particle size of the positively charged perfume-loaded NLC samples.

Sample name	Composition % (w/w)		Particle size analysis	
Kenzo 1	Apifil	11.5%	PCS (nm)	102 ± 1
	Kenzo	12.0%	PI	0.14 ± 0.00
	TegoCare 450	2.0%	d 50% (µm)	0.100 ± 0.001
	PlantaCare 2000	1.0%	d 90% (µm)	0.205 ± 0.008
	Maquat BTMC 85%	1.0%	d 95% (µm)	0.274 ± 0.024
	water	73.05%	d 99% (µm)	0.631 ± 0.330
Kenzo 2	Apifil	11.5%	PCS (nm)	101 ± 1
	Kenzo	12.0%	PI	0.16 ± 0.00
	TegoCare 450	2.0%	d 50% (µm)	0.110 ± 0.001
	PlantaCare 2000	1.0%	d 90% (µm)	0.200 ± 0.010
	Maquat SC 18	1.0%	d 95% (µm)	0.300 ± 0.020
	water	73.05%	d 99% (µm)	0.651 ± 0.230

The measured zeta potential of these two formulations confirmed that they have a positive charge. The zeta potenitail of Kenzo 1 and Kenzo 2 formulations was +60.3 ± 2 and +65.6 ± 3 respectively. This positive charge is due to the use of the cationic surfactants Maquat BTMC 85% and Maquat SC 18.

6.6.1 Panel's nose test

Four different formulas were tested to determine the sustainability of the perfume Kenzo using the positively charged NLC as a carrier system. The different samples were fabric softeners perfumed with either Kenzo perfume, Kenzo NLC 1, Kenzo NLC 2 or Kenzo cyclodextrin complex. The amount of the perfume loading in all samples was the same (2% (w/w)). The intensity of the perfume was assessed after 3, 6, 18, 24, 28 and 48 hrs (Figure 6-15). Each sample was tested three times (n=3). During the test period the intensity of the perfume was higher in the towels treated with the softeners containing the perfume-loaded NLC (both Kenzo NLC 1 and Kenzo NLC 2). The cyclodextrin perfume complex and the control showed less perfume intensities than the NLCs. After 28 hrs most of the perfume odor was gone from all the towels.

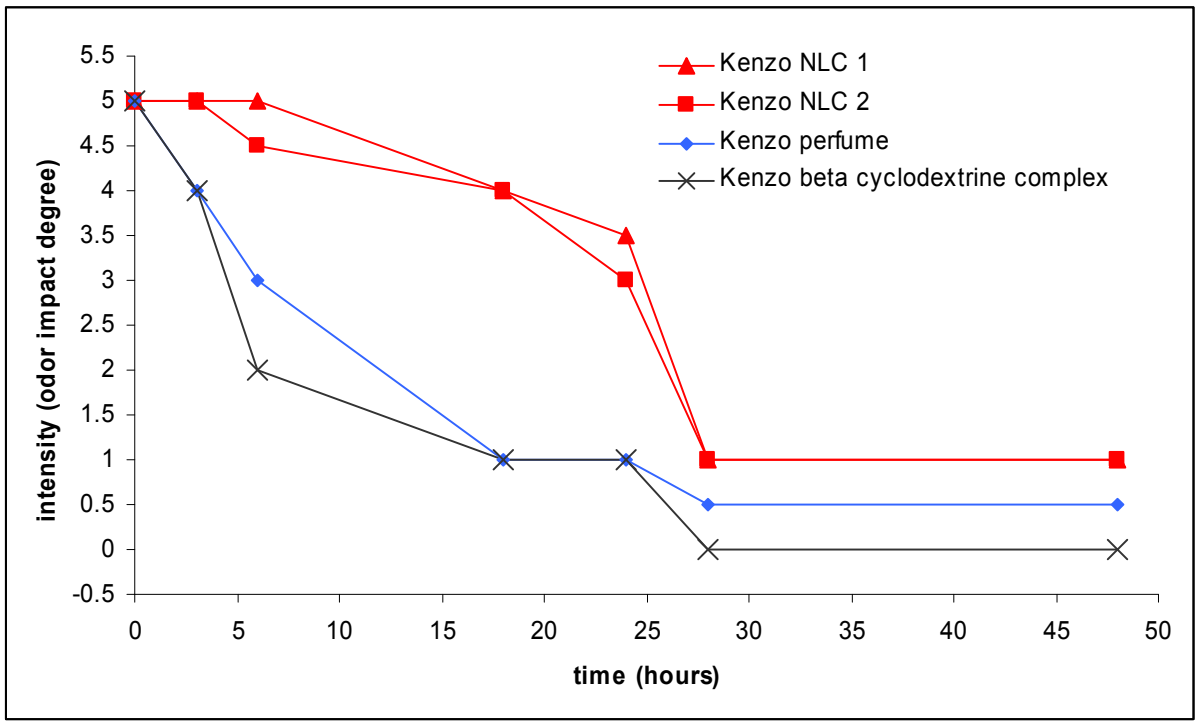

Figure 6-15: Panel's nose test results, the intensity of the perfume was assessed after 3, 6, 18, 24, 28 and 48 hrs. During the test period the intensity of the perfume was higher in the towels treated with the softeners containing the perfume-loaded NLC, (n=3).

6.6.2 Solid phase microextraction (SPME) test

Three samples were taken from each towel prepared for the panel's nose test (c.f. 6.6.1) and were analyzed using SPME. Figure 6-16 shows the spectra obtained.

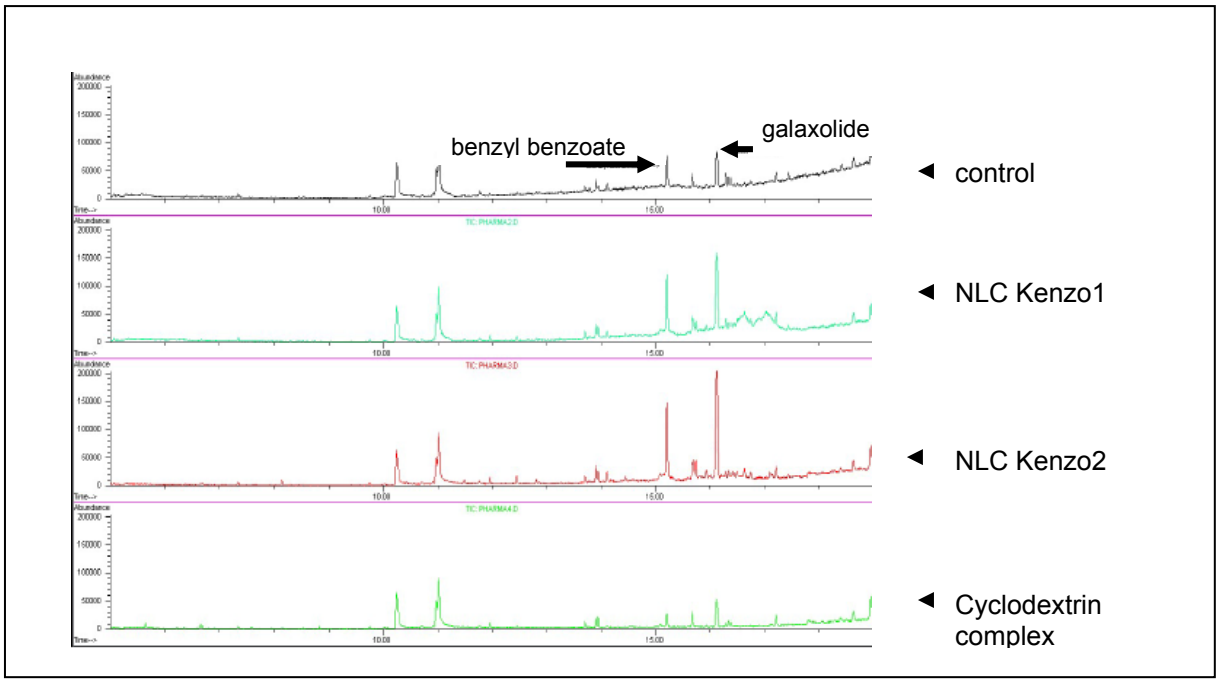

Figure 6-16: The SPME spectra of the control Kenzo fabric softener, two Kenzo-loaded NLC softeners and cyclodextrin-Kenzo complex softener.

From the SPME spectra perfume-loaded NLC made slight improvement on substantivity compared to the controls (free perfume and cyclodextrin complex). The perfume-loaded NLC failed to control the release of the volatile components of the perfume Kenzo (e.g. d-limonene, linalool) which have very poor substantivity. But they showed good control of the release of the heavy components (e.g. benzyl benzoate and galaxolide).

6.7 Conclusion

Technically, the incorporation of perfumes in NLC is possible. Many factors should be taken into consideration to produce a formulation that has a perfume prolonged release profile. It was found that the interaction between the perfume and the solid lipid is the essential factor. When the perfume was enclosed in the solid lipid matrix a slower release of the perfume from the lipid matrix of the NLC was achieved. This release follows *Higuchi equation* for release from a solid matrix. Fine tuning of the release profile could be achieved by controlling the particle size and by changing the type of lipid and surfactant used. Smaller particle sizes gave faster perfume release. Positively charged NLC were successfully produced and the positive charge maintained the NLC on the fabrics for a prolonged perfume release.

7 SUMMARY/ ZUSAMMENFASSUNG

7.1 Summary

The present work concentrates on the development of nanostructured lipid carriers (NLC) for dermal application. It also shows the advantages of using the NLC in dermal and personal care formulations and studies the factors that affect these advantages.

Production optimization of NLC

The optimal NLC production conditions were 2 homogenization cycles, 800 bar homogenization pressure and a homogenization temperature about 10°C above the melting point of the solid lipid. Increasing the surfactant concentration led to a decrease in the particle size. On the other hand, the particle size did not noticeably decrease when the concentration of the surfactant was over 2%. Moreover, excessive amount of surfactant led to foam formation during homogenization. After homogenization the formulations were cooled down using a 15°C water bath.

NLC as a carrier system for chemically labile actives

Coenzyme Q 10 and black currant seed oil loaded NLC and retinol-loaded NLC were produced and the physicochemical properties of these formulations were evaluated. The production of physically stable formulations, in terms of particle size, was successful for both formulations. By incorporating Coenzyme Q 10, black currant seed oil and retinol in NLC the chemical stability of these materials was improved. The developed formulations can be used in final topical products to achieve improved chemical stability. Regarding the Coenzyme Q 10 and black currant seed oil loaded NLC, the formulation based on carnauba wax and PlantaCare 2000 had the best physical and chemical stability. The most stable retinol formulations based on Retinol 15 D were the formulations containing 1% (w/w) retinol. The best two formulations were the NLC of the lipid Compritol ATO 888 and the surfactant Tween 80 and the NLC of the lipid Elfacos C 26 and the surfactant Miranol 32 (about 80% remaining retinol at RT after 1 year). Moreover, the formulation based on Retinol 50 C (containing 3% (w/w) retinol) showed a very good physical and chemical stability (about 77% remaining retinol at RT after 1 year).

NLC for ultraviolet (UV) radiation protection

This study showed that placebo NLC block UV radiation. This makes it possible to produce cosmetic products that have photoprotection properties without the need of using any sunscreens in the formulation. To achieve a maximum UV blocking activity the particle size of the NLC was optimized (about 400 nm).

Butyl methoxydibenzoylmethane (BMBM) as a model for organic UV blockers and titanium dioxide (TiO_2) as inorganic UV blocker, were successfully incorporated in NLC. This incorporation increased the UV blocking activity of these UV blockers. Hence, it is possible to reduce the UV blocker concentration in the finished products while maintaining the desired high UV blocking activity. This will decrease the possibility of allergic reactions and skin irritations and will also prevent, or at least reduce, the possible skin absorption of the organic UV blocker.

Perfume-loaded NLC

Different perfumes were successfully incorporated in NLC. Factors influencing the perfume release profile were studied. It was found that the interaction between the perfume and the solid lipid is an essential factor. When the perfume was enclosed in the solid lipid matrix a slower release of the perfume from the lipid matrix of the NLC was achieved. This release follows *Higuchi equation* for release from a solid matrix. Fine tuning of the release profile was achieved by controlling the particle size and by changing the type of lipid and surfactant used. Smaller particle sizes gave faster perfume release. Positively charged NLC were successfully produced and the positive charge maintained the NLC on the fabrics for a prolonged perfume release.

7.2 Zusammenfassung

Die hier vorliegende Arbeit beschäftigt sich mit der Entwicklung von NLC für die dermale Anwendung. Die Vorteile der Verwendung von NLC in Dermatika und Körperpflegeprodukten wurde aufgezeigt und die Faktoren, die diese Vorteile beeinflussen, untersucht.

Optimierung der Produktion von NLC

Als optimale Produktionsbedingungen für NLC erwiesen sich 2 Homogenisationszyklen, 800 bar Homogenisationsdruck und eine 10°C über dem Schmelzpunkt des festen Lipids liegende Homogenisationstemperatur. Eine Zunahme der Tensidkonzentration führte zu kleinerer Partikelgröße, welche sich jedoch ab einer Konzentration von 2% nicht mehr merklich verringerte und bei weiterem Überschuss Schaumbildung während der Homogenisation bewirkte. Nach der Homogenisation wurden die Formulierugen im Wasserbad auf 15°C abgekühlt.

NLC als Trägersystem für chemisch labile Wirkstoffe

Zuerst wurden NLC, beladen mit Coenzym Q 10 und Schwarzem Johannisbeerkernöl, sowie beladen mit Retinol hergestellt, dann wurden die physikalisch-chemischen Eigenschaften bestimmt. In Bezug auf die Partikelgröße war die Produktion von physikalisch stabilen Formulierungen für beide Erzeugnisse erfolgreich. Durch Einschluss von Coenzym Q 10, Schwarzem Johannisbeerkernöl und Retinol in die NLC wurde die chemische Stabilität verbessert. Die entwickelten Formulierungen können in topischen Endprodukten verwendet werden, um eine verbesserte chemische Stabilität der Wirkstoffen zu erreichen. Die mit Coenzym Q 10 und Schwarzem Johannisbeerkernöl beladenen NLC zeigten die beste physikalische und chemische Stabilität bei Verwendung von Carnaubawachs und PlantaCare 2000. Die stabilste Retinol-Formulierung wurde mit Retinol 15 D und einer Retinolkonzentration von 1% (w/w) erreicht. Als die zwei besten Formulierungen können die NLC des Lipids Compritol ATO 888 stabilisiert mit dem Tensid Tween 80 und die NLC des Lipids Elfacos C 26 stabilisiert mit dem Tensid Miranol 32 bezeichnet werden (ca. 80% Retinolgehalt nach 1 Jahr Lagerung bei RT). Ausserdem zeigten die Formulierungen, in denen Retinol 50 C benutzt wurde (Retinolkonzentration 3% (w/w)), sehr gute physikalische und chemische Stabilität (ca. 77% Retinolgehalt nach 1 Jahr Lagerung bei RT).

NLC zum Schutz vor ultravioletter (UV) Strahlung

Diese Studie zeigte, dass Placebo-NLC selbst schon UV-Strahlen blockieren. Dies erlaubt die Erzeugung von Lichtschutzeigenschaften aufweisenden Kosmetikprodukten ohne chemische Sonnenblocker. Um eine maximale UV-blockierende Aktivität zu erreichen, wurde die Partikelgröße der NLC optimiert (ca. 400 nm).

Sowohl die Modellsubstanz Butyl Methoxydibenzoylmethane (BMBM), ein organischer UV-Blocker als auch TiO_2, ein anorganischer UV-Blocker wurden erfolgreich in NLC inkorporiert, wobei eine erhöhte UV-blockierende Aktivität erzeugt wurde. Daher konnte die Konzentration der UV-Blocker im Endprodukt unter Beibehaltung der gewünschten hohen UV-blockierenden Aktivität niedrig gehalten werden. Dies reduziert mögliche allergische Reaktionen und Hautirritationen und verhindert bzw. vermindert eine eventuelle Absorption der organischen UV-Blockers in die Haut.

Parfüm-beladene NLC

Verschiedene Duftstoffe wurden mit Erfolg in NLC inkorporiert und die das Freisetzungsprofil beeinflussenden Faktoren untersucht. Es zeigte sich, dass die Interaktion zwischen dem Parfüm und dem festen Lipid für die Freisetzung ausschlaggebend ist. Durch Einschluss des Parfüms in die feste Lipidmatrix der NLC wurde eine verlangsamte Freisetzung erreicht, welche durch die *Higuchi-Gleichung* für die Freisetzung aus fester Matrix beschrieben werden kann. Eine Optimierung des Freisetzungsprofils wurde durch Kontrolle der Partikelgröße und Austausch von Lipidtyp und Tensid bzw. Stabilisator erzielt. Die Parfüms wurden bei kleinerer Partikelgröße schneller freigesetzt. Zudem ist es gelungen, positiv geladene NLC herzustellen, was zu verlängerter Haftung der NLC auf den Textilen führte und somit eine verlängerte Perfümwirkung auf den Textilen zu Folge hatte.

REFERENCES

1. Barratt, G.M., Therapeutic applications of colloidal drug carriers, **Pharm Sci Technolo Today**, 2000, 3(5): p. 163-71.
2. Mehnert, W., Mäder, K., Solid lipid nanoparticles: production, characterization and applications, **Adv Drug Deliv Rev**, 2001, 47(2-3): p. 165-96.
3. Mainardes, R.M., Silva, L.P., Drug delivery systems: past, present, and future, **Curr Drug Targets**, 2004, 5(5): p. 449-55.
4. Amidon, G.L., Lennernas, H., Shah, V.P., Crison, J.R., A theoretical basis for a biopharmaceutic drug classification: the correlation of in vitro drug product dissolution and in vivo bioavailability, **Pharm Res**, 1995, 12(3): p. 413-20.
5. van de Waterbeemd, H., The fundamental variables of the biopharmaceutics classification system (BCS): a commentary, **Eur J Pharm Sci**, 1998, 7(1): p. 1-3.
6. Dressman, J.B., Reppas, C., In vitro-in vivo correlations for lipophilic, poorly water-soluble drugs, **Eur J Pharm Sci**, 2000, 11(2): p. 73-80.
7. Gregoriadis, G., Florence, A.T., Patel, H.M., Liposomes in drug delivery, in **Drug Targeting and Delivery**, Florence, A.T., Gregoriadis, G., Editors. 1993, Harwood Academic Publishers GmbH: Chur.
8. Diederichs, J.E., Müller, R.H., Liposome in Kosmetika und Arzeimitteln, **Pharmazeutische Industrie**, 1994, 56(3): p. 267-75.
9. Bangham, A.D., Liposomes: realizing their promise, **Hosp Pract (Off Ed)**, 1992, 27(12): p. 51-6, 61-2.
10. Touitou, E., Junginger, H.E., Weiner, N.D., Nagai, T., Mezei, M., Liposomes as carriers for topical and transdermal delivery, **J Pharm Sci**, 1994, 83(9): p. 1189-203.
11. Janknegt, R., de Marie, S., Bakker-Woudenberg, I.A., Crommelin, D.J., Liposomal and lipid formulations of amphotericin B. Clinical pharmacokinetics, **Clin Pharmacokinet**, 1992, 23(4): p. 279-91.
12. Fassas, A., Anagnostopoulos, A., The use of liposomal daunorubicin (DaunoXome) in acute myeloid leukemia, **Leuk Lymphoma**, 2005, 46(6): p. 795-802.
13. Schubert, R., Liposomen in Arzneimitteln, in **Pharmazeutische Technologie: Moderne Arzneiformen**, Müller, R.H., Hildebrand, G.E., Editors. 1998, Wissenschaftliche Verlagsgesellschaft mbH: Stuttgart. p. 219-42.

14. Samad, A., Sultana, Y., Aqil, M., Liposomal drug delivery systems: an update review, **Curr Drug Deliv**, 2007, 4(4): p. 297-305.
15. Elsayed, M.M., Abdallah, O.Y., Naggar, V.F., Khalafallah, N.M., Lipid vesicles for skin delivery of drugs: reviewing three decades of research, **Int J Pharm**, 2007, 332(1-2): p. 1-16.
16. Müller, R.H., Mäder, K., Gohla, S., Solid lipid nanoparticles (SLN) for controlled drug delivery- a review of the state of the art, **Eur J Pharm Biopharm**, 2000, 50: p. 161-77.
17. Choi, M.J., Maibach, H.I., Liposomes and niosomes as topical drug delivery systems, **Skin Pharmacol Physiol**, 2005, 18(5): p. 209-19.
18. Cortesi, R., Nastruzzi, C., Liposomes, micelles and microemulsions as new delivery systems for cytotoxic alkaloids, **Pharm Sci Technolo Today**, 1999, 2(7): p. 288-98.
19. Santos, P., Watkinson, A.C., Hadgraft, J., Lane, M.E., Application of microemulsions in dermal and transdermal drug delivery, **Skin Pharmacol Physiol**, 2008, 21(5): p. 246-59.
20. Heuschkel, S., Goebel, A., Neubert, R.H., Microemulsions--modern colloidal carrier for dermal and transdermal drug delivery, **J Pharm Sci**, 2008, 97(2): p. 603-31.
21. Meinzer, A., Müller, E., Vonderscher, J., Perorale microemulsionsformulierung - Sandimmun Optoral®/Neoral®, in **Pharmazeutische Technologie: Moderne Arzneiformen**, Müller, R.H., Hildebrand, G.E., Editors. 1998, Wissenschaftliche Verlagsgesellschaft mbH: Stuttgart. p. 169-77.
22. Voigt, R., Pharmazeutische Technologie: für Studium und Beruf, 2000, Stuttgart: Deutscher Apotheker Verlag.
23. Benita, S., Levy, M.Y., Submicron emulsions as colloidal drug carriers for intravenous administration: comprehensive physicochemical characterization, **J Pharm Sci**, 1993, 82(11): p. 1069-79.
24. Block, L.H., Pharmaceutical Dosage Forms - Disperse Systems, in **Emulsions and microemulsions**, Lieberman, H.A., Rieger, M.M., Banker, G.S., Editors. 1989, Marcel Dekker Inc.: New York. p. 335-78.
25. Westesen, K., Wehler, T., Physicochemical characterization of a model intravenous oil-in-water emulsion, **J Pharm Sci**, 1992, 81(8): p. 777-86.
26. Klang, S., Benita, S., Submicron Emulsions in Drug Targeting and Delivery, in **Design and evaluation of submicron emulsions as colloidal drug carriers for**

intravenous administration, Benita, S., Editor. 1998, Harwood academic publishers: Amsterdam. p. 119-52.

27. Jumaa, M., Müller, B.W., The effect of oil components and homogenization conditions on the physicochemical properties and stability of parenteral fat emulsions, **Int J Pharm**, 1998, 163: p. 81-9.
28. Schmitt, J., Parenterale Fettemulsionen als Arzneistoffträger, in **Moderne Arzneiformen**, Müller, R.H., Hildebrand, G. E., Editor. 1998, Wissenschaftliche Verlagsgesellschaft: Stuttgart. p. 137-42.
29. Prankerd, R.J., Stella, V.J., The use of oil-in-water emulsions as a vehicle for parenteral drug administration, **J Parenter Sci Technol**, 1990, 44(3): p. 139-49.
30. Müller, R.H., Radtke, M., Wissing, S. A., Solid lipid nanoparticles (SLN) and nanostructured lipid carriers (NLC) in cosmetic and dermatological preparations, **Adv Drug Deliv Rev**, 2002, 54(1): p. 131-55.
31. Dingler, A., Blum, R.P., Niehus, H., Müller, R.H., Gohla, S., Solid lipid nanoparticles (SLN/Lipopearls)--a pharmaceutical and cosmetic carrier for the application of vitamin E in dermal products, **J Microencapsul**, 1999, 16(6): p. 751-67.
32. Benita, S., Friedman, D., Weinstock, M., Pharmacological evaluation of an injectable prolonged release emulsion of physostigmine in rabbits, **J Pharm Pharmacol**, 1986, 38(9): p. 653-8.
33. Alvarez-Roman, R., Barre, G., Guy, R.H., Fessi, H., Biodegradable polymer nanocapsules containing a sunscreen agent: preparation and photoprotection, **Eur J Pharm Biopharm**, 2001, 52(2): p. 191-5.
34. Andrieu, V., Fessi, H., Dubrasquet, M., Devissaguet, J.P., Puisieux, F., Benita, S., Pharmacokinetic evaluation of indomethacin nanocapsules, **Drug Des Deliv**, 1989, 4(4): p. 295-302.
35. Venier-Julienne, M.C., Benoit, J.P., Preparation, purification and morphology of polymeric nanoparticles as drug carriers, **Pharm Acta Helv**, 1996, 71(2): p. 121-8.
36. Kreuter, J., Nanoparticles, in **Colloidal Drug Delivery Systems**, Kreuter, J., Editor. 1994, Marcel Dekker Inc.: New York, Basel, Hong Kong. p. 219-342.
37. Gurny, R., Peppas, N.A., Harrington, D.D., Banker, G.S., Development of biodegradable and injectable latices for controlled release of potent drugs, **Drug Dev Ind Pharm**, 1981, 7: p. 1-25.
38. Bodmeier, R., Chen, H., Indomethacin polymeric nanosuspensions prepared by microfluidization, **J Control Release**, 1990, 12: p. 223-33.

39. Sukhorukov, G.B., et al., Nanoengineered polymer capsules: tools for detection, controlled delivery, and site-specific manipulation, **Small**, 2005, 1(2): p. 194-200.
40. Mayer, C., Nanocapsules as drug delivery systems, **Int J Artif Organs**, 2005, 28(11): p. 1163-71.
41. Vert, M., Polyvalent polymeric drug carriers, **Crit Rev Ther Drug Carrier Syst**, 1986, 2(3): p. 291-327.
42. Mu, L., Feng, S.S., PLGA/TPGS nanoparticles for controlled release of paclitaxel: effects of the emulsifier and drug loading ratio, **Pharm Res**, 2003, 20(11): p. 1864-72.
43. Smith, A., Hunneyball, l.M., Evaluation of poly (lactic acid) as a biodegradable drug delivery system for parenteral administration, **Int J Pharm**, 1986, 30(2-3): p. 215-20.
44. Lherm, C., Müller, R.H., Puisieux, F., Couvreur, P., Alkylcyanoacrylate Drug Carriers II: Cytotoxicity of Cyanoacrylate Nanoparticles with Different Alkyl Chain Length, **Int. J. Pharm.**, 1992, 84(1992): p. 13-22.
45. Lucks, J.S., Müller, R. H., Medication vehicles made of solid lipid particles (solid lipid nanospheres SLN), in EP0000605497. 1996: Germany.
46. Müller, R.H., Mäder, K., Lippacher, A., Jenning, V., Solid-liquid (semi-solid) liquid particles and method of producing highly concentrated lipid particle dispersions, in PCT/EP00/04565. 2000.
47. Müller, R.H., Mäder, K., Lippacher, A., Jenning, V., Fest-flüssige (halbfeste) Lipidpartikel und Verfahren zur Herstellung hochkonzentrierter Lipidpartikeldispersionen, in PCT/EP00/04112. 2000.
48. Saupe, A., Wissing, S. A., Lenk, A., Schmidt, C. Müller, R. H., Solid Lipid Nanoparticles (SLN) and Nanostructured Lipid Carriers (NLC) – Structural investigations on two different carrier systems, **Bio-Med Mater Eng**, 2005, 15: p. 393–402.
49. Müller, R.H., Radtke, M., Wissing, S.A., Nanostructured lipid matrices for improved microencapsulation of drugs, **Inte J Pharm**, 2002, 242(1-2): p. 121-8.
50. Jenning, V., Thunemann, A.F., Gohla, S.H., Characterisation of a novel solid lipid nanoparticle carrier system based on binary mixtures of liquid and solid lipids, **Int J Pharm**, 2000, 199(2): p. 167-77.
51. Jenning, V., Mäder, K., Gohla, S., Solid lipid nanoparticles (SLN) based on binary mixtures of liquid and solid lipids: a 1H-NMR study, **Int J Pharm**, 2000, 205(1-2): p. 15-21.

52. Müller, R.H., Lipid nanoparticles: recent advances, **Adv Drug Deliv Rev**, 2007, 59(6): p. 375-76.
53. Müller, R.H., Gohla, S., Dingler, A., Schneppe, T., Large scale production of solid lipid nanoparticles (SLN^{TM}) and nanosuspensions (DissoCubes^{TM}), in **Handbook of Pharmaceutical Controlled Release Technology** Wise, D.L., Editor. 2000. p. 359-76.
54. Üner, M., Preparation, characterization and physico-chemical properties of solid lipid nanoparticles (SLN) and nanostructured lipid carriers (NLC): their benefits as colloidal drug carrier systems **Die Pharmazie**, 2006, 61: p. 375-86.
55. Lukowski, G., Pflegel, P., Electron diffraction of solid lipid nanoparticles loaded with acyclovir, **Die Pharmazie**, 1997, 52: p. 642-43.
56. Cavalli, R., Bocca, C., Miglietta, A., Caputo, O., Gasco, M.R., Albumin adsorption on stealth and non-stealth solid lipid nanoparticles, **STP Pharma Sci**, 1999, 9: p. 183-89.
57. Fukui, H., Koike, T., Saheki, A., Sonoke, S., Seki, J., A novel delivery system for amphotericin B with lipid nano-sphere (LNS), **Int J Pharm**, 2003, 265(1-2): p. 37-45.
58. Fukui, H., Koike, T., Saheki, A., Sonoke, S., Tomii, Y., Seki, J., Evaluation of the efficacy and toxicity of amphotericin B incorporated in lipid nano-sphere (LNS), **Int J Pharm**, 2003, 263(1-2): p. 51-60.
59. Kristl, J., Volk, B., Gasperlin, M., Sentjurc, M., Jurkovic, P., Effect of colloidal carriers on ascorbyl palmitate stability, **Eur J Pharm Sci**, 2003, 19(4): p. 181-9.
60. Üner, M., Wissing, S.A., Müller, R.H., Solid Lipid Nanoparticles (SLN) and Nanostructured Lipid Carriers (NLC) for application of ascorbyl palmitate, **Die Pharmazie**, 2005, 60: p. 577-82.
61. Heiati, H., Tawashi, R., Phillips, N.C., Drug retention and stability of solid lipid nanoparticles containing azidothymidine palmitate after autoclaving, storage and lyophilization, **J Microencapsul**, 1998, 15(2): p. 173-84.
62. Sivaramakrishnan, R., Nakamura, C., Mehnert, W., Korting, H.C., Kramer, K.D., Schäfer-Korting, M., Glucocorticoid entrapment into lipid carriers -- characterisation by parelectric spectroscopy and influence on dermal uptake, **J Control Release**, 2004, 97(3): p. 493-502.
63. Masters, D.B., Domb, A.J., Liposphere local anesthetic timed-release for perineural site application, **Pharm Res** 1998, 15(7): p. 1038-45.
64. Garcia-Fuentes, M., Prego, C., Torres, D., Alonso, M.J., A comparative study of the potential of solid triglyceride nanostructures coated with chitosan or poly(ethylene

glycol) as carriers for oral calcitonin delivery, **Eur J Pharm Sci**, 2005, 25(1): p. 133-43.

65. Shahgaldian, P., Quattrocchi, L., Gualbert, J., Coleman, A.W., Goreloff, P., AFM imaging of calixarene based solid lipid nanoparticles in gel matrices, **Eur J Pharm Biopharm**, 2003, 55(1): p. 107-13.
66. Yang, S.C., Lu, L.F., Cai, Y., Zhu, J.B., Liang, B.W., Yang, C.Z., Body distribution in mice of intravenously injected camptothecin solid lipid nanoparticles and targeting effect on brain, **J Control Release**, 1999, 59(3): p. 299-307.
67. Yang, S.C., Zhu, J.B., Preparation and characterization of camptothecin solid lipid nanoparticles, **Drug Dev Ind Pharm**, 2002, 28(3): p. 265-74.
68. Yang, S., Zhu, J., Lu, Y., Liang, B., Yang, C., Body distribution of camptothecin solid lipid nanoparticles after oral administration, **Pharmaceut Res**, 1999, 16(5): p. 751-7.
69. Serpe, L., et al., Cytotoxicity of anticancer drugs incorporated in solid lipid nanoparticles on HT-29 colorectal cancer cell line, **Eur J Pharm Biopharm**, 2004, 58(3): p. 673-80.
70. Hu, F.Q., Yuan, H., Zhang, H.H., Fang, M., Preparation of solid lipid nanoparticles with clobetasol propionate by a novel solvent diffusion method in aqueous system and physicochemical characterization, **Int J Pharm**, 2002, 239(1-2): p. 121-28.
71. Souto, E.B., Wissing, S. A., Barbosa, C. M., Müller, R. H., Development of a controlled release formulation based on SLN and NLC for topical clotrimazole delivery, **Int J Pharm**, 2004, 278: p. 71–7.
72. Venkateswarlu, V., Manjunath, K., Preparation, characterization and in vitro release kinetics of clozapine solid lipid nanoparticles, **J Control Release**, 2004, 95(3): p. 627-38.
73. Manjunath, K., Venkateswarlu, V., Pharmacokinetics, tissue distribution and bioavailability of clozapine solid lipid nanoparticles after intravenous and intraduodenal administration, **J Control Release**, 2005, 107(2): p. 215-28.
74. Westesen, K., Bunjes, H., Koch, M.H.J., Physicochemical characterization of lipid nanoparticles and evaluation of their drug loading capacity and sustained release potential, **J Control Release**, 1997, 48(2-3): p. 223-36.
75. Zhang, Q., Yie, G., Li, Y., Yang, Q., Nagai, T., Studies on the cyclosporin A loaded stearic acid nanoparticles, **Inte J Pharm**, 2000, 200(2): p. 153-59.
76. Runge, S., Solid lipid nanoparticles (SLN) as colloidal drug carrierfor the oral application of cyclosporine A. PhD thesis. 1998, Freie Universität Berlin: Berlin.

77. Seki, J., Sonoke, S., Saheki, A., Fukui, H., Sasaki, H., Mayumi, T., A nanometer lipid emulsion, lipid nano-sphere (LNS$^{(R)}$), as a parenteral drug carrier for passive drug targeting, **Int J Pharm**, 2004, 273(1-2): p. 75-83.
78. Sznitowska, M., Gajewska, M., Janicki, S., Radwanska, A., Lukowski, G., Bioavailability of diazepam from aqueous-organic solution, submicron emulsion and solid lipid nanoparticles after rectal administration in rabbits, **Eur J Pharm Biopharm**, 2001, 52(2): p. 159-63.
79. Cavalli, R., Caputo, O., Gasco, M.R., Solid lipospheres of doxorubicin and idarubicin, **Int J Pharm**, 1993, 89: p. 9-12.
80. zur Mühlen, A., Schwarz, C., Mehnert, W., Solid lipid nanoparticles (SLN) for controlled drug delivery - Drug release and release mechanism, **Eur J Pharm Biopharm**, 1998, 45(2): p. 149-55.
81. Harivardhan Reddy, L., Sharma, R.K., Chuttani, K., Mishra, A.K., Murthy, R.S.R., Influence of administration route on tumor uptake and biodistribution of etoposide loaded solid lipid nanoparticles in Dalton's lymphoma tumor bearing mice, **J Control Release**, 2005, 105(3): p. 185-98.
82. Souto, E.B., Anselmi, C., Centini, M., Müller, R.H., Preparation and characterization of n-dodecyl-ferulate-loaded solid lipid nanoparticles (SLN®), **Int J Pharm**, 2005, 295: p. 261-68.
83. Mao, S., Wang, P., Bi, D., Investigations on 5-fluorouracil solid lipid nanoparticles (SLN) prepared by hot homogenization, **Die Pharmazie**, 2005, 60: p. 273-77.
84. Morel, S., Terreno, E., Ugazio, E., Aime, S., Gasco, M.R., NMR relaxometric investigations of solid lipid nanoparticles (SLN) containing gadolinium(III) complexes, **Eur J Pharm Biopharm**, 1998, 45(2): p. 157-63.
85. Hu, F.Q., Hong, Y., Yuan, H., Preparation and characterization of solid lipid nanoparticles containing peptide, **Int J Pharm**, 2004, 273(1-2): p. 29-35.
86. Cavalli, R., Peira, E., Caputo, O., Gasco, M.R., Solid lipid nanoparticles as carriers of hydrocortisone and progesterone complexes with beta-cyclodextrins, **Int J Pharm**, 1999, 182(1): p. 59-69.
87. Zara, G.P., Bargoni, A., Cavalli, R., Fundaro, A., Vighetto, D., Gasco, M.R., Pharmacokinetics and tissue distribution of idarubicin-loaded solid lipid nanoparticles after duodenal administration to rats, **J Pharm Sci**, 2002, 91(5): p. 1324-33.

88. Ricci, M., Puglia, C., Bonna, F., Di Giovanni, C., Giovagnoli, S., Rossi, C., Evaluation of indomethacin percutaneous absorption from nanostructured lipid carriers (NLC): in vitro and in vivo studies, **J Pharm Sci**, 2005, 94(5): p. 1149-59.

89. Yaziksiz-Iscan, Y., Wissing, S., Müller, R.H., Hekimoglu, S., Different production methods for solid lipid nanoparticles (SLN) containing the insect repellent DEET, in The 4th World Meeting Pharmacy, Biopharmacy and Pharmaceutical Technology,Florenz, 2002.

90. Wissing, S., Mäder, K., Müller, R. H., Prolonged efficacy of the insect repellent lemon oil by incorporation into solid lipid nanoparticles (SLN™), in Proceeding in the 3rd World Meeting of Pharmacy, Biopharmacy and Pharmceutical Technology,Berlin, 2000.

91. Trotta, M., Cavalli, R., Carlotti, M.E., Battaglia, L., Debernardi, F., Solid lipid micro-particles carrying insulin formed by solvent-in-water emulsion-diffusion technique, **Int J Pharm**, 2005, 288(2): p. 281-88.

92. Souto, E.B., Müller, R. M., SLN and NLC for topical delivery of ketoconazole, **J Microencapsul**, 2005, 22(5): p. 501–10.

93. Igartua, M., Saulnier, P., Heurtault, B., Pech, B., Proust, J.E., Pedraz, J.L., Benoit, J.P., Development and characterization of solid lipid nanoparticles loaded with magnetite, **Int J Pharm**, 2002, 233(1-2): p. 149-57.

94. Hou, D., Xie, C., Huang, K., Zhu, C., The production and characteristics of solid lipid nanoparticles (SLNs), **Biomaterials**, 2003, 24(10): p. 1781-5.

95. Kumar, V.V., Chandrasekar, D., Ramakrishna, S., Kishan, V., Rao, Y.M., Diwan, P.V., Development and evaluation of nitrendipine loaded solid lipid nanoparticles: influence of wax and glyceride lipids on plasma pharmacokinetics, **Int J Pharm**, 2007, 335(1-2): p. 167-75.

96. Zhang, D.R., Ren, T.C., Lou, H.X., Xing, J., [The tissue distribution in mice and pharmacokinetics in rabbits of oridonin-solid lipid nanoparticles], **Yao Xue Xue Bao**, 2005, 40(6): p. 573-6.

97. Chen, D.B., Yang, T.Z., Lu, W.L., Zhang, Q., In vitro and in vivo study of two types of long-circulating solid lipid nanoparticles containing paclitaxel, **Chem Pharm Bull (Tokyo)**, 2001, 49(11): p. 1444-7.

98. Chen, H., Chang, X., Du, D., Liu, W., Liu, J., Weng, T., Yang, Y., Xu, H., Yang, X., Podophyllotoxin-loaded solid lipid nanoparticles for epidermal targeting, **J Control Release**, 2006, 110(2): p. 296-306.

99. Maia, C.S., Mehnert, W., Schäfer-Korting, M., Solid lipid nanoparticles as drug carriers for topical glucocorticoids, **Int J Pharm**, 2000, 196(2): p. 165-7.

100. Jenning, V., Gohla, S.H., Encapsulation of retinoids in solid lipid nanoparticles (SLN), **J Microencapsul**, 2001, 18(2): p. 149-58.

101. Morel, S., Ugazio, E., Cavalli, R., Gasco, M.R., Thymopentin in solid lipid nanoparticles, **Int J Pharm**, 1996, 132: p. 259-261.

102. Cavalli, R., Bargoni, A., Podio, V., Muntoni, E., Zara, G.P., Gasco, M.R., Duodenal administration of solid lipid nanoparticles loaded with different percentages of tobramycin, **J Pharm Sci**, 2003, 92(5): p. 1085-94.

103. Mei, Z., Li, X., Wu, Q., Hu, S., Yang, X., The research on the anti-inflammatory activity and hepatotoxicity of triptolide-loaded solid lipid nanoparticle, **Pharmacol Res**, 2005, 51(4): p. 345-351.

104. Mei, Z., Chen, H., Weng, T., Yang, Y., Yang, X., Solid lipid nanoparticle and microemulsion for topical delivery of triptolide, **Eur J Pharm Biopharm**, 2003, 56(2): p. 189-96.

105. Bunjes, H., Drechsler, M., Koch, M.H., Westesen, K., Incorporation of the model drug ubidecarenone into solid lipid nanoparticles, **Pharm Res**, 2001, 18(3): p. 287-93.

106. Wissing, S.A., Muller, R.H., Manthei, L., Mayer, C., Structural Characterization of Q10-Loaded Solid Lipid Nanoparticles by NMR spectroscopy, **Pharm Res**, 2004, 21(3): p. 400-5.

107. Teeranachaideekul, V., Souto, E.B., Junyaprasert, V.B., Müller, R.H., Cetyl palmitate-based NLC for topical delivery of Coenzyme Q(10) - development, physicochemical characterization and in vitro release studies, **Eur J Pharm Biopharm**, 2007, 67(1): p. 141-8.

108. Yaziksiz-Iscan, Y., Wissing, S.A., Hekimoglu, S., Müller, R.H., Development of a novel carrier system for vitamin K using solid lipid nanoparticles (SLN™), in The 4th World Meeting Pharmacy, Biopharmacy and Pharmaceutical Technology,Florence, 2002.

109. Wissing, S., Lippacher, A., Muller, R., Investigations on the occlusive properties of solid lipid nanoparticles (SLN), **J Cosmet Sci**, 2001, 52(5): p. 313-24.

110. Wissing, S.A., Müller, R.H., Cosmetic applications for solid lipid nanoparticles (SLN), **Int J Pharm**, 2003, 254(1): p. 65-8.

111. Wissing, S., Müller, R., The influence of the crystallinity of lipid nanoparticles on their occlusive properties, **Int J Pharm**, 2002, 242(1-2): p. 377-9.

112. Wissing, S.A., Müller, R.H., The influence of solid lipid nanoparticles on skin hydration and viscoelasticity--in vivo study, **Eur J Pharm Biopharm**, 2003, 56(1): p. 67-72.

113. Teeranachaideekul, V., Boonme, P., Souto, E.B., Müller, R.H., Junyaprasert, V.B., Influence of oil content on physicochemical properties and skin distribution of Nile red-loaded NLC, **J Control Release**, 2008, 128(2): p. 134-41.

114. Müller, R.H., Hommoss A., Pardeike, J.,Schmidt, C., Lipid nanoparticles (NLC) as novel carrier for cosmetics - Special features & state of commercialisation, **SÖFW**, 2007(9): p. 40-46.

115. Zhai, H., Maibach, H.I., Effects of skin occlusion on percutaneous absorption: an overview, **Skin Pharmacol Appl Skin Physiol**, 2001, 14(1): p. 1-10.

116. Schäfer-Korting, M., Mehnert, W., Korting, H.C., Lipid nanoparticles for improved topical application of drugs for skin diseases, **Adv Drug Deliv Rev**, 2007, 59(6): p. 427-43.

117. Dingler, A., Fest Lipid-Nanopartikel als kolloidale Wirkstoffträgersysteme zur dermalen Applikation. PhD thesis. 1998, Freie Universität Berlin: Berlin.

118. Pardeike, J., Müller, R.H., Coenzyme Q10 loaded NLCs: preparation, occlusive properties and penetration enhancement **Pharm Technol Eur**, 2007 July.

119. Jenning, V., Schäfer-Korting, M., Gohla, S., Vitamin A-loaded solid lipid nanoparticles for topical use: drug release properties, **J Control Release**, 2000, 66(2-3): p. 115-26.

120. Stecova, J., et al., Cyproterone acetate loading to lipid nanoparticles for topical acne treatment: particle characterisation and skin uptake, **Pharm Res**, 2007, 24(5): p. 991-1000.

121. Liu, J., Hu, W., Chen, H., Ni, Q., Xu, H., Yang, X., Isotretinoin-loaded solid lipid nanoparticles with skin targeting for topical delivery, **Int J Pharm**, 2007, 328(2): p. 191-5.

122. Joshi, M., Patravale, V., Nanostructured lipid carrier (NLC) based gel of celecoxib, **Int J Pharm**, 2008, 346(1-2): p. 124-32.

123. Joshi, M., Patravale, V., Formulation and evaluation of Nanostructured Lipid Carrier (NLC)-based gel of Valdecoxib, **Drug Dev Ind Pharm**, 2006, 32(8): p. 911-8.

124. Shah, K.A., Date, A.A., Joshi, M.D., Patravale, V.B., Solid lipid nanoparticles (SLN) of tretinoin: Potential in topical delivery, **Int J Pharm**, 2007, 345(1-2): p. 163-71.

125. Wissing, S.A., Müller, R.H., Solid lipid nanoparticles (SLN)--a novel carrier for UV blockers, **Pharmazie.**, 2001, 56(10): p. 783-6.
126. Wissing, S.A., Müller, R.H., Solid lipid nanoparticles as carrier for sunscreens: in vitro release and in vivo skin penetration, **J Control Release**, 2002, 81(3): p. 225-33.
127. Song, C., Liu, S., A new healthy sunscreen system for human: solid lipid nanoparticles as carrier for 3,4,5-trimethoxybenzoylchitin and the improvement by adding Vitamin E, **Int J Biol Macromol**, 2005, 36(1-2): p. 116-9.
128. Villalobos-Hernandez, J.R., Müller-Goymann, C.C., Novel nanoparticulate carrier system based on carnauba wax and decyl oleate for the dispersion of inorganic sunscreens in aqueous media, **Eur J Pharm Biopharm**, 2005, 60(1): p. 113-22.
129. Teeranachaideekul, V., Müller, R.H., Junyaprasert, V.B., Encapsulation of ascorbyl palmitate in nanostructured lipid carriers (NLC)--effects of formulation parameters on physicochemical stability, **Int J Pharm**, 2007, 340(1-2): p. 198-206.
130. Jenning, V., Solid lipid Nanoparticles (SLN) as a carrier system for the dermal application of retinol. PhD thesis. 1999, Freie Universität Berlin: Berlin.
131. Wissing, S.A., Kayser, O., Müller, R. H., Solid lipid nanoparticles for parenteral drug delivery, **Adv Drug Deliv Rev**, 2004, 56: p. 1257-72.
132. Liedtke, S., Wissing, S., Muller, R.H., Mader, K., Influence of high pressure homogenisation equipment on nanodispersions characteristics, **Int J Pharm**, 2000, 196(2): p. 183-5.
133. Priano, L., Esposti, D., Esposti, R., Castagna, G., De Medici, C., Fraschini, F., Gasco, M.R., Mauro, A., Solid lipid nanoparticles incorporating melatonin as new model for sustained oral and transdermal delivery systems, **J Nanosci Nanotechnol**, 2007, 7(10): p. 3596-601.
134. Gasco, M.R., Solid lipid nanspheres from warm microemuslion, **Pharm Technol Eur**, 1997, 9: p. 32-42.
135. Gasco, M.R., Method for producing solid lipid microspheres having a narrow size distribution, in US Patent US 5 250 236. 1993: USA.
136. Trotta, M., Debernardi, F., Caputo, O., Preparation of solid lipid nanoparticles by a solvent emulsification-diffusion technique, **Int J Pharm**, 2003, 257(1-2): p. 153-60.
137. Sjöström, B., Bergenstahl, B., Preparation of submicron drug particles in lecithin-stabilized o/w emulsions I. Model studies of the precipitation of cholesteryl acetate, **Int J Pharm**, 1992, 88: p. 53-62.

138. Schubert, M.A., Muller-Goymann, C.C., Solvent injection as a new approach for manufacturing lipid nanoparticles--evaluation of the method and process parameters, **Eur J Pharm Biopharm**, 2003, 55(1): p. 125-31.
139. Garcý-Fuentes, M., Torres, D., Alonso, M., Design of lipid nanoparticles for the oral delivery of hydrophilic macromolecules, **Colloid Surface B** 2002, 27(2002): p. 159-68.
140. Heurtault, B., Saulnier, P., Pech, B., Proust, J.E., Benoit, J.P., A novel phase inversion-based process for the preparation of lipid nanocarriers, **Pharm Res**, 2002, 19(6): p. 875-80.
141. Puglia, C., Blasi, P., Rizza, L., Schoubben, A., Bonina, F., Rossi, C., Ricci, M., Lipid nanoparticles for prolonged topical delivery: An in vitro and in vivo investigation, **Int J Pharm**, 2008, 357(1-2): p. 295-304.
142. Charcosset, C., El-Harati, A., Fessi, H., Preparation of solid lipid nanoparticles using a membrane contactor, **J Control Release**, 2005, 108(1): p. 112-20.
143. El-Harati, A.A., Charcosset, C., Fessi, H., Influence of the formulation for solid lipid nanoparticles prepared with a membrane contactor, **Pharm Dev Technol**, 2006, 11(2): p. 153-7.
144. Gattefossé AG, Deutschland.
145. Fiedler, H.P., Lexikon der Hilfsstoffe für Pharmazie, Kosmetik und angrenzender Gebiete, 4th ed, 1996, Aulendorf: Edition Cantor Verlag.
146. Bees wax. 2007, Wikipedia http://en.wikipedia.org/wiki/Main_Page.
147. Carnauba wax 2442. 2007, Kahl & Co. http://www.kahlwax.de/.
148. Carnauba wax 2442 L. 2007, Kahl & Co. http://www.kahlwax.de/.
149. Sasol Germany GmbH, 58453 Witten, Germany.
150. Syncrowax ERLC. 2007, Croda http://www.croda.com.
151. Hem, S.L., Feldkamp, J.R., White, J.L., Basic chemical principles related to emulsions and suspension dosage forms, in **The theory and practice of industrial pharmacy**, Lachman, L., Lieberman, H.A., Kanig, J.L., Editors. 1986, Lea & Febiger: Philadelphia. p. 100-22.
152. Rhodia GmbH, Miranol Ultra C 32. 2007.
153. Westesen, K., Siekmann, B., Investigation of the gel formation of phospholipid-stabilized solid lipid nanoparticles, **Int J Pharm**, 1997, 151: p. 35-45.
154. PLANTACARE® 2000 UP. 2007, Cognis, http://www.cognis.de.
155. Tego®Care 450. 2007, Degussa, http://www.degussa.de.

156. European Pharmacopoeia, 2001.
157. Mason Chemical Company, Maquat SC 18. 2007.
158. Mason Chemical Company, Maquat BTMC-85%. 2007.
159. Frei, B., Kim, M.C., Ames, B.N., Ubiquinol-10 is an effective lipid-soluble antioxidant at physiological concentrations, **Proc Natl Acad Sci U S A**, 1990, 87(12): p. 4879-83.
160. Nohl, H., Kozlov, A.V., Staniek, K., Gille, L., The multiple functions of coenzyme Q, **Bioorg Chem**, 2001, 29(1): p. 1-13.
161. Fuller, B., Smith, D., Howerton, A., Kern, D., Anti-inflammatory effects of CoQ10 and colorless carotenoids, **J Cosmet Dermatol**, 2006, 5(1): p. 30-8.
162. Yang, H.Y., Song, J.F., High-sensitive determination of coenzyme Q(10) in iodinate-beta-cyclodextrin medium by inclusion reaction and catalytic polarography, **Anal Biochem**, 2006, 348(1): p. 69-74.
163. Yang, H.Y., Song, J.F., Inclusion of coenzyme Q10 with beta-cyclodextrin studied by polarography, **Yao Xue Xue Bao**, 2006, 41(7): p. 671-4.
164. Matsuda, Y., Masahara, R., Photostability of solid-state ubidecarenone at ordinary and elevated temperatures under exaggerated UV irradiation, **J Pharm Sci**, 1983, 72(10): p. 1198-203.
165. Blackcurrant. 2008, Wikipedia, the free encyclopedia.
166. Blackcurrant oil. 1998, 1001 Herbs. http://www.1001herbs.com/blackcurrant-oil/index.html.
167. Stransky, K., Zarevucka, M., Wimmer, Z., Gas chromatography analysis of blackcurrant oil in relation to its stability, **Food Chemistry**, 2005, 92(3): p. 569-73.
168. Bartlova, M., Bernasek, P., Sykora, J., Sovova, H., HPLC in reversed phase mode: Tool for investigation of kinetics of blackcurrant seed oil lipolysis in supercritical carbon dioxide, **J Chromatogr B Analyt Technol Biomed Life Sci**, 2006, 839(1-2): p. 80-4.
169. Sporn, M.B., Roberts, A.B., Goodman, D.S., TheRetinoids: Biology, Chemistry, and Medicine, 2nd ed, 1994, New York: Raven Press.
170. Lee, C.M., Boileau, A.C., Boileau, T.W., Williams, A.W., Swanson, K.S., Heintz, K.A., Erdman, J.W., Jr., Review of animal models in carotenoid research, **J Nutr**, 1999, 129(12): p. 2271-7.

171. Baumann, L., Vujevich, J., Halem, M., Martin, L.K., Kerdel, F., Lazarus, M., Pacheco, H., Black, L., Bryde, J., Open-label pilot study of alitretinoin gel 0.1% in the treatment of photoaging, **Cutis**, 2005, 76(1): p. 69-73.

172. Kafi, R., et al., Improvement of naturally aged skin with vitamin A (retinol), **Arch Dermatol**, 2007, 143(5): p. 606-12.

173. Lee, S., Yuk, H., Lee, D., Lee, K., Hwang, Y., Ludescher, R., Stabilization of Retinol through Incorporation into Liposomes, **J Biochem Mol Biol**, 2002, 35(4): p. 358-363.

174. Maier, T., Korting, H.C., Sunscreens - which and what for?, **Skin Pharmacol Physiol**, 2005, 18(6): p. 253-62.

175. Tarras-Wahlberg, N., Stenhagen, G., Larko, O., Rosen, A., Wennberg, A.M., Wennerstrom, O., Changes in ultraviolet absorption of sunscreens after ultraviolet irradiation, **J Invest Dermatol**, 1999, 113(4): p. 547-53.

176. Gange, R.W., Soparkar, A., Matzinger, E., Dromgoole, S.H., Sefton, J., DeGryse, R., Efficacy of a sunscreen containing butyl methoxydibenzoylmethane against ultraviolet A radiation in photosensitized subjects, **J Am Acad Dermatol**, 1986, 15(3): p. 494-9.

177. Seite, S., Colige, A., Piquemal-Vivenot, P., Montastier, C., Fourtanier, A., Lapiere, C., Nusgens, B., A full-UV spectrum absorbing daily use cream protects human skin against biological changes occurring in photoaging, **Photodermatol Photoimmunol Photomed**, 2000, 16(4): p. 147-55.

178. Antoniou, C., Kosmadaki, M., Stratigos, A., Katsambas, A., Sunscreens - what's important to know, **J Eur Acad Dermatol Venereol**, 2008.

179. Anderson, M.W., Hewitt, J.P., Spruce, S.R., Broadspectrum physical sunscreens: titanium dioxide and zinc oxide, in **Sunscreens: Development, Evaluation and Regulatory Aspects**, Lowe, N.J., Shaath, N.A., Pathak, M.A., Editors. 1997, Dekker: New York. p. 353–97.

180. Tan, M.H., Commens, C.A., Burnett, L., Snitch, P.J., A pilot study on the percutaneous absorption of microfine titanium dioxide from sunscreens, **Australas J Dermatol**, 1996, 37(4): p. 185-7.

181. Miller, G., Cosmetics, nanotoxicity and skin penetration – a brief summary of the toxicological and skin penetration. 2006, Friends of the Earth Australia.

182. Dondi, D., Albini, A., Serpone, N., Interactions between different solar UVB/UVA filters contained in commercial suncreams and consequent loss of UV protection, **Photochem Photobiol Sci**, 2006, 5: p. 835–43.

183. Britton, G., Structure and properties of carotenoids in relation to function, **Faseb J**, 1995, 9(15): p. 1551-8.

184. Arita, S., Otsuki, K., Osaki, K., Murata, Y., Shimoishi, Y., Tada, M., Reduction in photostability by the esterification of beta-cryptoxanthin, **Biosci Biotechnol Biochem**, 2004, 68(2): p. 451-3.

185. Subagio, A., Wakaki, H., Morita, N., Stability of lutein and its myristate esters, **Biosci Biotechnol Biochem**, 1999, 63: p. 1784–6.

186. Goulson, M.J., Warthesen, J.J., Stability and Antioxidant Activity of Beta Carotene in Conventional and High Oleic Canola Oil, **J Food Sci**, 1999, 64(6): p. 996-9.

187. Ager, D.J., Schroeder, S.A., Stabilization of carotenoid colorants and uses in low-fat food systems, in **Science for the Food Industry of the 21st Century**, Yalpani, M., Editor. 1993, ATL Press: Shrewsbury, Mass. p. 285–310.

188. Paquin, P., Technological properties of high pressure homogenizers: the effect of fat globules, milk proteins, and polysaccharides **Int Dairy J**, 1999, 9(3): p. 329-35.

189. Pereda, J., Ferragut, V., Quevedo, J.M., Guamis, B., Trujillo, A.J., Effects of ultra-high pressure homogenization on microbial and physicochemical shelf life of milk, **J Dairy Sci**, 2007, 90(3): p. 1081-93.

190. Wang, X.Q., Huang, J., Dai, J.D., Zhang, T., Lu, W.L., Zhang, H., Zhang, X., Wang, J.C., Zhang, Q., Long-term studies on the stability and oral bioavailability of cyclosporine A nanoparticle colloid, **Int J Pharm**, 2006, 322(1-2): p. 146-53.

191. Product discription: High pressure pumps and homogenizers. 2005, GEA Niro Soavi, http://www.nirosoavi.com.

192. Jinno, J., et al., Effect of particle size reduction on dissolution and oral absorption of a poorly water-soluble drug, cilostazol, in beagle dogs, **J Control Release**, 2006, 111(1-2): p. 56-64.

193. Krause, K.P., Kayser, O., Mäder, K., Gust, R., Müller, R.H., Heavy metal contamination of nanosuspensions produced by high-pressure homogenisation, **Int J Pharm**, 2000, 196(2): p. 169-72.

194. Jahnke, I.S., The theory of high-pressure homogenisation, in **Dispersion techniques for laboratory and industrial scale processing**, Müller, R.H., Böhm, B.H.L., Editors. 2001, Wissenschaftliche Verlagsgesellschaft GmbH: Stuttgart.

195. Maschke, A., Cali, N., Appel, B., Kiermaier, J., Blunk, T., Gopferich, A., Micronization of insulin by high pressure homogenization, **Pharm Res**, 2006, 23(9): p. 2220-9.

196. Müller, R.H., Böhm, B.H.L., Nanosuspensions, in **Emulsions and Nanosuspensions for the Formulation of Poorly Soluble Drugs**, Müller, R.H., Benita, S., Böhm, B.H.L., Editors. 1998, Medpharm Scientific: Stuttgart. p. 149-74.
197. Fiese, E.F., Hagen, T.A., Pre-formulation, in: The theory and practice of industrial pharmacy, ed. Lachman, L., Lieberman, H.A., Kanig, J.L., 1986, Philadelphia: Lea & Febiger.
198. Keck, C., Cyclosporine nanosuspensions: Optimised size characterisation & oral formulations. PhD thesis. 2006, Free University of Berlin: Berlin.
199. Müller, R.H., Schuhmann, R., Teilchengrößenmessung in der Laborpraxis, 1996, Stuttgart: Wissenschaftliche Verlagsgesellschaft mbH. 191.
200. Xu, R., Extracted polarization intensity differential scattering for particle characterization, in United States Patent 6859276. 2003, Coulter International Corp.
201. Xu, R., Improvements in particle size analysis using light scattering, in **Particle and surface characterisation methods**, Müller, R.H., Mehnert, W., Editors. 1977, Medpharm Scientific: Stuttgart. p. 27-56.
202. Washington, C., Particle Size Analysis in Pharmaceutics and Other Industries: Theory and Practice., 1992, West Sussex: Ellis Horwood Ltd.
203. Schuhmann, R., Physikalische Stabilität parenteraler Fettemulsionen, Entwicklung eines Untersuchungsschemas unter besonserem Aspekt analytischer Möglichkeiten, PhD thesis. 1995, Freie Universität Berlin: Berlin.
204. Müller, R.H., Colloidal carriers for controlled drug delivery and targeting. Modification, characterization, and In vivo distribution, 1991, Stuttgart, Boston: Wissenschaftliche Verlagsgesellschaft GmbH, CRC Press.
205. Kaszuba, M., McKnight, D., Connah, M.T., McNeil-Watson, F.K., Nobbmann, U., Measuring sub nanometre sizes using dynamic light scattering, **J Nanopart Res**, 2007, 10(5): p. 823-9.
206. Thode, K., Müller, R.H., Kresse, M., Two-time window and multiangle photon correlation spectroscopy size and zeta potential analysis--highly sensitive rapid assay for dispersion stability, **J Pharm Sci**, 2000, 89(10): p. 1317-24.
207. Malvern Instruments, New dynamic light scattering technology for high sensitivity and measurement at high concentration (NIBS). 2008, Malvern Instruments Ltd.
208. Instruments, M., Zeta Potential Theory. 2008, Malvern Instruments Ltd.

209. Thode, K., Müller, R.H., Kresse, M., Two-time window and multiangle photon correlation spectroscopy size and zeta potential analysis - highly sensitive rapid assay for dispersion stability, **J Pharm Sci**, 2000, 89(10): p. 1317-24.
210. Müller, R.H., Zetapotential und Partikeladung in der Laborpraxis, 1996, Suttgart: Wissenschaftliche Verlagsgeselschaft mbH. 254.
211. Malvern Instruments, Zeta potential: An introduction in 30 minutes. 2008, Malvern Instruments Ltd.
212. Ford, J.L., Timmins, P., Horwood, E., Pharmaceutical thermal analysis - techniques and applications, ed. Horwood, E., 1989, West Sussex, England: Ellis Horwood Limited.
213. Clas, S.D., Dalton, C.R., Hancock, B.C., Differential scanning calorimetry: applications in drug development, **Pharm Sci Technolo Today**, 1999, 2(8): p. 311-20.
214. Freitas, C., Müller, R.H., Correlation between long-term stability of solid lipid nanoparticles (SLN) and crystallinity of the lipid phase, **Eur J Pharm Biopharm**, 1999, 47(2): p. 125-32.
215. Bunjes, H., Unruh, T., Characterization of lipid nanoparticles by differential scanning calorimetry, X-ray and neutron scattering, **Adv Drug Deliv Rev**, 2007, 59(6): p. 379-402.
216. Unruh, T., Bunjes, H., Westesen, K., Koch, M.H.J., Observation of Size-Dependent Melting in Lipid Nanoparticles, **J Phys Chem B**, 1999, 103(47): p. 10373-77.
217. Unruh, T., Bunjes, H., Westesen, K., Koch, M.H.J., Investigations on the melting behaviour of triglyceride nanoparticles, **Colloid Polym Sci**, 2001, 279(4): p. 398-403.
218. Al-Shora, H.I., Determination of ubidecarenone by high performance liquid chromatography, **Pharmazie**, 1987, 42: p. 56-7.
219. Andersson, S., Determination of coenzym Q 10 [ubidecarenone] by non-aqueous reversed-phase liquid chromatography, **J Chromatogr**, 1992, 626(2): p. 272-6.
220. Zhiri, A., Belichard, P., Reversed-phase liquid chromatographic analysis of coenzym Q 10 and stability study in human plasma, **J Liquid Chromatogr**, 1944, 17(2): p. 2633-40.
221. DFG standard methods, Wheeler peroxide number. 2002.
222. Hommoss, A., Souto, E.B., Müller, R.H., Assessment of the release profiles of a perfume incorporated into NLC dispersions in comparison to reference nanoemulsions, in Abstract of the annual meeting of the American Association of Pharmaceutical Scientists (AAPS),Nashville, USA, Nov. 6-10, 2005.

223. Barri, T., Jonsson, J.A., Advances and developments in membrane extraction for gas chromatography: Techniques and applications, **J Chromatogr A**, 2008, 1186(1-2): p. 16-38.

224. Stashenko, E.E., Martinez, J.R., Sampling flower scent for chromatographic analysis, **J Sep Sci**, 2008, 31(11): p. 2022-31.

225. Hyotylainen, T., Riekkola, M.L., Sorbent- and liquid-phase microextraction techniques and membrane-assisted extraction in combination with gas chromatographic analysis: A review, **Anal Chim Acta**, 2008, 614(1): p. 27-37.

226. Ferrero, L., Pissavini, M., Dehais, A., Marguerie, S., Zastrow, L., Importance of substrate roughness for in vitro sun protection Assessment, **Int J Cosmet Sci**, 2007, 29(1): p. 59.

227. Diffey, B.L., Sunscreens and UVA protection: a major issue of minor importance, **Photochem Photobiol**, 2001, 74(1): p. 61-3.

228. Lott, D.L., Stanfield, J., Sayre, R.M., Dowdy, J.C., Uniformity of sunscreen product application: a problem in testing, a problem for consumers, **Photodermatol Photoimmunol Photomed**, 2003, 19(1): p. 17-20.

229. Jenning, V., Lippacher, A., Gohla, S.H., Medium scale production of solid lipid nanoparticles (SLN) by high pressure homogenization, **J Microencapsul**, 2002, 19(1): p. 1 - 10.

230. Almeida, A.J., Runge, S., Müller, R.H., Peptide-loaded solid lipid nanoparticles (SLN): Influence of production parameters, **Int J Pharm**, 1997, 149(2): p. 255-65.

231. Lippacher, A., Müller, R.H., Mäder, K., Semisolid SLN dispersions for topical application: influence of formulation and production parameters on viscoelastic properties, **Eur J Pharm Biopharm**, 2002, 53(2): p. 155-60.

232. Schubert, M.A., Müller-Goymann, C.C., Characterisation of surface-modified solid lipid nanoparticles (SLN): Influence of lecithin and nonionic emulsifier, **Eur J Pharm Biopharm**, 2005, 61(1-2): p. 77-86.

233. Lander, R., Manger, W., Scouloudis, M., Ku, A., Davis, C., Lee, A., Gaulin homogenization: a mechanistic study, **Biotechnol Prog**, 2000, 16(1): p. 80-5.

234. Arii, K., Fukuta, Y., Kai, T., Kokuba, Y., Preparation of fine emulsified fat particles without glycerol for intravenous nutrition, **Eur J Pharm Sci**, 1999, 9(1): p. 67-73.

235. Salgueiro, A., Egea, M.A., Espina, M., Valls, O., Garcia, M.L., Stability and ocular tolerance of cyclophosphamide-loaded nanospheres, **J Microencapsul**, 2004, 21(2): p. 213-23.

236. Yoon, K.A., Burgess, D.J., Mathematical modelling of drug transport in emulsion systems, **J Pharm Pharmacol**, 1998, 50(6): p. 601-10.

237. Grit, M., Underberg, W.J., Crommelin, D.J., Hydrolysis of saturated soybean phosphatidylcholine in aqueous liposome dispersions, **J Pharm Sci**, 1993, 82(4): p. 362-6.

238. Müller, R.H., Petersen, R.D., Hommoss, A., Pardeike, J., Nanostructured lipid carriers (NLC) in cosmetic dermal products, **Adv Drug Deliv Rev**, 2007, 59(6): p. 522-30.

239. State Pharmacopoeia Committee of the People's Republic of China. Pharmacopoeia of the People's Republic of China, 2000, Beijing, China: Chemical Industry Press.

240. Dragićević-Ćurić, N., Blume, G., Stupar, M., Milić, J., M., S., Influence of liposomes on the photostability of coenzyme Q10 in carbomer gels, **SÖFW Journal**, 2004, 130: p. 10-14.

241. Xia, S., Xu, S., Zhang, X., Optimization in the preparation of coenzyme Q10 nanoliposomes, **J Agric Food Chem**, 2006, 54(17): p. 6358-66.

242. Nehilla, B.J., Bergkvist, M., Popat, K.C., Desai, T.A., Purified and surfactant-free coenzyme Q10-loaded biodegradable nanoparticles, **Int J Pharm**, 2008, 348(1-2): p. 107-14.

243. Thunemann, A.F., General, S., Nanoparticles of a polyelectrolyte-fatty acid complex: carriers for Q10 and triiodothyronine, **J Control Release**, 2001, 75(3): p. 237-47.

244. Hsu, C.H., Cui, Z., Mumper, R.J., Jay, M., Preparation and characterization of novel coenzyme Q10 nanoparticles engineered from microemulsion precursors, **AAPS PharmSciTech**, 2003, 4(3): p. E32.

245. Siekmann, B., Westesen, K., Preparation and physicochemical characterization of aqueous dispersions of coenzyme Q10 nanoparticles, **Pharm Res**, 1995, 12(2): p. 201-8.

246. Ratnam, D.V., Ankola, D.D., Bhardwaj, V., Sahana, D.K., Kumar, M.N., Role of antioxidants in prophylaxis and therapy: A pharmaceutical perspective, **J Control Release**, 2006, 113(3): p. 189-207.

247. Pardeike, J., Müller, R.H., Penetration Enhancement and Occlusion Properties of Coenzyme Q10-loaded NLC, in The American Association of Pharmaceutical Scientists (AAPS),San Antonio, Texas, USA, 2006.

248. Petersen, R.D., Hommoss, A., Peter, M., Müller, R.H. , Nanostructured lipid carrier – A delivery system with protective functions, **SÖFW**, 2006(4): p. 64-9.

249. Cannelle, J.S., Fundamentals of stability testing, **Int J Cosmet Sci**, 1985, 7: p. 291-303.
250. Guidlines on stability testing of cosmetic products, The European Cosmetic Toiletry and Perfumery Association (CTFA). 2004 [cited; Available from: www.colipa.com.
251. Semenova, E., Cooper, A., Wilson, C., Converse, C. , Stabilization of All-trans-retinol by Cyclodextrins: A Comparative Study Using HPLC and Fluorescence Spectroscopy **J Inclus Phenom Mol**, 2002, 44: p. 155-8.
252. Saupe, A., Pharmazeutisch-kosmetische Anwendungen Nanostrukturierter Lipidcarrier (NLC): Lichtschutz und Pflege. 2004, Freie Universität Berlin.
253. Jee, J.P., Lim, S.J., Park, J.S., Kim, C.K., Stabilization of all-trans retinol by loading lipophilic antioxidants in solid lipid nanoparticles, **Eur J Pharm Biopharm**, 2006, 63(2): p. 134-9.
254. Swanson, L.N., OTC dermatological agents, in **Comprehensive Pharmaceutical Review**, Shargel, L., Mutnick, A.H., Souney, P.F., Swanson, L.N., Editors. 2007, Wolters Kluwer, Lippincott, Williams and Wilkins.
255. Villalobos-Hernández, J.R., Müller-Goymann, C.C., Artificial sun protection: sunscreens and their carrier systems, **Curr Drug Deliv**, 2006, 3(4): p. 405-15.
256. Ultraviolet. 2008, Wikipedia http://en.wikipedia.org/wiki/Ultraviolet.
257. Scarlett, W.L., Ultraviolet radiation: sun exposure, tanning beds, and vitamin D levels. What you need to know and how to decrease the risk of skin cancer, **J Am Osteopath Assoc**, 2003, 103(8): p. 371-5.
258. Wolf, R., Wolf, D., Morganti, P., Ruocco, V., Sunscreens, **Clin Dermatol**, 2001, 19(4): p. 452-9.
259. Mackie, B.S., Mackie, L.E., The PABA story, **Australas J Dermatol**, 1999, 40(1): p. 51-3.
260. Loeppky, R., Hastings, R., Sandbothe, J., Heller, D., Bao, Y., Nagel, D., Nitrosation of tertiary aromatic amines related to sunscreen ingredients, **IRAC Sci Publ**, 1991, 105: p. 244-32.
261. Schauder, S., Ippen, H., Contact and photocontact sensitivity to sunscreens. Review of a 15-year experience and of the literature, **Contact Dermatitis**, 1997, 37(5): p. 221-32.
262. Jiang, R., Roberts, M.S., Collins, D.M., Benson, H.A., Absorption of sunscreens across human skin: an evaluation of commercial products for children and adults, **Br J Clin Pharmacol**, 1999, 48(4): p. 635-7.

263. Sarveiya, V., Risk, S., Benson, H.A., Liquid chromatographic assay for common sunscreen agents: application to in vivo assessment of skin penetration and systemic absorption in human volunteers, **J Chromatogr B Analyt Technol Biomed Life Sci**, 2004, 803(2): p. 225-31.

264. Gustavsson Gonzalez, H., Farbrot, A., Larko, O., Percutaneous absorption of benzophenone-3, a common component of topical sunscreens, **Clin Exp Dermatol**, 2002, 27(8): p. 691-4.

265. Hany, J., Nagel, R., Nachweis von UV-Filtersubstanzen in Muttermilch, **Dtsch Lebensmittel Rundschau**, 2001, 91: p. 341-5.

266. Schlumpf, M., Cotton, B., Conscience, M., Haller, V., Steinmann, B., Lichtensteiger, W., In vitro and in vivo estrogenicity of UV screens, **Environ Health Perspect**, 2001, 109(3): p. 239-44.

267. Patel, M., Jain, S.K., Yadav, A.K., Gogna, D., Agrawal, G.P., Preparation and characterization of oxybenzone-loaded gelatin microspheres for enhancement of sunscreening efficacy, **Drug Deliv**, 2006, 13(5): p. 323-30.

268. Perugini, P., Simeoni, S., Scalia, S., Genta, I., Modena, T., Conti, B., Pavanetto, F., Effect of nanoparticle encapsulation on the photostability of the sunscreen agent, 2-ethylhexyl-p-methoxycinnamate, **Int J Pharm**, 2002, 246(1-2): p. 37-45.

269. Lapidot, N., Gans, O., Biagini, F., Sosonkin, L., Rotmann, C., Advanced sunscreens: UV absorbers encapsulated in Sol-Gel glass microcapsules **J Sol-Gel Sci Technol**, 2003, 26: p. 67-72.

270. Sayre, R.M., Kollias, N., Roberts, R.L., Baqer, A., Sadiq, I., Physical sunscreens, **J Soc Cosmet Chem** 1990, 41: p. 103–9.

271. Mitchnick, M.A., Fairhurst, D., Pinnell, S.R., Microfine zinc oxide (Z-cote) as a photostable UVA/UVB sunblock agent, **J Am Acad Dermatol**, 1999, 40(1): p. 85-90.

272. Wamer, W.G., Yin, J.J., Wei, R.R., Oxidative damage to nucleic acids photosensitized by titanium dioxide, **Free Radic Biol Med**, 1997, 23(6): p. 851-8.

273. www.kemira.com, UV-Titan.

274. Hoet, P.H., Bruske-Hohlfeld, I., Salata, O.V., Nanoparticles - known and unknown health risks, **J Nanobiotechnology**, 2004, 2(1): p. 12.

275. A review of the scientific literature on the safety of nanoparticulate titanium dioxide or zinc oxide in sunscreens, Department of Health and Ageing Ausrtalian Government, Editor. 2006.

276. Kim, S., et al., Near-infrared fluorescent type II quantum dots for sentinel lymph node mapping, **Nat Biotechnol**, 2004, 22(1): p. 93-7.

277. Peters, K., Unger, R.E., Kirkpatrick, C.J., Gatti, A.M., Monari, E., Effects of nano-scaled particles on endothelial cell function in vitro: studies on viability, proliferation and inflammation, **J Mater Sci Mater Med**, 2004, 15(4): p. 321-5.

278. Lademann, J., Weigmann, H., Rickmeyer, C., Barthelmes, H., Schaefer, H., Mueller, G., Sterry, W., Penetration of titanium dioxide microparticles in a sunscreen formulation into the horny layer and the follicular orifice, **Skin Pharmacol Appl Skin Physiol**, 1999, 12(5): p. 247-56.

279. Nohynek, G.J., Schaefer, H., Benefit and risk of organic ultraviolet filters, **Regul Toxicol Pharmacol**, 2001, 33(3): p. 285-99.

280. Lansdown, A.B., Taylor, A., Zinc and titanium oxides: promising UV-absorbers but what influence do they have on the intact skin?, **Int J Cosmet Sci**, 1997, 19(4): p. 167-72.

281. Bennat, C., Müller-Goymann, C.C., Skin penetration and stabilization of formulations containing microfine titanium dioxide as physical UV filter, **Int J Cosmet Sci**, 2000, 22(4): p. 271-83.

282. Memorandum: Firm Clients and Friends. . 2008, Bergeson & Campbell, P.C.: San Jose, CA.

283. Oberdorster, G., Oberdorster, E., Oberdorster, J., Nanotoxicology: an emerging discipline evolving from studies of ultrafine particles, **Environ Health Perspect**, 2005, 113(7): p. 823-39.

284. Schulz, J., et al., Distribution of sunscreens on skin, **Adv Drug Deliv Rev**, 2002, 54(1): p. 157-63.

285. Sipzner, L., Stettin, J., The penetration of titanium dioxide nanoparticles: from dermal fibroblasts to skin tissue, in abstract in APS,Baltimore, MD, 2006.

286. Hallmans, G., Liden, S., Penetration of 65Zn through the skin of rats, **Acta Derm Venereol**, 1979, 59(2): p. 105-12.

287. Pinnell, S.R., Fairhurst, D., Gillies, R., Mitchnick, M.A., Kollias, N., Microfine zinc oxide is a superior sunscreen ingredient to microfine titanium dioxide, **Dermatol Surg**, 2000, 26(4): p. 309-14.

288. El-Boury, S., Couteau, C., Boulande, L., Paparis, E., Coiffard, L.J., Effect of the combination of organic and inorganic filters on the Sun Protection Factor (SPF) determined by in vitro method, **Int J Pharm**, 2007, 340(1-2): p. 1-5.

289. Reisch, M.S., New-wave Sunscreens, **Chem Eng News**, 2005, 83(15): p. 18-22.

290. Wissing, S.A., Müller, R.H., The development of an improved carrier system for sunscreen formulations based on crystalline lipid nanoparticles, **Int J Pharm**, 2002, 242(1-2): p. 373-5.

291. Villalobos-Hernandez, J.R., Müller-Goymann, C.C., Sun protection enhancement of titanium dioxide crystals by the use of carnauba wax nanoparticles: the synergistic interaction between organic and inorganic sunscreens at nanoscale, **Int J Pharm**, 2006, 322(1-2): p. 161-70.

292. Villalobos-Hernandez, J.R., Müller-Goymann, C.C., Physical stability, centrifugation tests, and entrapment efficiency studies of carnauba wax-decyl oleate nanoparticles used for the dispersion of inorganic sunscreens in aqueous media, **Eur J Pharm Biopharm**, 2006, 63(2): p. 115-27.

293. Edlich, R.F., Winters, K.L., Lim, H.W., Cox, M.J., Becker, D.G., Horowitz, J.H., Nichter, L.S., Britt, L.D., Long, W.B., Photoprotection by sunscreens with topical antioxidants and systemic antioxidants to reduce sun exposure, **J Long Term Eff Med Implants**, 2004, 14(4): p. 317-40.

294. Aquino, R., Morelli, S., Tomaino, A., Pellegrino, M., Saija, A., Grumetto, L., Puglia, C., Ventura, D., Bonina, F., Antioxidant and photoprotective activity of a crude extract of Culcitium reflexum H.B.K. leaves and their major flavonoids, **J Ethnopharmacol**, 2002, 79(2): p. 183-91.

295. Bissett, D.L., McBride, J., Skin conditioning with glycerol, **J Am Acad Dermatol**, 1996, 34: p. 187-95.

296. Fuchs, J., Kern, H., Modulation of UV-light-induced skin inflammation by D-alpha-tocopherol and L-ascorbic acid: a clinical study using solar simulated radiation, **Free Radic Biol Med**, 1998, 25(9): p. 1006-12.

297. Wright, F.J., Beneficial effects of topical application of free traditional scarvengers, **Appl Cosmetol**, 1996(13): p. 41-50.

298. Roelandts, R., Sohrabvand, N., Garmyn, M., Evaluating the UVA protection of sunscreens, **J Am Acad Dermatol**, 1989, 21(1): p. 56-62.

299. Bauckhage, K., Nutzung unterschiedlicher Streulichtanteile zur Partikelgrößen-Bestimmung in dispersen Systemen, **Chemie Ingenieur Technik**, 1993, 65(10): p. 1200-5.

300. Garti, N., Sato, K., Crystallization and Polymorphism of Fats and Fatty Acids, ed. Dekker, M., 1998, New York and Basel.

301. Perfume. 2008, Wikipedia, the free encyclopedia.
302. Bauer, K.H., Frömming, K.-H., Führer, C., Pharmayeutische Technologie, 1989, Stuttgart, New Zork: Georg Thieme Verlag.
303. Lai, F., Wissing, S.A., Müller, R.H., Fadda, A.M., Artemisia arborescens L essential oil–loaded solid lipid nanoparticles for potential agricultural application: preparation and characterization, **AAPS PharmSciTech**, 2006, 7(1): p. Article 2.
304. Wissing, S.A., Mäder, K., Müller, R.H., Solid Lipid Nanoparticles (SLN) as a novel carrier system offering prolonged release of the perfume allure (Chanel), in Proceeding in International Symposium on Controlled Release of Bioactive Materials, 2000.
305. Yonezawa, Y., Ishida, S., Sunada, H., Release from or through a wax matrix system. VI. Analysis and prediction of the entire release process of the wax matrix tablet, **Chem Pharm Bull (Tokyo)**, 2005, 53(8): p. 915-8.
306. Yonezawa, Y., Ishida, S., Suzuki, S., Sunada, H., Release from or through a wax matrix system. II. Basic properties of release from or through the wax matrix layer, **Chem Pharm Bull (Tokyo)**, 2002, 50(2): p. 220-4.
307. Higuchi, T., Physical chemical analysis of percutaneous absorption process from creams and ointments, **J Soc Cosmetic Chemists**, 1960, 11: p. 85-97.
308. Higuchi, T., Rate of release of medicaments from ointments bases containing drug in suspension, **J Pharm Sci**, 1961, 50: p. 874-5.
309. Higuchi, T., Mechanism of sustained action medication: Theoretical analysis of rate of release of solid drugs dispersed in solid matrices, **J Pharm Sci**, 1963, 52: p. 1149-63.
310. Noguchi, H., Takasu, M., Adhesion of nanoparticles to vesicles: a Brownian dynamics simulation, **Biophys J**, 2002, 83(1): p. 299-308.

ACKNOWLEDGEMENTS

Here I would like to take the chance to express my gratitude to the following:

To my supervisor, Prof. Dr. Rainer Müller, for giving me the opportunity to start my PhD in Berlin and for his support to me in all means during the four years of my work in his group. I appreciate his vast knowledge and skill in many areas and his assistance, which have on occasion made me "GREEN" with envy.

To the Deutscher Akademischer Austausch Dienst (DAAD), a sincere thank for opening the door to many scientists to perform their research in Germany and for funding my research.

To Jana Pardeike for her suggestions and efforts to make this work better and her friendship and the good times in Germany and all over the world.

To Dr. Cornelia Keck for her help through this work and for her valuable suggestions.

To Dr. Eliana Souto for her supervision at the beginning of my studies in Berlin and for her precious friendship.

To Mrs. Inge Volz and Mrs. Corinna Schmidt. Thank you very much for the assistance, support and good times.

To Dr. Wolfgang Mehnert for his time, help and counseling and for the scientific discussions that enriched this work in many parts.

To Rachmat Mauludin for his dear friendship and brotherhood during the past years, it means a lot to me.

To my colleagues and later my friends who helped me with some parts of this work, Mohammad Al-Samman and Hendrikje Immig. Thank you for your cooperation and friendship.

To all of the members of the Kelchstrasse family, my friends and colleagues who shared their time with me. To Dr. Lothar Schwabe, Mrs. Gabriela Karsubke, Dr. Nadiem Bushrab, Dr. Norma Hernandez-Kirstein, Dr. Vee Teeranachaideekul, Dr. Boris Petri, Dr. Torsten Göppert, Dr. Jan Möschwizer, Dr. Andreas Lemke, Kay Schwabe, Marc Muchow, JensUwe Jughanns, Jörg Hanisch, Szymon Kobierski, Senem Acar, Mirko Jansch and Ansgar Brinkmann.

To Dr. Hassan Tarabishi for the things I learned from him and his support.

To Dr. Emma Blumer, Dr. Maged Yousef, Loaye Al-Shaal, Eng. Hasan Shammout, Dr. Mahmoud Dallal and Dr. Sabah Sulaiman. I have no words to thank all their love, their moral support and friendship during all these years.

To my sisters and brother and to my uncles Dr. Ghassan Hommoss and Eng. Anas Hommoss.

To my parents who taught me my values and raised me to be who I am. I want to thank them from all of my heart for the immeasurable love, support and encouragement.

Last but not least, to God to whom I owe everything I have and everything I will have.

PUBLICATION LIST

Book chapter:

Keck, C., Hommoss, A., Müller, R. H., *Lipid nanoparticles (SLN, NLC, LDC) for the enhancement of oral absorption*, in *Modified Release Drug Delivery Technology*, Rathbone, M. J., Editor. 2008, Egerton: New York.

Journals:

1. Pardeike, J., Hommoss, A., Müller, R.H., *Lipid nanoparticles (SLN, NLC) in cosmetic and pharmaceutical dermal products*, Int J Pharm, in press.
2. Müller, R. H., Hommoss, A., *Nanostructured Lipid Carrier (NLC) Technology for Delivery of Cosmetic Actives,* Int J Pharm, submitted.
3. Müller, R. H., Immig, H., Hommoss, A., *Prolonged release of perfumes by nano lipid carriers (NLC) technology,* Euro Cosmetics, 2007 (11/12).
4. Müller, R. H., Rimpler, C., Petersen, R., Hommoss, A., Schwabe, K., *A new dimension in cosmetic products by nanostructured lipid carriers (NLC) technology,* Euro Cosmetics, 2007 (3): p. 32-37.
5. Muller, R. H., Petersen, R. D., Hommoss, A., Pardeike, J., *Nanostructured lipid carriers (NLC) in cosmetic dermal products,* Adv Drug Deliv Rev, 2007. **59** (6): p. 522-530.
6. Müller, R. H., Pardeike, J., Petersen, R., Hommoss, A., *Nano lipid carriers (NLC): The new cosmetic carrier generation,* SÖFW, 2007 (5).
7. Keck, C., Hommoss, A., Müller, R. H., *Lipid nanoparticles for encapsulation of actives: dermal & oral formulations,* Am Pharm Rev, 2007 (11/12).
8. Müller, R. H., Hommoss A., Pardeike, J.,Schmidt, C., *Lipid nanoparticles (NLC) as novel carrier for cosmetics -Special features & state of commercialisation,* SÖFW Journal, 2007 (9).
9. Petersen, R. D., Hommoss, A., Peter, M., Müller, R.H. , *Nanostructured lipid carrier – A delivery system with protective functions,* SÖFW, 2006 (4): p. 64-69.
10. Rimpler, C., Müller, R. H., Hommoss, A., Schwabe, K., *Lipophiler Wirkstofftransport durch NLC-Technologie,* Euro Cosmetics, 2005 (11/12): p. 2-5.

Proceedings:

1. Hommoss, A., Al-Samman, M., Müller, R. H., *TiO_2-loaded nanostructured lipid carriers (NLC): A nanosave dermal carrier*, proceeding in the *Annual Meeting of the Controlled Release Society (CRS)*, New York, USA, July 11-16, 2008
2. Hommoss, A., Müller, R. H., *Nanostructured lipid carriers (NLC): Efficient formulation to stabilize retinol*, proceeding in the *Annual Meeting of the Controlled Release Society (CRS)*, New York, USA, July 11-16, 2008
3. Hommoss, A., Müller, R. H., *Stabilization of retinol by nanostructured lipid carriers (NLC)*, proceeding in the *6th World Meeting on Pharmaceutics, Biopharmaceutics and Pharmaceutical Technology*, Barcelona, April 7-10, 2008
4. Hommoss, A., Peter, M., Müller, R. H., *Sun Protection Factor (SPF) Increase Using Nanostructured Lipid Carriers (NLC)*, proceeding in the *Annual Meeting of the Controlled Release Society (CRS)*, Long Beach, USA, No. 760, July 7-11, 2007
5. Hommoss, A., Al-Samman, M., Müller, R. H., *Stabilization of chemically labile actives using nanostructured lipid carriers (NLC)*, proceeding in the *Annual Meeting of the Controlled Release Society (CRS)*, Long Beach, USA, No. 591, July 7- 11, 2007
6. Hommoss, A., Müller, R. H., *Release of perfumes: Modulation by type of matrix lipid in NLC*, proceeding in the *5th World Meeting on Pharmaceutics, Biopharmaceutics and Pharmaceutical Technology*, Geneva, March 27- 30, 2006
7. Müller, R. H., Hommoss, A., Schwabe, K., Rimpler, C., *Nanorepair Q10 – First dermal product on the market based on nanostructured lipid carrier (NLC) technology*, proceeding in the *5th World Meeting on Pharmaceutics, Biopharmaceutics and Pharmaceutical Technology*, Geneva, March 27-30, 2006
8. Müller, R. H., Hommoss, A., Pardeike, J., Schmidt, C., *Lipid nanoparticles (NLC) as novel carrier for cosmetics – Special features & state of commercialisation*, proceeding in the *Cosmetic Science Conference (CSC) at In-Cosmetics*, Barcelona, Spain, April 5, 2006

Abstracts:

1. Hommoss, A., Al-Samman, Müller R. H., *UV radiation blocker based on nanostructured lipid carriers (NLC),* abstract in the *Annual Meeting of the American Association of Pharmaceutical Scientists (AAPS)*, Atlanta, USA, November 16-20, 2008

2. Hommoss, A., Kim, C., Müller R. H., *Positively charged nanostructured lipid carriers (NLC) for a prolonged perfume release*, abstract in the *Annual Meeting of the American Association of Pharmaceutical Scientists (AAPS)*, Atlanta, USA, November 16-20, 2008
3. Hommoss, A., Schwabe, K., Rimpler, C., Müller, R. H., *Nanostructured lipid carriers (NLC) in cosmetic dermal formulations,* abstract in the *7th European Workshop on Particulate Systems (EWPS)*, Berlin, May 30-31, 2008
4. Hommoss, A., Keck, C., Müller, R. H., *Retinol loaded nanostructured lipid carriers: A design for higher chemical stability*, abstract in the *Menopause Andropause Anti-Aging*, Vienna, Austria, December 6-8, 2007
5. Hommoss, A., Al-Samman, M., Müller, R. H., *UV radiation blocking activity booster depending on nanostructured lipid carriers (NLC)*, abstract in the *Annual Meeting of the American Association of Pharmaceutical Scientists (AAPS)*, San Diego, USA, No. 2269, November 11-15, 2007
6. Hommoss, A., Acar, S., Kim, C., Müller, R. H., *Prolonged release of perfume from nanostructured lipid carriers (NLC)*, abstract in the *Annual Meeting of the American Association of Pharmaceutical Scientists (AAPS)*, San Diego, USA, No. 1999, November 11-15, 2007
7. Hommoss, A., Immig, H., Müller, R. H., *Perfume loaded nanostructure lipid carrier (NLC) - an approach to controlled release*, abstract in the *Annual Meeting of the American Association of Pharmaceutical Scientists (AAPS)*, San Antonio, USA, No. W4260, October 29- November 2, 2006
8. Müller, R. H., Hommoss, A., Schwabe, K., Rimpler, C., *Dermal coenzyme Q10 formulations based on nanostructured lipid carrier (NLC)*, abstract in the *Annual Meeting of the American Association of Pharmaceutical Scientists (AAPS)*, San Antonio, USA, No. M1269, October 29 - November 2, 2006
9. Müller, R. H., Hommoss, A., Rimpler, C., *Lipid Nanoparticles (SLN, NLC) – Present state of development for dermal delivery*, abstract in the *European Workshop on Particulate Systems (EWPS)*, Geneva, March 23-25, 2006
10. Hommoss, A., Souto, E. B., Müller, R. H., *Assessment of the release profiles of a perfume incorporated into NLC dispersions in comparison to reference nanoemulsions*, abstract in the *Annual Meeting of the American Association of Pharmaceutical Scientists (AAPS)*, Nashville, USA, No. M1238, November 6-10, 2005